
实验室学术委员会

顾问

苏纪兰 中国科学院院士，自然资源部第二海洋研究所研究员

主任

陈大可 中国科学院院士，自然资源部第二海洋研究所研究员

副主任

吴立新 中国科学院院士，中国海洋大学教授

张 经 中国科学院院士，华东师范大学教授

委员

秦大河 中国科学院院士，中国科学院寒区旱区环境与工程研究所研究员

王成善 中国科学院院士，中国地质大学（北京）教授

彭平安 中国科学院院士，中国科学院广州地球化学研究所研究员

周成虎 中国科学院院士，中国科学院地理科学与资源研究所研究员

陈发虎 中国科学院院士，中国科学院青藏高原研究所研究员

戴民汉 中国科学院院士，厦门大学教授

宗永强 香港大学教授

赵冲久 新疆维吾尔自治区人民政府副主席，原中华人民共和国交通运输部研究员

唐丹玲 中国科学院南海海洋研究所研究员

魏 皓 天津大学教授

杨守业 同济大学教授

王厚杰 中国海洋大学教授

丁平兴 华东师范大学教授

高 抒 华东师范大学教授

实验室领导：

主任：高 抒

副主任：吴 辉 张卫国 江红

SKLEC Academic Committee:

Advisory Members

Prof. Dr. SU Jilan, Second Institute of Oceanography, MNR, and Academician of CAS

Chair

Prof. Dr. CHEN Dake, Second Institute of Oceanography, MNR, and Academician of CAS

Vice Chairs

Prof. Dr. WU Lixin, Ocean University of China, and Academician of CAS

Prof. Dr. ZHANG Jing, East China Normal University, and Academician of CAS

Members

Prof. Dr. QIN Dahe, Cold and Arid Regions Environmental and Engineering Research Institute, CAS, and Academician of CAS

Prof. Dr. WANG Chengshan, China University of Geosciences, and Academician of CAS

Prof. Dr. PENG Ping'an, Guangzhou Institute of Geochemistry, CAS, and Academician of CAS

Prof. Dr. ZHOU Chenghu, Institute of Geographic Sciences and Natural Resources Research, CAS, and Academician of CAS

Prof. Dr. CHEN Fahu, Institute of Tibetan Plateau Research, CAS, and Academician of CAS

Prof. Dr. DAI Minhan, Xiamen University, and Academician of CAS

Prof. Dr. ZONG Yongqiang, the University of Hong Kong

Prof. Dr. ZHAO Chongjiu, Vice Governor of the People's Government of Xinjiang Uygur Autonomous Region, and former senior researcher of MOC

Prof. Dr. TANG Danning, South China Sea Institute of Oceanology, CAS

Prof. Dr. WEI Hao, Tianjin University

Prof. Dr. YANG Shouye, Tongji University

Prof. Dr. WANG Houjie, Ocean University of China

Prof. Dr. DING Pingxing, East China Normal University

Prof. Dr. GAO Shu, East China Normal University

CAS – Chinese Academy of Sciences

MNR – Ministry of Natural Resource of the People's Republic of China

MOC – Ministry of Transport of the People's Republic of China

SKLEC Board of Directors

Director: Prof. Dr. GAO Shu

Deputy Directors: Prof. Dr. WU Hui, Prof. Dr. ZHANG Weiguo, Dr. JIANG Hong

实验室行业技术委员会

主任

王光谦 中国科学院院士，青海大学校长

委员

张连云 中国工程院院士，南京水利科学研究院教授级高工

傅伯杰 中国科学院院士，中国科学院生态环境研究中心研究员

王超 中国工程院院士，河海大学教授

胡春宏 中国工程院院士，中国水利水电科学研究院教授级高工

李家彪 中国工程院院士，自然资源部第二海洋研究所研究员

蒋兴伟 中国工程院院士，国家卫星海洋应用中心研究员

张洪涛 国务院参事，原国土资源部总工程师

仲志余 水利部长江水利委员会总工程师

李文学 水利部黄河水利委员会总工程师

石小强 中国长江三峡集团公司上海勘测设计研究院有限公司董事长

朱剑飞 交通部长江口航道管理局总工程师

崔丽娟 中国林业科学研究院湿地研究所研究员

汤臣栋 上海市绿化和市容管理局副局长

潘增弟 自然资源部东海分局研究员

SKLEC Technical Committee

Chair

WANG Guangqian, President of Qinghai University, and Academician of CAS

Members

ZHANG Jianyun, Nanjing Hydraulic Research Institute, and Academician of CAE

FU Bojie, Research Center for Eco-Environmental Sciences, CAS, and Academician of CAS

WANG Chao, Hohai University, and Academician of CAE

HU Chunhong, China Institute of Water Resources and Hydropower Research, and Academician of CAE

LI Jiabiao, Second Institute of Oceanography, MNR, and Academician of CAE

JIANG Xingwei, National Satellite Ocean Application Service, and Academician of CAE

ZHANG Hongtao, Former Chief Engineer of MLR, and counsellor of the State Council of China

ZHONG Zhiyu, Chief Engineer of Changjiang Water Resources Commission of the Ministry of Water Resources

LI Wenxue, Chief Engineer of Yellow River Water Resources Commission of the Ministry of Water Resources

SHI Xiaoqiang, Shanghai Investigation, Design and Research Institute Company, LTD

ZHU Jianfei, Chief Engineer of Yangtze river estuary waterway administration bureau of MOC

CUI Lijuan, Institute of Wetland Research, Chinese Academy of Forestry

TANG Chendong, Deputy Director General of Shanghai Landscaping and City Appearance Administrative Bureau

PAN Zengdi, East China Sea Branch of MNR

CAS – Chinese Academy of Sciences

CAE – Chinese Academy of Engineering

MNR – Ministry of Natural Resource of the People's Republic of China

MOC – Ministry of Transport of the People's Republic of China

MLR – Ministry of Land and Resources

LTD- Limited Liability Company

目录

CONTENTS



1

实验室简介
SKLEC Introduction

2

大事记
Headlines

6

科研课题与进展
Research Programs
& Highlights

117

交流与合作
Academic Communi-
cations & Cooperations

131

论文专著
List of Peer Reviewed
Publications

145

获奖与专利
Awards & Patents

148

平台设施与野外观测
Facilities & Field
Observations

153

人才培养
Student Programs

160

研究队伍
Research Staff

实验室简介 SKLEC Introduction

河口海岸学国家重点实验室缘自1957年由教育部批复建立的华东师范大学河口研究室，依托华东师范大学，于1989年由原国家计委批准筹建，1995年12月通过国家验收并正式向国内外开放。

经过二十多年的建设，实验室已拥有一支结构合理、多学科交叉、专业互补、老中青结合的研究队伍；配备了先进的野外勘测及室内测试与分析仪器。实验室现有固定人员93人，其中研究人员83人（教授/研究员40人，副教授/副研究员20人，讲师/助理研究员4人，博士后19人；全部具有博士学位），技术人员7人，管理人员3人。秉承“开放、流动、联合、竞争”的运行机制，实验室瞄准国际学科前沿，围绕国家重大需求，在河口海岸学科前沿领域深入进行应用基础性研究，已成为代表我国河口海岸最高水平的科研基地与高层次人才培养基地。

State Key Laboratory of Estuarine and Coastal Research (SKLEC) is affiliated to East China Normal University (ECNU), Shanghai. SKLEC was established on the research achievement of China in 1989, and went into operation in December 1995. It is now co-sponsored by East China Normal University and Ministry of Science and Technology of China.

Since 1989, the laboratory has formed a number of multidisciplinary research teams, equipped with advanced instruments both for fieldwork and laboratory analysis. There are 93 fulltime faculties and staff members in the laboratory, which include 83 research faculties (40 professors, 20 associate professors, 4 lecturers and 19 post-doctors, all research faculties with Ph.D. degree), 7 technicians and 3 administrative staff.

SKLEC carries out a large amount of theoretical and applied research projects to serve the demands of national development, social sustainability, and frontline science. Guided by the philosophy of “Openness, Exchange, Cooperation and Competition”, it has become a high level research and training base for estuarine and coastal studies in China.



大事记 Headlines

运行管理

Operations and Managements

2018年1月，河口海岸学国家重点实验室第六届学术委员会第二次会议召开。

In January 2018, SKLEC's Academic Committee Meeting was held in Shanghai.

2018年11月，河口海岸学国家重点实验室正式搬迁闵行校区新河口海岸大楼。

In November 2018, SKLEC was officially relocated to the new building of Minhang campus.

研究生培养

Student Programs

我室获批国家留学基金委2018年创新型人才国际合作培养项目。

SKLEC was approved the International Cooperation Training Program for innovative talents by CSC(China Scholarship Council) in 2018.

我室完成海洋科学(港口海岸及近海工程)学位点自评估。

SKLEC have completed the Academic Degree Self-assessment of Marine Science (including Port Coastal and Offshore Engineering).

学术交流

Academic Communications

2018年4月，华东师范大学海外青年科学家论坛-海洋科学分论坛顺利举行。来自美国、英国、加拿大、澳大利亚、新加坡等国的10位海外青年学者应邀出席。会议以学术报告的形式围绕河口海岸沉积动力学与海岸工程、河口水文过程演变、滨海湿地碳循环、海岸生物地球化学、极地生态系统演变、全新世海平面变化等领域展开交流。此次论坛为海内外青年学者提供了良好的交流平台。

The 2018 International Forum for Outingstanding Oversea Young Scholars in marine science was held on 28, April in ECNU. 10 oversea young scholars joined this forum and gave talks on physical oceanography, oceanographically remote sensing, marine ecosystem, marine geology and ocean chemistry. This forum provided a platform to enhance the exchange between SKLEC and oversea young scholars.

2018年4月，“第二届海洋微塑料污染与控制国际学术研讨会”开幕。二十余名国内外知名专家学者在为期三天的研讨会中带来了精彩的学术报告，并和与会专家一起围绕海洋微塑料在海洋中的来源和归趋、海洋微塑料输运数值模型、海洋微塑料与化学污染物的相互作用、微塑料对海洋生物的生态效应、公民科学家参与解决海洋垃圾问题及海洋微塑料防治措施等议题进行探讨交流。

The 2nd symposium is organized by the State Key Laboratory of Estuarine and Coastal Research (SKLEC) and the Plastic Marine Debris Research Center (PMDRC), East China Normal University, co-organized by Intergovernmental Oceanographic Commission Sub-Commission for the Western Pacific, and the State Oceanic

Administration of China was held in April. More than 70 famous experts and scientists from 7 different countries joined the symposium. They discussed four key topics of microplastic research: 1) Occurrence and fate of microplastics in the marine environment; 2) Microplastics interacting with biological and chemical contaminants; 3) Influences of microplastics on the marine biota; 4) Citizens science and possible solutions/remediation measure for marine microplastics.

2018年9月，“海洋生物地球化学与西太平洋生物圈可持续发展”国际研讨会议暨第八届中-日-韩“海洋生物圈整合研究”研讨会召开。来自日本、韩国、泰国、印度、巴基斯坦、斯里兰卡、马来西亚、加拿大和中国等国家和地区的近30家海洋科研机构及大学的100余名代表参会，大会围绕主题集中探讨了气候变化和人类活动影响下西太平洋地区生态系统所承载的压力及其可持续化发展问题。

The 8th China-Japan-Korea IMBeR Symposium and Training Course (IMBeR CJK 2018) was held from September 17 to 19 in 2018 at the East China Normal University (ECNU) in Shanghai, China, with the focus on Marine Biogeochemical Sciences for the Sustainability of the West Pacific Biosphere. The State Key Laboratory of Estuarine and Coastal Research (SKLEC) & ECNU, China GLOBEC-IMBeR project and IMBeR Regional Project Office co-hosted the event. IMBeR CJK 2018 attracted over 100 delegates including scientists, young researchers and students from almost 30 marine scientific research institutions and universities, which were from China, Japan, Korea, Thailand, India, Pakistan, Sri Lanka, Malaysia and Canada.

2018年10月，实验室主办的大河三角洲国际研讨会在上海召开，会议针对国际海洋研究科学委员会工作组申请框架进行了讨论，从海洋视角探讨了大河三角洲面临问题的根源，以及多学科、多方位的综合解决方案。

International Symposium for Mega Deltas organized by State Key Laboratory of Estuarine and Coastal Research (SKLEC) was held in Shanghai during October 15-16, 2018. The meeting presented: 1) the evolution of mega deltas; 2) challenges and disasters faced. Then, participants discussed the solutions to the various problems identified and the application of Scientific Committee on Oceanic Research (SCOR).

国际合作 International Cooperation

2018年1月，华东师范大学和加拿大科学出版社合作学术期刊《Anthropocene Coasts》（中译名《人新世海岸》）正式上线，第一篇论文于加拿大时间2018年1月3日正式发表。

Anthropocene Coasts is an innovative international partnership journal, jointly developed and co-owned by Canadian Science Publishing (CSP) and East China Normal University (ECNU). It was launched in January 2018. The first paper was officially published on Canadian time January 3, 2018.

2018年3月，克罗地亚Vladimir Bermanec院士代表团访问我校，双方座谈会在我室举行。

In March 2018, a delegation of Croatian Academician visited our university, and the bilateral meeting was held in State Key Laboratory of Estuarine and Coastal Research (SKLEC).

2018年3月，海洋生物圈整合研究（IMBeR）和未来地球海岸国际计划（Future Earth Coasts, FEC）联合成立新的陆架边缘研究工作组（Continental Margins Working Group, CMWG）。

In March 2018, Integrated Marine Biogeochemistry and Ecosystem Research (IMBeR) and Future Earth Coasts (FEC) jointly established the new Continental Margins Working Group (CMWG).

科研项目 Research projects

由我室何青教授领衔的国家重点研发计划政府间国际科技创新合作重点专项“应对转型中的河口三角洲”项目启动会及学术研讨会在华东师范大学举行。该项目是由中国科技部(MOST)和荷兰皇家科学院(KNAW)联合发起的政府间科技合作项目，意在确立中国与荷兰长期的科学战略合作关系。

The kick-off meeting of the joint research project "Coping with Deltas in Transition", which is the intergovernmental cooperation on science and technology innovation of the National Key Research and Development Program, was held at East China Normal University (ECNU) during May 15-16, 2018. This project is supported by the Programme Strategic Scientific Alliances (PSA) between China and the Netherlands and funded by Ministry of Science and Technology of the Peoples' Republic of China (MOST) and Koninklijke Nederlandse Akademie Van Wetenschappen (KNAW), with the vision of establishing a new framework of long-term scientific cooperation with mutual benefit to the Netherlands and China.

由我室张卫国教授领衔的国家重点研发计划政府间国际科技创新合作重点专项“中美大河三角洲侵蚀灾害与应对策略比较研究”项目获批立项。

The intergovernmental cooperation on science and technology innovation of the National Key Research and Development Program "Comparative Study on Erosion Hazards and Coping Strategies in River Deltas between China and America" hosted by Prof. ZHANG Weiguo was approved.

由我室客座教授SHEN Jian主持申请的上海市科委社会发展领域重大(点)项目“崇明东滩生态修复评估与调控技术研究”项目获批。

The Social Development Key Program of Shanghai Science and Technology Commission "Research on Ecological Restoration Assessment and Regulation Technology of Chongming Dongtan Wetland" hosted by Prof. SHEN Jian was approved.

我室唐剑武教授获得全国海洋标准化技术委员会自然资源(海洋领域)标准制定项目，标准名称为“蓝碳生态系统碳库规模调查与评估技术规程 盐沼”，标准级别HYT。

The standard setting project named "Carbon Pool Scale Survey and Assessment Technical Specification in Blue Carbon Ecosystems • Salt Marsh" was awarded by the National Technical Committee on Marine Standardization of China in 2018.

人物 People

侯立军教授发明专利“一种基于膜入口质谱仪分析溶解态氮同位素含量的方法”获得授权。

Prof. HOU Lijun was authorized one National Invention Patent.

瞿建国副教授发明专利“一种连续提取沉积物样品中各形态硫的实验装置”获得授权。

Prof. QU Jianguo was authorized one National Invention Patent.

2018年，程和琴教授领衔完成的科研成果“长江口海平面上升对上海城市安全影响及其应对关键技术研究”荣获上海市水务海洋科学技术奖二等奖。

The project entitled "Research on the Impact of Rising Sea Level on the City Security and Key Adaptive Technologies" awarded the second prize of Shanghai Marine Science and Technology Award in 2018.

李道季教授领衔的政协委员提案“关于加强长三角区域一体化合作与发展的建议”荣获上海市政协2018年优秀提案奖。

The proposal entitled “Suggestions on Strengthening the Regional Integration Cooperation and Development of the Yangtze River Delta” was awarded the Excellent Proposal Award by Shanghai CPPCC in 2018.

陈启晴博士入选“紫江青年学者”。

Dr. CHEN Qiqing was selected into the Zijiang Young Scholar Program of ECNU.

科研课题与进展

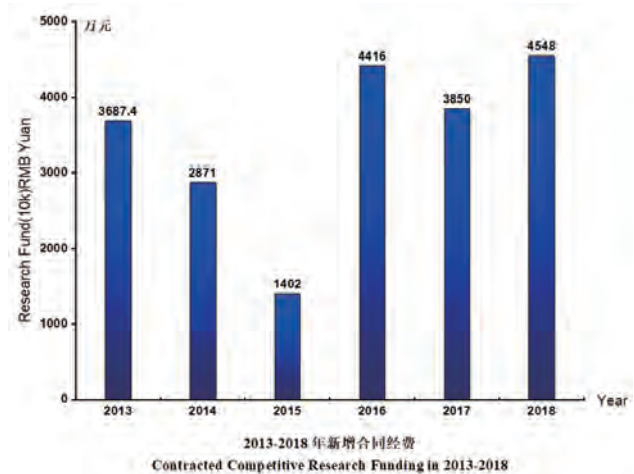
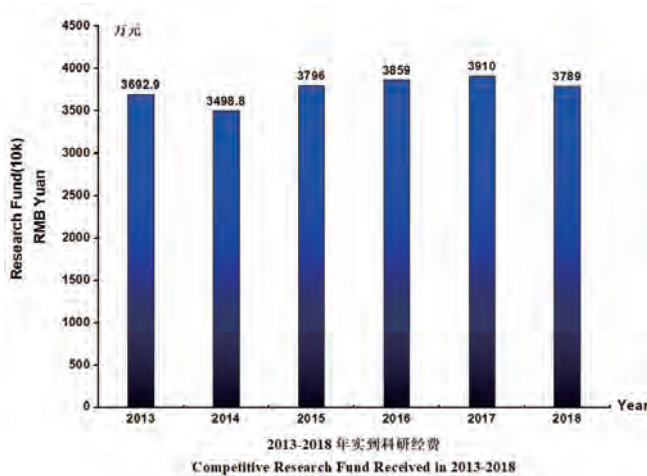
Research Programs and Highlights

科研课题

Research Programs

2018年度，实验室新增项目92项，新增合同经费4548余万元。其中，新增国家、省部级项目33项，新增合同经费3621余万元。2018年度，实验室合计承担课题200余项，实到经费3789余万元，其中国家和省部级课题100余项，实到经费2990万元。此外，实验室还获得科技部国家重点实验室专项经费700万元，其中300万元用于自主研究课题的部署，400万元用于实验室管理运行和开放课题。

Ninety-two new projects were granted in 2018 with total funding of 45.48 million RMB. Among them, more than 33 projects were awarded from national or provincial funding agencies, which total 36.21 million RMB. In 2018, more than 200 research projects were carried out with total funding of 37.89 million RMB. Among them, more than 100 projects were granted by national, provincial and ministerial funding agencies, which totaled 29.90 million RMB. In addition, SKLEC received special funding from the Ministry of Science and Technology (MOST) of China, among which 3 million RMB was specifically aimed at scientific research, 4 million RMB for administration and operation of SKLEC.



在研重要项目进展 Progress of Important Projects

国家重点研发计划项目：海洋微塑料监测和生态环境效应评估技术研究（2016YFC1402200） The National Key R&D Program of China: Marine Microplastics Monitoring and Ecological Risk Assessment Technology Research Project (2016.09-2020.12)

本项目从2016年启动到2018年，计划进展顺利，任务的实施进展情况良好。

本项目已完成确定水体和生物体中微塑料样品采集和实验室筛选分离、消化处理和分析鉴定方法，编制《海洋微塑料监测技术规程》。结束了渤海、黄海、东海共6条关键断面季节性航次采样，及长江口、珠江口微塑料入海通量季节性和洪、枯季研究现场采样。在海洋微塑料的分布、源解析、输运和归趋机制研究方面，开发了微塑料颗粒分析软件；对不同来源的塑料垃圾进行采样调查，形成微塑料来源数据集，为构建指纹信息库储备数据；建立一套完整的漂浮型和悬浮型微塑料的数值模式，模拟得到长江口塑料颗粒运移的3条主要路径，对评估微塑料的污染状况提供了有力的科学数据。在对微塑料自身及吸附的化学污染物在海洋食物链中的传递与转化过程研究方面，完成微塑料-有机污染物吸附解吸机理研究，开展了微塑料对有机污染物在海洋生物体内积累途径及转化的影响研究。在微塑料对海洋生物的毒性效应及机制研究方面，开展进行了室内毒理实验预实验，初步确定实验环境与暴露浓度背景值，建立了环境特征微塑料制备技术。在微塑料附着生物传播与微塑料海洋生态风险评估技术研究方面，确定了长江口及邻近海域，以及东南部沿海“微塑料圈”中的重点细菌属；初步构建了海洋微塑料生态风险评估方法；成功建立一套中国塑料垃圾产生量预测模型，对未来20年中国入海塑料垃圾量进行合理预测。

本年度申请专利7项（其中授权5项），发表论文35篇。

In 2018, this project went smoothly and accomplished the planned tasks.

We have built the methods of sampling collection, laboratory screening separation, digestion, treatment and identification of microplastics in water bodies, sediments and organisms; compiled the Technical Regulations for Monitoring Marine Microplastics and applied to the research in offshore and polar ocean. We have completed sampling in Bohai Sea, Yellow Sea, East China Sea, the Changjiang Estuary and Pearl River Estuary on different seasonal voyages. We have built database to identify source of microplastics; established a set of numerical models of floating and suspended microplastics, which provided powerful scientific data for the assessment of marine microplastics pollution. We have studied microplastics - organic pollutants adsorption and desorption mechanism, and impact of microplastics to organic pollutants in the marine biological accumulation and transformation. We have surveyed field mussels and fish along the coast of the East China Sea; carried out the preliminary toxicology experiment of accumulation, discharge and toxicity effect of microplastics on marine organisms. We have analyzed ecological effects of attached bio-communities of microplastics in the Changjiang Estuary as well as the southeast coast and preliminarily constructed marine microplastic ecological risk assessment method under the microplastic pollution investigation. A set of prediction model of plastic waste production in China has been established successfully.

This year, we applied for 7 patents (5 of which were authorized) and published 35 papers.

国家重点研发计划项目：长三角典型河口湿地生态恢复与产业化技术（2017YFC0506000）**The National Key R&D Program of China: Ecological Restoration and Resources Utilization of Yangtze Estuarine Wetlands (2017.07-2020.12)**

2018年度，本项目按计划完成了潮滩植被-光滩前沿和植被带内部水动力、泥沙、地貌高程和生物数据的采集，将纳入正在构建的“水动力-地貌-植被模型”；研发了多项海三棱藨草恢复技术，并构建生态修复示范区约1000亩；在分析不同植被类型水质净化功能基础上，初步形成盐沼湿地水质净化的物理-生态技术措施；分析了主要鱼类和底栖动物胁迫因子，筛选出适用于生境恢复的动物类群；完成连续型能量自维持生物炭制备装置的加工，以及生物炭基护岸材料、水质净化材料的加工试制、性能测试，实现批量生产，并在金山基地示范；获得生物矿质液产品生产许可批文，实现了米草固体饮料试生产，完成米草添加剂奶牛饲喂试验和试生产，形成互花米草草渣-菌菇-蚯蚓-生物有机肥培育工艺；对不同生态修复、利用方式的成本、效益进行了分析，并将应用于不同岸段的植被修复。本年度申请专利18项（其中授权2项，国际专利1项），出版论著1部，发表论文22篇。

In 2018, this project went smoothly and accomplished the planned tasks. We have made field observations in the vegetation zones and vegetation-tidal flat fronts, and obtained data for the hydro-sediment-morpho-vegetation model. We have developed several technics to restore *Scirpus mariquetter*, and established demonstration sites with a total area over 60 hectares. We analyzed the purification function of different saltmarsh vegetation species, and developed methods to improve the brackish water quality in the newly enclosed area. We investigated the major factors that threatens the fish and benthic species, and delineated the fauna species for rehabilitation. The project team developed the self-energy consistant biochar-preparation equipment, produced bio-char based embankment and water purification materials, and demonstrated their efficiency at the Jinshan Coast. We also obtained the production licence for *Spartina alterniflora* based bio-liquid, and got the first batch of testing beverage product. The *Spartina* based addition agent is being tested for cows, while the *Spartina* residuals – mushroom culture substrates – earthworm culture – bio-fertilizer production chain is being formed. Finally, we analyzed the cost and benefit of wetland vegetation restoration and utilization, which will be applied in the future restoration projects at different sections of the coastline.

部分新增项目 Selected New Projects

| 国家重点研发计划项目 The National Key Research and Development Program of MOST | |
|---|-----------------------|
| 应对转型中的河口三角洲(2016YFE0133700) Coping with deltas in transition (2018.01-2021.12) | 何青 HE Qing |
| 中美大河三角洲侵蚀灾害与应对策略比较研究(2017YFE0107400) Comparative study on erosion hazards and coping strategies in river deltas between China and America (2018.01-2020.12) | 张卫国 ZHANG Weiguo |
| 国家自然科学基金杰青项目 NSFC Distinguished Young Scholars | |
| 河口环境过程与生态效应(41725002) Environmental processes and ecological effects in estuaries (2018.01-2021.12) | 侯立军 HOU Lijun |
| 国家自然科学基金重点项目 NSFC Key Program | |
| 河口泥沙运动关键过程与滩槽格局转化研究(51739005) Research on key processes of flow and sediment transport and alveolar pattern transform in estuaries (2018.01-2021.12) | 何青 HE Qing |
| 国家自然科学基金联合基金重点支持项目 NSFC Collaborative Fund Supported Program | |
| 黄河三角洲地貌演变的动力机制与环境效应(U1706214) Dynamic mechanisms and environmental effects of geomorphic deformation in the Yellow River Delta (2018.01-2021.12) | 陈沈良 CHEN Shenliang |
| 国家自然科学基金面上项目 NSFC General Project | |
| 长江和钱塘江河口早-中全新世物源演化及其对地貌塑造的意义(41771226) Sediment provenance of the Yangtze and Qiantang estuaries during the Early to Mid-Holocene and its geomorphological implication (2018.01-2021.12) | 陈静 CHEN Jing |
| 高浊度河口近底高浓度泥沙形成机制与数值模拟研究(41776104) Mechanism and Numerical Study on Formation of Near-bed High-Concentrated Mud Suspension in the High-turbidity Estuary (2018.01-2021.12) | 葛建忠 GE Jianzhong |
| 基于释光技术的全新世苏北平原埋藏潮成砂体演化研究 (41771009) Holocene evolution of buried tidal sand body in North Jiangsu Plain based on luminescence dating (2018.01-2021.12) | 年小美 NIAN Xiaomei |
| 海岸水体浮游植物粒级的生物光学特性及遥感反演研究(41771378) Remote sensing inversion and bio-optical properties of phytoplankton size class in coastal waters (2018.01-2021.12) | 沈芳 SHEN Fang |
| 环境和生物样品中小粒径微塑料的分离和鉴定方法(41776123) Separation and identification methods of small graded microplastics in environmental and biological samples (2018.01-2021.12) | 施华宏 SHI Huahong |
| 近岸长江冲淡水跨陆架运动的机理及生态效应(41776101) Cross-shelf transport of nearshore Changjiang diluted water and its ecological effects (2018.01-2021.12) | 吴辉 WU Hui |

国家自然科学基金青年科学基金项目 NSFC Young Scientist Fund

| | |
|---|---------------------|
| 基于稳定同位素和脂肪酸技术的中华绒螯蟹溯河洄游期食物来源研究(41706128) Diet sources of Chinese mitten crab (<i>Eriocheir sinensis</i>) during its upstream migration indicated by the stable isotopes and fatty acid composition (2018.01-2020.12) | 崔莹 CUI Ying |
| 地下河口对海岸带地下水排放可溶性无机氮通量的调节作用研究(41706081) Evaluation of subterranean estuaries on the modulation of dissolved inorganic nitrogen fluxes from submarine groundwater discharge (2018.01-2020.12) | 江山 JIANG Shan |
| 跨陆架水交换控制下苏北沿岸海域水体存留时间的数值研究(41706011) Numerical study on water residence time under the control of cross-shelf water exchange in Subei coast (2018.01-2020.12) | 林磊 LIN Lei |
| 长江口南槽泥沙输移和地貌冲淤机制研究(41706093) Research on mechanisms of sediment transportation and geomorphological erosion/deposition in the South Passage of the Changjiang Estuary (2018.01-2020.12) | 梅雪菲 MEI Xuefei |
| 不同水环境中铅-210、铯-137和钚同位素定年的对比研究(41706089) Intercomparison between lead-210, cesium-137 and plutonium isotopes chronology in different aquatic environments (2018.01-2020.12) | 王锦龙 WANG Jinlong |
| 潮汐环境中千年尺度风暴强度的沉积记录解译(41706095) Sediment records interpretation of millennium-scale storm intensity in tidally dominated coastal environments (2018.01-2020.12) | 杨阳 YANG Yang |
| 长江口外低氧现象的成因机制研究(41706015) Mechanisms controlling hypoxia formation and sustain off the Changjiang estuary (2018.01-2020.12) | 张文霞 ZHANG Wenxia |
| 海南岛南部海岸风暴巨砾沉积揭示的风暴强度(41706096) Reconstructing storm intensities responsible for coastal boulder deposits from southern coast of Hainan Island (2018.01-2020.12) | 周亮 ZHOU Liang |

国家自然科学基金海外及港澳学者合作研究基金 NSFC Overseas Chinese, Hong Kong and Macao Young Scientists Joint Research Fund

| | |
|---|--------------------|
| 盐沼湿地恢复过程中的蓝碳效应及其调控机制研究(31728003) Coastal blue carbon, the control, and the underlying mechanism during restoration of salt marsh (2018.01-2019.12) | 唐剑武 TANG Jianwu |
|---|--------------------|

国家社科基金项目 (National Social Science Foundation)

| | |
|---|-------------------|
| 气候变化与苏沪海岸传统适应研究(18BZS156) Study on climate change and traditional adaptation of suhu coast (2018.07-2022.06) | 鲍俊林 BAO Junlin |
|---|-------------------|

省部级项目 Project Funded by Provincial and Ministerial Commission

| | |
|--|---------------------|
| 多瑙河三角洲近期环境变化及其对流域人类活动的响应(18230743100) Recent environmental changes in the Danube delta and their responses to human activities in the basin (2018.10-2020.09) | 张卫国 ZHANG Weiguo |
| 季节性低氧对长江口外关键功能菌群的影响(18ZR1410600) Effects of seasonal hypoxia on key functional flora outside the Yangtze estuary (2018.06-2021.05) | 叶祁 YE Qi |
| 崇明东滩生态修复评估与调控技术研究(18DZ1204802) Research on ecological restoration assessment and regulation technology of Chongming Dongtan Wetland (2018.07-2020.06) | SHEN Jian |

| | |
|--|---------------------|
| 长江口微塑料与典型有机污染物的复合污染研究(18PJ1403400) Study on compound pollution of microplastics and typical organic pollutants in changjiang estuary (2018.07-2020.06) | 陈启晴 CHEN Qiqing |
| 基于目标表面反射特性的LiDAR激光强度数据改正(18YF1406800) LiDAR laser intensity data correction based on target surface reflection (2018.05-2020.04) | 谭凯 TAN Kai |
| 介形虫——近海地区污染新指示(2018M630415) Ostracoda - new indication of pollution in offshore areas (2018.06-2020.12) | 晏达达 YAN Dada |
| 基于硒稳定同位素的长江口硒在悬浮泥沙—水分配的探讨(2018M632062) Discussion on the distribution of selenium in suspended sediment and water in changjiang estuary based on stable selenium isotope (2018.06-2020.12) | 常燕 CHANG Yan |
| 拉让河口无机氮时空分布及其生物地球化学调控机制研究(2018M630416) Temporal and spatial distribution of inorganic nitrogen and its biogeochemical regulation mechanism in the lajan estuary (2018.06-2020.12) | 江山 JIANG Shan |
| 海水中Bi-210的地球化学行为及其颗粒物输运示踪研究(2018T110373) Study on geochemical behavior of bi-210 in seawater and trace transport of particulate matter (2018.06-2019.12) | 王锦龙 WANG Jinlong |
| 长江口北支河势的地貌-水文-能耗协同性与稳定性研究(2018M630414) Study on the coordination and stability of geomorphology, hydrology and energy consumption in the north branch of the changjiang estuary (2018.06-2020.12) | 张敏 ZHANG Min |

获批重要项目 Selected Approved Projects

| | |
|---|-----------------------|
| 中尺度过程对海洋上层水体溶解有机物迁移和转化的影响(国家自然科学基金面上项目) (41876074) Impact of mesoscale process on the transport and transform of marine dissolved organic matter in the upper layer (NSFC General Project)(2019.01-2022.12) | 吴莹 WU Ying |
| 人类活动影响下的长江水下三角洲地貌动力系统状态转换(国家自然科学基金面上项目) (41876092) Regime shift of the Changjiang Subaqueous Delta morphodynamic system under the anthropogenic influence (NSFC General Project) (2019.01-2022.12) | 贾建军 JIA Jianjun |
| 厚壁硅藻具槽帕拉藻在黄海增殖成因及对生物硅循环的影响(国家自然科学基金面上项目) (41876127) The cause of heavily silicified Paralia sulcata increase and its impact on the BSi cycle in the Yellow Sea (NSFC General Project) (2019.01-2022.12) | 刘东艳 LIU Dongyan |
| 周期性淹水下红树根际微生物的多样性及其对铁膜的形成的作用(国家自然科学基金面上项目) (41877413) The diversity of rhizosphere microbes of mangrove and its effect on the iron plaque formation under periodic flooding conditions (NSFC General Project) (2019.01-2022.12) | 闫中正 YAN Zhongzheng |
| 河口近口段地貌的减沙失衡效应及再平衡研究(国家自然科学基金面上项目) (41876091) Tidal river morphodynamic equilibrium restoration and implications on sediment flux to the sea (NSFC General Project) (2019.01-2022.12) | 郭磊城 GUO Leicheng |

| | |
|--|--------------------|
| 海平面上升对盐沼湿地碳库要素稳定性与固碳效率的影响及预测(国家自然科学基金面上项目) (41871088) Influence mechanism and effect prediction of sea level rise on the constancy of key carbon pools and the consequent carbon sequestration in the salt marshes (NSFC General Project) (2019.01-2022.12) | 葛振鸣 GE Zhenming |
| 溶解态铅的稳定同位素在海洋中的剖面特点(国家自然科学基金面上项目) (41876071) Profiles of Stable Isotopes for Dissolved Lead in the Ocean (NSFC General Project) (2019.01-2022.12) | 张经 ZHANG Jing |
| 长江口盐沼湿地生态系统稳态转换过程与机制研究(国家自然科学基金面上项目) (41876093) Study on the process and mechanisms of the regime shifts in saltmarsh wetland ecosystem at the Yangtze esuary (NSFC General Project) (2019.01-2022.12) | 袁琳 YUAN Lin |
| 滨海盐沼植被日光诱导叶绿素荧光与总初级生产力的关联机制(国家自然科学基金青年项目) (41801253) Mechanistic up-scaling from solar-induced chlorophyll fluorescence to gross primary productivity of coastal salt marshes (NSFC Young Scientist Fund) (2019.01-2021.12) | 黄颖 HUANG Ying |
| 热带西太平洋溶解态硒同位素组成及其生物地球化学示踪初探(国家自然科学基金青年项目) (41806096) Selenium stable isotopes in the Western Tropical Pacific: Tracer of selenium biogeochemical cycles (NSFC Young Scientist Fund) (2019.01-2021.12) | 常燕 CHANG Yan |
| 环境条件下微塑料对多氯联苯在斑马鱼体内富集的影响(国家自然科学基金青年项目) (21806038) The Influence of Microplastics on Bioaccumulation of Polychlorinated Biphenyls in Zebrafish under Environmental Conditions (NSFC Young Scientist Fund) (2019.01-2021.12) | 陈启晴 CHEN Qiqing |
| 长三角河口海岸沉积物介形虫变化指示的环境污染研究(国家自然科学基金青年项目) (41806105) Study on Environment Pollution indicated by Ostracod Assemblage Changes in Sediments at the Changjiang River Delta Coast (NSFC Young Scientist Fund) (2019.01-2021.12) | 晏达达 YAN Dada |
| 长江口崇明东滩响应风暴作用的沉积动力过程(国家自然科学基金青年项目) (41806106) Sediment dynamic response of the Eastern Chongming Shoal, Changjiang Estuary, to storms (NSFC Young Scientist Fund) (2019.01-2021.12) | 魏稳 WEI Wen |

科技部实验室专项基金 MOST Special Fund

2018年，科技部实验室专项共资助团队项目7项，人才队伍项目10项。

Laboratory special fund, supported by the Ministry of Science and Technology (MOST) of China, granted to 17 projects including task team projects and talent funds.

专项基金资助一览表

List of Receipients of Special Fund

| 项目名称 Project | 负责人 Investigator |
|---|-----------------------|
| 长江未来五十年 Next 50 Years of the Yangtze River | 陈中原 CHEN Zhongyuan |
| 综合模型 Community Modelling | 朱建荣 ZHU Jianrong |
| 近海动力与环境 Coastal Ocean Dynamics Environment | 吴辉 WU Hui |
| 海岸与陆架耦合的生态动力学过程模拟 Marginal Seas (MARSEAS) working group | Richard Bellerby |
| 河口海岸初级生产和食物网 Primary Production and Food Web of Coastal Waters | 刘东艳 LIU Dongyan |
| 观测体系建设 Development of Observation System | 张卫国 ZHANG Weiguo |
| 科普工作 Popularization of Science | 童春富 TONG Chunfu |
| 环境特征微塑料对海洋生物的生态毒性效应和机制研究 The ecotoxicological effects of environmental microplastics on marine organisms and mechanism research | 陈启晴 CHEN Qiqing |
| 海岸过程比较研究 Study on the comparison of coastal processes | 晏达达 YAN Dada |
| 常态及极端事件下的潮滩沉积地貌过程 Morpho-sedimentary dynamics of mudflats under normal conditions and extreme events | 魏稳 WEI Wen |
| 浮游动物对微塑料颗粒的选择性摄食和行为研究 Selective feeding and behaviors of zooplankton fed on microplastic particles | 徐佳奕 XU Jiayi |
| 东海近岸海域的黑潮水入侵变异对营养盐和浮游植物的影响研究 The influences of the kuroshio intrusion onto the coastal water of the East China Sea on nutrient and phytoplankton | 梅衍俊 MEI Yanjun |
| 南海砗磲反映局地气候环境演化及气候极端事件 Records of Tridacna in South China Sea: climate change and extreme climate events | 徐凡 XU Fan |
| 声学方法反演悬沙浓度关键技术研究 Study on the key technique of acoustic inversion of suspended sediment concentration | 张文祥 ZHANG Wenxiang |
| 宽量程悬沙浓度光学现场测量技术探究 Study on optical field measurement technology of suspended sediment concentration with wide range | 李为华 LI Weihua |

科研进展 Research Programs

2018年度，河口海岸学国家重点实验室在科技部、国家自然科学基金委员会和上海市科委等国家、省部级各类项目和国际合作项目及应用研究项目的支持下，在实验室的三大研究方向上围绕国家重大需求、聚焦前沿科学问题，持续地展开了科学研究，取得以下成果进展。

In 2018, supported by Ministry of Science and Technology (MOST), National Natural Fund Committee (NNFC), Shanghai Science and Technology Committee and international cooperation projects and application research projects, the State Key Laboratory of Estuarine and Coastal Research (SKLEC) focused on vital demand and frontier science, carried out scientific research and made important progress.

河口演变规律与河口沉积动力学 Estuarine Evolution and Sediment Dynamics

实验室人员采用现场调查、数值模拟和海图及卫星遥感分析等多种手段，研究了河口滩槽动力过程，入口水沙通量，以及在自然因素和人类活动双重影响下的演变机理，取得了系列的成果。采用高分辨率多种仪器综合集成的近底三脚架系统观测了长江口最大浑浊带核心北槽区域的近底水沙动力，确定在显著垂向层化背景下河口高浓度泥沙的形成机制；利用数值模型模拟了长江口北槽的横向流，利用动力平衡分析探索了横向流对河口环流的驱动作用，发现从潮平均的时间尺度上看，横向对流加速使更多的水体从深槽进入河口，从浅滩向外海输运，使得深槽的向陆余流增加；基于在Scheldt河口Kapellebank潮滩持续约1个月的定点泥沙絮凝过程观测，研究了风暴与常态天气期间，悬浮泥沙的絮凝特性，随水动力的变化过程以及对风暴侵蚀后潮滩淤积恢复的影响；提出了数值模型超浅水水域的底摩擦参数化方案，显著改进了北支盐水倒灌的数值模拟精度；利用1958年来的海图地形资料系统分析了近70年来的河口大范围地貌变化特征，指出长江河口三角洲地貌演变对流域减沙的响应，为进一步理解大型河口地貌演化规律和对减沙的响应特征提供了重要基础；利用1880-2013年的海图数值化地形及相关水沙资料，揭示出长江分汉型河优型河口北港动力地貌主要经历河槽平顺、沙洲并陆及落潮槽为主向河槽弯曲、沙洲零散发育与涨落潮复式槽共存的变化过程；基于1996-2016年黄河入海水沙数据和现行河口区实测水下地形资料，研究了近20年黄河入海水沙情势，以及现行黄河水下三角洲地貌演变过程；利用水文监测资料、海图地形和卫星遥感图像等，系统分析了以三峡大坝为代表的人类重大活动对长江水沙通量、江一湖（如鄱阳湖和洞庭湖）水沙交换、河道与沙洲地形地貌等状态变化，探讨了在自然规律和人类活动双重影响下的河湖系统演变规律。

The Laboratory has conducted multi-disciplinary methods, including field cruise, numerical simulation and remote sensing, to study the morphodynamics of river channels and shoals, discharge of water and sediment into the estuary, and their evolution mechanism under natural and anthropogenic influences. The tripod system integrated with multiple high-resolution instruments has been deployed in bottom layer of the core region of the turbidity maximum in the Changjiang Estuary. With the observational hydrodynamics and sediment dynamics, the effect of strong vertical stratification has been revealed in the formation of high-concentrated benthic mud suspension. The numerical model has been applied to study the lateral current in the North Passage of the Changjiang Estuary. With the momentum balance analysis, it is found that lateral current has a driving effect on estuarine circulation. Within the tide-averaged timescale, the lateral advection acceleration drives more water from deep channel into the estuary, and be transported from shallow shoal to offshore region, leading increasing onshore residual current. Based on one-month continuous mooring flocculation observation in the Kappellebank in Scheldt estuary, the flocculation process has been examined under different dynamic conditions, including calm and storm conditions, indicating that was changing according to the hydrodynamics. In addition, the mudflat's restoration was also been studied with this observation. The parameterization of bottom friction in very shallow water condition has been proposed, and the results shown this method could significantly improve the model prediction of saltwater intrusion in the North Branch of the Changjiang Estuary. Based on the analysis of bathymetric data between 1880 and 2013 and related hydrological data, we developed the first study on the centennial bathymetric variations of the North Channel. It is found that the bathymetric changes of NC include two main modes, the first is observable deposition in the mouth bar and its outer side area (lower reach); the second mode demonstrates channel deepening along the inner side of the mouth bar (upper reach) during 1970–2013. Based on the discharge of water and sediment of Huang River from 1996-2016 and observed bathymetry around the Huanghe Estuary, the variation of sediment and water flux

have been revealed, as well as the morphological evolution of Huanghe submarine delta. The hydrological data, marine bathymetry and remote sensing has been jointly merged to systemically analyze the major anthropogenic activities' impacts on sediment and water discharge of Changjiang River, and their exchange between Changjiang River and its connected major lakes, such as Poyang Lake and Dongting Lake, as well as the morphological variation in river channels and sandbanks. Particularly, the evolution mechanism of river-lake system under natural and anthropogenic influence has been discussed.

海岸动力地貌与动力沉积过程 Coastal Morphodynamics and Sedimentary Process

实验室人员研究了不同时间尺度下河流入海物质在三角洲及邻近水域的搬运、堆积过程，探讨了陆上三角洲、水下三角洲和远端泥质区的泥沙收支和地形地貌演变规律，取得了系列的成果。利用庞大的钻孔数据库研究了全新世以来在海平面上升和泥沙供给变化双重因素作用下的长江三角洲建设和破坏过程，并在21世纪海平面加速上升和流域泥沙供给减少背景下，预测海平面与泥沙之间的不平衡关系将导致长江口面临从建设型向破坏型的转变；通过在苏北水域布设坐底三角架系统进行观测，揭示了典型冬季偏北季风下长江口和苏北水域的水体物质输送方向为逆风北向，并从物理海洋学的基本原理出发解释了其形成机理；研究发现河口深水航道、土地围垦等重大工程对河流入海物质运输有着类似于“蝴蝶效应”的影响，使得东北向扩展减弱、南向扩展加强，可对长江口外的低氧和赤潮等分布格局产生影响；利用数值模拟和资料分析，揭示了潮汐混合对长江冲淡水沿浙闽海岸扩展的动力机制，提出了潮汐海域浮力沿岸流的新机制；从宏观和微观两个尺度量化分析了长江三角洲体系（包括陆上三角洲、水下三角洲及其远端泥即“浙闽沿岸泥”）的泥沙收支及滞留时间，回答了长江陆上三角洲的淤进、水下三角洲的稳定及浙闽沿岸潮滩生长发育等地貌动力学的科学问题；根据潮位标定模型和正交断面方法，建立了一个新的岸线指标方法，实现了高时间频率连续的岸线动态监测，加深了对快速变化中的黄河三角洲海岸的精细演变过程和动力机制的理解。

The Laboratory studied the transport and accumulation of river-to-sea sediments in Delta and adjacent waters at different time scales, and discussed the sediment budget and topographic evolution of deltas, underwater deltas and distal muddy areas, and gained a series of results. The process of construction and destruction of the Yangtze River Delta under the dual effects of sea level rise and sediment supply change since Holocene were studied by using a large core database. Under the background of accelerated sea level rise and sediment supply decrease in the basin in the 21st century, it is predicted that the unbalanced relationship between sea level and sediment will lead to the transformation of the Yangtze River Estuary from construction to destruction. Based on the observation of the triangle-frame system in the northern Jiangsu waters, it is revealed that the direction of sediment transport in the Yangtze Estuary and the northern Jiangsu waters is northward in the north-northerly monsoon in winter, and its formation mechanism is explained from the basic principles of physical oceanography. It is found that major projects such as deepwater channel and land reclamation in estuaries have a similar "butterfly effect" on sediment transport into the sea, which weakens the north-eastern expansion and strengthens the southern expansion, and can affect the distribution pattern of hypoxia and red tide outside the Yangtze Estuary. Based on numerical simulation and data analysis, the dynamic mechanism of tidal mixing on the expansion of Yangtze River diluted fresh water along Zhejiang and Fujian coasts is revealed, and a new mechanism of buoyant coastal current in tidal coastal ocean is proposed. The sediment budget and retention time of the Yangtze River Delta system (including land delta, underwater delta and its far-end mud, i.e. "coastal mud of Zhejiang and Fujian") were quantitatively analyzed at macro and micro scales. The scientific geomorphological dynamics of the siltation of the Yangtze River land delta, the stability of the underwater delta and the growth and development of tidal flats along the coast of Zhejiang and Fujian are answered. According to the tidal level calibration model and the orthogonal section method, a new coastline index method is established, which realizes the continuous coastline dynamic monitoring with high time and frequency, and deepens the understanding of the evolution process and dynamic mechanism of the Yellow River Delta coast in rapid change.

河口海岸生态与环境 Estuarine and Coastal Ecology and Environment

实验室人员广泛研究了河口海岸地区的各种生态环境过程。在湿地生态方面发现盐度和淹水胁迫一定程度上会促进互花米草的散布扩张，本地种在高盐环境下倾向于分配更多生物量至地下根系，这对维持盐沼滩面海拔高程更为有利，以应对持续上升的海平面；研究了湿地植物如互花米草等吸附固化潮滩湿地土壤中重金属的过程、机理，以及在不同淹水时间和背

景重金属浓度下的固化能力；研究了芦苇这一我国海典型本地种和互花米草这一外来入侵植物对潮汐和盐度等水文因子的适应性，发现未来海平面上升引起的长期淹水和盐水负荷可引发中国海岸线本土植物的退化和外来种的进一步入侵；通过测定两种水生植物（沉水植物 *Egeria densa* 和挺水植物 *Juncus effus*）在三种 AgNPs 释放情景下的生理响应和酶促反应，研究了 AgNPs 对水生植物的毒性影响；研究长江口湿地微型底栖动物功能多样性对环境因子自然梯度的响应，发现盐度、沉积物粒径和水动力条件都会对其群落的物种和功能特征组成产生影响；研究揭示了区域内滨海湿地生态系统高强度人类活动影响下的演化过程，区域土地利用变化的转化方式以及湿地生态系统的退化路径。

The researchers of the laboratory have extensively investigated various ecological and environmental processes in the estuarine and coastal areas. They found that the salinity and flooding stresses would to a certain extent lead to further invasion of exotic *Spartina alterniflora*. Under the increased salinity and inundation, the native plants (e.g. *Phragmites* and *Scirpus* species) allocated more biomass to the root system belowground, which is favorable for maintaining the elevation of salt marsh and coping with sea level rise. The mechanisms of adsorption and solidification of heavy metals in wetland soil colonized by marsh vegetation (such as *S. alterniflora*) were studied. The researchers also assessed the ability of wetland plants to solidify heavy metals with varying flooding times and heavy metal concentrations. The ecophysiological characteristics of native and exotic marsh vegetation grown under waterlogging and salinity were investigated to explore their adaptation potential to sea level rise. The results indicated a degradation of native species and further colonization of *S. alterniflora* under prolonged flooding and saltwater intrusion from sea level rise on the coastline of China. The toxicological responses and enzymatic reactions of a submerged plant (*Egeria densa*) and an emergent aquatic plant (*Juncus effuse*) to three types of AgNPs treatments were studied. The studies on responses of microbenthos to the natural gradient of environmental factors showed that salinity, sediment particle size and hydrodynamic conditions synergistically affected the species abundance and functional biodiversity of the benthos community. The researchers revealed the evolution processes of coastal wetland ecosystem under the influence of high-intensity human activities, the transformation mode of regional land use change and the degradation path of wetland ecosystem.

在河口近海生物地球化学方面，研究了1997年至2010年长江水系悬浮沉积物的有机地球化学特征变化，揭示了大型河流系统中颗粒有机物(pom)年龄的时空分布特征，填补了全球碳循环理解中的一个重要知识缺口；揭示了东中国海溶解铅的分布，并探讨了其从边缘海到开阔大洋的跨陆架运动过程；定量评估了通过地下水进入红树林的碳通量，发现它可相当于全球河流输入海洋碳通量的29-48%，以此阐明了海底地下水排放的碳是近岸红树林湿地碳收支的重要组成部分；通过对2013年10月份采集的东海海水样品中碘同位素的分析，揭示了东海碘同位素的来源以及洋流运输，结果表明长江冲淡水在10月份可以输送到江苏沿岸；利用放射性同位素 ^7Be 、 ^{234}Th 、 ^{210}Pb 示踪和磁学参数联合分析，量化了长江入海泥沙跨陆架搬运的过程，并探讨了其动力机制；揭示了氨氧化群落动态对河口盐度梯度的响应机制，探究了长江口典型盐度断面硝化细菌(AOB)与古菌(AOA)的多样性、丰度、菌群结构以及硝化速率的变化特征，为进一步认识河口氨氧化过程的微生物驱动机制提供了新的见解；揭示了沉积物固氮过程在调控氮收支平衡的重要性，提升了对河口近海氮循环过程的认识；研究估算显示长江口沉积物年固氮量约占河流无机氮输入通量的9.3%，反映底栖沉积物固氮是一个重要的活性氮来源，可进一步加剧河口海岸生态系统的氮污染；通过富集培养证明了长江口潮滩沉积物中全程氨氧化微生物的存在，并分析了河口地区全程氨氧化微生物菌群的多样性、丰度及潜在活性。

With respect to estuarine and coastal biogeochemistry, we studied the organic geochemistry nature of the suspended particles in the Changjiang River system between 1997 and 2010. We revealed the particulate organic matter age distribution pattern within a large river system, filling an important blank in global carbon cycle. We revealed the dissolved lead distribution pattern in the East China Sea, discussing its cross-shelf transportation process. We quantitatively assessed the carbon flux via subground discharge into mangrove system, suggesting that it accounts for 29-48% of the total riverine carbon export to the sea. By analyzing the iodine isotope in the East China Sea seawater samples that collected in October 2013, we revealed the source of iodine and the ocean current transportation feature in the key marginal sea, finding that the Changjiang diluted water can be transported to Jiangsu coast in October. By using the radioisotopes of ^7Be , ^{234}Th and ^{210}Pb , together with magnetism parameters, we quantified the cross-shelf transportation process and mechanism for Changjiang River suspended sediment. We revealed the dynamics of microbial nitrification community responding to estuarine salinity gradient, assessed the biodiversity, abundance, community structure and nitrifying rate of nitrifier bacteria (AOB) and archaea (AOA) in a typical section in the Changjiang Estuary, which is novel in microbial-driven estuarine nitrification process. We proposed the importance of sedimentary nitrogen fixation process in the nitrogen cycle, which improved our

understanding of nitrogen cycling in estuarine and coastal regions. We found that the Changjiang sedimentary nitrogen fixation can account for 9.3% of the annual riverine inorganic nitrogen flux, which indicates that the sedimentary nitrogen fixation can be an important labile nitrogen source, and this further enhances the nitrogen contamination in estuaries. By carrying out culture experiment, we provided the evidence of ammonification microbial in Changjiang estuarine tidal flat, and we analyzed their biodiversity, abundance and potential activity.

在近海生态环境方面，采用2003-2015年卫星海表面温度梯度资料，并通过对126处表层沉积物中共计345种进行双向指示种分析，揭示锋面这一不同水团之间窄过渡带对海洋浮游植物群落的划分起到至关重要的作用；根据黄海2个富营养化海湾的古生态学和现代海水数据，揭示冬季氮富集后，重度硅化硅藻的出现显著增加；结合现场观测和数值模拟，揭示了台风天气下长江冲淡水分布的变化和恢复过程，以及在此过程中产生的初级生产力增加现象；利用数值模型揭示了潮汐和快速变化的风场下长江口外低氧区域的短时间尺度变化规律；提出了一个卫星遥感浮游植物粒径算法，利用遥感数据了反演浑浊的、受大河影响的中国东大陆架边缘海浮游植物粒径分布。

With respect to coastal ecology and environment, we used the satellite data of sea surface temperature gradient, together with analyzing the 345 tracing species in the surface sediment, to reveal the importance of estuarine and coastal front in dividing the marine phytoplankton community into different groups. We analyzed the paleo ecology in two eutrophic bays and its contemporary marine water data, and we found a dramatic increase of heavily silicified diatoms after the nitrogen-accumulation in winter. Combing the in situ observation and numerical modelling, we revealed the distribution and recovery pattern of Changjiang diluted water in typhoon events, and the corresponding primary production increase. With the help of numerical modelling, we revealed the hypoxia zone dynamics in short time scale under the influence of tide and dynamic wind field. We proposed a novel algorithm for remote sensing phytoplankton grain size, and accordingly we derived the phytoplankton grain size distribution in the turbid east China marginal sea area, which is under large river impact.

在海洋微塑料研究方面，发现了检测微塑料密度这一重要指标参数的最佳制备密度梯度溶液，开发了简单有效的测定方法；调查了微塑料在城市河道中的分布规律，对沉积环境中微塑料的生态风险进行了评估，提出了环境风险评估的基本框架；系列研究调查揭示了微塑料通过摄食、沾染等方式进入鱼、蝌蚪、贻贝和牡蛎等生物体的方式，并分析了类二 英效应等化学毒性。

In the research of marine microplastics, the optimal preparation density gradient solution for detecting the microplastic density was found, for which a simple and effective measurement method was developed. The occurrence and distribution of microplastics in urban rivers were investigated, and the ecological risks of microplastics were evaluated and the basic framework of environmental risk assessment was proposed. A series of researches revealed the way in which microplastics entered by organisms (such as fish, tadpoles, mussels and oysters) through ingestion and adherence, and the toxicity of the associated dioxin-like chemicals on microplastics was also analyzed.

河口演变规律与河口沉积动力学 *Estuarine Evolution and Sediment Dynamics*

Investigation of flocculation dynamics under changing hydrodynamic forcing on an intertidal mudflat

Guo C, He Q, Van Prooijen B, et al. *Marine Geology*, 2018, 395:120-132.

In situ floc size and turbulent shear stress were measured together with suspended sediment concentration to investigate the floc properties under changing hydrodynamic forcing over the intertidal mudflat. A tripod system was established in the field for a period of approximately one month, including ~6 days of stormy conditions in the middle of the investigation period. Mean floc size exhibited strong temporal variations within a tidal cycle, and inverse relationship was found between mean floc size and shear stress. Suspended sediment concentration (SSC) can modulate the flocculation dynamics when shear stress decreases down to enhancing flocculation. Asymmetrical behaviors of floc sizes between flood and ebb phases were identified, with overall larger floc sizes in flood than in ebb tide under the same shear stresses. Floc structure showed different properties under calm and stormy conditions, and the variable fractal dimension and variable primary particle size were more convincing in simulating the variation of floc effective density with mean floc size during the storm period, which was inferred to be related to the resuspension of bed sediment as well as organic matter. A total of 110 mm bed erosion was measured during the storm, and erosion events occurred only around low water, due to the high current-wave combined bed shear stress and off-shore current. After the storm, ~40% of the erosion recovered within one week, and the fast settling of large flocs around high water plays significant role in the deposition process, leading to ~60% of the recovery.

潮滩是陆地与河口之间的过渡区以及陆地的保护屏障，并且在区域生态系统发展方面具有重要功能。已有研究表明，在潮周期尺度内潮滩表层沉积物主要以絮团的形式存在，因此开展潮滩泥沙絮凝沉降动力过程研究，对潮滩悬沙沉降、输运及潮滩发育的影响研究均有重要的科学和应用意义。基于在Schendt河口Kapellebank潮滩持续约1个月的定点水沙运动，特别是泥沙絮凝过程的现场观测结果，研究了风暴与常态天气期间，悬浮泥沙的絮凝特性，随水动力的变化过程以及对风暴侵蚀后潮滩淤积恢复的影响。研究发现：（1）泥沙絮凝过程受到剪切动力主控。无论是常态天气还是风暴天气，絮团粒径大小均在潮周期内显著变化，且絮团粒径随着床面剪切应力的增大而减小。在涨潮和落潮过程中，絮团粒径的变化呈现出不对称的特性，在相同剪切作用下，涨潮期间絮团粒径普遍比落潮期间大；（2）絮团有效密度变化过程及控制机制。絮团有效密度整体上随着粒径的增大呈减小趋势，在风暴期间，絮团粒径超过100 μm时，絮团有效密度随着粒径的进一步增大转变为呈增大趋势，主要是由于风暴期间床面泥沙再悬浮导致形成絮团的分散态泥沙颗粒粒径组成发生改变，使用变分散颗粒粒径和变絮团分形维数的改进方法可以较好地模拟整个变化过程；（3）风暴期泥沙絮凝沉降及潮滩快速恢复机制。在风暴导致潮滩侵蚀后，潮滩床面高程可以在一周内快速恢复约40%，其中65%的淤积发生在高水位时段，缘于絮团粒径和沉降速度达到最大，同时悬沙浓度较高，综合导致产生较大的悬沙沉降通量，促进潮滩的淤积。

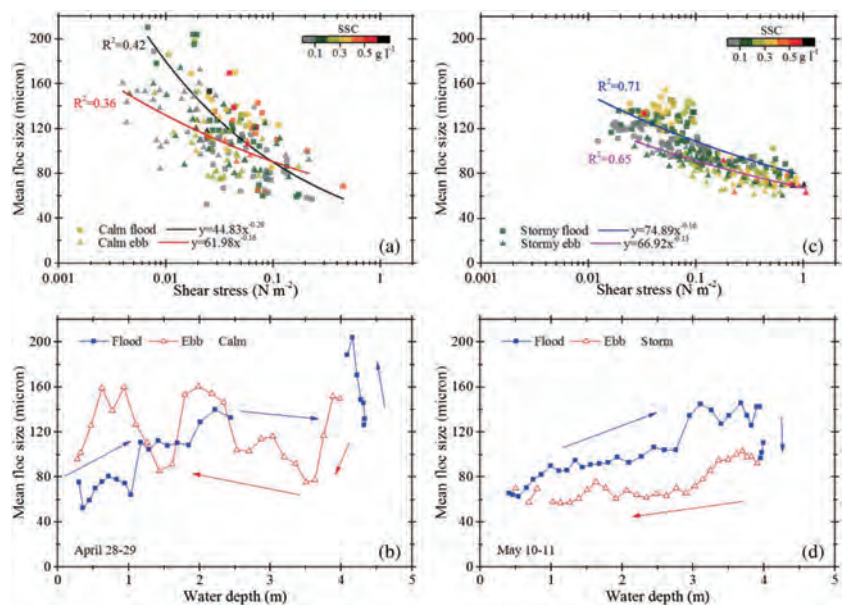


Fig. 8. (a)(c) Variation of mean floc size and shear stress under calm flood/ebb and stormy flood/ebb conditions, respectively; (b)(d) Typical variation of mean floc size with water depth in a tidal cycle under calm and stormy conditions on April 28–29 and May 10–11, respectively. In (a) and (c), solid lines are the regression results, and colour bar indicates corresponding suspended sediment concentration SSC. In (b) and (d), blue and red symbols represent flood and ebb tide, respectively. (For interpretation of the references to colour in this figure legend, the reader is referred to the web version of this article.)

Modeling lateral circulation and its influence on the along-channel flow in a branched estuary

Zhu L, He Q, Shen J. *Ocean Dynamics*, 2018, 68(2):177-191.

A numerical modeling study of the influence of the lateral flow on the estuarine exchange flow was conducted in the north passage of the Changjiang estuary. The lateral flows show substantial variabilities within a flood-ebb tidal cycle. The strong lateral flow occurring during flood tide is caused primarily by the unique cross-shoal flow that induces a strong northward (looking upstream) barotropic force near the surface and advects saltier water toward the northern part of the channel, resulting in a southward baroclinic force caused by the lateral density gradient. Thus, a two-layer structure of lateral flows is produced during the flood tide. The lateral flows are vigorous near the flood slack and the magnitude can exceed that of the along-channel tidal flow during that period. The strong vertical shear of the lateral flows and the salinity gradient in lateral direction generate lateral tidal straining, which are out of phase with the along-channel tidal straining. Consequently, stratification is enhanced at the early stage of the ebb tide. In contrast, strong along-channel straining is apparent during the late ebb tide. The vertical mixing disrupts the vertical density gradient, thus suppressing stratification. The impact of lateral straining on stratification during spring tide is more pronounced than that of along-channel straining during late flood and early ebb tides. The momentum balance along the estuary suggests that lateral flow can augment the residual exchange flow. The advection of lateral flows brings low-energy water from the shoal to the deep channel during the flood tide, whereas the energetic water is moved to the shoal via lateral advection during the ebb tide. The impact of lateral flow on estuarine circulation of this multiple-channel estuary is different from single-channel estuary. A model simulation by blocking the cross-shoal flow shows that the magnitudes of lateral flows and tidal straining are reduced. Moreover, the reduced lateral tidal straining results in a decrease in vertical stratification from the late flood to early ebb tides during the spring tide. By contrast, the along-channel tidal straining becomes dominant. The model results illustrate the important dynamic linkage between lateral flows and estuarine dynamics in the Changjiang estuary.

本文研究利用数值模型模拟了长江口北槽的横向流，并利用动力平衡分析探索了横向流对河口环流的驱动作用。创新发现：1) 滩槽水体交换是长江河口横向环流产生的主要机制，涨潮时在水体表层的高流速横向流主要由越滩流形成的水位梯度引起，而在底层水体，横向盐度梯度形成的斜压力造成了向南的横向流；落潮时，越滩流消失，横向的盐度梯度减小，这使横向流流速大为减小。横向流的最大值出现在涨憩附近，其流速甚至超过了纵向的潮流流速。2) 横向流的垂向梯度与横向的盐度梯度相互作用，产生横向的潮汐应变，成为盐度分层的一个重要机制。与纵向潮流产生的应变不同，横向潮汐应变一般出现在涨潮后期，这使得水体在涨憩附近的分层最强。在大潮期间，横向潮汐应变的作用超过了纵向潮汐应变。3) 横向流产生的横向对流加速也是河口环流形成的机制之一。在涨潮时，浅滩的水体被输送至深槽，而在落潮期间，深槽的高流速水体被带到两侧浅滩。从潮平均的时间尺度上看，横向对流加速使更多的水体从深槽进入河口，从浅滩向外海输运，使得深槽的向陆余流增加。

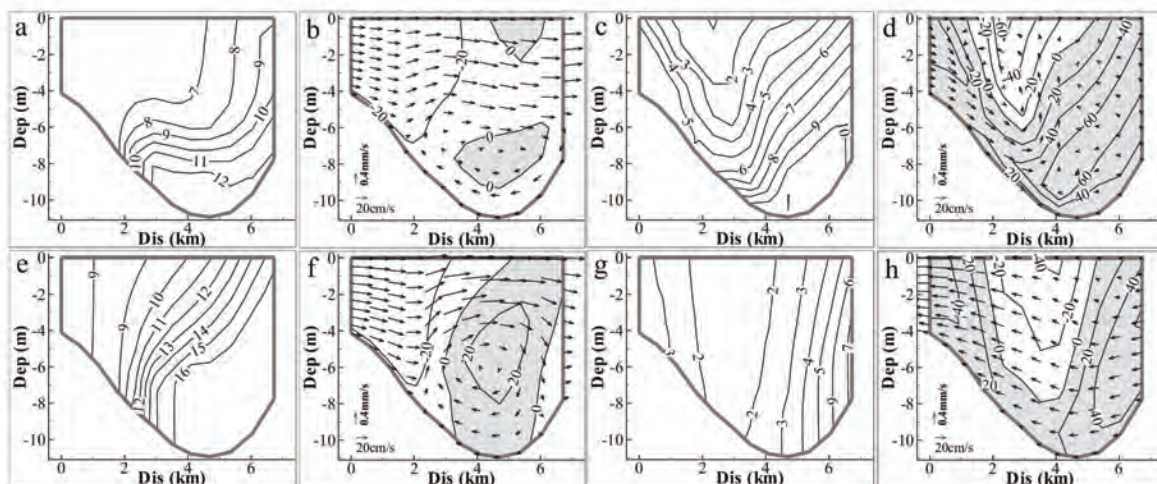


Fig. 7 The transverse structure of salinity (a, c, e, g) and tidal currents (b, d, g, h) during the flood slack (a, b, e, f) and ebb slack (c, d, g, h). The upper panels denote the neap tide, and the lower panels denote the spring tide. The along-channel flow is contoured in 20 cm/s intervals with the landward component shaded gray. Lateral flows are shown as arrows, and salinity is contoured in 1 psu

Impact of anthropogenic drivers on subaqueous topographical change in the Datong to Xuliujing reach of the Yangtze River

Zheng S, Cheng H, Shi S, et al. *Science China Earth Sciences*, 2018, 61(7):940-950.

Changes of subaqueous topography in shallow offshore water pose safety risks for embankments, navigation, and ports. This study conducted measurements of subaqueous topography between Datong and Xuliujing in the Yangtze River using a SeaBat 7125 multi-beam echo sounder, and the channel change from 1998 to 2013 was calculated using historical bathymetry data. The study revealed several important results: (1) the overall pattern of changes through the studied stretch of the river was erosion–deposition–erosion. Erosion with a volume $700 \times 10^6 \text{ m}^3$ occurred in the upper reach, deposition of about $204 \times 10^6 \text{ m}^3$ occurred in the middle reach, and erosion of about $602 \times 10^6 \text{ m}^3$ occurred in the lower reach. (2) Dunes are the most common microtopographic feature, accounting for 64.3% of the Datong to Xuliujing reach, followed by erosional topography and flat river topography, accounting for 27.6% and 6.6%, respectively. (3) Human activities have a direct impact on the development of the microtopography. For instance, the mining of sand formed holes on the surface of dunes with lengths of 20–35 m and depths of 3–5 m. We concluded that the overall trend of erosion (net erosion volume of $468 \times 10^6 \text{ m}^3$) occurred in the study area mainly because of the decreased sediment discharge following the closure of the Three Gorges Dam. However, other human activities were also impact factors of topographic change. Use of embankments and channel management reduced channel width, restricted river meandering, and exacerbated the erosion phenomenon.

近浅海水下地形演变事关堤岸、航运及港口安全，一直是地理学和工程学界研究的热点。利用多波束测深系统对长江大通至徐六泾河段水下地形进行了测量和统计分析，结合历史资料分析了该河段1998~2013年的冲淤格局。结果表明：(1) 1998年至2013年大通至徐六泾河段总体呈“冲淤-冲”特征。其中，上段冲刷 $0.70 \times 10^8 \text{ m}^3$ ；中段淤积 $2.04 \times 10^8 \text{ m}^3$ ；下段冲刷 $6.02 \times 10^8 \text{ m}^3$ 。(2) 沙波是研究河段航道中最常见的床面地形，约占整个河段的64.3%；其次为各类冲刷地形(约27.6%)；平床地形约占6.6%。(3) 人类活动可直接影响水下地形形态的自然发育，如于沙波表面形成直径20~35 m，深3~5 m的采砂坑。分析认为三峡大坝的修建导致了流域来沙量急剧下降，是研究河段整体上呈冲刷趋势(净冲刷约 $4.68 \times 10^8 \text{ m}^3$)的主要原因，而其他人类活动，如岸线利用、航道整治束窄了河道，制约了河流的横向摆动，加剧了受冲岸段的岸坡冲刷。

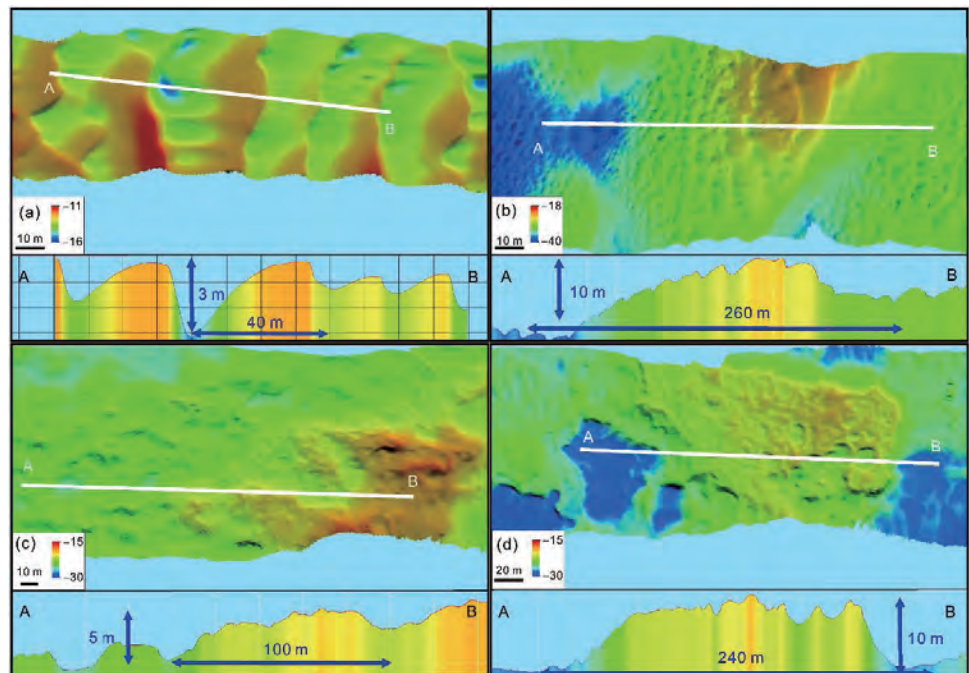


Figure 3 Maps showing the microtopography in the Yangtze River between Datong and Xuliujing (grid resolution of $0.5 \text{ m} \times 0.5 \text{ m}$). (a) Large dunes, (b) very large dunes, (c) complex topography, (d) composite topography.

Connection of the proto-Yangtze River to the East China Sea traced by sediment magnetic properties

Liu X, Chen J, Maher B A, et al. *Geomorphology*, 2018, 303:162-171.

The evolution of the Yangtze River, and specifically how and when it connected to the East China Sea, has been hotly debated with regard to possible linkages with the so-called 'Cenozoic Topographic Reversal' (tectonic tilting of continental east China in the Cenozoic) and particularly the relationship to the uplift history of the Tibetan Plateau. Resolving this key question would shed light on the development of large Asian rivers and related changes in landforms and monsoon climate during this interval. Here, we use the magnetic properties of both Plio-Quaternary sediments in the Yangtze delta and of surficial river sediments to identify a key mid-late Quaternary switch in sediment source-sink relationships. Our results reveal a fundamental shift in sediment magnetic properties at this time; the upper 145 m of sediment has magnetic mineral concentrations 5 to 10 times higher than those of the underlying late Pliocene/early Quaternary sediments. We show that the distinctive magnetic properties of the upper core sediments closely match those of surficial river sediments of the upper Yangtze basin, where the large-scale E'mei Basalt block ($2.5 \times 10^5 \text{ km}^2$) is the dominant magnetic mineral source. This switch in sediment magnetic properties occurred at around the Jaramillo event ($\sim 1.2\text{--}1.0 \text{ Ma}$), which indicates that both the westward extension of the proto-Yangtze River into the upper basin and completion of the connection to the East China Sea occurred no later than at that age.

长江水系的演化，尤其是它是何时流入东海，一直是学术界争论关心的热点问题。本文通过对长江三角洲新生代沉积物的磁性特征为切入点，并结合长江流域支流沉积物的磁性特征，综合探讨了长江上游物质到达三角洲的年限。研究发现，长江三角洲沉积物磁性特征发生根本转变约在早更新世中晚期，上部地层沉积物表现出高磁性特征，约是下部早更新世早期和上新世地层的5~10倍，这一特征和现代长江流域中上游地区玄武岩强磁性特征非常吻合。这一转型发生于贾拉米洛事件时期，约1.2~1.0Ma，意味着古长江流入东海不晚于这个时间。

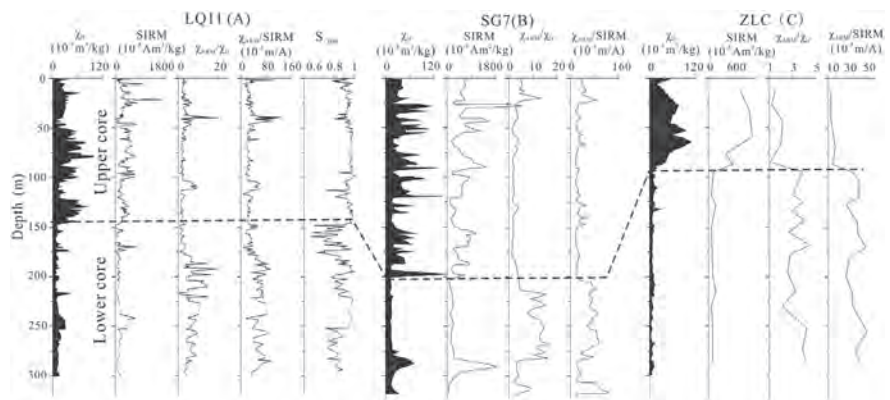


Fig. 5. Comparison of magnetic properties of sediments from cores (A) LQ11, (B) SG7 (Tao, 2007), and (C) ZLC collected from the middle Yangtze (Zhang et al., 2008), and correlation of the magnetic transition at $\sim 1.2\text{--}1.0 \text{ Ma BP}$.

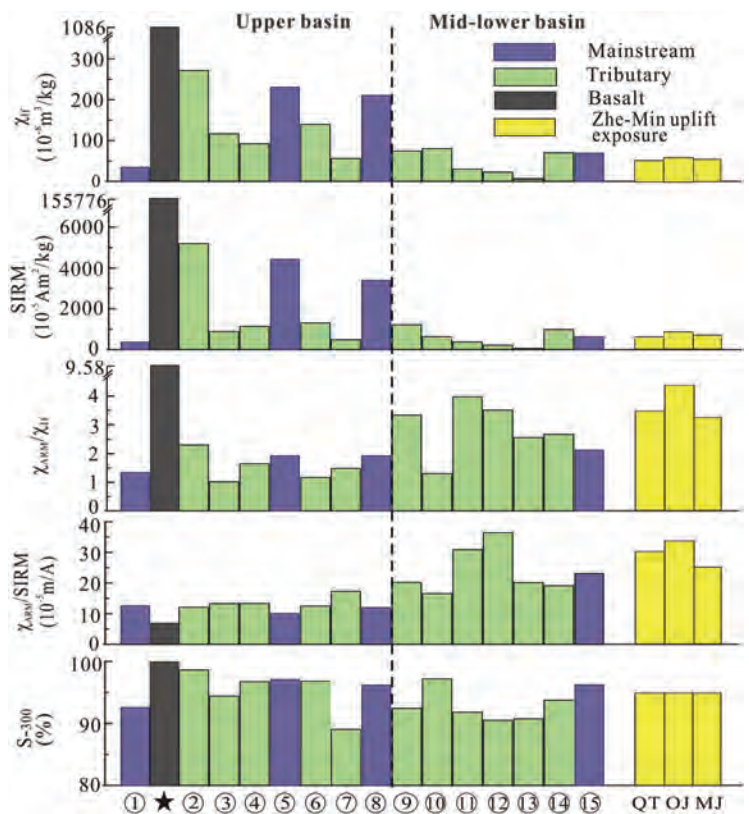


Fig. 7. Distribution of magnetic properties of surficial Yangtze sediments with comparison to the E'mei Basalt and Zhe-Min uplift (①-⑮, ★, and QT, OJ, and MJ see Fig. 1). Samples sourced from tributaries with carbonate and sedimentary rocks have much lower χ_{lf} than those in which basalt is widely distributed in the catchment.

An analysis on half century morphological changes in the Changjiang Estuary: Spatial variability under natural processes and human intervention

Zhao J, Guo L, He Q, et al. *Journal of Marine Systems*, 2018, 181:25-36.

Examination of large scale, alluvial estuarine morphology and associated time evolution is of particular importance regarding management of channel navigability, ecosystem, etc. In this work, we analyze morphological evolution and changes of the channel-shoal system in the Changjiang Estuary, a river- and tide-controlled coastal plain estuary, based on bathymetric data between 1958 and 2016. We see that its channel-shoal pattern is featured by meandering and bifurcated channels persisting over decades. In the vertical direction, hypsometry curves show that the sand bars and shoals are continuously accreted while the deep channels are eroded, leading to narrower and deeper estuarine channels. Intensive human activities in terms of reclamation, embankment, and dredging play a profound role in controlling the decadal morphological evolution by stabilizing coastlines and narrowing channels. Even though, the present Changjiang Estuary is still a pretty wide and shallow system with channel width-to-depth

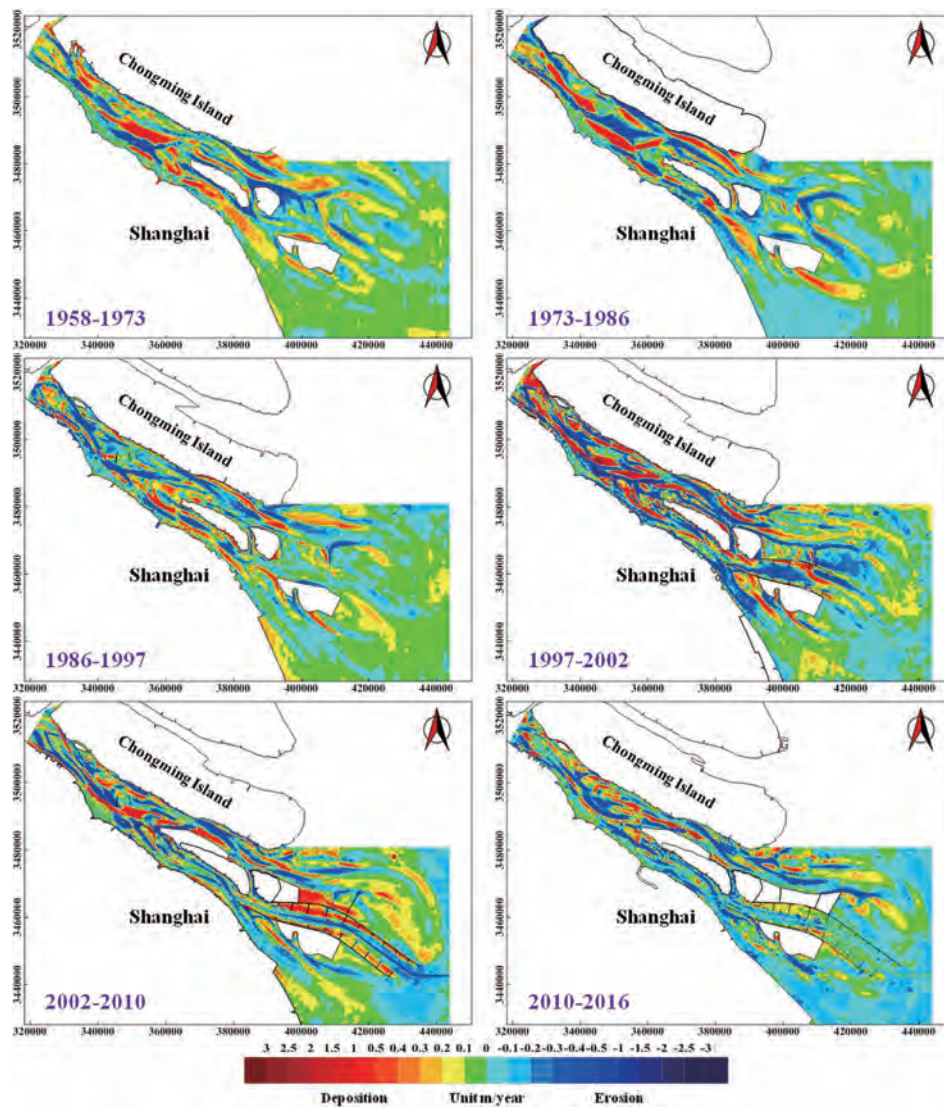


Fig. 4. Bathymetry changes of the study area during different periods (1958–1973, 1973–1986, 1986–1997, 1997–2002, 2002–2010, and 2010–2016) (unit: m/year).

ratios > 1000, much larger than usual fluvial rivers and small estuaries. In-depth analysis suggests that the Changjiang Estuary as a whole exhibited an overall deposition trend over 59 years, i.e., a net deposition volume of $8.3 \times 10^8 \text{ m}^3$. Spatially, the pan-South Branch was net eroded by $9.7 \times 10^8 \text{ m}^3$ whereas the mouth bar zone was net deposited by $18 \times 10^8 \text{ m}^3$, suggesting that the mouth bar zone is a major sediment sink. Over time there is no directional deposition or erosion trend in the interval though riverine sediment supply has decreased by 2/3 since the mid-1980s. We infer that the pan-South Branch is more fluvial-controlled therefore its morphology responds to riverine sediment load reduction fast while the mouth bar zone is more controlled by both river and tides that its morphological response lags to riverine sediment supply changes at a time scale > 10 years, which is an issue largely ignored in previous studies. We argue that the time lag effect needs particular consideration in projecting future estuarine morphological changes under a low sediment supply regime and sea-level rise. Overall, the findings in this work can have implications on management of estuarine ecosystem, navigation channel and coastal flooding in general.

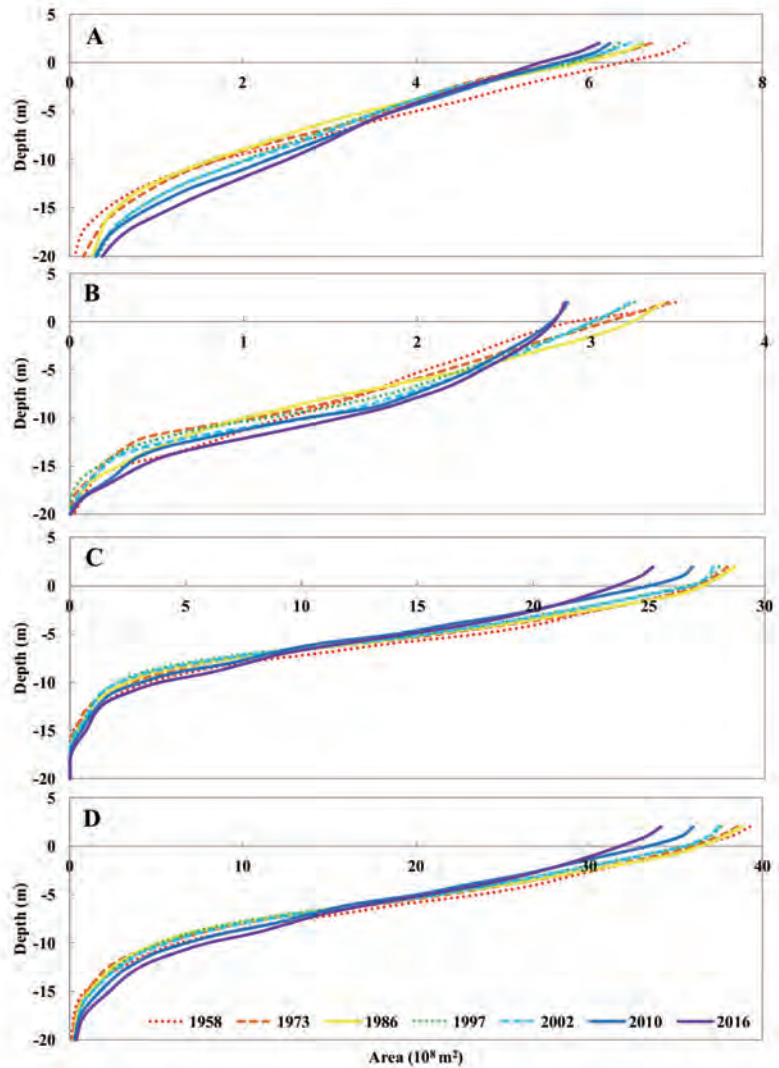


Fig. 5. Hypsometry changes of region A (A), region B (B), region C (C), and entire study area (D) from 1958 to 2016.

长江河口是一个径潮作用为主的大型冲积性三角洲型河口，其地貌演变受到陆海双重因素的影响，在河流来沙锐减的背景下，其地貌演变过程和规律受到日益广泛的关注。已有研究或者关键局部河段，或者采用的地形数据的时间跨度不长。本研究系统分析了自1958年以来的近70年的河口大范围的地貌变化特征，得到关键科学认识包括：(1) 进一步证实了特大洪水在长江河口三角洲地貌演变中的作用，认识到特大洪水的两个关键特征，即洪量大、挟沙显著不饱和是导致河口三角洲冲刷的关键；(2) 发现长江河口三角洲地貌响应的空间分异性特征，包括滩淤槽冲，河口河道向窄深趋势发展（图1）；指出河口内河道和口门拦门沙不同的响应特征，其中拦门沙区域对流域减沙具有显著更强的弹性(resilience)；(3) 首次指出长江河口三角洲地貌演变对流域来沙减少的滞后响应(time lag effect)，即河口三角洲侵蚀变化滞后于河流来沙量变化，初步估算得到滞后的时间尺度在10-30年，由此反映河口三角洲系统内部的地貌再平衡作用。这些认识为进一步理解大型河口的地貌演化规律和对减少的响应特征提供了重要基础。

Impacts of historical records on extreme flood variations over the conterminous United States

Mei X, Dai Z, Tang Z, et al. *Journal of Flood Risk Management*, 2018, 11(1):S359-S369.

Evaluation of flood variations over time, especially for floods with large return periods, is of great significance to flood risk assessment. 'Historical' data that have been recorded before the construction of a gauging station provide an effective way to analyse the temporal changes of extreme floods. Here, comparison of maximum likelihood method, L-moment method and Bayesian theory are made to calculate the Gumbel distribution parameters via Monte Carlo simulation experiment. The best option is applied to 37 unregulated rivers over the conterminous United States to analyse their 100-year flood variations. The Monte Carlo simulation results indicate that L-moment method is substantially better than the other two estimators for both systematic and unsystematic series. Over 70% of studied river catchments detect 100-year flood decrease when the historical data are considered. The impacts of historical records on 100-year flood variation estimations are closely related to censoring threshold and historical period length.

正确评估极端洪水的变化对洪水风险预测意义重大。进行洪水评估时，将历史上有记录且远远早于实测记录的特大洪水纳入参考，可以更有效地分析极端洪水的变化。本文首先基于蒙特卡罗模拟实验，对比研究了最大似然法、线性矩法和贝叶斯理论三种经典参数估计方法在评估Gumbel分布各个参数时的最优性。结果表明线性矩法在分析连续实测记录和间断洪水记录时均明显优于其他两种参数估计方法。随后，将线性矩法运用到美国37条河流以评估其百年一遇洪水的变化。研究发现参考历史洪水记录后，美国70%的河流百年一遇洪水预测值有所降低。研究进一步显示历史洪水记录的计算结果与阈值选择及洪水记录时间密切相关。

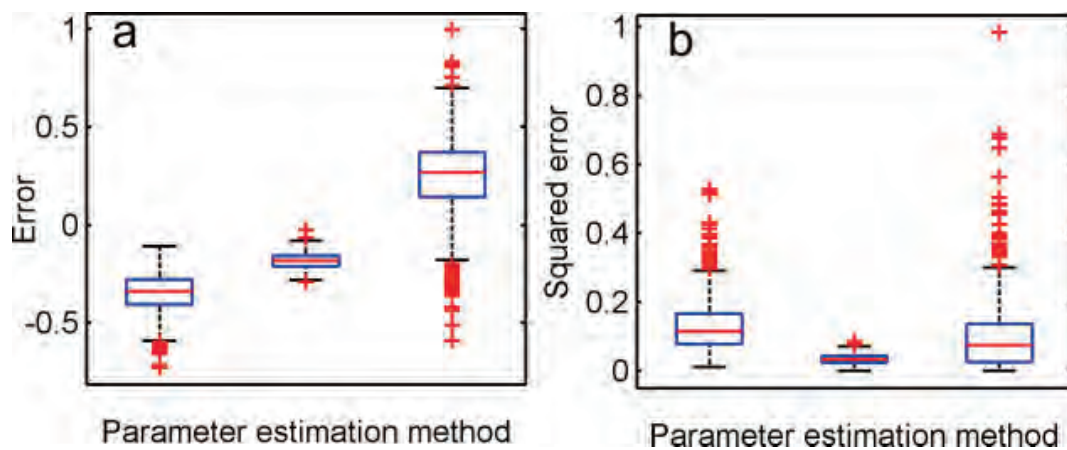


Figure 3 Performance of Maximum Likelihood Method, L-Moment Method and Bayesian method for systematic records. (a) Error results; and (b) squared error results.

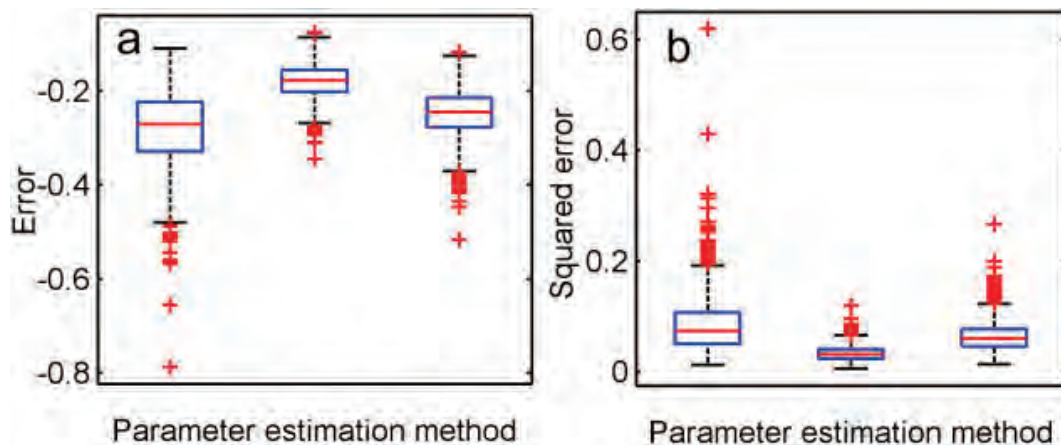


Figure 4 Performance of Maximum Likelihood Method, L-Moment Method and Bayesian method for unsystematic records. (a) Error results; and (b) squared error results.

Fluctuations in the tidal limit of the Yangtze River estuary in the last decade

Shi S, Cheng H, Xuan X, et al. *Science China Earth Sciences*, 2018, 61(8):1136-1147.

The tidal limit is the key interface indicating whether water levels will be affected by tidal waves, which is of great significance to navigation safety and regional flood control. Due to limitations in research methods, recent changes in the Yangtze River tidal limit, caused by sea level rise and large-scale engineering projects, urgently need to be studied. In this study, spectrum analysis was undertaken on measured water level data from downstream Yangtze River hydrological stations from 2007 to 2016. The bounds of the tidal limit were identified through comparisons between the spectra and red noise curves, and the fluctuation range and characteristics were summarized. The results showed that: (1) During the extremely dry period, when the flow rate at Jiujiang station was about 8440 m³/s, the tidal limit was near Jiujiang; whereas during the flood season, when the flow rate at Jiujiang station was about 66700 m³/s, the tidal limit was between Zongyang Sluice and Chikou station. (2) From the upper to lower reach, the effect of the Jiujiang flow rate on the tidal limit weakens, while the effect of the Nanjing tidal range increases. The tidal limit fluctuates under similar flow rates and tidal ranges, and the fluctuation range increases with increasing flow rate and decreasing tidal range. (3) With the continued influence of rising sea levels and construction in river basin estuaries, the tidal limit may move further upstream.

潮区界是标志水位是否受潮动力影响的关键界面,对港航安全与区域防洪意义重大.限于研究方法,近期海平面上升以及大规模工程建设运行背景下的潮区界变动情况亟待研究.对2007~2016年长江下游水文站实测水位资料进行频谱分析,结合红噪声检验判断水位过程中的潮差变化,分析了长江河口潮区界变动范围与特征.结果显示:(1)特大枯水时期,九江站流量约8440 m³/s时,潮区界在九江附近;特大洪水时期,九江站流量约66700 m³/s时,潮区界在枞阳闸与池口之间;(2)自上而下九江流量对潮区界的影响沿程减弱,南京潮差的影响则沿程增强,相近流量/潮差下潮区界位置有变动,变动范围随流量的增大而增大,随潮差的减小而增大;(3)在海平面上升以及流域河口工程建设的持续影响下,未来潮区界或将进一步上移.

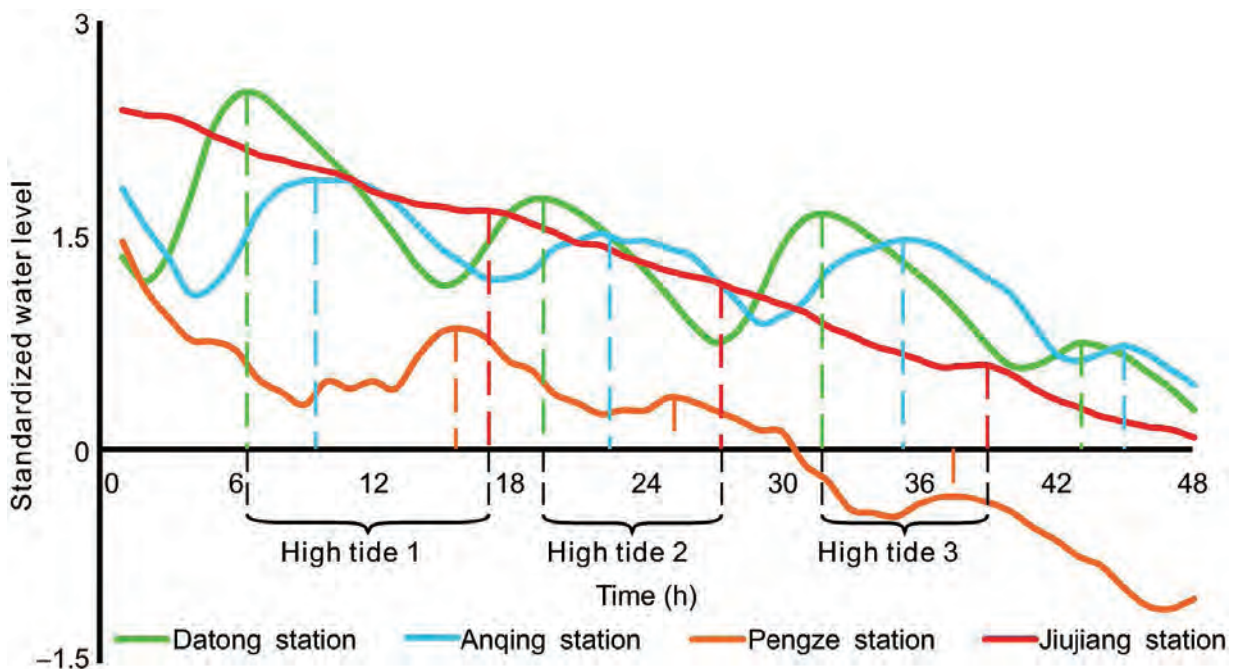


Figure 13 Tidal wave propagation along the Jiujiang-Datong reach, 18–19 December 2007.

Immediately downstream effects of Three Gorges Dam on channel sandbars morphodynamics between Yichang-Chenglingji Reach of the Changjiang River, China

Wang J, Dai Z, Mei X, et al. *Journal of Geographical Sciences*, 2018, 28(5):629-646.

Sandbars are of vital ecological and environmental significance, which however, have been intensively influenced by human activities. Morphodynamic processes of sandbars along the Yichang-Chenglingji Reach of the Changjiang River, the channel immediately downstream of the Three Gorges Dam (TGD), are assessed based on remote sensing images between 2000 and 2016. It can be found that the entire area of sandbars reduces drastically by 19.23% from 149.04 km² in 2003 to 120.38 km² in 2016, accompanied with an increase in water surface width. Owing to differences in sediment grain size and anti-erosion capacity, sandbar area in the upstream sandy gravel reach (Yichang-Dabujie) and downstream sandy reach (Dabujie-Chenglingji) respectively decreases by 45.94% (from 20.79 km² to 11.24 km²) and 14.93% (from 128.30 km² to 109.14 km²). Furtherly, morphological evolutions of sandbars are affected by channel type: in straight-microbend channel, mid-channel sandbars exhibit downstream moving while maintaining the basic profile; in meandering channel, point sandbars show erosion and deposition in convex and concave bank respectively, with mid-channel sandbars distributing sporadically; in bending-branching channel, point sandbars experience erosion and move downstream while mid-channel sandbars show erosion in the head part along with retreating outline. We document that the primary mechanism of sandbars shrinkages along the Yichang-Chenglingji Reach can be attributed to TGD induced suspended sediment concentration decreasing and increasing in unsaturation of sediment carrying capacity. Additionally, channel type can affect the morphological evolution of sandbars. Along the Yichang-Chenglingji Reach, sandbars in straight-microbend channel are more affected by water flow than that in bending-branching channel.

沙洲具有非常重要的生态与环境价值。然而，沙洲一直受到强烈的人类活动影响。基于此，本文以离三峡大坝最近的宜昌-城陵矶河段的沙洲作为案例，基于长时间遥感影像和水文数据研究沙洲如何响应人类活动作用的动力地貌过程。研究发现该河段所有沙洲面积从2003年的149.04平方公里减少到2016年的120.38平方公里。由于泥沙粒径和扛侵蚀能力的差异，沙洲面积在砂砾石河段和沙质河段各自减少了45.94%和14.93%。同时，沙洲地貌受控于河型的影响：直线微弯河段，河槽中央沙洲展示形态基本不变但向下游移动；曲线河段，边缘沙洲经历侵蚀和向下游移动，而中央沙洲是头部侵蚀撤退。

此外，我们论证了沙洲萎缩的基本机制来自三峡大坝引起的水体悬浮泥沙浓度减少和夹砂能力增加。河槽形态也是影响地貌演变的一个方面。沙洲在直线微弯河段更容易被水体作用而发生变化。

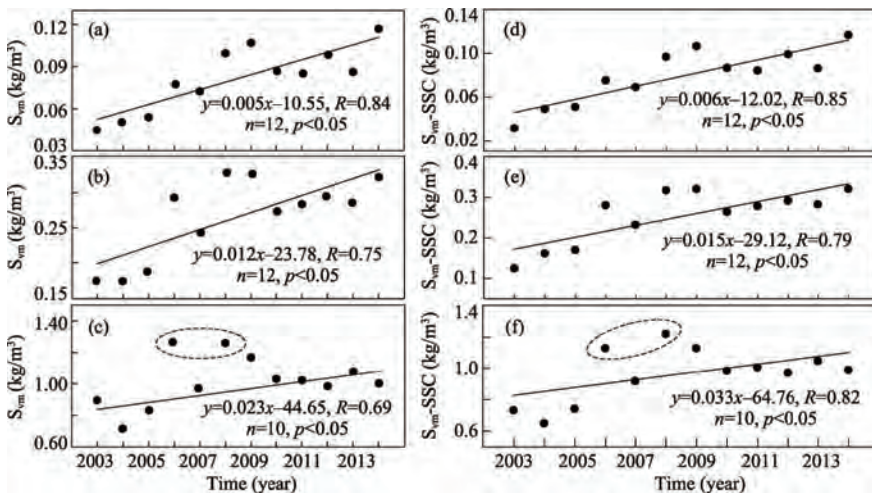


Figure 12 Temporal variation of (a-c) calculated sediment carrying capacity (Svm) and (d-e) the difference between calculated SCC and SSC (Svm-SSC) under different water discharge scenarios, with (a, d) 5000 m³/s; (b, e) 10000 m³/s; (c, f) 20000 m³/s

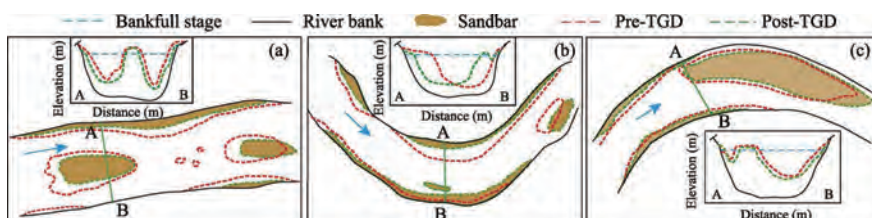


Figure 14 Evolution model of sandbars in different channel types along the Yichang-Chenglingji Reach following the impact of TGD: (a) straight-microbend channel; (b) meandering channel; and (c) bending-branching channel

Riverbed erosion of the final 565 kilometers of the Yangtze River (Changjiang) following construction of the Three Gorges Dam

Zheng S, Xu Y, Cheng H, et al. *Scientific Reports*, 2018, 8(1):11917.

The world's largest hydropower dam, the Three Gorges Dam (TGD), spans the upper Yangtze River in China, creating a 660-km long and 1.1-km wide reservoir upstream. Several recent studies reported a considerable decline in sediment load of the Lowermost Yangtze River (LmYR) and a rapid erosion in the subaqueous delta of the river mouth after the closure of the TGD in 2003. However, it is unknown if the TGD construction has also affected river channel and bed formation of the LmYR. In this study, we compared bathymetric data of the last 565 kilometers of the Yangtze River's channel between 1998 and 2013. We found severe channel erosion following the TGD closure, with local riverbed erosion up to 10 m deep. The total volume of net erosion from the 565-km channel amounted to 1.85 billion m^3 , an equivalent of 2.59 billion metric tons of sediment, assuming a bulk density of $1.4 t/m^3$ for the riverbed material. The largest erosion occurred in a 100-km reach close to the Yangtze River mouth, contributing up to 73% of the total net eroded channel volume.

作为世界上最大的水利发电站，三峡大坝横亘于长江上游并在其上游河段形成了长660km宽1.1km的库区。2003年三峡大坝修建之后，长江下游来沙量大幅度减少，很少有研究对长江入海最后565km的河势演变与底床微形态进行系统的研究。但是，三峡大坝的修建是否对该河段的河势演变与底床微形态变化有影响尚不可知。本研究利用1998年和2013年长江下游最后565km河段的水下地形资料进行分析，发现该河段发生了剧烈的冲刷，局部冲刷深度可至10m。净冲刷用量可达18.5亿立方米，即按照 $1.4t/m^3$ 换算的话，约有25.9亿吨河床泥沙被冲刷。值得注意的是，最大冲刷河段位于距离吴淞口上游约100km的河段，该河段冲刷量占研究河段总冲刷量的73%。

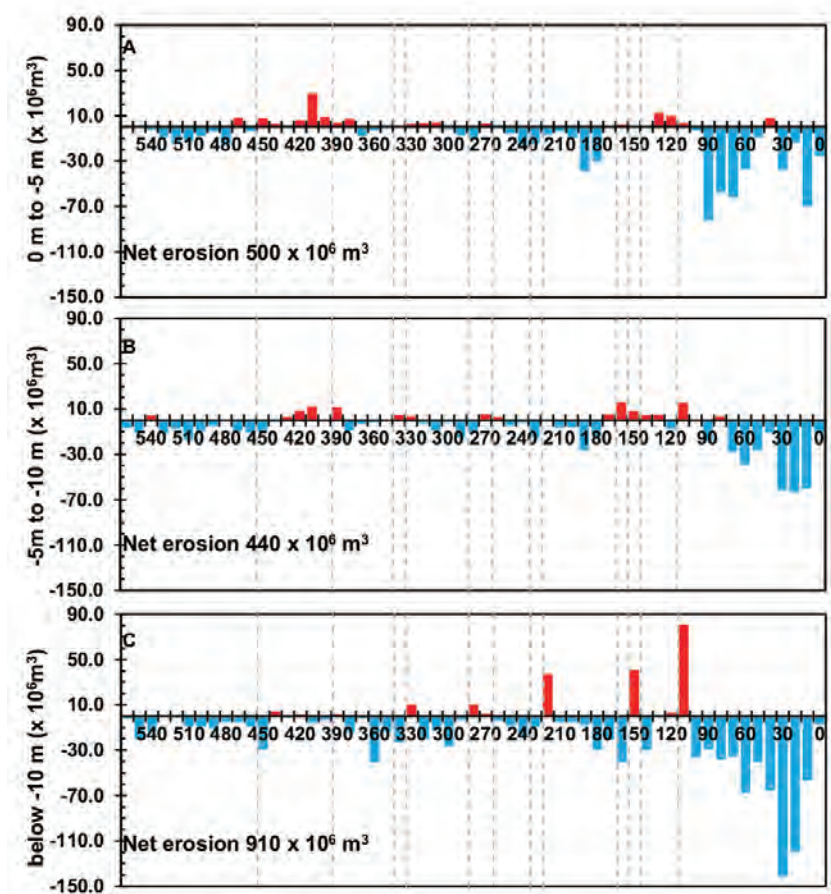


Figure 7. Erosion, deposition, and net change (i.e. erosion – deposition) of channel volume along the final 565 kilometers of the Yangtze River. Blue and red histograms indicate erosion and deposition volumes, respectively, between 0 m to –5 m (A), between –5 m to –10 m (B), and below –10 m (C) in the Lowermost Yangtze River during 1998–2013.

How have the river discharges and sediment loads changed in the Changjiang River basin downstream of the Three Gorges Dam?

Guo L, Su N, Zhu C, et al. *Journal of Hydrology*, 2018, 560:259-274.

Streamflow and sediment loads undergo remarkable changes in worldwide rivers in response to climatic changes and human interferences. Understanding their variability and the causes is of vital importance regarding river management. With respect to the Changjiang River (CJR), one of the largest river systems on earth, we provide a comprehensive overview of its hydrological regime changes by analyzing long time series of river discharges and sediment loads data at multiple gauge stations in the basin downstream of Three Gorges Dam (TGD). We find profound river discharge reduction during flood peaks and in the wet-to-dry transition period, and slightly increased discharges in the dry season. Sediment loads have reduced progressively since 1980s owing to sediment yield reduction and dams in the upper basin, with notably accelerated reduction since the start of TGD operation in 2003. Channel degradation occurs in downstream river, leading to considerable river stage drop. Lowered river stages have caused a 'draining effect' on lakes by fostering lake outflows following TGD impoundments. The altered river-lake interplay hastens low water occurrence inside the lakes which can worsen the drought given shrinking lake sizes in long-term. Moreover, lake sedimentation has decreased since 2002 with less sediment trapped in and more sediment flushed out of the lakes. These hydrological changes have broad impacts on river flood and drought occurrences, water security, fluvial ecosystem, and delta safety.

长江流域的工程和人类活动日益增多，显著改变了河流入海的径流和泥沙通量。本文即基于长系列的水沙资料(1950-2016)，首先给出了三峡水库过去14年的实际运行方式及其对出库流量的影响；继而系统分析了三峡大坝及宜昌以下的中下游河湖系统的径流和泥沙变化过程，研究发现：(1)除了1955年的一个转折点外，中下游及进入河口的年径流没有显著变化；但径流的季节性变化显著，集中表现为夏秋季径流显著减小、冬春季微弱增加；(2)河流泥沙从1980年代中期开始逐步减小，反映长江上游减沙的影响；三峡水库2003年蓄水运行导致泥沙加剧减少，三峡的年平均泥沙截留量为1.26亿吨每年；(3)中下游由于沙的亏缺，河床发生冲刷，外加两湖采沙而引起出湖泥沙增加，两者引起宜昌至大通的泥沙沿程恢复；(4)径流和泥沙变化引起中下游河湖系统的变化，其中干流径流减小、河床冲刷导致水位下降，进而导致对两湖的回水效应减弱，甚至引起抽吸效应。这种变化使得两湖蓄水能力减弱，一定程度上加剧了湖内枯水和干旱的发生，威胁两湖生态系统。

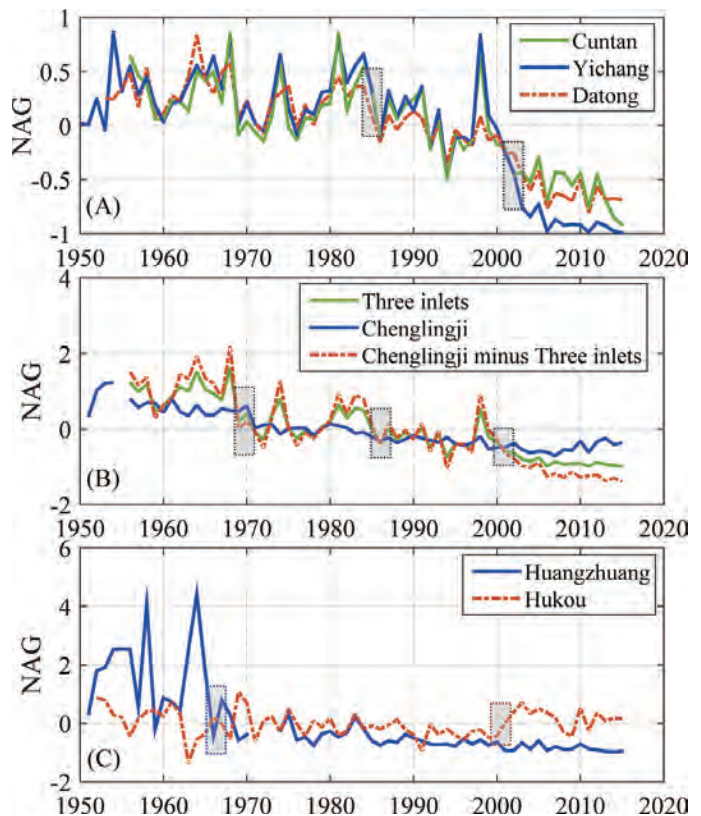


Fig. 8. The normalized anomaly of sediment loads (NAG) (A) at Cuntan (plus Wulong), Yichang, and Datong, (B) at three inlets, Chenglingji, and that at Chenglingji minus at three inlets, and (C) at Huangzhuang and Hukou. The shade bars indicate change points.

A 14 ka high-resolution $\delta^{18}\text{O}$ lake record reveals a paradigm shift for the process-based reconstruction of hydroclimate on the northern Tibetan Plateau

Wünnemann B, Yan D, Andersen N, et al. *Quaternary Science Reviews*, 2018, 200:65-84.

The influence of the mid-latitude westerlies (MLW) competing with the Asian summer monsoons (ASM) over the Tibetan Plateau (TP) remains a matter of discussion on how and to which extent both atmospheric systems have been controlling hydro-climate during the Holocene. Depleted oxygen isotopes in lake deposits were commonly interpreted in terms of enhanced summer monsoon moisture supply, implying a migration of the ASM deep into the interior of the plateau during Holocene periods. In order to test this relationship we used a high resolution oxygen isotope record (mean 20 yr resolution) in combination with carbonates and mineral phases, titanium flux, grain size and ostracod abundances derived from a 6.84m long sediment core in the endorheic Kuhai Lake basin, north-eastern TP. The results confirm 1) continuous positive co-variance between enriched $\delta^{18}\text{O}_{\text{carb}}$ and total carbonates during the last 14 ka, indicative of dominant seasonal influence on multi-decadal to centennial scale isotopic signatures in lake water and respective carbonate precipitation, 2) negative co-variance between allochthonous sediment flux and $\delta^{18}\text{O}_{\text{carb}}$ (and carbonates) attributed to relative increase of flux rates during non-summer seasons, 3) correspondence of lake level variations with carbonate mineral phases and the occurrence/disappearance of ostracod assemblages, and 4) inverse relationships between isotopic signatures in ASM-dominated and MLW-controlled lake records across the TP. Enriched $\delta^{18}\text{O}_{\text{carb}}$ in Kuhai Lake sediments was primarily a result of high evaporation during the summer seasons, while ASM-related rainfall amount did not play an important role, likely counterbalanced by isotopic signatures from different water sources. Conversely, depleted $\delta^{18}\text{O}_{\text{carb}}$ was mainly attributed to water supply during nonsummer seasons of colder temperatures and generally light isotopic signatures from MLW-derived sources. This finding may lead to a paradigm shift in such way that depleted $\delta^{18}\text{O}$ in carbonates is primarily not the result from ASM-related rainfall as previously assumed. The reconstructed hydro-climatic history of Kuhai Lake indicates the dominance of westerly-derived climate during the Younger Dryas interval (12.8-11.5 ka) under very shallow pond-like conditions. Despite climate amelioration during the early Holocene (11.5-7.5 ka) hydrological conditions remained unstable with frequent alternations between dominance of summer and winter seasons. During the middle Holocene (7.5-5.5 ka) the lake experienced highest lake levels dominated by summer monsoon-related water supply, assigned to the Holocene hydro-climatic optimum. Frequent high-amplitude fluctuations afterwards (5.1-2.9 ka) refer to cooling/drying events under enhanced MLW influence accompanied by a strong lake level decline. The late Holocene (2.9 ka- Present) period experienced moderate isotopic variations and fluctuating lake levels in response to variable influence of summer- or winter-related hydro-climatic conditions. This seesaw-like pattern with amplitudes of $>10\%$ in $\delta^{18}\text{O}_{\text{carb}}$ resembles fluctuations in cave records and variations between air and seawater (Dole effect). High correspondence with cooling events derived from North Atlantic drift ice and meltwater discharge indicate close ties to northern hemispheric climate transmitted by the MLW across the TP.

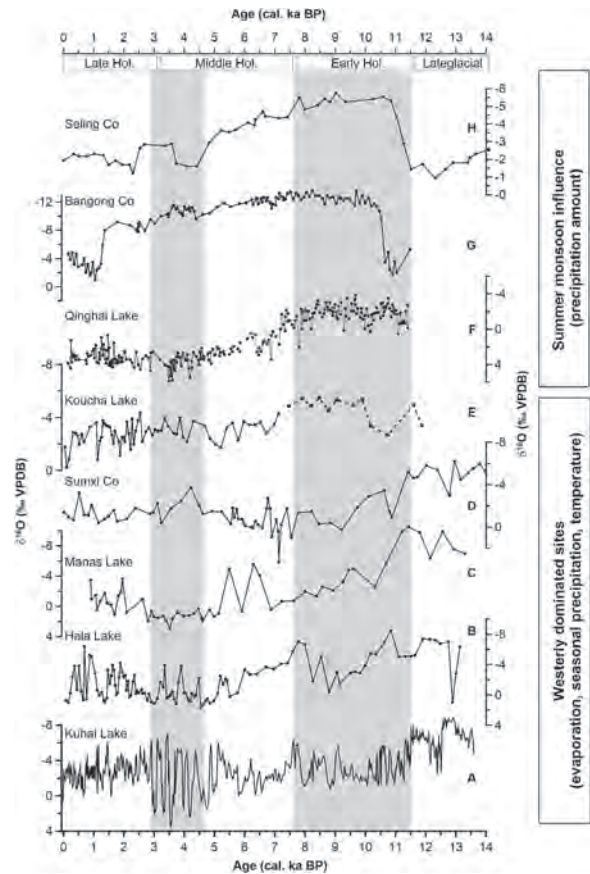


Fig. 9. Comparison of isotope records from various lakes on the Tibetan Plateau. Westerly domain: Kuhai Lake (this study), Hala Lake (Yan and Wünnemann, 2014), Manas Lake (Rhodes et al., 1996), Sumxi Co (Gasse et al., 1991; Wei and Gasse, 1999); ASM influenced domains: Koucha Lake (Mischke et al., 2008), dotted line indicates unclear chronology; Qinghai Lake (An et al., 2012), Bangong Co (Gasse et al., 1996; Wei and Gasse, 1999), Seling Co (Gu et al., 1993; Wei and Gasse, 1999), all redrawn according to published individual chronologies and related uncertainties. Shaded areas mark unstable climatic conditions during the early Holocene and late middle Holocene.

Morphological variability of the active Yellow River mouth under the new regime of riverine delivery

Ji H, Chen S, Pan S, et al. *Journal of Hydrology*, 2018, 564:329-341.

The Yellow River subaqueous delta (YRSD), once the most rapid depo-center among river deltas worldwide, has been under the risks of subsidence and degradation due to the new regime of riverine delivery affected by human interventions. Utilizing hydrologic and bathymetric surveying datasets, we examined the latest regime of river input from the perspective of water-sediment relationship, and the responding morphological evolutionary processes of active YRSD over a period of 20 years between 1996 and 2016. Results show that the new discharge regime is strongly interfered by the Water-Sediment Regulation Scheme (WSRS), characterized by a more drastic decline of sediment load than that of water discharge; more harmonious relationship between water and sediment discharges in the lower reach of the river to the sea; coarser sediment delivery and low suspended sediment concentration (SSC). We identified inverse erosion-accretion trends in the subaqueous region: net accretion of 0.15 m/yr in the

active Yellow River mouth (AYRM) and severe erosion of 0.1 m/yr in the Gudong littoral zone (GDLZ). As the primary sink for sediment delivery, AYRM received approximately 68% of sediment delivery during the study period and sedimentation was mainly occurred in the shallower area where water depth was less than 10 m. In addition, recent morphological evolution of AYRM is found to have undergone through four stages, namely: moderate accretion (1996–2002), rapid accretion (2002–2007), reduced accretion (2007–2015) and rapid erosion (2015–2016). The new regime of riverine delivery presents multiple spatiotemporal scales in shaping deltaic morphology. Compared with the previous research, we present the morphological evolution of deltaic system over decadal timescale is strongly influenced by reduction of sediment supply derived from basinscale human impacts, and the variability of subaqueous portion during the study period is closely related to inter-annual variability of river input. Besides, the building of AYRM is shaped by event-scale WSRS induced floodwater, and decade-scale change of sediment pathway governed by frequent mouth channel migration. The results show, for the first time, that

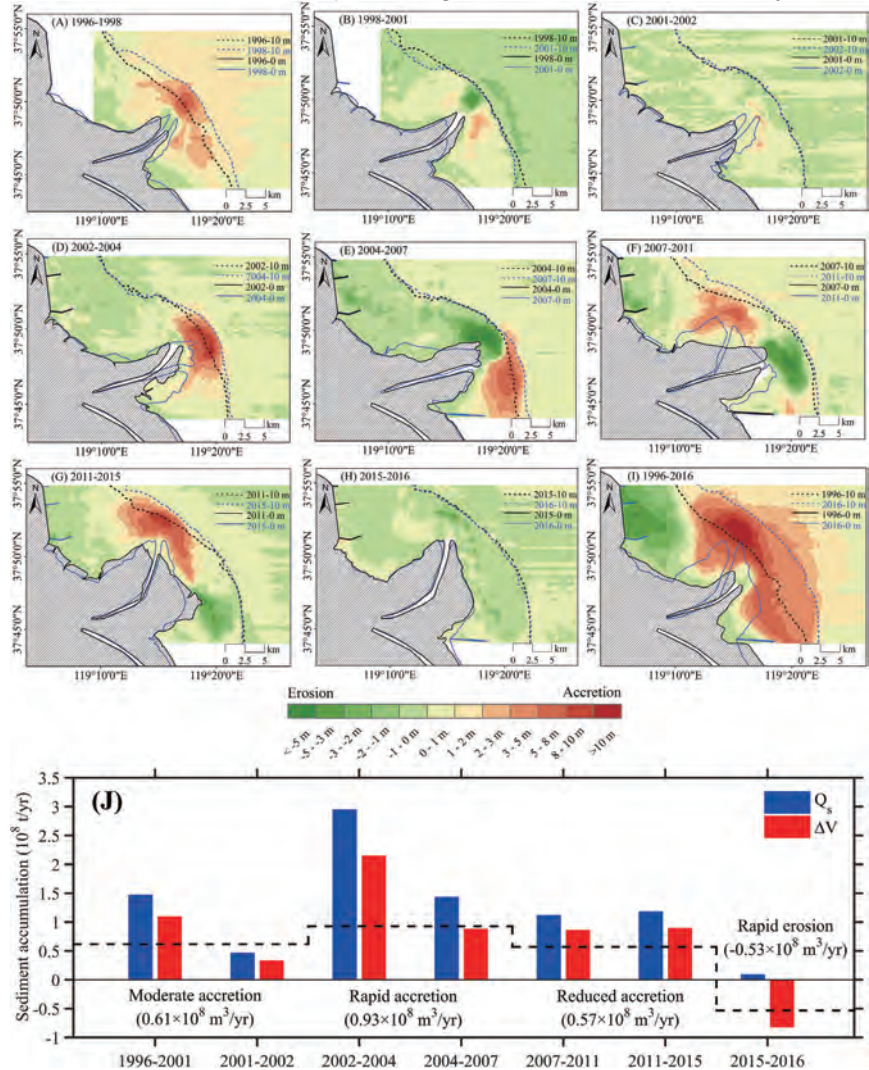


Fig. 5. Bathymetric changes in AYRM during (A) 1996–1998; (B) 1998–2001; (C) 2001–2002; (D) 2002–2004; (E) 2004–2007; (F) 2007–2011; (G) 2011–2015; (H) 2015–2016 and the entire 20-yr time span (I). The black and blue dash line indicated the shoreline and 10-m depth contour position of AYRM in adjacent years; (J) Erosion-accretion volume in AYRM (ΔV) and suspended sediment discharging to the sea (Q_s) during 1996–2016. The black dash line represents average volume change in AYRM in different period, indicating four different stages in AYRM variation. (For interpretation of the references to colour in this figure legend, the reader is referred to the web version of this article.)

AYRM has experienced a significant erosion since the implementation of WSRS, with a decline of 99% sediment delivery in 2016 compared to the natural mode during 1950s. The results also indicate that to maintain the erosion-accretion balance of AYRM, an estimation of 41.4–62.3 Mt/yr sediment delivery should be kept. Due to the fluvial regime change from the natural to the highly human-regulated modes, the AYRM, as well as the whole YRSD, is expected to be transforming from the accretion to erosion states.

近年来，受流域气候变化和强烈的人类活动干预，黄河入海水沙出现了新的情势。黄河三角洲曾是世界上造陆最快的沉积中心，目前正面临沉降和退化的风险。基于1996-2016年黄河入海水沙数据和现行河口区实测水下地形资料，从水沙关系的角度，研究了近20年黄河新的入海水沙情势，以及现行黄河水下三角洲地貌演变过程。结果表明，受调水调沙的强烈干预，黄河入海水沙情势已由“水少沙多”向“枯水少沙”转变，入海泥沙持续减少，水沙关系更趋协调，泥沙颗粒粗化，悬沙浓度降低。研究发现，现行黄河水下三角洲出现淤涨和侵蚀的两种不同态势，即现行河口的净淤积和孤东近岸的严重侵蚀。作为泥沙输送的主要归宿，现行河口近20年间堆积了68%的来沙。黄河口近期地貌演变经历了四个阶段，即中度淤积（1996-2002）、快速淤涨（2002-2007）、淤涨减缓（2007-2015）和快速侵蚀（2015-2016）。研究揭示了年代尺度的河口地貌演化受流域人类活动引起的来沙减少的强烈影响，水下三角洲演变与入海水沙的年际变化密切相关。研究发现，现行河口演变主要受调水调沙人造洪水和口门出汉的控制。2016年由于水量极枯，调水调沙首次中断，河口滨海区出现了大面积蚀退。计算结果表明，为了维持现行黄河口的冲淤平衡，需4140-6230万t/a来沙量。黄河高度受控于水库调控，入海泥沙大幅降低，现行河口和整个水下三角洲将面临从淤涨向侵蚀的转型。

Fluvial sediment transfer in the Changjiang (Yangtze) river-estuary depositional system

Dai Z, Mei X, Darby S E, et al. *Journal of Hydrology*, 2018, 566:719-734.

Knowledge of the transfer of sediment through river systems is essential for understanding the physical, chemical and biological processes on the Earth's surface. A holistic analysis of long-term records of water discharge, sediment transport, riverbed morphology and estuarine hydrology is here used to quantify spatial and temporal variations in fluvial sediment fluxes along the Changjiang River. We show that the establishment of the Three Gorges Dam (TGD) has directly changed the fluvial sediment-transport process by annually trapping 1.23×10^8 t of sediment. The upper Changjiang reach has switched from being the main sediment source before 2003 to a depositional sink of fluvial sediment subsequently. The major lakes, such as Dongting Lake and Poyang Lake, have shifted from being local sediment sinks before 2003 to sediment sources thereafter, such that they now provide sediment to the Changjiang River. Since the 2003 closure of the TGD the riverbed of the middle-lower Changjiang has become the major source of sediment being transmitted downstream, now providing almost 50% of the material entering the estuary. Shoals in the estuarine channels and landward sediment transport from the sea have become major sediment sources for the river estuary. We conclude that dams currently in preparation along the upper Changjiang reach and adjacent lakes may cause the cessation of sediment supply to downstream reaches. Rising sea levels and frequent storms may terminate landward sediment transport, increasing estuarine erosion and inducing seaward sediment transport. It can therefore be expected that substantial erosion could occur in the near future in the Changjiang estuary system.

理解河流系统的泥沙转换对于地球表面物理、化学和生物过程的研究具有非常重要的价值。因而，一套综合、全面和长时间的水、泥沙运输、河床地貌及河口水动力被利用以定量长江河流泥沙通量的时空变化。我们的研究表明三峡大坝的构建通过捕获每年约1.23亿吨泥沙已经直接改变河流泥沙运输过程。长江上游从三峡构建前的主要泥沙物源转为目前的泥沙沉降区。主要湖泊，如洞庭与鄱阳湖，从局部的泥沙沉降区转变为提供泥沙给长江干流。自从2003年三峡构建，中下游河槽成为主要的泥沙物源区，提供了约50%的泥沙进入河口。河口河槽的浅滩和来自海域向陆运输的泥沙成为河口的主要物源。我们推定上游和湖泊正在构建的大坝将可能引起泥沙补给到下游中断。上升的海平面和频繁的风暴将终止泥沙向陆运输，增加河口侵蚀和诱发泥沙向海运输。在不久的将来，实质性的侵蚀将会在长江河口系统发生。

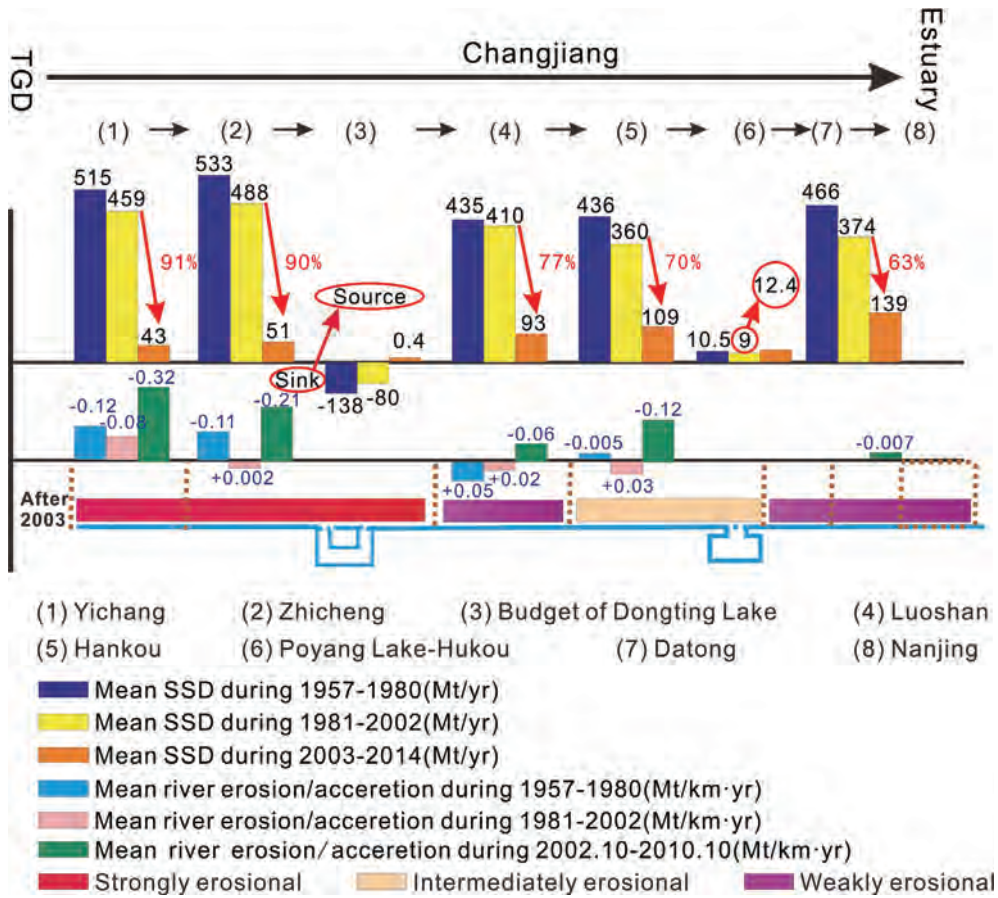


Fig. 8. Sediment transfer shifts along the middle-lower Changjiang reach (Revision after Dai and Liu (2013))

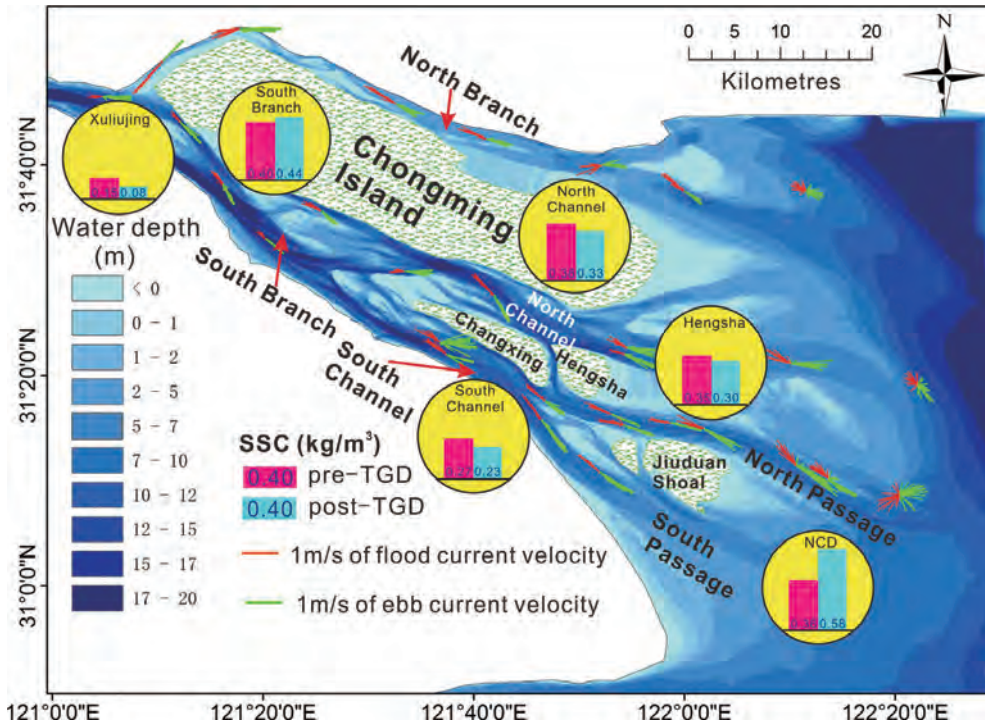


Fig. 16. Mean tidal-current variation in the Changjiang Estuary (Synchronous survey data: 22 Sept. 2002), also showing the variations in mean suspended sediment concentration (SSC).

Hydromorphological processes of Dongting Lake in China between 1951 and 2014

Yu Y, Mei X, Dai Z, et al. *Journal of Hydrology*, 2018, 562:254-266.

Under the impact of intensive anthropogenic activities and in the context of global climate change, the hydromorphological processes of most lakes around the world have changed dramatically. Here, based on hydrologic and topographic data, we analyzed secular variations in hydromorphological characteristics and their influencing factors at Dongting Lake, the second-largest freshwater lake in China. The entire time series (1951–2014) was divided into four subperiods based on the anthropogenic modifications of the Changjiang (Yangtze) River, including the construction of the Lower Jingjiang Cutoff Project and the operation of the Gezhou Dam (GD) and the Three Gorges Dam (TGD). The results indicated that there were obvious stepwise decreasing trends in the annual water discharge and suspended sediment discharge (SSD) from 1951 to 2014. Seasonal differences in water discharge and SSD over the recent 60 years exhibited a tendency of “less flooding during the flood season and more drying during the dry season”. Meanwhile, the deposition-erosion budget of Dongting Lake shifted from a deposition rate of 120×10^6 t/yr from 1951 to 2003 to an erosion rate of 2×10^6 t/yr with the serious degradation of the Ouchi and Xiangjiang deltas after 2003. The hydrological processes of Dongting Lake are dominated by different anthropogenic activities at different stages. The Jingjiang Cutoff Project is the main driver of the decreases in water discharge and SSD from 1967 to 1980. The operation of the GD along the Changjiang River and other reservoirs, as well as land-use changes in the Dongting Lake basin, should be responsible for the hydrological variations from 1981 to 2003. The high sediment retention rate, geometric adjustment of the channel, and flow regulation induced by the operation of the TGD are the main drivers for the hydromorphological variations in Dongting Lake in 2004–2014.

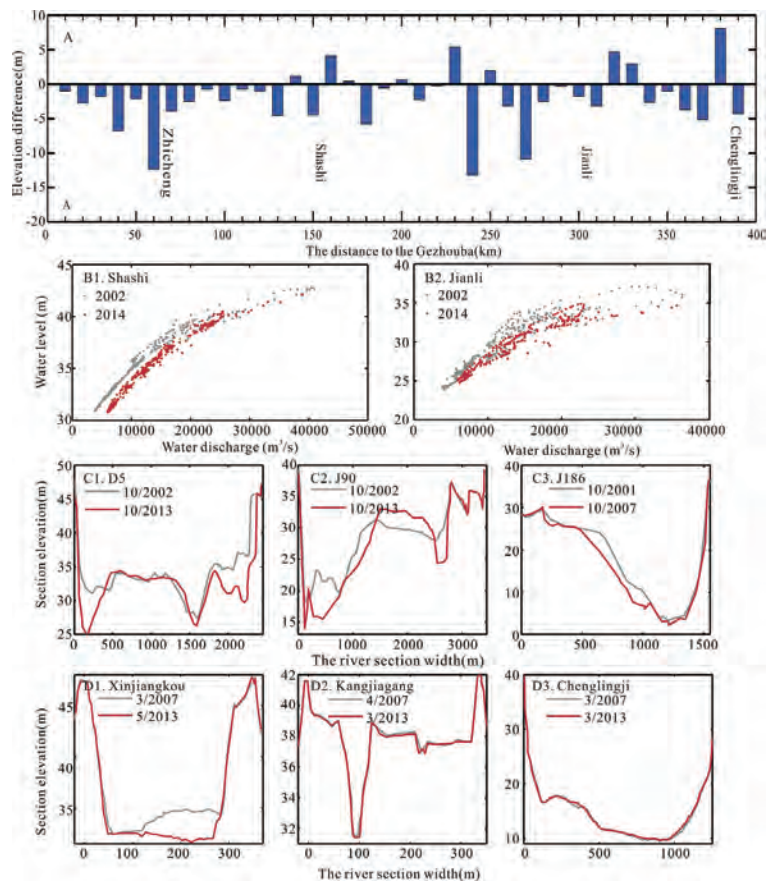


Fig. 11. (A) Thalweg changes along the Changjiang River; (B) Daily water level and water discharge comparison between 2002 and 2014 at Shashi and Jianli; and cross-section variations (C) along the Changjiang River and; (D) Dongting Lake basin.

在强烈的人类活动和全球气候变化背景下，全球大部分湖泊水文-地貌过程已经发生戏剧性的改变。这儿，利用水文和地形资料，我们分析了中国第二大湖泊洞庭湖的水文-地貌长期变化及影响因素。整个时间尺度自1951-2014年包括了荆江裁弯工程、葛洲坝和三峡构建。结果表明洞庭湖每年水和泥沙有阶段性的减少趋势。季节性的变化则展示洪季不洪、枯季更枯的特征。同时，洞庭湖的沉积侵蚀模式由1951-2003年的年沉积1.2亿吨转为目前年均侵蚀2百万吨，同时在藕池和湘江三角洲有严重的侵蚀特征。洞庭湖的水文过程主要受不同阶段的人类活动控制。荆江裁弯工程控制了1967-1980年的水沙减少，葛洲坝和同期湖泊建坝及土地利用影响1981-2003年的湖泊水文过程。大坝高的捕获泥沙速率、槽的地貌调整和流的约束直接改变洞庭湖的近期水文地貌过程。

Decadal Sedimentation in China's Largest Freshwater Lake, Poyang Lake

Mei X, Du J, Dai Z, et al. *Geochemistry, Geophysics, Geosystems*, 2018, 19(8):2384-2396.

Lakes, as key recorders of sedimentation regime variations, have undergone dramatic erosion/deposition worldwide in response to global warming and increasing anthropogenic interference. Poyang Lake, China's largest freshwater lake, has not escaped these variations. Herein, we show that the sedimentation in Poyang Lake has likely undergone a unique phase shift from sediment sink (annually storing 421×10^4 t) during 1960–1999 to sediment source (yearly losing 782×10^4 t) during 2000–2012, with respect to the Changjiang (Yangtze) River. In comparison with sedimentation during 1960–1999, Poyang Lake sedimentation during the period 2000–2012 is characterized by no deposition during the flood season and enhanced erosion during the dry season. Furthermore, Poyang Lake's largest delta, the Ganjiang Delta, prograded at a rate of 32.7 m/a from 1983 to 1996, which increased to 52.8 m/a from 1996 to 2005 but dropped significantly to 1.7 m/a from 2005 to 2015. A sediment core collected in the shallow-water shoal of the central lake indicates a stable increase in sedimentation flux from 1960 to 2002, with a mean value of $0.27 \text{ g}/(\text{cm}^2 \cdot \text{a})$, followed by a decline in sedimentation flux after 2002. Our findings show that the tributary sediment input from the lake catchment dominated the sedimentation of Poyang Lake prior to 2000, when it was significantly larger than the sediment output to the Changjiang River. However, thereafter, the contribution of tributary sediment to the output dropped by 50%, and the rest has been provided by the lake itself. Namely, channels along Poyang Lake's waterway became the additional source of the lake's sediment output in the 2000s.z

湖泊，作为一种重要的沉积体系，其地貌演变直接反映了地表沉积系统对气候变化和人类活动的响应。本研究通过分析中国第一大淡水湖鄱阳湖1960s-2010s的沉积记录，探讨了其年代际变化过程和相关控制因素。结果表明鄱阳湖在1960-1999期间淤积泥沙421万吨/年，而在2000-2012期间侵蚀泥沙782万吨/年，从而由泥沙的汇转变成了源，并表现出了“洪季不淤，枯季更冲”的季节性特征。通过剖析鄱阳湖年代际遥感影像，揭示出鄱阳湖最大的三角洲，赣江三角洲向湖淤进速率首先由32.7米/年（1983-1996）逐步增加到52.8米/年（1996-2005），之后迅速下降到1.7米/年（2005-2015）。与此同时，鄱阳湖浅滩处采集的沉积柱样表明，通江河道浅滩的淤积速率在2002年后出现下降趋势。通过进一步探讨相关控制因素，研究发现鄱阳湖近期的严重侵蚀主要由支流入湖泥沙下降和出湖泥沙上升共同导致。

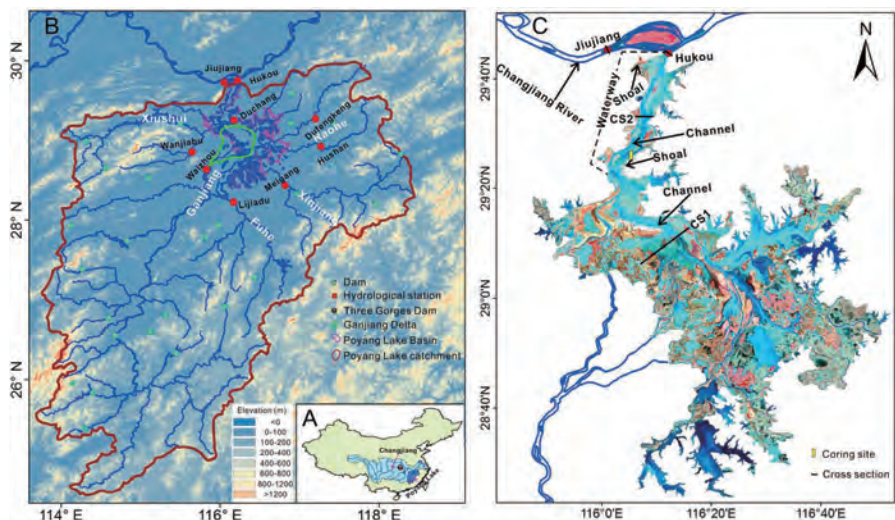


Figure 1. Study area of Poyang Lake, with (a) Poyang Lake's location relative to the Changjiang River, the Three Gorges Dam, and the East China Sea; (b) Poyang Lake Catchment; (c) Poyang Lake basin, where the cross sections CS1 and CS2 refer to the cross section shown in Figure 6 and the cross section Jiujiang and Hukou refer to the cross section shown in Figure 7.

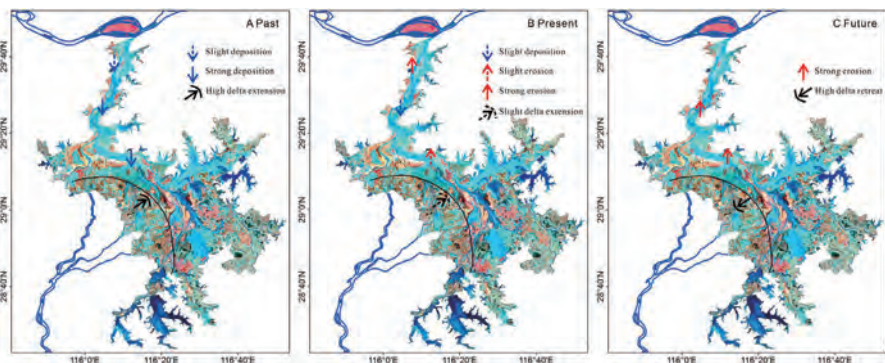


Figure 8. Dynamic sedimentation of Poyang Lake: (a) past, (b) present, and (c) future.

Modulation of Extreme Flood Levels by Impoundment Significantly Offset by Floodplain Loss Downstream of the Three Gorges Dam

Mei X, Dai Z, Darby S E, et al. *Geophysical research letters*, 2018, 45(7):3147-3155.

River flooding—the world's most significant natural hazard—is likely to increase under anthropogenic climate change. Most large rivers have been regulated by damming, but the extent to which these impoundments can mitigate extreme flooding remains uncertain. Here the catastrophic 2016 flood on the Changjiang River is first analyzed to assess the effects of both the Changjiang's reservoir cascade and the Three Gorges Dam (TGD), the world's largest hydraulic engineering project on downstream flood discharge and water levels. We show that the Changjiang's reservoir cascade impounded over $30.0 \times 10^3 \text{ m}^3/\text{s}$ of flow at the peak of the flood on 25 July 2016, preventing the occurrence of what would otherwise have been the second largest flood ever recorded in the reach downstream of the TGD. Half of this flood water storage was retained by the TGD alone, meaning that impoundment by the TGD reduced peak water levels at the Datong hydrometric station (on 25 July) by 1.47 m, compared to pre-TGD conditions. However, downstream morphological changes, in particular, extensive erosion of the natural floodplain, offset this reduction in water level by 0.22 m, so that the full beneficial impact of floodwater retention by the TGD was not fully realized. Our results highlight how morphological adjustments downstream of large dams may inhibit their full potential to mitigate extreme flood risk.

评估长江上游链珠式水库，包括世界最大的水利工程三峡大坝，对下游河口极端洪水流量及水位的调控效应。研究表明，自1870年以来最强的ENSO事件在长江流域产生了最严重的降雨，然而，相应的洪水事件在河口潮区界大通的洪水流量记录中仅位居第7。成果揭示，长江上游链珠式水库在2016年7月25日蓄水超过 $30000 \text{ m}^3/\text{s}$ ，从而阻止了历史第二大洪水在下游河段的出现，其中三峡水库蓄水贡献约50%，有效降低大通洪水位1.47m。但是，三峡水库大规模拦截上游泥沙导致下游河漫滩发生普遍侵蚀。下游河漫滩的损失削弱了其对洪水的阻滞作用，进而导致洪水上升0.22m。可见，三峡大坝蓄水对极端洪水位的调控作用被下游河漫滩的损失削弱。成果进而指出，随着全球变暖导致的极端洪水事件持续加强，在未来的一段时间内，长江下游河段类似2016年的洪水事件可能将不断发生，甚至成为常态现象。

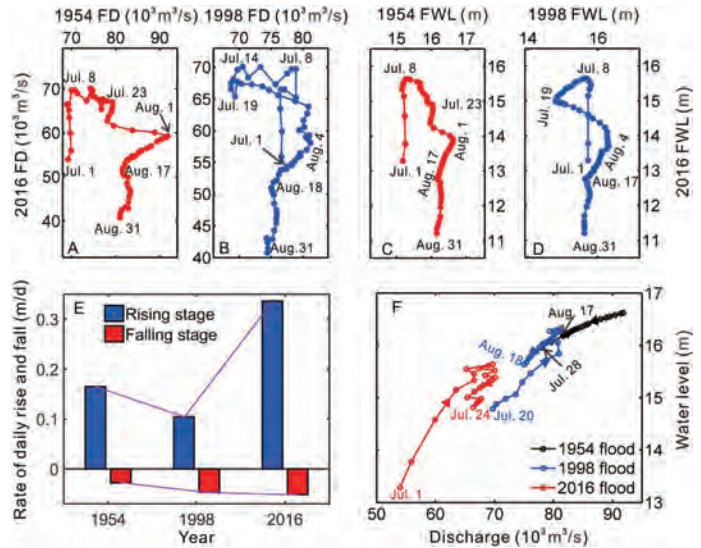


Figure 2. Comparison of flood characteristics observed at the Datong hydrometric station. (a, b) Daily flood discharge (FD); (c, d) daily water level (FWL) for the 2016 versus the 1954 and 1998 floods; (e) rate of daily rise and fall of water level during the 1954, 1998, and 2016 floods; and (f) loop-rating curves of the daily water level versus water discharge for the 1954, 1998, and 2016 flood events.

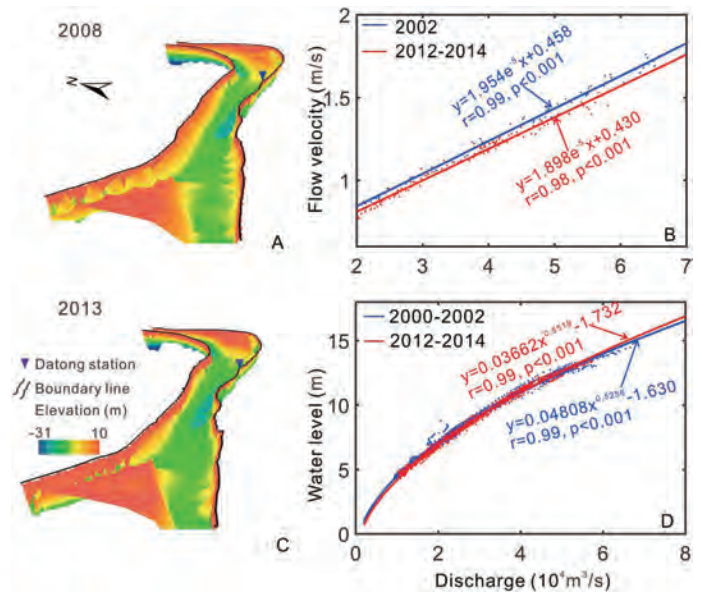


Figure 4. Channel erosion along the Changjiang River around the Datong hydrometric station as detected from bathymetric maps between (a) 2008 and (c) 2013; (b) relationship between cross-sectional average flow velocity and flow discharge in the pre-TGD (2002) and post-TGD (2003–2013) periods; (d) relationship between daily discharge and water level during the pre-TGD (2000–2002) and post-TGD (2012–2014) periods. Note that the flow velocity data, discharge, and water level data used here were provided by the Changjiang Water Resources Commission, China.

Secular bathymetric variations of the North Channel in the Changjiang (Yangtze) Estuary, China, 1880–2013: causes and effects

Mei X, Dai Z, Wei W, et al. *Geomorphology*, 2018, 303:30-40.

As the interface between the fluvial upland system and the open coast, global estuaries are facing serious challenges owing to various anthropogenic activities, especially to the Changjiang Estuary. Since the establishment of the Three Gorges Dam(TGD), currently the world's largest hydraulic structure, and certain other local hydraulic engineering structures, the Changjiang Estuary has experienced severe bathymetric variations. It is urgent to analyze the estuarine morphological response to the basin-wide disturbance to enable a better management of estuarine environments. North Channel (NC), the largest anabranching estuary in the Changjiang Estuary, is the focus of this study. Based on the analysis of bathymetric data between 1880 and 2013 and related hydrological data, we developed the first study on the centennial bathymetric variations of the NC. It is found that the bathymetric changes of NC include two main modes, with the first mode representing 64% of the NC variability, which indicates observable deposition in the mouth bar and its outer side area (lower reach); the second mode representing 11% of the NC variability, which further demonstrates channel deepening along the inner side of the mouth bar (upper reach) during 1970–2013. Further, recent erosion observed along the inner side of the mouth bar is caused by riverine sediment decrease, especially in relation to TGD induced sediment trapping since 2003, while the deposition along the lower reach since 2003 can be explained by the landward sediment transport because of flood-tide force strengthen under the joint action of TGD induced seasonal flood discharge decrease and land reclamation induced lower reach narrowing. Generally, the upper and lower NC reach are respectively dominated by fluvial and tidal discharge, however, episodic extreme floods can completely alter the channel morphology by smoothing the entire channel. The results presented herein for the NC enrich our understanding of bathymetric variations of the Changjiang Estuary in response to human activities, which can be well applied to other estuaries subject to similar interferences.

世界大河入海泥沙的变化对河口三角洲的影响一直是未来地球海岸计划的研究热点，但涉及到不同类型的河口，其对上游泥沙变化的响应并非一致。本文利用1880-2013年的海图数字化地形及相关水沙资料，揭示出长江分汉型河优型河口北港动力地貌主要经历河槽平顺、沙洲并陆及落潮槽为主向河槽弯曲、沙洲零散发育与涨落潮复式槽共存的变化过程。进而总结出北港河道百余年来地貌演变主要呈现下段严重淤积和上段深槽持续侵蚀两种模式。其中，上游泥沙减少是导

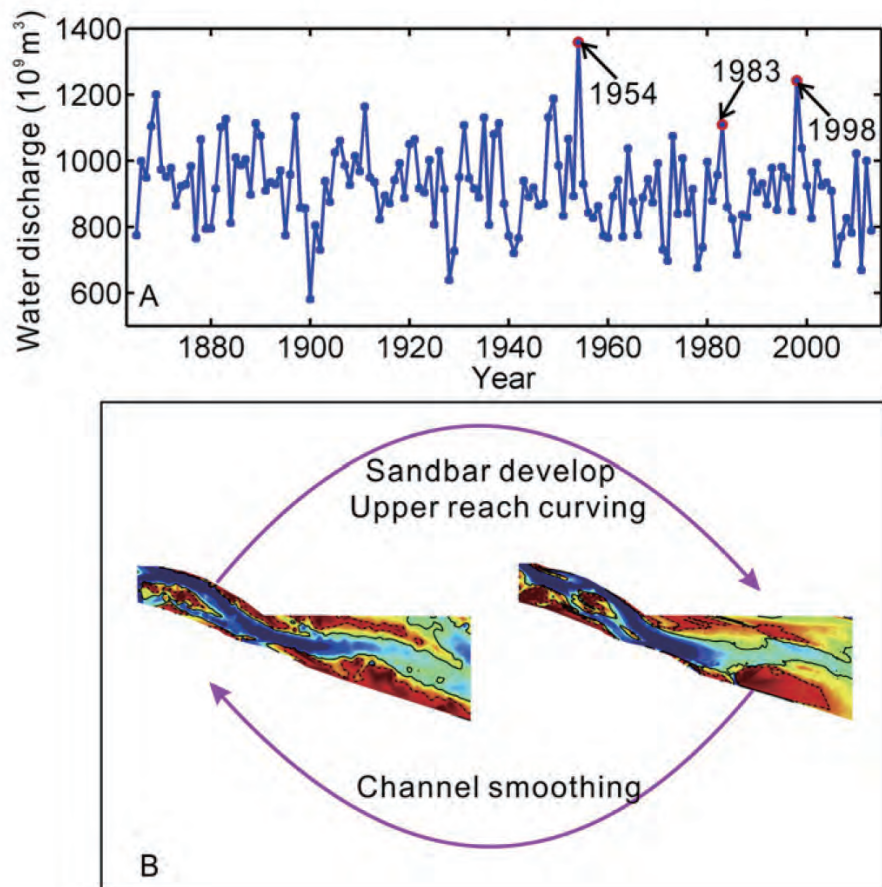


Fig. 14. A) Yearly water discharge into the Changjiang Estuary with recent extreme floods highlighted by the red cycles; B) Cyclic evolution of the North Channel relative to the extreme floods

致拦门沙以浅区域出现河槽侵蚀的主控因素；拦门沙屏障与涨潮动力作用则是拦门沙以深区域仍维持淤积状态的主要原因。此外，极端洪水可冲刷整个北港，导致其地貌发生根本改变。

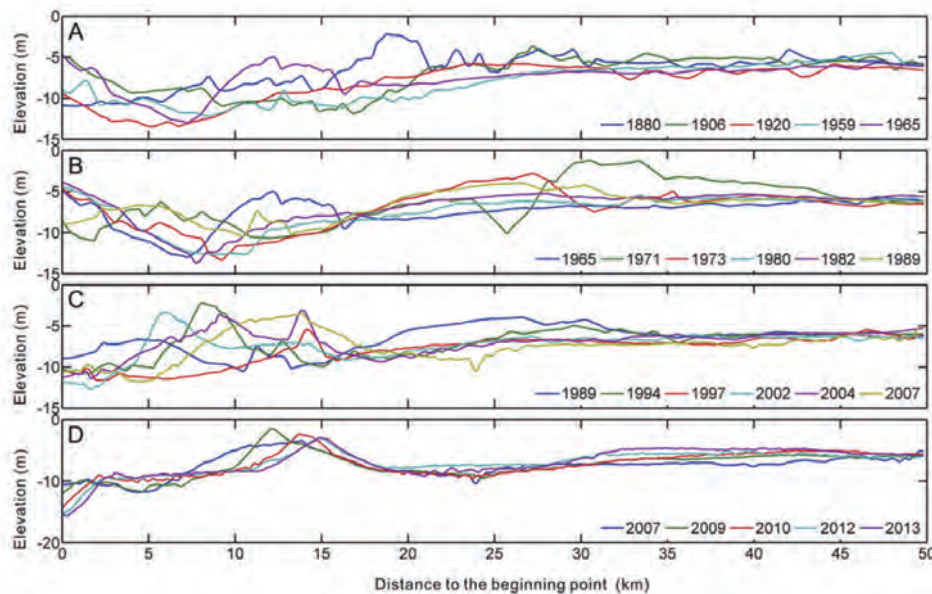


Fig. 7. Temporal bathymetric variations of the North Channel from 1842 to 2013. The location of the longitudinal section is shown in Fig. 1.

Response of lake-catchment processes to Holocene climate variability: Evidences from the NE Tibetan Plateau

Yan D, Wünnemann, B, Zhang Y, et al. *Quaternary Science Reviews*, 2018, 201:261-279.

Investigating the so-called Third Pole Environment (TPE) became a major concern during the last decades since it was recognized that the high-altitude region of the Tibetan Plateau (TP) is a key area for the understanding of cause-effect mechanisms driven by climate change and geodynamic processes. Studies on the hydro-climatic evolution during the Late Quaternary were mainly carried out by single lake records or alternatively by individual terrestrial sites. Integrated source-to sink studies considering lake catchment interactions were extremely seldom utilized. We investigated such relationships in the Kuhai Basin on the north-eastern Tibetan Plateau and analysed sedimentary processes based on 30 onshore sections and three sediment cores from different locations and water depth in the lake basin. Grain size variations, ostracod assemblages, geochemical proxies and absolute dating (luminescence, radiocarbon, $^{210}\text{Pb}/^{137}\text{Cs}$) were applied as key indicators that reveal interacting sediment fluxes under different hydro-climatic settings during the Younger Dryas interval and the Holocene. Our results indicate that wind-induced transportation processes and allocation of respective aeolian sands in the catchment are attributed to distinct phases of reduced effective moisture availability during summer time. Those phases corresponded to weak summer monsoon influence during the Younger Dryas interval, the Early Holocene (11.6-7.5 ka), dry-cold interlude (DCI: ca. 4.5-3.0 ka), Dark Ages Cold Period (DACP: ca. 1.8-1.1 ka) and the Little Ice Age (LIA: ca. 0.6-0.1 ka). Contemporaneous low lake levels during these periods corresponded with respective aeolian sand flux and variable composition of mixed sediments (fluvial and aeolian) in lake deposits. Different flux rates at the core sites could be assigned to local conditions in respect to inflow behaviour of individual drainage systems and nearshore morphology. Aeolian deposits in the catchment were not always preserved and underwent re-mobilisation during succeeding episodes and/or erosion during phases of high water availability. Wetter climatic conditions during the Mid-Holocene (ca. 7.5-5.1 ka), Roman Warm Period (RWP: ca. 2.8-1.5 ka) and Medieval Climate Anomaly (MCA: ca. 0.9-0.6 ka) revealed significant lake level rise due to enhanced river discharge, well documented by highest suspended flux rates, disappearance of ostracod communities at core sites and very low sand input. Climate shifts during the Holocene were linked to variations in effective moisture supply under the influence of the Asian summer monsoon (ASM) and the interplay with the mid-latitude westerlies (MLW). Cold-dry phases were likely a response to North Atlantic climatic anomalies transmitted by the MLW across the TP.

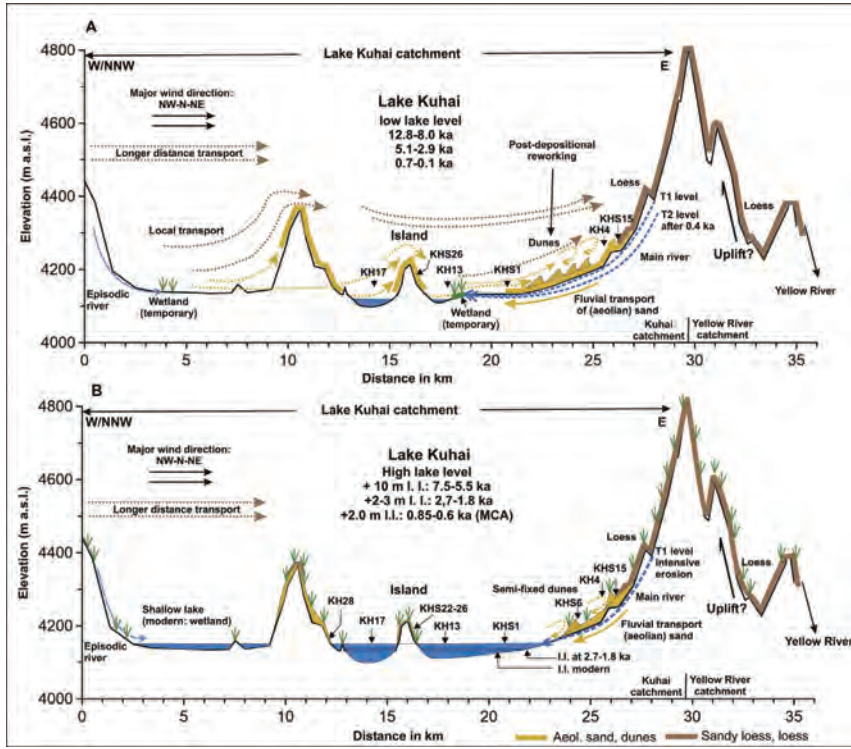


Fig. 10. Transect (sketch) across the Kuhai catchment from W/NNW to E. (A) Periods of higher lake level with reduced aeolian activity and higher river discharge/erosion (formation of terrace T1?) and (B) periods of low lake levels with stronger aeolian processes and reduced runoff. Dunes underwent several re-mobilisation phases after the early Holocene. River incision formed the terrace T2 after ca. 0.4 ka BP. Brown dotted lines with arrow indicate loess transport from local and longer distances; brown areas mark loess deposits. Yellow dotted lines with arrow indicate local sand transport; yellow areas depict aeolian sand sheets and dunes. Aeolian deposits, water depth and plant cover are unscaled. (For interpretation of the references to color in this figure legend, the reader is referred to the Web version of this article.)

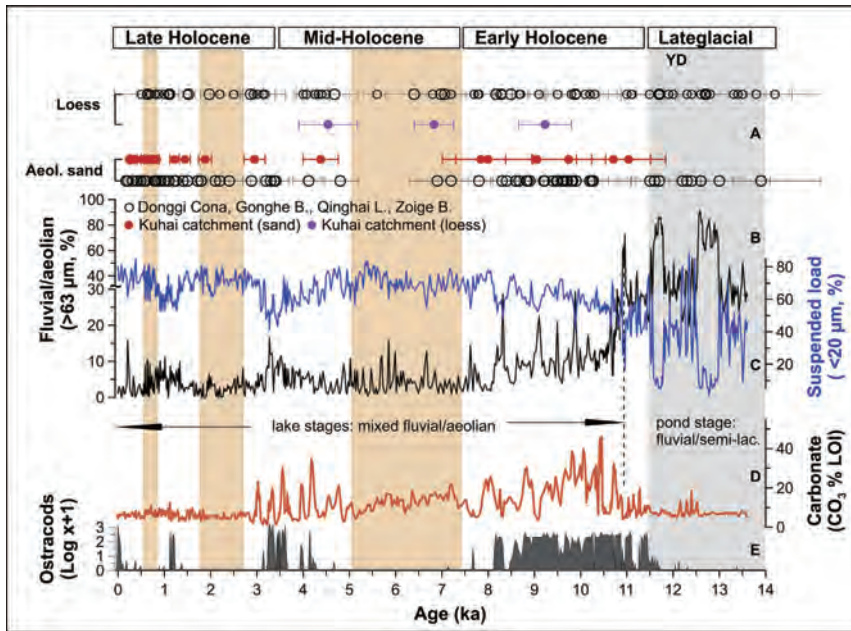


Fig. 9. (A) OSL ages from aeolian sediments (sand, loess) in sections of the Kuhai catchment in comparison with ages from adjacent regions; (B, C) grain size (fluvial/aeolian, >63 μm) and suspended load (<20 μm) records from core KH17, lake center; (D) carbonate (CO₃) content and (E) ostracod abundances. YD¼ Younger Dryas. Shaded areas (gray) mark the lateglacial period with negative water budget. Positive water balances with higher-than-present lake level refer to orange areas. (For interpretation of the references to color in this figure legend, the reader is referred to the Web version of this article.)

Role of mudflat-creek sediment exchanges in intertidal sedimentary processes

Xie W, He Q, Wang X, et al. *Journal of Hydrology*, 2018, 567:351-360.

Intertidal environments, including bare mudflats, tidal creeks, and vegetated salt marshes, are of significant physical and ecological importance in estuaries. Their morphodynamics are closely linked by mudflats and creek networks. Understanding water motion and sediment transport in mudflats and tidal creeks is fundamental to understand intertidal morphodynamics in intertidal environments. To explore dynamic interactions between tidal creeks and mudflats, we conducted field campaigns monitoring water depths, tidal currents, waves, suspended sediments, and bed-level changes at sites in both mudflats and tidal creeks in the Eastern Chongming tidal wetland in the Yangtze Delta for a full spring-neap tidal cycle. We saw that under fair weather conditions, the bed-level changes of the tidal creek site displayed a contrary trend compared with those of the mudflat site, indicating the source-sink relationship between tidal creek and mudflat. During over-marsh tides, the tidal creek site with relatively high bed shear stresses (averagely, 0.37 N/m^2) was eroded by 35mm whereas the mudflat site was accreted by 29mm under low bed shear stresses (averagely, 0.18 N/m^2). To the contrast, during creek-restricted tides, deposition occurred in the tidal creek site by 20mm under low bed shear stresses (averagely, 0.09 N/m^2) whereas erosion occurred in the mudflat site by 25mm under relatively high bed shear stresses (averagely, 0.21 N/m^2). Over a spring-neap tidal cycle, the net bed level changes were 15mm (erosion) and 4mm (deposition) in tidal creeks and mudflats, respectively. These results suggested that there were alternated erosion-deposition patterns in spring and neap tides, and a sediment source and sink shift between mudflats and creeks. We found that the eroded sediments in mudflats were transported landward into tidal creeks and deposited therein in neap tides, and these newly deposited sediments would be resuspended and transported to surrounding marshes (over-marsh deposition) at spring tides. The coherent sediment transport and associated erosion-deposition pattern within the mudflat-creek system at spring-neap tidal time scales thus played a fundamental role in intertidal morphodynamic development. These findings suggest that management and restoration of intertidal ecosystem need to take the entire mudflat-creek-marsh system as a unit into consideration rather than focusing on single elements.

潮滩是河口海岸地区重要组成部分，具有显著的社会经济价值和生态环境效益。潮滩一般由光滩、潮沟、盐沼植被带组成，其中光滩-潮沟系统在潮滩动力地貌过程中发挥着重要作用。因此，探究光滩-潮沟系统的水沙输运过程对于研究潮滩动力地貌过程尤为关键。本研究以长江口崇明东滩典型潮滩为研究对象，在光滩和潮沟分别布点观测，获取了两站点平常天气下覆盖大中小潮完整周期的水深、流速、波浪、含沙量、地形变化等数据。分析数据可知，潮沟与光滩的地形变化在潮周期内呈现相反的变化趋势：大潮期间，潮沟站平均床面剪切应力较大，达 0.37 N/m^2 ，潮沟床面侵蚀35 mm，而同期光滩站平均床面剪切应力较小，滩面淤积29 mm；小潮期间，潮沟站平均床面剪切应力较小，为 0.09 N/m^2 ，潮沟床面淤高25 mm，而小潮光滩站平均床面剪切应力相对较大，滩面冲刷25 mm；整个潮周期潮沟站净冲刷15 mm而光滩站净淤高4 mm。这些研究结果表明，指征潮沟与光滩二者间的泥沙供给在大-小潮周期内存在源汇交替互换的关系：小潮期间，光滩泥沙作为潮沟的泥沙来源，被侵蚀启动后输运至潮沟并沉积于此；大潮期间，潮沟新淤积的泥沙作为盐沼植被带的泥沙来源，通过漫滩水流输运并沉积于盐沼带，同期外海的泥沙作为光滩的泥沙来源淤积与光滩。因此，整个光滩-潮沟系统在潮周期内的泥沙输运以及相应冲淤过程决定了潮滩的动力地貌过程。基于此，本文认为研究潮滩动力地貌过程不能仅对潮滩单一地貌类型孤立研究，而应统筹光滩-潮沟-盐沼带等潮滩地貌单元开展系统研究。

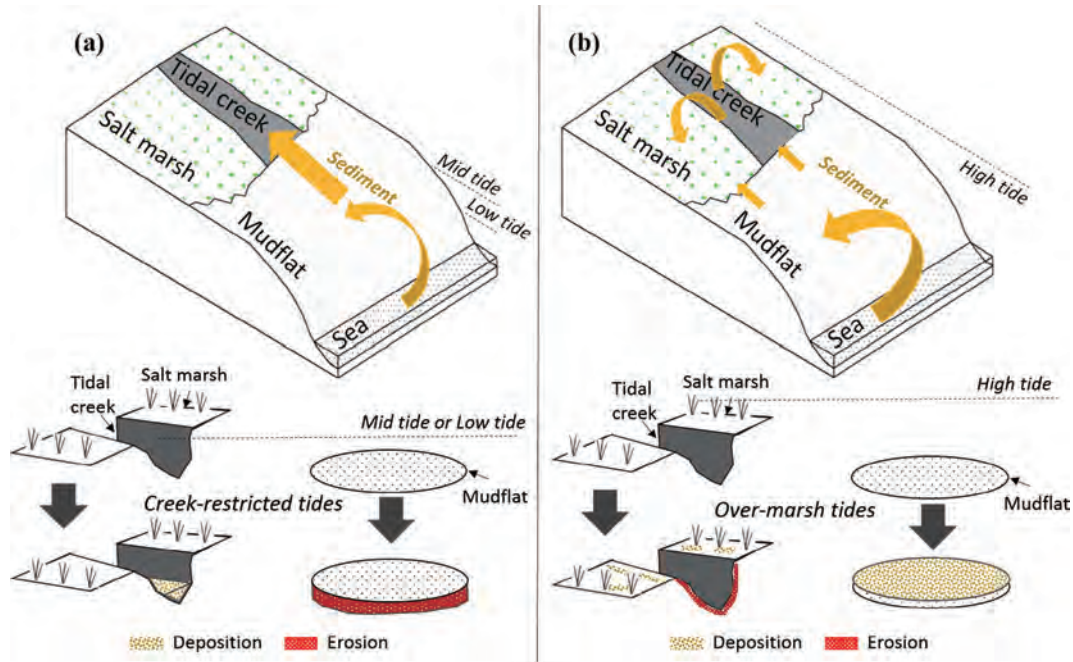


Fig. 8. Conceptual model for the sedimentary process in the intertidal environments of the Yangtze Delta under fair weather conditions, based on the mudflat-creek system. (a) during low tides (neap tides) and (b) high tides (spring tides).

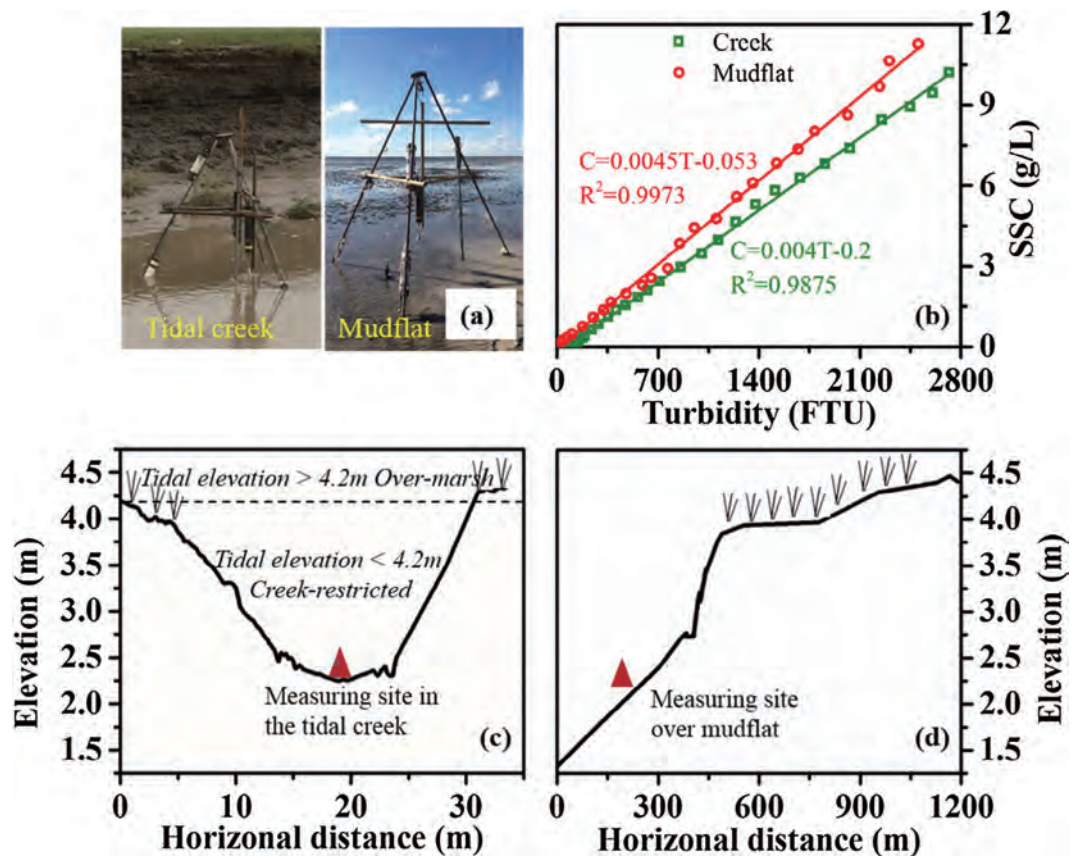


Fig. 2. (a) Measuring sites in the tidal creek (left) and the mudflat (right), (b) calibration of the optical backscatter signal with SSC data, (c) creek cross section, (d) location of the mudflat site.

Impact of tropical cyclones on the evolution of the monsoon-driven upwelling system in the coastal waters of the northern South China Sea

Zheng B, Li Y, Li J, et al. *Ocean Dynamics*, 2018, 68(2):223-237.

An upwelling system exists in the coastal waters of the northern South China Sea (NSCS), a region that is frequently affected by tropical cyclones in summer. This study investigates the evolution of the NSCS monsoon-driven upwelling system and the effects of the Talim and Doksuri tropical cyclones on the system using in situ observational data obtained at three mooring stations, one land-based meteorological station, and concurrent satellite remote sensing data for the NSCS coastal waters from May to July 2012. The results show that the occurrence and evolution of the upwelling system were mainly controlled by the Asian southwest monsoon, while the eastward current also made important contributions to the upwelling intensity. A decrease in the bottom water temperature and shifts in the along-shore and cross-shore currents were direct evidence of the establishment, existence, and recovery of this upwelling. Tropical cyclones have significant impacts on hydrodynamics and can thus influence the evolution of the NSCS upwelling system by changing the local wind and current fields. Variations in water level and local current systems impeded the development of upwelling during tropical cyclones Talim and Doksuri in the study area, which have low-frequency fluctuations of approximately 2–10 days. These variations were the results of the coupled interactions between local wind fields, coastal trapped waves, and other factors. The hydrodynamic environment of the marinewater (including coastal upwelling system) rapidly recovered to normal sea conditions after each cyclone passed due to the relatively short duration of the impact of a tropical cyclone on the dynamic environment of the waters.

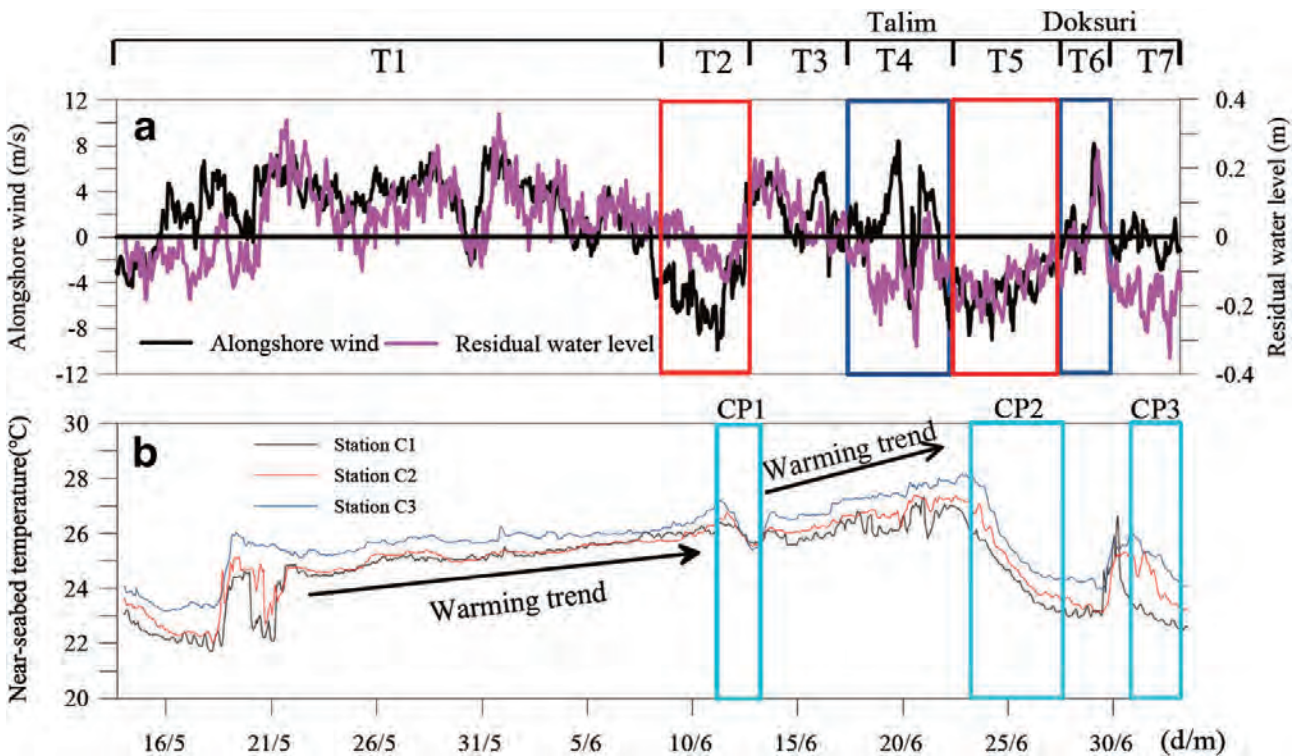


Fig. 4 Variation curves of the a alongshore wind and residual water level, and b bottom seawater temperature data obtained at the continuous observation stations between May 13 and July 3, 2012. Orange and blue boxes signify the southwesterly wind, and tropical cyclones Talim and Doksuri, respectively; and (a) light blue boxes (CP1-CP3) signify events when the bottom seawater temperature decreases (b)

Human impacts on sediment in the Yangtze River: A review and new perspectives

Yang H, Yang S, Xu K, et al. *Global and Planetary Change*, 2018, 162:8-17.

Changes in riverine suspended and riverbed sediments have environmental, ecological and social implications. Here, we provide a holistic review of water and sediment transport and examine the human impacts on the flux, concentration and size of sediment in the Yangtze River in recent decades. We find that most of the fluvial sediment has been trapped in reservoirs, except for the finest portion. Furthermore, soil-conservation since the 1990s has reduced sediment yield.

From 1956-1968 (pre-dam period) to 2013-2015 (post-dams and soil-conservation), the sediment discharge from the sub-basins decreased by 91%; in the main river, the sediment flux decreased by 99% at Xiangjiaba (upper reach), 97% at Yichang (transition between upper and middle reaches), 83% at Hankou (middle reach), and 77% at Datong (tidal limit). Because the water discharge was minimally impacted, the suspended sediment concentration decreased to the same extent as the sediment flux. Active erosion of the riverbed and coarsening of surficial sediments were observed in the middle and lower reaches. Fining of suspended sediments was identified along the river, which was counteracted by downstream erosion. Along the 700-km-long Three Gorges Reservoir, which retained 80% of the sediment from upstream, the riverbed gravel or rock was buried by mud because of sedimentation after impoundment. Along with these temporal variations, the striking spatial patterns of riverine suspended and riverbed sediments that were previously exhibited in this large basin were destroyed or reversed. Therefore, we conclude that the human impacts on sediment in the Yangtze River are strong and systematic.

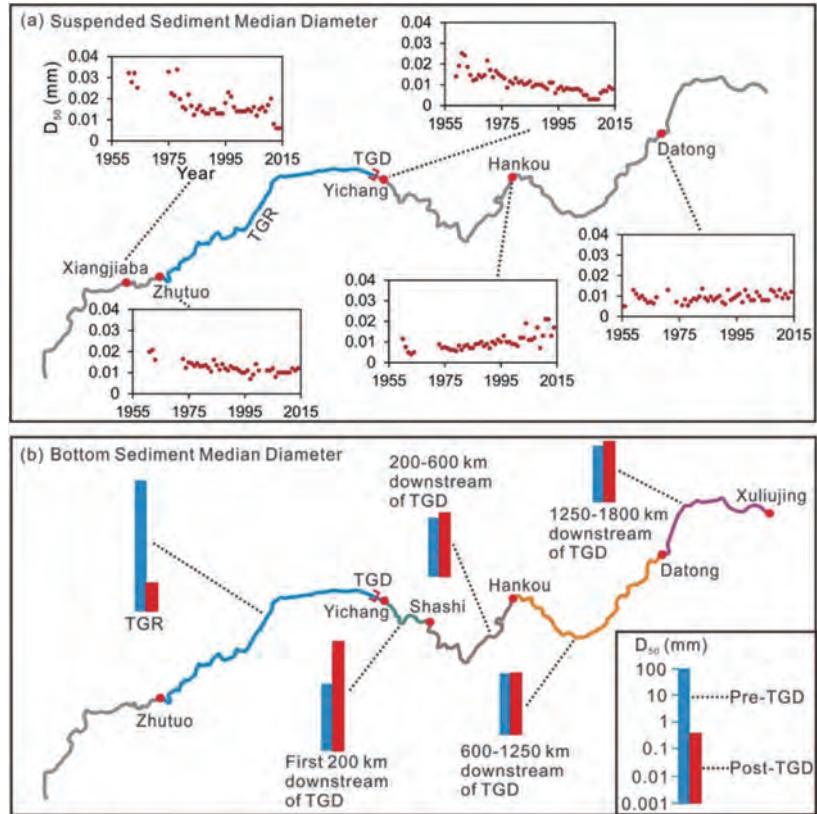


Fig. 7. Temporal changes in the grain size of sediments in the Yangtze River. (a) Annually averaged median size (D_{50}) of suspended sediments at the gauging stations. (b) Comparison of the reach-averaged D_{50} of riverbed sediments between the pre-TGD and post-TGD periods.

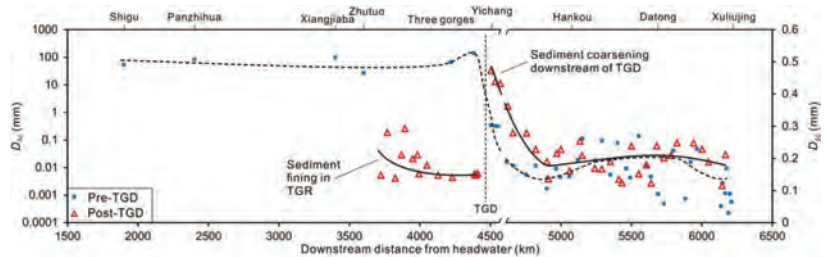


Fig. 8. Median sizes of riverbed sediments along the Yangtze River. After the impoundment of the TGR, fining of surficial sediments was found in the reservoir, whereas coarsening of surficial sediments was observed downstream of the TGD.

Recent coarsening of sediments on the southern Yangtze subaqueous delta front: A response to river damming

Yang H, Yang S, Meng Y, et al. *Continental Shelf Research*, 2018, 155:45-51.

After more than 50,000 dams were built in the Yangtze basin, especially the Three Gorges Dam (TGD) in 2003, the sediment discharge to the East China Sea decreased from 470 Mt/yr before dams to the current level of ~140 Mt/yr. The delta sediment's response to this decline has interested many researchers. Based on a dataset of repeated samplings at 44 stations in this study, we compared the surficial sediment grain sizes in the southern Yangtze subaqueous delta front for two periods: pre-TGD (1982) and post-TGD (2012). External factors of the Yangtze River, including water discharge, sediment discharge and suspended sediment grain size, were analysed, as well as wind speed, tidal range and wave height of the coastal ocean. We found that the average median size of the sediments in the delta front coarsened from 8.0 μm in 1982 to 15.4 μm in 2012. This coarsening was accompanied by a decrease of clay components, better sorting and more positive skewness. Moreover, the delta morphology in the study area changed from an overall accretion of 1.0 cm/yr to an erosion of 0.6 cm/yr. At the same time, the riverine sediment discharge decreased by 70%, and the riverine suspended sediment grain size increased from 8.4 μm to 10.5 μm . The annual wind speed and wave height slightly increased by 2% and 3%, respectively, and the tidal range showed no change trend. Considering the increased wind speed and wave height, there was no evidence that the capability of the China Coastal Current to transport sediment southward has declined in recent years. The sediment coarsening in the Yangtze delta front was thus mainly attributed to the delta's transition from accumulation to erosion which was originally generated by river damming. These findings have important implications for sediment change in many large deltaic systems due to worldwide human impacts.

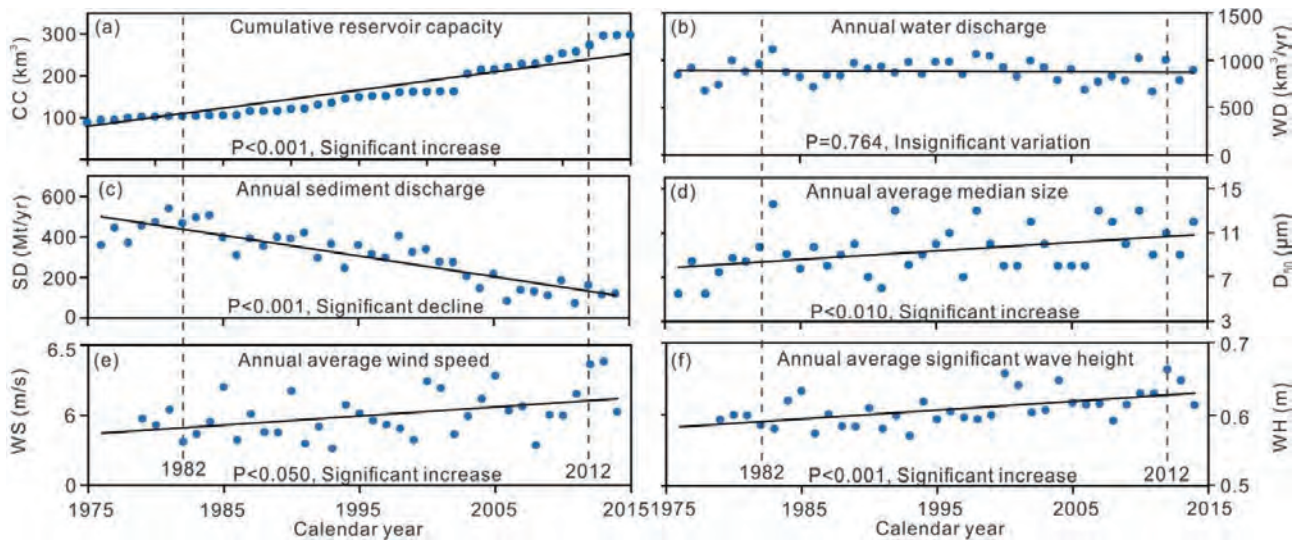


Fig. 5. Scatter plots showing the cumulative reservoir storage capacity (a), annual water discharge (b), annual sediment discharge (Mt/yr) (c) and annual average median size (d) at Datong Station; annual average wind speed (e) and annual average significant wave height (f) at Dajishan Station. CC: Cumulative capacity, WD: water discharge, SD: sediment discharge, D50: median size, WS: wind speed and WH: wave height.

The influence of seasonal climate on the morphology of the mouth-bar in the Yangtze Estuary, China
Zhang M, Townend I, Cai H, et al. *Continental Shelf Research*, 2018, 153:30-49.

The geomorphology of the Yangtze Estuary in the Changjiang River Delta in Eastern China has been the subject of extensive research. This study extends previous work to examine the influence of wind-waves on the mouthbar, where about half of the river-borne material settles to the bed. The site is located just outside of Changjiang River mouth, which is meso-tidal and subject to seasonally varying river flows and wind-wave conditions. Modeling was performed with a coupled wave-current hydrodynamic model using TELEMAC and TOMAWAC and validated against observed data. Bottom Shear Stress (BSS) from river, tide and waves based on the numerical model output was used to infer the respective contribution to the evolution of the subaqueous delta. Our examination did not however extend to modeling the sediment transport or the morphological bed changes. The results suggest that (i) the dominance of river discharge is limited to an area inside the mouth, while outside, the mouth-bar is tide-wave dominant; (ii) considering just the tide, the currents on the shallow shoals are flood dominant and deep channels are ebb dominant, which induces continued accretion over the shallows and erodes the deeper parts of the mouth-bar until the tidal currents become too weak to transport sediment; (iii) whereas waves are very efficient at reshaping the shallow shoals, with the effect being subtly dependent on the depth distribution over the mouth-bar; (iv) the stability of shallow shoal morphology is highly dependent on the presence of seasonal wind-waves and characterized as “summer storing and winter erosion”, while deep channels perform like corridors of water and sediment, exporting sediment all year round. The nature of the mouth-bar response has important implications for coastal management, such as the ongoing deep water channel maintenance, reclamations and coastal defense measures.

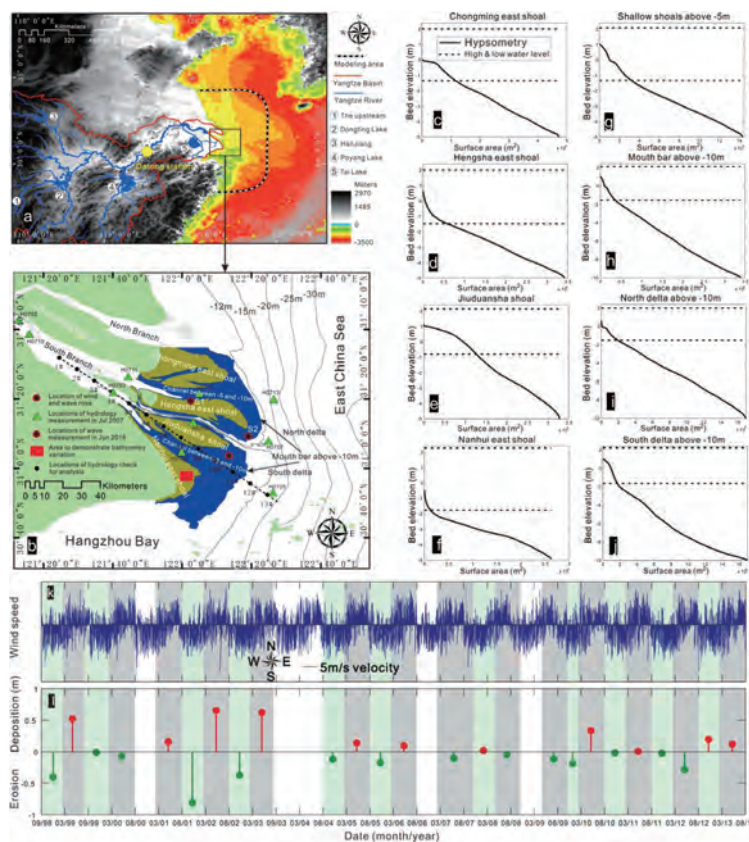


Fig. 1. (a) Location map and bathymetry for the east coast of China; (b) mouth of the Yangtze showing the regional enlarged map of mouth-bar area (blue and yellow colors), the locations of field hydrology measurement (green triangle) in July 2007, June 2016, location of wind and wave rose, and seasonal bathymetry validation (red square) from September 1998 to August 2013; (c-j) bed hypsometry for the areas denoted in (b); (k) wind vector off Nanhui coast; (l) averaged erosion and deposition thickness over the red square frame denoted in (b) derived from subtraction of consecutive bathymetry maps in the time series, positive (red) is deposition and negative (green) is erosion. The colored background indicates the duration of changes that happened, in which gray is around the summer season and green is around the winter season (for the data available, the duration is not strictly following summer-winter division). (For interpretation of the references to color in this figure legend, the reader is referred to the web version of this article.)

海岸动力地貌与动力沉积过程 *Coastal Morphodynamics and Sedimentary Process*

Mega estuarine constructions modulate the Changjiang River plume extension in adjacent seas

Wu H, Wu T, Bai M. *Estuaries and Coasts*, 2018, 41(5):1234-1252.

Mega constructions have been built in many river estuaries, but their environmental consequences in the adjacent coastal oceans are not well understood. This issue was addressed with an example of the Changjiang River Estuary, where massive navigation and reclamation constructions were recently built on the tidal flats that separate the three major outlets. Based on numerical model twin validations against data from eight cruises and the scenario simulations, we found that the estuarine constructions have profoundly affected the plume extension and the associated physical stratification in a surprisingly large area. Before the constructions were built, the water masses in the two southern outlets were transported across the tidal flats to the northern outlet by the lateral tidal residual transports. However, this lateral exchange was gradually blocked as the constructions were built, so the freshwater in the two southern outlets now exits the river mouth directly. The overall effect is that the northeastward offshore plume extension has been weakened, whereas the southward along-shelf plume extension has been strengthened. The ecological consequences of this shift in plume regime are speculated. Previously, the Three Gorges Dam (TGD) was thought to be responsible for some offshore environmental changes by modulating the river plume, but our results show that its effects on the river plume characteristics are secondary. The TGD and the mega estuarine constructions were built during a similar period; hence, their influences need to be reconsidered.

世界上许多河口都建造有大型河口工程，但这些工程对邻近海域的环境影响尚未被深入研究。对此问题，本文以长江河口重大工程为例，研究其对邻近海域的影响。近些年来，长江河口的滩涂上进行了大规模的深水航道和滩涂围垦建设，这些河口工程将长江河口的三个主要水道分隔开来。基于数值模型结果对8次走航观测数据的孪生验证，本文发现长江河口工程对很大区域内的长江冲淡水扩展形态及其在邻近海域形成的垂向层化产生了深远影响。在建造工程之前，南槽和北槽的淡水可以通过横向潮余运输越过滩涂进入北港。然而，随着河口工程的建造，这种横向交换逐渐被切断，因此现在南槽和北槽的所有淡水都直接从对应的口门流出。河口工程的总体效果是削弱了冲淡水向东北方向的离岸扩展，而加强了其南向的沿岸扩展。这种冲淡水扩展状态的转变可能会带来深远的生态影响。以往的研究认为，三峡工程是调整长江冲淡水扩展形势进而影响长江河口及邻近海域生态环境的主要因素。但本文的结果显示三峡工程对长江冲淡水扩展形态的影响是次要的。三峡工程和河口工程是在同一时期建设的，因此，研究人员需要重新考量它们对长江河口及其邻近海域的影响。

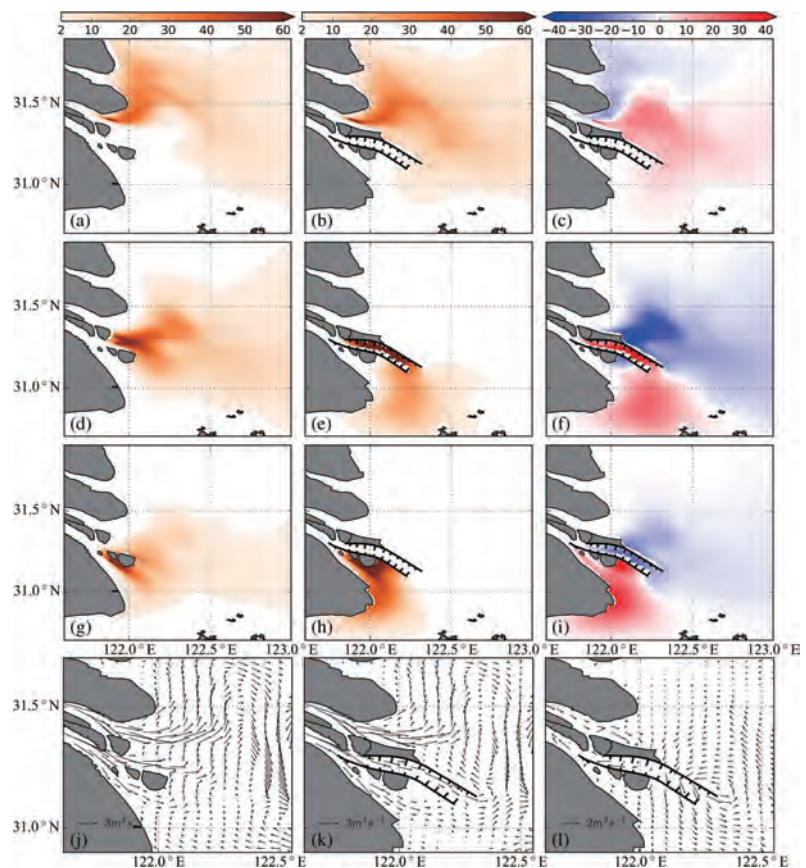


Fig. 11 Passive tracer movements 8 days after being released in the North Channel (a, b), North Passage (d, e), and South Passage (g, h), during the spring tide in July, without (a, d, g) and with (b, e, h) the estuarine constructions, respectively. Their differences ("with" minus "without") are shown in c, f, and i. Residual transports during the spring tide in July are shown in j and k for the simulations without and with the estuarine constructions, respectively, and their difference is shown in l

Winter Counter-Wind Transport in the Inner Southwestern Yellow Sea

Wu H, Gu J, Zhu P. *Journal of Geophysical Research Oceans*, 2018, 123(1):411-436.

Coastal currents generally flow downshelf with land on the right side (Northern Hemisphere) under the geostrophic balance, and are often strengthened by downwelling-favorable winds. However, the recent mooring observation in the inner southwestern Yellow Sea showed that coastal transport direction can be substantially changed by tidal forcing. In the survey, the tidal-averaged transports at two out of three sites remained northward (i.e., in the upshelf direction) and opposite the downwelling-favorable northerly wind, except during a brief neap tide period. Numerical experiments showed that the incoming Poincaré wave tide from the East China Sea plays a key role in forming this counter-wind transport system. This tidal wave produces a shoreward tidal stress south of 33.5°N in the inner southwestern Yellow Sea, driving an upshelf transport under the Earth's rotation. Counterpropagating tidal waves from the East China Sea and the northern Yellow Sea collide in coastal water in 32.5–34°N, which produce a standing tidal wave and therefore a mean sea-surface setup with alongshore and cross-shelf scales of both >100 km. This seasurface setup causes an alongshore sea surface gradient, which veers the upshelf transport to the offshore direction under geostrophic balance. The strong tidal current increases the tidal-mean bottom resistance in the SCW, thus reduces the wind-driven current to a magnitude smaller than the tide-induced residual transport velocity. Therefore, upshelf transport persists in the inner southwestern Yellow Sea, and the Changjiang River Estuary becomes a major source area for the inner southwestern Yellow Sea.

该研究发现，冬季西南黄海（也称作苏北水域）近岸的苏北沿岸流方向为逆风北向，而不是传统观点认为的顺风南下。这一新发现改变了关于长江口与苏北海域之间源汇关系的认识，从而有可能对研究长江入海物质归宿和苏北海域环境灾害背后驱动因子等提供新的思路。传统观点认为，受地球自转科氏力和偏北东亚季风的影响，冬季苏北水域存在南向的苏北沿岸流。然而，以往由于该水域地形复杂、潮流强劲、风浪较大、观测困难，直接测流数据较少，关于此沿岸流的认识在一定程度上是一种推断。2017年1月，在国家自然科学基金委员会项目的支持下，河口海岸学国家重点实验室科研人员在苏北水域投放了3个座底三脚架观测系统，对该海域的水体输送进行了为期约20天的连续观测。观测期间覆盖了完整的大小潮周期，经历了数次强烈的寒潮北风天气，因此结果可以反应典型冬季气象条件下的沿岸流特征。

观测结果显示，虽然近表层非常薄的水体的运动方向受风向影响，但绝大多数时间垂向整体的潮平均输送速度（即余流）为沿岸北上，即使在强北风气象条件下也是如此。从传统物理海洋学观点看，这一北向沿岸流与地球自转效应和风生流方向均相反，为“逆向”，但它却与苏北水域长期存在低盐水和来自长江的营养盐泥沙物质的观测事实相符。北向沿岸流主要在近岸，在外侧的测点（离岸约50 km）余流方向开始偏东北。只有在小潮期间短暂的两天沿岸流方向才与风向一致为向南流动。进一步数值模拟显示，苏北近岸水域的北向沿岸流发端于长江口，延伸至废黄河口南侧水域，然后与海州湾内南向沿岸流辐合后转为离岸运动。

为了解释这一北向沿岸流的物理机制，该研究首先用数值模拟的方法再现了观测期间的物理过程。在此基础上分析发现，产生北向沿岸流的关键在于向岸潮波造成了指向海岸的潮汐应力(tidal stress)，它与科氏力平衡后造成了北向的潮平均输送。研究发现，只有向岸潮波才能造成这种逆向沿岸运动，而常见的以Kelvin波形式存在的顺岸潮波则不会。因此，苏北水域北向沿岸流的生成与该区域独特的潮波特征有关。该研究进一步探讨了风生流和潮流的联合作用机制，发现由于海底摩擦的非线性，潮流作用下有效底摩擦迅速增加，导致了潮流环境下风生流的显著减弱。以上两个机制联合作用，造成冬季偏北季风下苏北海域的沿岸流方向为逆风北上。仅在小潮期间的少数几天潮汐作用减弱，沿岸流方向才转为和风向一致。夏季盛行偏南风，可以推断苏北沿岸流方向依然为北向，甚至更强，数值模拟的结果也证实了这一点。

进一步，研究人员利用数值模拟量化了长江对苏北水域的影响程度。结果表明，在33.5°N以南的苏北水域长江是主要的淡水来源，34.5°N以北地方河流是主要淡水来源，在两者之间则受到两个来源的共同影响。长江冲淡水抵达苏北海域的动力机制就是上述的北向潮致沿岸流。总体而言，冬季苏北海域70%的冲淡水来自长江，夏季这一比例则上升到了80%。苏北水域长江淡水含量的峰值要落后于长江径流峰值约2个月。在秋冬季节，苏北水域的长江冲淡水主要为前期长江冲淡水的残留，受北向沿岸流的影响得以维持。

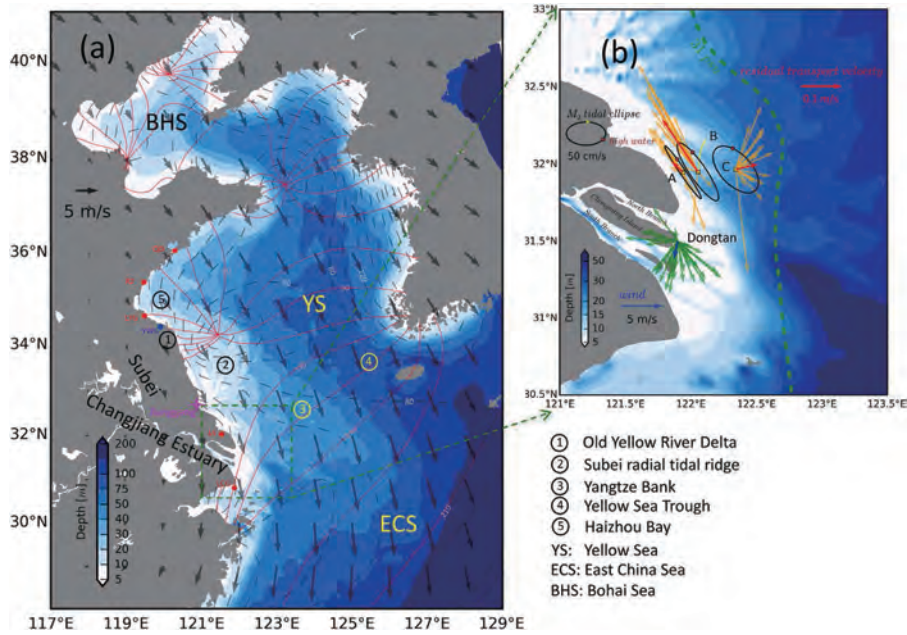


Figure 1. (a) Map and bathymetry of the East China Sea and the Yellow Sea. Solid contours are cophase lines for the M2 tide with an interval of 308, and dashed contours are the co-amplitude lines with an interval of 20 cm, which are both digitized from Editorial Board for Marine Atlas (1992). Vectors signify the climatological wind in January. QD (Qingdao), RZ (Rizhao), LYG (Lianyungang), YWG (Yanweigang), LS (Lvsi), and LCG (Luhaogang) are the tidal gauge stations. (b) Three tripod sites (A, B, and C) and their measured residual transport velocities (orange arrows for daily values and red arrows for the record-means). The M2 tidal ellipses at three sites are shown, with the high-water times relative to the tidal current phases are marked on the ellipses. The rotations of the tidal ellipses are clockwise. Green arrows and a blue arrow denote the daily and record-mean wind vectors, respectively. The green-dashed line represents the climatological 31 psu contour in January (Editorial Board for Marine Atlas, 1992).

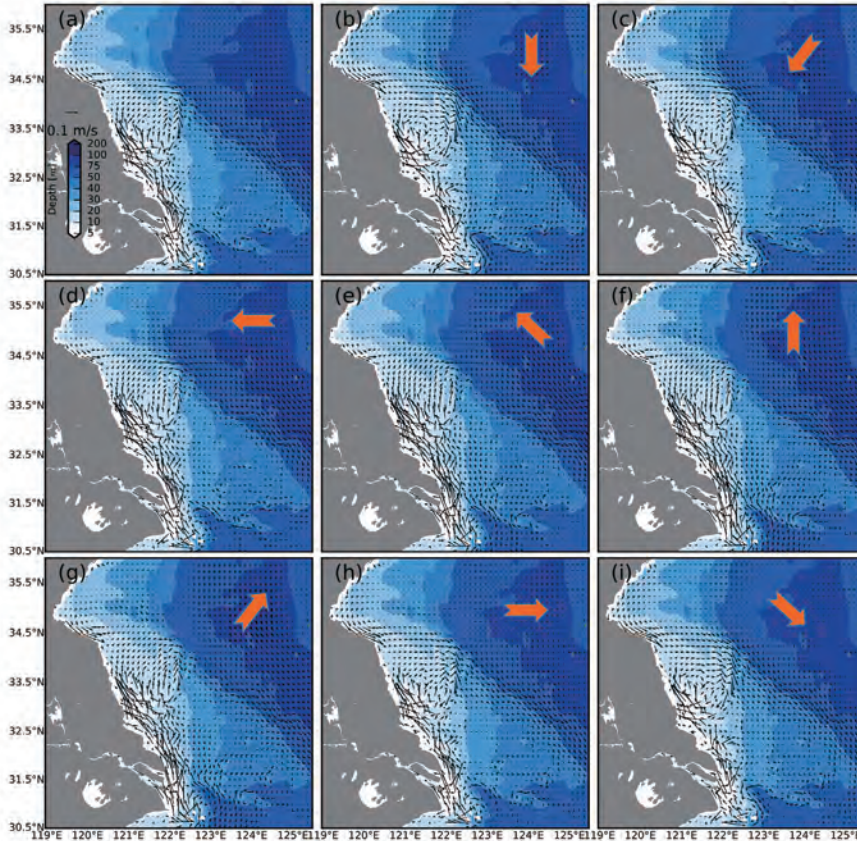


Figure 8. Modeled residual transport velocity under tide only (a) and under both tide and wind ((b)–(i)) during spring tide. The wind speed is 6 m/s; the wind directions are labeled on each panel.

Shoreline dynamics of the active Yellow River delta since the implementation of Water-Sediment Regulation Scheme: A remote-sensing and statistics-based approach

Fan Y, Chen S, Zhao B, et al. *Estuarine, Coastal and Shelf Science*, 2018, 200:406-419.

The Active Yellow River (Huanghe) Delta (AYRD) is a complex landform in which rapid deposition takes place due to its geologic formation and evolution. Continuous monitoring of shoreline dynamics at hightemporal frequency is crucial for understanding the processes and the driving factors behind this rapidly changing coast. Great efforts have been devoted to map the changing shoreline of the Yellow River delta and explain such changes through remote sensing data. However, the temporal frequency of shoreline in the obtained datasets are generally not fine enough to reflect the detailed or subtly variable processes of shoreline retreat and advance. To overcome these limitations, we continuously monitored the dynamics of this shoreline using time series of Landsat data based on tidal-level calibration model and orthogonaltransect method. The Abrupt Change Value (ACV) results indicated that the retreat-advance patterns had a significant impact regardless of season or year. The Water-Sediment Regulation Scheme (WSRS) plays a dominant role in delivering river sediment discharge to the sea and has an impact on the annual average maximum ACV, especially at the mouth of the river. The positive relationship among the average ACV, runoff and sediment load are relatively obvious; however, we found that the Relative Exposure Index (REI) that measures wave energy was able to explain only approximately 20% of the variation in the data. Based on the abrupt change at the shoreline of the AYRD, river flow and time, we developed a binary regression model to calculate the critical sediment load and water discharge for maintaining the equilibrium of the active delta from 2002 to 2015. These values were approximately 0.48×10^8 t/yr and 144.37×10^8 m³/yr. If the current water and sediment proportions released from the Xiaolangdi Reservoir during the WSRS remain stable, the erosion-accretion patterns of the active delta will shift from rapid accretion to a dynamic balance.

黄河三角洲大冲大淤，堆积快速，演变复杂。高时间频率连续的岸线动态监测，对于理解快速变化中的黄河三角洲海岸的精细演变过程和动力机制至关重要，特别是可以揭示黄河调水调沙短期行为对河口海岸的影响。根据潮位标定模型和正交断面方法，我们建立了一个新的岸线指标方法。基于系列高分辨率遥感影像和新的岸线指标，研究了2002年黄河调水调沙以来至2015年现行河口岸线精细演变过程，定量评估了调水调沙对河口海岸的影响。并根据现行黄河口岸线的突变、径流量和时间，我们建立了一个二元回归模型，计算得出维持现行河口冲淤平衡的临界年输沙量为0.48亿吨，临界年径流量144亿立方米。现行黄河三角洲的冲淤格局已由快速淤涨向动态平衡转变。

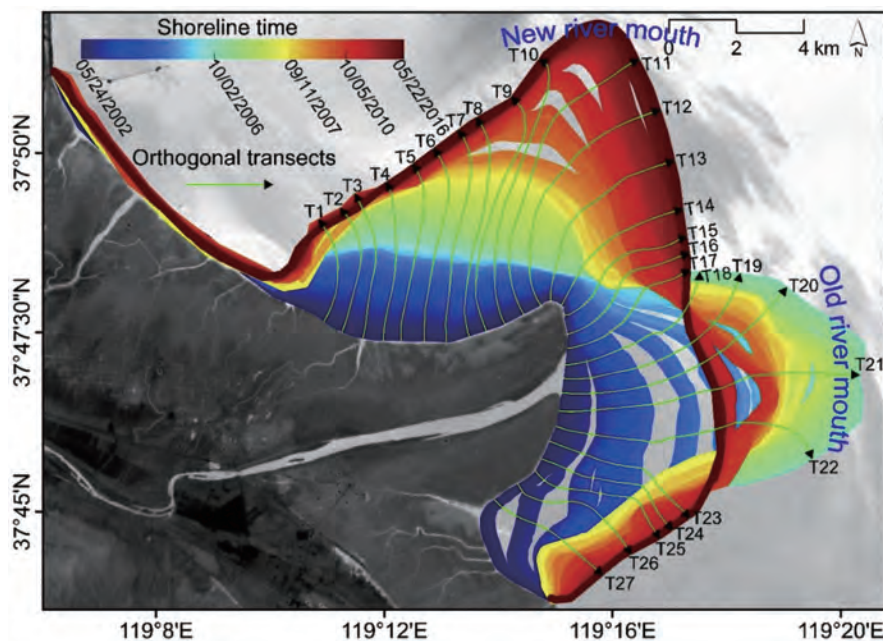


Fig. 5. Shoreline dynamics in active delta from May 2002 to May 2016. A total of 27 orthogonal transects were created at 500 m spacing. Landsat 5 TM, acquired on May 24, 2002, combine the base map.

Middle Holocene marine flooding and human response in the south Yangtze coastal plain, East China

Wang Z, Ryves D B, Lei S, et al. *Quaternary Science Reviews*, 2018, 187:80-93.

Coastal flooding catastrophes have affected human societies on coastal plains around the world on several occasions in the past, and are threatening 21st century societies under global warming and sealevel rise. However, the role of coastal flooding in the interruption of the Neolithic Liangzhu culture in the lower Yangtze valley, East China coast has been long contested. In this study, we used a well-dated Neolithic site (the Yushan site) close to the present coastline to demonstrate a marine drowning event at the terminal stage of the Liangzhu culture and discuss its linkage to relative sea-level rise. We analysed sedimentology, chronology, organic elemental composition, diatoms and dinoflagellate cysts for several typical profiles at the Yushan site. The field and sedimentary data provided clear evidence of a palaeotyphoon event that overwhelmed the Yushan site at ~2560 BCE, which heralded a period of marine inundation and ecological deterioration at the site. We also infer an acceleration in sea-level rise at 2560-2440 BCE from the sedimentary records at Yushan, which explains the widespread signatures of coastal flooding across the south Yangtze coastal plain at that time. The timing of this mid-Holocene coastal flooding coincided with the sudden disappearance of the advanced and widespread Liangzhu culture along the lower Yangtze valley. We infer that extreme events and flooding accompanying accelerated sea-level rise were major causes of vulnerability for prehistoric coastal societies.

海岸带的水涝灾害是21世纪所面临的重大风险之一。在人类历史上，新石器文化期间，海岸带的古人类社会可能也曾经因为水涝灾害发生文化衰变。本研究利用一个位于当前海岸线附近的新石器文化遗址-鱼山遗址的高分辨率地层记录，探讨了良渚文化末期的一次海水浸淹事件及其与海平面上升的关系。本研究进行了沉积学、年代学、有机地球化学和微体古生物学等多项分析，研究结果揭示了一次发生于公元前约2560年（距今约4500年）的超强台风事件以及其后长时间的海水入侵和生态破坏。鱼山遗址的地层记录还指示了公元前2560-2440年期间的一次海平面加速上升事件，从而解释了该时间段长江口滨海平原普遍存在的水涝现象。这次大规模的水涝灾害在时间上与良渚文化的突然衰变非常吻合，因此我们推测，海平面上升和极端事件导致的海岸带水涝灾害是长江三角洲史前人类社会瓦解的重要原因。

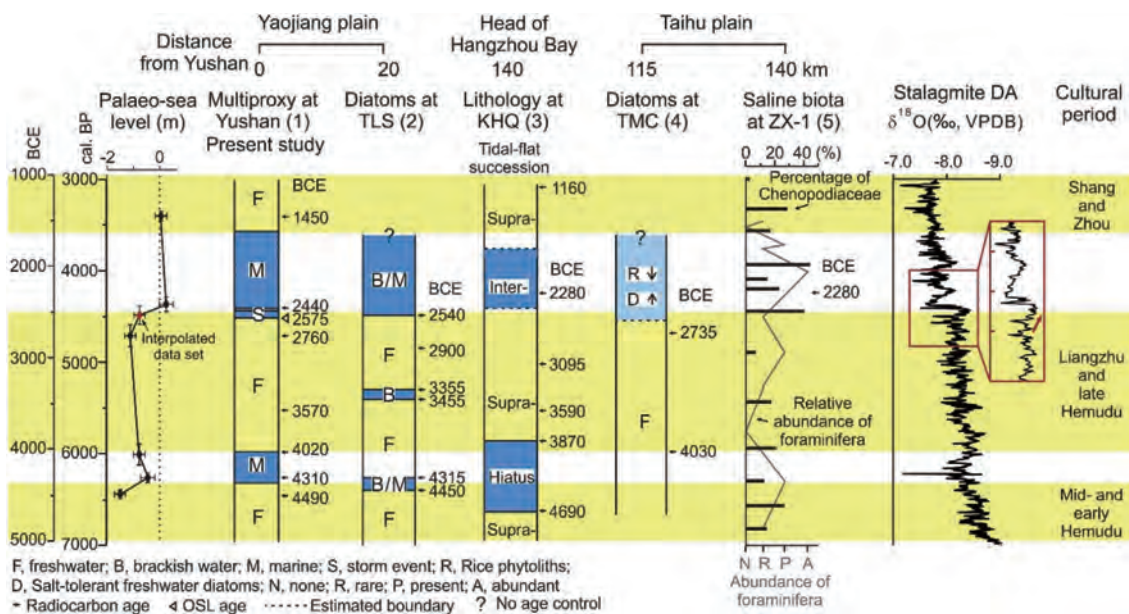


Fig. 6. Comparison of the relative sea-level change and regional marine flooding records on the south Yangtze coast from the Yaojiang and Taihu plains and the head of Hangzhou Bay. In the sea-level curve, calibrated radiocarbon ages are presented with error bars of 2s; horizontal error bars represent the indicative meaning (range of relative sea level) of each sea-level indicator. The interpolated data point is calculated from the data set derived from the estimated storm age and original peat top (Table 4; see text for details). Sediment profiles are numbered as in Fig. S2 (with increasing distance from Yushan); data sources are given in Tables 4 and S2. The oxygen isotopic record ($\delta^{18}\text{O}$) of stalagmite DA from Dongge Cave (the cave location is marked in Fig. 1A; Wang et al., 2005) denotes a short period of strengthening, yet variable, Asian summer monsoon linked to the warming climate (denoted by the red arrow) during the latter stages of the Liangzhu culture. (For interpretation of the references to colour in this figure legend, the reader is referred to the Web version of this article.)

Mid- to late Holocene geomorphological and hydrological changes in the south Taihu area of the Yangtze delta plain, China

Chen T, Ryves D B, Wang Z, et al. *Palaeogeography Palaeoclimatology Palaeoecology*, 2018, 498:127-142.

The Taihu Plain of the Lower Yangtze valley, China was a centre of rice agriculture during the Neolithic period. Reasons for the rapid development of rice cultivation during this period, however, have not been fully understood for this coastal lowland, which is highly sensitive to sea-level change. To improve understanding of the geomorphological and hydrological context for evolution of prehistoric rice agriculture, two sediment cores (DTX4 and DTX10) in the East Tiaoxi River Plain, south Taihu Plain, were collected, and analysed for radiocarbon dating, diatoms, organic carbon and nitrogen stable isotopes ($\delta^{13}\text{C}$ and $\delta^{15}\text{N}$), grain size and lithology. These multiproxy analyses revealed that prior to ca. 7500 cal. yr BP, the East Tiaoxi River Plain was a rapidly aggrading high-salinity estuary (the Palaeo-Taihu Estuary). After ca. 7500 cal. yr BP, low salinity conditions prevailed as a result of strong Yangtze freshwater discharge. Subsequently, seawater penetration occurred and saltmarsh developed between ca. 7000 and 6500 cal. yr BP due to accelerated relative sea-level rise. This transgression event influenced a large area of the Taihu Plain during the Holocene, as shown by multiple sediment records from previous studies. Persistent freshwater marsh (or subaerial land) formed due to dramatic shrinkage/closure of the Palaeo-Taihu Estuary after ca. 5600 cal. yr BP when sea level was relatively stable. We speculate that geomorphological and hydrological changes of the East Tiaoxi River Plain played an important role in agricultural development across the Taihu Plain during the Neolithic period. The closure of the Palaeo-Taihu Estuary and the formation of stable freshwater marsh (or subaerial land) after ca. 5600 cal. yr BP were critical preconditions encouraging the rapid rise of rice productivity in the Liangzhu period (5500–4500 cal. yr BP). This development changed the landscape and river systems, and thus provided adequate freshwater supply to the Taihu Plain.

本研究通过对太湖平原西南部两个钻孔测年、硅藻、有机地球化学等分析，以揭示古太湖湾的水文地貌环境演变过程及其对太湖平原新石器文明发展的影响。研究结果显示，距今7500年前，古太湖湾为高盐度的古海湾，7500年以来，在长江径流影响下，盐度降低；但是在距今7000-6500年前的某个时候，受海平面上升影响，盐度再次增大，太湖平原西侧大面积成为盐沼环境；直到大约距今5600年前，古太湖湾明显萎缩，成为淡水湖沼平原，从而极大地丰富了太湖平原的淡水和土地资源，为该区良渚文化及其稻作农业的高度发展提供了重要的环境条件。

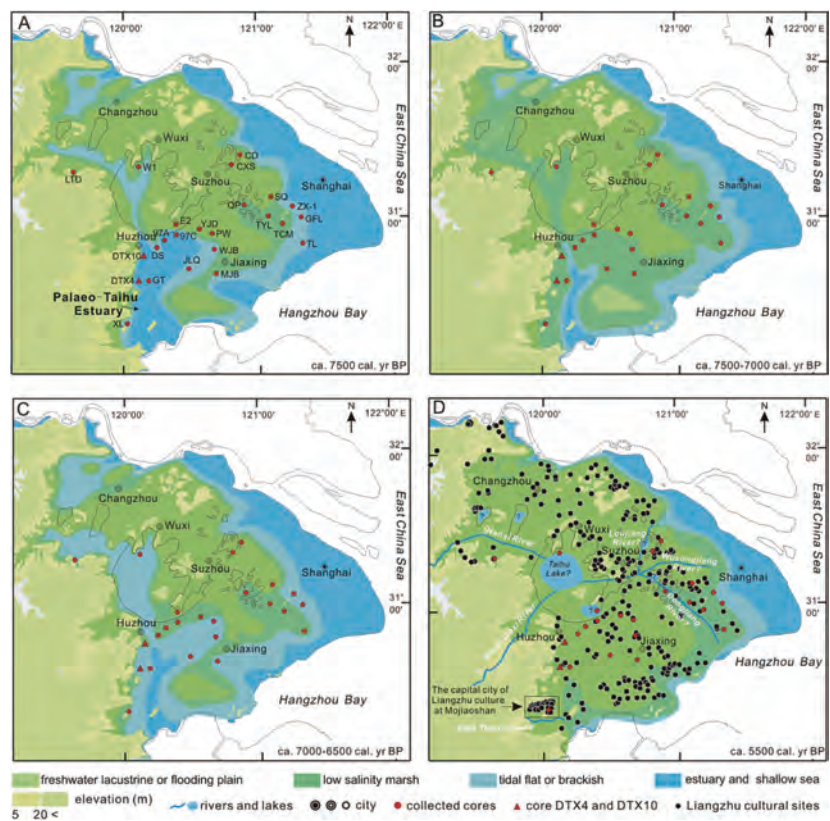


Fig. 9. Palaeogeographic map for the Taihu Plain before ca. 7500 cal. yr BP (A), during ca. 7500–7000 cal. yr BP (B), during ca. 7000–6500 cal. yr BP (C), and at ca. 5500 cal. yr BP (D). Rivers in (D) are based on Hong (1991), and the possible formation of Taihu Lake is based on Wang et al. (2001). The number of Liangzhu (5500–4500 cal. yr BP) cultural sites grew rapidly to 461, while it is only 78 and 93 during the Majiabang (7000–5800 cal. yr BP) and Songze (5800–5500 cal. yr BP) period, respectively (from Zheng, 2002; Chen, 2002; Xu, 2015).

Impact of the bottom drag coefficient on saltwater intrusion in the extremely shallow estuary

Lyu H, Zhu J. *Journal of Hydrology*, 2018, 557:838-850.

The interactions between the extremely shallow, funnel-shaped topography and dynamic processes in the North Branch (NB) of the Changjiang Estuary produce a particular type of saltwater intrusion, saltwater spillover (SSO), from the NB into the South Branch (SB). This dominant type of saltwater intrusion threatens the winter water supplies of reservoirs located in the estuary. Simulated SSO was weaker than actual SSO in previous studies, and this problem has not been solved until now. The improved ECOM-si model with the advection scheme HSIMT-TVD was applied in this study. Logarithmic and Chézy-Manning formulas of the bottom drag coefficient (BDC) were established in the model to investigate the associated effect on saltwater intrusion in the NB. Modeled data and data collected at eight measurement stations located in the NB from February 19 to March 1, 2017, were compared, and three skill assessment indicators, the correlation coefficient (CC), root-mean-square error (RMSE), and skill score (SS), of water velocity and salinity were used to quantitatively validate the model. The results indicated that the water velocities modeled using the Chézy-Manning formula of BDC were slightly more accurate than those based on the logarithmic BDC formula, but the salinities produced by the latter formula were more accurate than those of the former. The results showed that the BDC increases when water depth decreases during ebb tide, and the results based on the Chézy-Manning formula were smaller than those based on the logarithmic formula. Additionally, the landward net water flux in the upper reaches of the NB during spring tide increases based on the Chézy-Manning formula, and saltwater intrusion in the NB was enhanced, especially in the upper reaches of the NB. At a transect in the upper reaches of the NB, the net transect water flux (NTWF) is upstream in spring tide and downstream in neap tide, and the values produced by the Chézy-Manning formula are much larger than those based on the logarithmic formula. Notably, SSO during spring tide was 1.8 times larger based on the Chézy-Manning formula than that based on the logarithmic formula. The model underestimated SSO and salinity at the hydrological stations in the SB based on the logarithmic BDC formula but successfully simulated SSO and the temporal variations in salinity in the SB using the Chézy-Manning formula of BDC.

长江河口北支盐水倒灌南支是一个独特的现象，也是南支水源地的最大威胁。以往的数值模拟中存在着北支倒灌盐通量大潮期间偏小、中期和小潮期间偏大的现象，一直难于解决，是盐水入侵数值预报误差的主要来源。对一般河口和陆架水域，底摩擦拖曳系数采用对数率公式，但北支为超浅的河道，水深特浅，落潮期间大量滩涂出露，基于底边界层的对数率可能不再适用。

针对这个难题，实验室于2017年2月在北支开展了8点座底系统和半小时垂向OBS剖面定点观测，分小潮、小潮后中潮、大潮和大潮后中潮4个潮型，每个潮型连续观测至少3天，获得了高质量的流速、流向和盐度等资料。针对北支

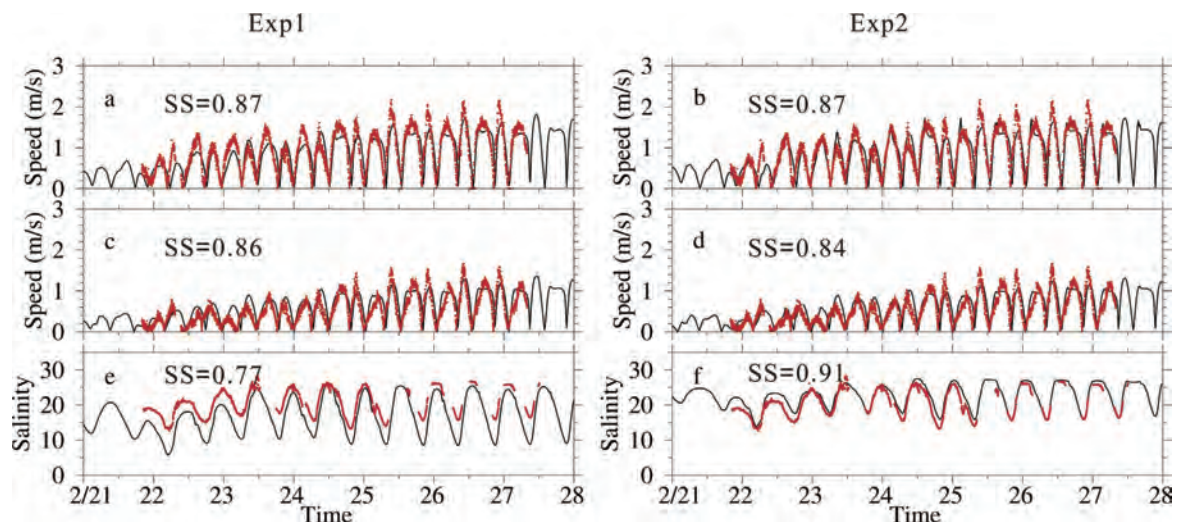


Fig. 6. Comparisons between the modeled data (blank line) and observed data (red dots) at measured station G in Exp1 (left panel) and in Exp2 (right panel). a, b: surface current velocity; c, d: bottom current velocity; e, f: surface salinity. (For interpretation of the references to colour in this figure legend, the reader is referred to the web version of this article.)

超浅河道的特点，提出底摩擦拖曳系数需采用随水深变化的谢才-曼宁公式。应用长江河口盐水入侵三维数值模式和上述实测资料，采用底摩擦拖曳系数为对数率公式和随水深变化的谢才-曼宁公式，对模式作严格验证，结果表明底摩擦拖曳系数采用谢才-曼宁公式大幅提升了盐度计算精度。

进一步从底摩擦拖曳系数在大潮和小潮期间最高潮位和最低潮位时刻的分布、单宽余通量分布、北支横断面盐通量、大潮和小潮期间涨憩盐度分布，详细分析和揭示了底摩擦拖曳系数在北支盐水入侵中的作用。底拖曳系数在落潮期间随水深减小而增大，基于谢才-曼宁公式的结果比基于对数率的结果要小。基于谢才-曼宁公式计算的北支上段向陆净水通量大潮期间增加，北支盐水入侵增强，特别在北支上段。在北支上段横断面，净断面水通量大潮期间向下游，小潮期间向上游，由谢才-曼宁公式产生的值远比基于对数率公式得到的值大。值得注意的，基于谢才-曼宁公式计算的大潮期间北支盐水倒灌比基于对数率公式计算的值大1.8倍。基于对数率公式模式低估了北支盐水倒灌和南支水文站盐度，但使用谢才-曼宁公式能成功模拟北支盐水倒灌和南支盐度随时间的变化。

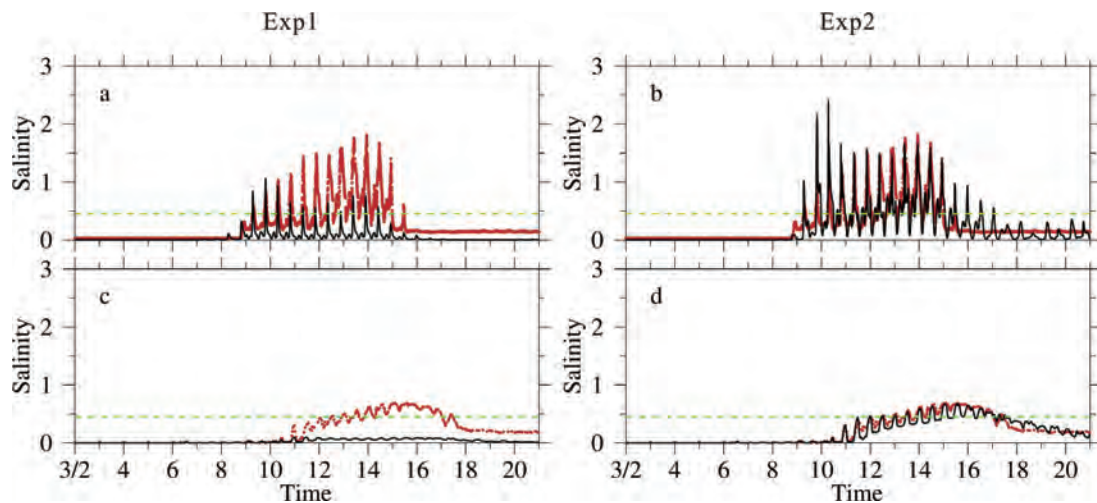


Fig. 12. Temporal variation of salinity in Exp1 (left panel) and in Exp2 (right panel) during March 2 to 20, 2016. a, b: at Chongxi hydrological station; c, d: at Nanmen hydrological station. The black line denotes modeled data and red dots denote measured data. The green dashed line is salinity 0.45, the standard of drink water. (For interpretation of the references to colour in this figure legend, the reader is referred to the web version of this article.)

Sediment accumulation and retention of the Changjiang (Yangtze River) subaqueous delta and its distal muds over the last century

Jia J, Gao J, Cai T, et al. *Marine Geology*, 2018, 401:2-16.

Mega-deltas are major sinks of river-borne sediments and important sources of terrigenous sediments for open shelves. Their evolution has far-reaching impacts on adjacent coastal waters, from the point of view of alongshelf morphodynamics and biogeochemistry. However, the complex budgeting patterns of input, storage, bypass, and final accumulation of sediment are still poorly understood. The Changjiang (Yangtze River) in China is among the world's largest river systems, not only in terms of water and sediment discharges but also the massive amount of sediment deposited in its subaqueous delta and distal muds. Here we discuss about the along-shelf sediment redistribution in the Changjiang Subaqueous Delta and Distal Mud (CSDDM) over the last century. For the purpose of understanding its spatial diversity in detail, we divided the study area into three spatially connected parts, namely the Changjiang subaqueous deltaic mud (CJM), the Zhejiang inner-shelf mud (ZJM), and the Fujian inner-shelf mud (FJM). The concept of sediment retention index helps understand the overall evolution of this mega-delta. Hydrological survey data from the peripheral rivers and short marine-sediment cores are used to evaluate the amount of sediment supplied to and deposited in the study area. The results show that over the last century, the rate of sediment supply to the CSDDM reached $\sim 645 \text{ Mt year}^{-1}$ on average (ranging between 535 and 725 Mt year^{-1}), while the total sediment deposition in the CSDDM reached $\sim 683 \text{ Mt year}^{-1}$ on average ($390\text{--}976 \text{ Mt year}^{-1}$), with the ratio for the deposits in the CJM, ZJM and FJM being close to 3:5:2. As such, the input and output of sediment were generally in balance. The sediment retention indices are estimated to be 0.35, 0.86 and 1.00 for

CJM, ZJM and FJM, respectively. This study contributes to our knowledge of marine sediment fluxes, facilitates a better understanding of the growth and development of mega-deltas under system regime shifts, and helps identify a sustainable development model for areas of high population density, heavy economic activity and rapid urbanization.

长江是东海沉积物之陆源物质的最大来源，在现代东海沉积物源—汇体系中，长江来源的物质占70%-90%。早在20世纪60年代，以秦蕴珊为代表的中国学者已经认识到，分布于浙闽沿岸的狭长泥质沉积在物源与沉积动力上与长江水下三角洲具有一致性。这一认识促成了中国海洋沉积动力学者对三角洲沉积体系的新见解：长江三角洲体系包括陆上三角洲、水下三角洲及其远端泥（即“浙闽沿岸泥”）。由此带来的问题是，长江沉积物在上述各个子系统的“留下”与“出走”各有多少，这关系到长江陆上三角洲的淤进、水下三角洲的稳定及浙闽沿岸潮滩生长发育等地貌动力学问题，及沿岸围垦的可持续性和围垦工程的稳定性等实践应用问题。

回答上述问题有宏观和微观两条技术路线可行。宏观上，可以沉积物滞留系数为抓手，统计、分析和估算每个子系统沉积物的输入量、沉积量和输出量。研究人员进行了覆盖流域—河口—浅海的大范围沉积物采样，结合文献收集，获得260个百年尺度沉积速率站点，经过插值计算发现：（1）研究区百年尺度的沉积物收支基本平衡，大陆河流(长江及浙闽沿岸中小河流)、台湾西海岸河流、南黄海等来源的沉积物总量为645 Mt/yr (535–725 Mt/yr)，同期沉积通量为683 Mt/yr(390–976 Mt/yr)。（2）百年尺度内，长江水下三角洲、浙江沿岸泥和福建沿岸泥的沉积物滞留系数分别为0.35、0.86和1.00。由于考虑了南黄海对东海内陆架的供应，该研究得到长江水下三角洲滞留系数较以往的认识略低。这项工作将丰富全球变化和人类活动影响的科学认识，加深河口—水下三角洲—内陆架沉积体系的物质转运与沉积过程的了解，有利于在人口密度高、人类活动强、经济密集的区域评估海岸带资源，进行可持续开发利用战略评估和防灾减灾的应对措施优选。

微观上，可以评估悬沙的平流输运与再悬浮作用，对河口区的悬沙输运过程和地貌演化进行解释。研究人员在长江口南槽口外三个站位进行现场观测，获得了潮周期内的水位、流速、悬沙浓度、盐度、海底切应力等数据；在此基础上，建立了一个理想化的箱式模型，并基于海底冲淤测量验证了模型的可靠性。该模型的价值在于：（1）突破了水体悬沙浓度定量分离为平流输运组分与再悬浮组分的技术难点；（2）进一步分析表明，由于长江入海泥沙通量大幅减少，来自径流平流运输的泥沙已经难以补充河口区向外海搬运的损失量，导致长江口“洪淤不再、枯冲依旧”的格局改变为“洪淤不再、枯冲依旧”。这个认识对于长江三角洲发生系统状态转变给出了沉积动力学和地貌动力学的解释。

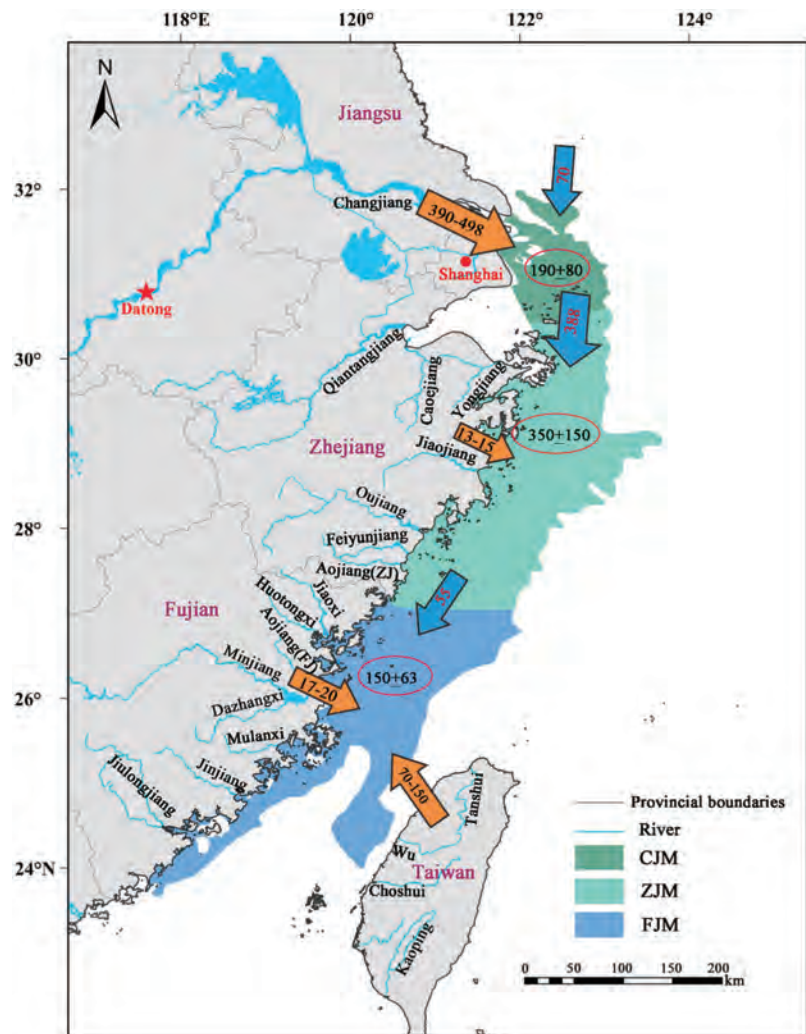


Fig. 6. Summary of sediment input, deposition, and output in the CJM, ZJM, and FJM (units: Mt year^{-1}). Brown arrows indicate riverine sediment input, blue arrows indicate shelf-derived input, and red circles indicate deposition fluxes. (For interpretation of the references to colour in this figure legend, the reader is referred to the web version of this article.)

Differentiating the effects of advection and resuspension on suspended sediment concentrations in a turbid estuary

Li Y, Jia J, Zhu Q, et al. *Marine Geology*, 2018, 403:179-190.

Suspended sediment concentration (SSC) has a significant impact on the estuarine environment and its morphological evolution. At any given location, the temporal variability of depth-averaged SSC is due to a combination of two processes: horizontal advection and local resuspension. In this study, we investigated the sediment dynamics at three anchored monitoring stations close to the maximum turbidity zone of the Changjiang Estuary, and developed a box model to differentiate the effects of advection and resuspension. Further, settling velocities were estimated using the ADV Reynolds flux method, excluding the advection SSC component. We found that predicted changes in advection- and resuspension-induced SSCs were consistent with the bottom shear stress and accretion/erosion observations. The combination of observed bed accretion/erosion changes and the predicted advection-induced SSCs indicates that the advective transport of suspended sediment is an important process in accelerating persistent erosion at the monitoring stations. Although SSC variations due to advection and resuspension are of similar magnitudes, our model results indicate that if resuspension dominates, the resuspension-induced component can reach up to twice the magnitude of the advection-induced component. We conclude that the box model is a valuable tool for evaluating subaqueous delta accretion/erosion in response to sediment reduction caused by upstream dam construction and climate change.

长江是东海沉积物之陆源物质的最大来源，在现代东海沉积物源—汇体系中，长江来源的物质占70%-90%。早在20世纪60年代，以秦蕴珊为代表的中国学者已经认识到，分布于浙闽沿岸的狭长泥质沉积在物源与沉积动力上与长江水下三角洲具有一致性。这一认识促成了中国海洋沉积动力学对三角洲沉积体系的新见解：长江三角洲体系包括陆上三角洲、水下三角洲及其远端泥（即“浙闽沿岸泥”）。由此带来的问题是，长江沉积物在上述各个子系统的“留下”与“出走”各有多少，这关系到长江陆上三角洲的淤进、水下三角洲的稳定及浙闽沿岸潮滩生长发育等地貌动力学问题，及沿岸围垦的可持续性和围垦工程的稳定性等实践应用问题。

回答上述问题有宏观和微观两条技术路线可行。宏观上，可以沉积物滞留系数为抓手，统计、分析和估算每个子系统沉积物的输入量、沉积量和输出量。研究人员进行了覆盖流域—河口—浅海的大范围沉积物采样，结合文献收集，获得260个百年尺度沉积速率站点，经过插值计算发现：（1）研究区百年尺度的沉积物收支基本平衡，大陆河流（长江及浙闽沿岸中小河流）、台湾西海岸河流、南黄海等来源的沉积物总量为645 Mt/yr (535–725 Mt/yr)，同期沉积通量为683 Mt/yr(390–976 Mt/yr)。（2）百年尺度内，长江水下三角洲、浙江沿岸泥和福建沿岸泥的沉积物滞留系数分别为0.35、0.86和1.00。由于考虑了南黄海对东海内陆架的供应，该研究得到长江水下三角洲滞留系数较以往的认识略低。这项工作将丰富全球变化和人类活动影响的科学认识，加深河口—水下三角洲—内陆架沉积体系的物质转运与沉积过程的了解，有利于在人口密度高、人类活动强、经济密集的区域评估海岸带资源，进行可持续开发利用战略评估和防灾减灾的应对措施优选。

微观上，可以评估悬沙的平流输运与再悬浮作用，对河口区的悬沙输运过程和地貌演化进行解释。研究人员在长江口南槽口外三个站位进行现场观测，获得了潮周期内的水位、流速、悬沙浓度、盐度、海底切应力等数据；在此基础上，建立了一个理想化的箱式模型，并基于海底冲淤测量验证了模型的可靠性。该模型的价值在于：（1）突破了水体悬沙浓度定量分离为平流输运组分与再悬浮组分的技术难点；（2）进一步分析表明，由于长江入海泥沙通量大减少，来自径流平流输运的泥沙已经难以补充河口区向外海搬运的损失量，导致长江口“洪淤枯冲”的格局改变为“洪淤不再、枯冲依旧”。这个认识对于长江三角洲发生系统状态转变给出了沉积动力学和地貌动力学的解释。

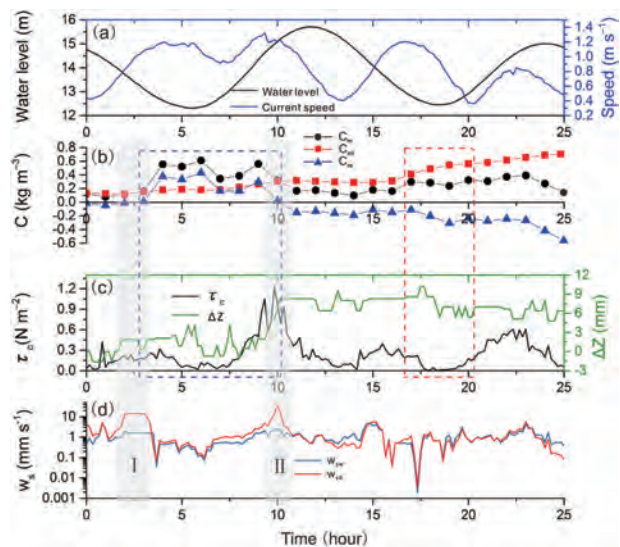


Fig. 8c) exhibits a significant increase from 0.1 to a maximum of 1.2 Nm^{-2} between hours 7.5 and 10. Cumulative bed-level changes (Δz ; mm) calculated from Eq. (15) are shown in Fig. 8c (green line). When τ_c increased from 0.1 to 1.2 Nm^{-2} , there was a large concomitant increase in Δz of approximately 8 mm, after which Δz remained almost unchanged during the hour 10–18 period before decreasing to a sustained value of about 6 mm. Between hour 10 and hour 15 C_{ad} exceeded C_m (Fig. 8b), indicating that bed accretion occurred. However, Δz measured over the same period did not exhibit a sustained decrease, indicating that the ADV is incapable of measuring discrete elevation changes. Therefore, our study suggests that more accurate altimeter measurements are required to increase the accuracy of bed-level change estimates.

Three-dimensional evolution of the Yangtze River mouth, China during the Holocene: impacts of sea level, climate and human activity

Wang Z, Saitoc Y, Zhan Q, et al. *Earth-Science Reviews*, 2018, 185:938-955.

The Yangtze (Changjiang) mega-delta, China, has a high risk of coastal erosion owing to the recent high rate of relative sea-level rise and reduced sediment supply. The study of the Holocene evolution of the delta can provide information about its response to rapid sea-level rise and changes in sediment supply caused by climate or human activity, although this has yet to be fully explored because of the lack of integrated studies using ageconstrained sedimentary records. Here we document stratigraphic architecture and morphological changes over the last 11,700 years and estimate the amount of sediment trapped in the delta region on a millennial scale using a dataset of 344 sediment cores, 658 radiocarbon and 28 optically stimulated luminescence (OSL) ages (of which we obtained 64 cores, 345 radiocarbon and 28 OSL ages, and the others we sourced from the literature). Using this dataset we present the temporal and spatial morphodynamic evolution of the entire Yangtze River mouth from its early Holocene transgressive estuary to a mid- to late-Holocene regressive delta, making it possible to reduce a quantitative and sequential analysis of sediment deposition. A destructive phase of the river mouth region was identified at 10 to 8 cal. kyr BP, including significant coastal erosion of tidal flats and troughs within the estuary and of tidal ridge-and-trough topography offshore; these resulted from the reshaping of the river mouth morphology caused by rapid sea-level rise at that time. As a result, the rate of sediment trapping at the river mouth declined from an average of 224 Mt/yr at 11.7–10 cal. kyr BP to 137 Mt/yr between 10 and 8 cal. kyr BP. Since delta initiation 8000 years ago, a retreat of the subaqueous delta occurred and the sediment trapping rate declined from 151 Mt/yr at 8–6 cal. kyr BP to 99–113 Mt/yr between 6 and 2 cal. kyr BP, caused by the reduction in sediment supply linked to summer monsoon weakening ~6000 years ago. In the last 2000 years the sediment trapping rate has increased to 162 Mt/yr due to intensified human activity. The present-day level of sedimentation in delta (49 Mt/yr in 2003–2011), after the completion of the Three Gorges Dam, is far lower than the 'natural' range in the Holocene. We thus infer a potential for system regime shift in terms of coastal erosion and a transition to a new equilibrium in delta morphology in the near future.

世界各地三角洲普遍面临海平面上升与泥沙不足的双重压力，长江三角洲是其中的一个典型例子。据最新预测，到2100年，全球平均海平面将比2005年上升 65 ± 12 cm；同时，未来长江入海泥沙量非常可能下降到只有~110 Mt/yr，只有1960年代的20%。

海平面上升速率和泥沙堆积速率之间的平衡关系决定了河口处于建设状态还是破坏状态。为保障长江口海岸地质环境的安全，急需对21世纪长江口的海平面与泥沙的平衡关系做出科学评估。全新世海平面以及气候控制下的入海水沙量均经历显著变化，因此重建全新世长江口的演变过程，揭示海平面和泥沙平衡关系在其演变中的作用，对于科学评估21世纪长江口的海平面-泥沙平衡关系具有重要指导

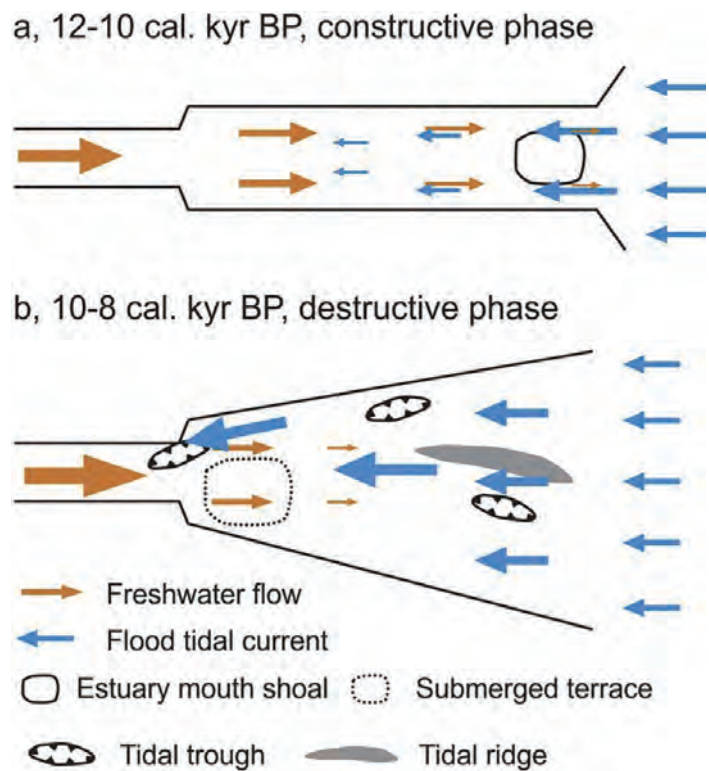


Fig. 10. Schematic diagram comparing the morphology and hydrodynamics in the Yangtze estuary as it changed from a constructive phase at 12–10 cal. kyr BP (a) to a destructive phase from 10 to 8 cal. kyr BP (b). Incoming tidal currents weakened rapidly because of friction, while fluvial flow remained relatively strong in the elongated estuary at 12 to 10 cal. kyr BP. In contrast, from 10 to 8 cal. kyr BP, fluvial flow dissipated rapidly because of the open funnel-shaped river mouth, while tidal currents strengthened landward in the narrowing estuary. Tidal trough and ridge structures developed in the funnel-shaped estuary owing to the strong tidal currents. Size of the arrow indicates the intensity of the flow or currents.

意义。

实验室科研人员通过庞大的钻孔数据库，对全新世长江口演变这一研究工作取得重要进展。该研究显示，距今10000-8000年前，由于海平面的快速上升（平均速率12.5 mm/yr），长江口普遍发生侵蚀，使其呈现为破坏型河口状态，具体表现在潮滩、潮汐通道的强烈侵蚀，以及水下地形被改造成为潮流砂脊与潮汐通道相间分布的格局。另外在此期间，下切古河谷内的晚更新世阶地上游，发生了潮汐通道的强烈下蚀，下蚀幅度可达到30 m，同时伴随显著的侧向侵蚀与岸滩崩塌。

该研究还计算了全新世千年尺度的泥沙堆积通量，结果显示，在全新世初期的近2000年里，河口的泥沙堆积率为224 Mt/yr；而距今10000-8000年前，下降到137 Mt/yr。距今8000-6000年前，随着三角洲的建设，堆积率恢复到151 Mt/yr。距今6000年前，夏季风的衰退，导致水下三角洲沉积体大幅度后退，泥沙堆积率也显著下降，距今6000-2000年前的堆积率为99-113 Mt/yr。而最近2000年，流域人类活动的增强使入海泥沙增多，河口的泥沙堆积率上升到162 Mt/yr。

按照前人研究的结果，长江泥沙在河口地区的沉积量占入海泥沙总量约68%（Liu et al., 2007）。以此比例来估算全新世河口泥沙堆积率最低阶段（距今6000-4000年前）的入海泥沙量，大约为146 Mt/yr；而距今10000-8000年前的入海泥沙量则应超过200 Mt/yr。因此，未来长江入海泥沙量（~110 Mt/yr）显然低于全新世任何阶段。考虑到21世纪海平面加速上升，长江口海平面与泥沙之间的不平衡关系成为必然，长江口面临从建设型向破坏型的转变。

Fingerprinting Sediment Transport in River-Dominated Margins Using Combined Mineral Magnetic and Radionuclide Methods

Wang J, Zhang W, Baskaran M, et al. *Journal of Geophysical Research: Oceans*, 2018, 123(8): 5360-5374.

Both magnetic properties and radionuclides are widely used to trace sediment transport in aquatic environments; however, these methods have not been used in combination. In this study, the East China Sea (ECS), a typical river-dominated margin, was chosen to demonstrate the advantages of combining these two methods to track sediment movements on a seasonal to annual timescale. The ratios between saturation isothermal remnant magnetization and anhysteretic remnant magnetization ($\chi_{ARM}/SIRM$) and ${}^7\text{Be}/{}^{210}\text{Pb}_{ex}$ activity ratios as well as mass balance of ${}^7\text{Be}$ provide information on the seasonal transport of sediment from the Changjiang Estuary to the neighboring shelf. Both ${}^{210}\text{Pb}$ budget and SIRM distribution in the inner shelf of the ECS show that a small fraction (at most 14% of annual Changjiang sediment discharge) of particles could be transported offshore. Most of ${}^7\text{Be}$ activities in inner shelf sediments of the ECS were below detection limit due to relatively lower residence times and dilution by the older sediment. The observation that radionuclide activities exhibit a better correlation with $\chi_{ARM}/SIRM$ ratios than with grain size suggests that iron oxides are the primary carriers of ${}^7\text{Be}$, ${}^{210}\text{Pb}$, and ${}^{234}\text{Th}$. The absorption of radionuclides onto magnetic minerals further reinforces the reliability of this combined approach in tracing sediment transport. Our study indicates that radionuclides, with different half-lives, can be utilized for quantifying sediment dynamics, whereas magnetic properties can yield more detailed information on

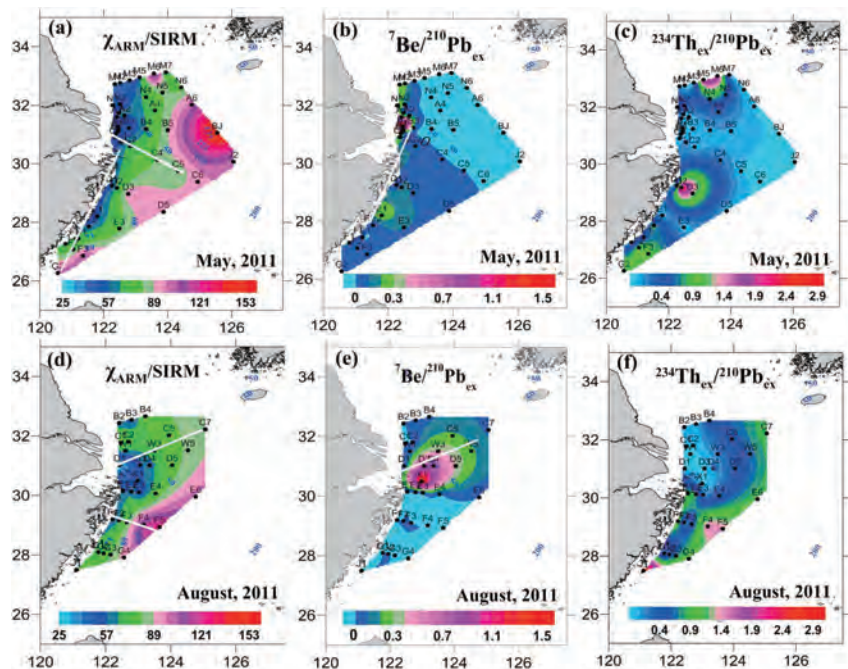


Figure 5. Spatial distribution of $\chi_{ARM}/SIRM$ ratios and ${}^7\text{Be}/{}^{210}\text{Pb}_{ex}$, ${}^{234}\text{Th}/{}^{210}\text{Pb}_{ex}$ activity ratios in (a-c) May and (d-f) August.

sediment transport directions. The combined analysis of magnetic parameters and radionuclides offers a better understanding of sediment transport in river-dominated areas.

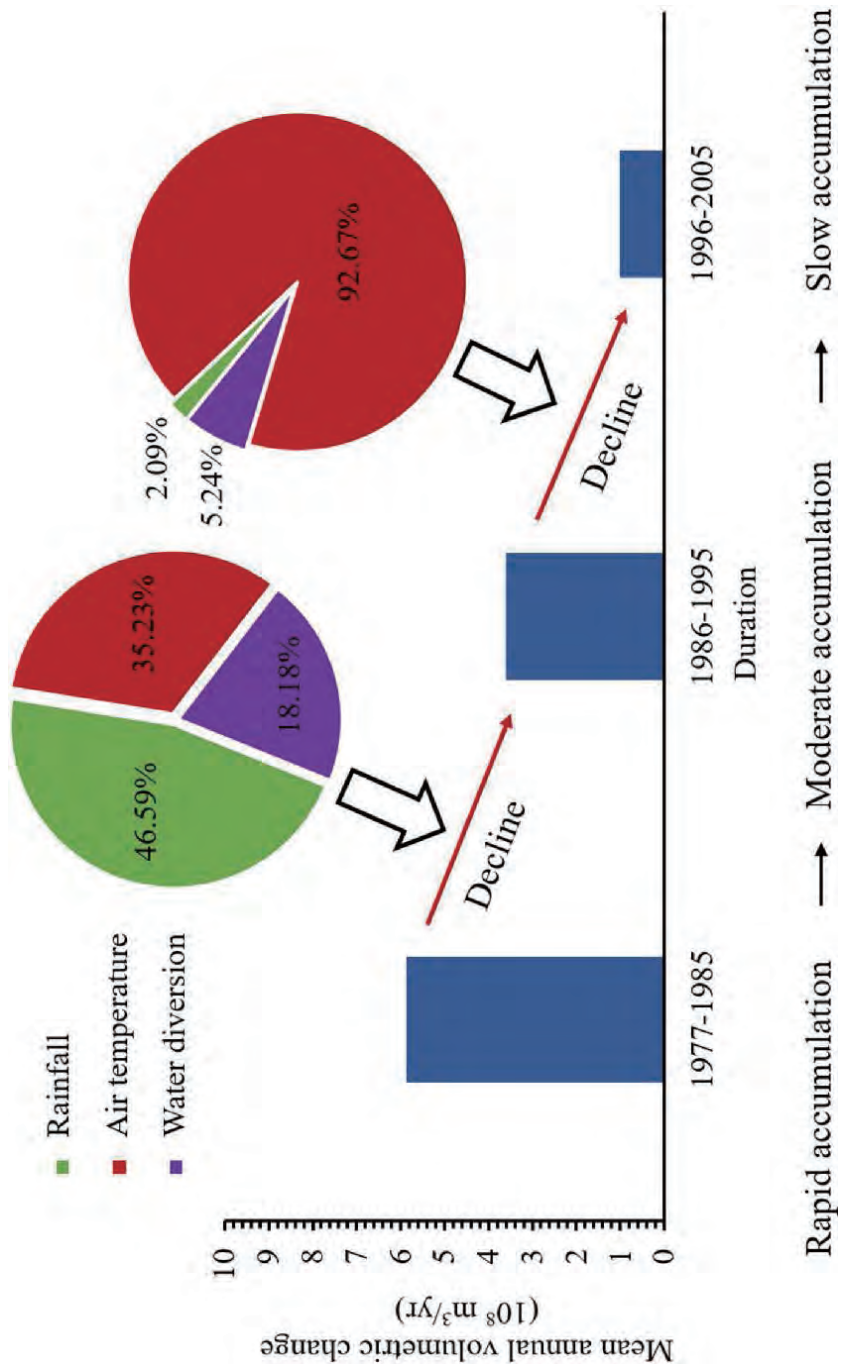
河流入海泥沙不仅是地貌塑造单元的重要物质，而且作为许多污染物和营养盐的载体，对海岸环境颗粒活性物质的迁移、转化和埋藏起着决定性作用。新沉积在近岸区域的一部分泥沙可以在一定动力条件下再悬浮和再运输，这部分泥沙在河口海岸区域的运输对于泥沙沉积/再悬浮过程和生物地球化学进程具有重要控制作用。不同放射性同位素 (^7Be 、 ^{234}Th 、 ^{210}Pb) 半衰期不同，具有颗粒活性，是泥沙来源和运输过程的天然示踪剂。本文通过对2011年5月和8月在东海采集的表层沉积物中以上核素和相关磁学参数的分析，发现中 $^7\text{Be}/^{210}\text{Pb}_{\text{ex}}$ 的高值在春季主要存在于南部，在夏季主要分布于长江口附近区域磁学参数 $\chi_{\text{ARM}}/\text{SIRM}$ 在春季由河口向东南方向增大，在夏季则向东北向增大；这些参数的变化规律与长江冲淡水 (CDW) 的季节性变化规律相似，表明泥沙在在河口附近，受 CDW 的影响呈现季节性的运输趋势。在浙闽沿岸的一些区域， $^7\text{Be}/^{210}\text{Pb}_{\text{ex}}$ 呈现离岸减小， $\chi_{\text{ARM}}/\text{SIRM}$ 呈现离岸增加的趋势，说明了泥沙存在离岸输送。通过 $^{210}\text{Pb}_{\text{ex}}$ 的质量平衡模型，本文估算出最多有约占长江年均泥沙输入量14%的泥沙可以输出内陆架至中陆架。本文在2011年春、夏季都观测到了泥沙的离岸输送，说明其输运动力机制可能不是由季节性变化的沿岸流主导。 $^{234}\text{Th}_{\text{ex}}/^{210}\text{Pb}_{\text{ex}}$ 的分布说明长江输入的泥沙在沿岸向南运输的过程中存在明显的再悬浮过程。磁学参数 χ 和 SIRM 的分布进一步说明该区域的泥沙可能源于苏北沿岸区域的细颗粒泥沙与北部残留砂的混合。最后，本文提出结合磁学参数和放射性核素可以更好地示踪研究大河影响下的陆架边缘海区域的泥沙运输。

Geomorphic evolution of the Yellow River Delta: Quantification of basin scale natural and anthropogenic impacts

Jiang C, Chen S, Pan S, et al. *Catena*, 2018, 163:361-377.

The intensified impacts of both natural and anthropogenic processes in river basins on the sustainabilities of river deltas worldwide have necessitated serious international socioeconomic and environmental concerns. The Yellow River Delta (YRD), which formed within a relatively weak coastal dynamic environment, provides an excellent opportunity for a quantitative study of basin-scale natural and human influences on deltaic transformation. An examination of long-term bathymetric data demonstrates that the annual volumetric change of the YRD has experienced a statistically distinct declining trend during 1977–2005 with substantial inter-annual variations. Consequently, the decadal geomorphic evolution of the YRD has successively undergone three stages, namely, quick, stable and slow accumulation stages. Taking the fluvial supply as a link in combination with long-term hydro-meteorological data, the geomorphologic processes of the YRD are closely associated with the rainfall, air temperature and water diversion within the Yellow River catchment. A significant quantitative relationship exists between the deltaic land accretion and basin controls, indicating that annual morphological change will decrease by $4 \times 10^8 \text{ m}^3/\text{yr}$ with every decrease of $100 \text{ mm}/\text{yr}$ in annual precipitation, decline by $2.49 \times 10^8 \text{ m}^3/\text{yr}$ with every increase of $1 \text{ }^\circ\text{C}/\text{yr}$ in annual air temperature, and diminish by $1 \times 10^8 \text{ m}^3/\text{yr}$ with every increase of $100 \times 10^8 \text{ m}^3/\text{yr}$ in annual water abstraction. Further non-dimensional analysis reveals that 50.55%, 36.26% and 13.19% of the inter-annual variation of the morphological change can be attributed to inter-annual variations of the precipitation, air temperature and water diversion, respectively. Natural environmental changes can account for 86.81% of the overall variations, while human-induced changes can explain the rest. Moreover, the contributions from rainfall, air temperature and water diversion to the decadal landform evolution transition from quick accumulation to stable accumulation were estimated as 46.59%, 35.23% and 18.18%, respectively, and their respective contributions to the transition to the subsequent slow accumulation stage were 2.09%, 92.67% and 5.24%. The natural contributions to the inter-decadal shifts were calculated as 81.82% and 94.76%, which are much greater than the respective human-related contributions of 18.18% and 5.24%. Our quantification results highlight that since the late 1970s, the changes of natural environment throughout the watershed have played a strikingly important role in both the inter-annual and interdecadal changes of the sedimentary processes of the YRD. This study provides valuable quantitative references for the validation of basin-delta process-based research and for the sustainable development of the YRD. Furthermore, the YRD can be regarded as a typical case for deltaic systems that are currently being subjected to catchment-scale natural and anthropogenic influences, thereby suggesting the direction of future research.

流域自然过程和人类活动对三角洲可持续性的影响日益加剧，已引起了广泛的关注。黄河三角洲形成于相对弱的海洋动力环境，为量化研究流域自然变化和人类活动对三角洲转型的影响，提供了很好的案例。基于长期水深测量数据研究表明，黄河三角洲的年淤积量变化在1977-2005年间呈现明显的下降趋势，年际变化幅度较大。黄河三角洲年代际地貌演化经历了快速堆积、中度堆积和缓慢堆积三个阶段。黄河三角洲淤涨和流域控制之间存在一个重要的定量关系：流域年降水量每减少100 mm/a，三角洲淤积减少4亿m³/a；流域气温每增加1° C/a，三角洲淤积减少2.49亿m³/a；流域引水量每增加100亿m³/a，淤积量减少1亿m³/a。黄河流域以河流补给为纽带，结合长期水文气象资料，黄河三角洲地貌过程与流域降雨、气温、引水密切相关。基于30年的数据分析，量化了流域降水、气温和引水对黄河三角洲地貌演变的影响。无量纲分析显示，年际尺度上，流域降水、气温和引水对黄河三角洲地貌变化贡献分别为50.55%、36.26%和13.19%，自然环境变化占了86.81%；在年代际尺度上，降水、气温和引水对三角洲地貌变化贡献分别为46.59%、35.23%和18.18%；2.09%、92.67%和5.24%。自然环境变化占了81.82%和94.76%。研究发现流域引水量维持在高水平的情况下，流域气温的上升对黄河三角洲淤积下降起到了主要的控制作用。本研究为流域-三角洲过程研究的验证和可持续发展提供了有价值的定量参考。并且，黄河三角洲可视为目前受流域自然和人为影响的三角洲系统的典型案例，从而为今后的研究指明了方向。



Scaling properties of estuarine beaches

Dai Z, Fagherazzic S, Gao S, et al. *Marine Geology*, 2018,404:130-136.

Estuarine beaches near large rivers are dynamic systems constantly shaped by tides, waves, and fluvial sediment inputs. However, little research has been done on the intrinsic characteristics of these geomorphic systems. Using eleven high resolution bathymetries, our results show that human disturbance mingled with natural forcings have induced bathymetric changes in Nanhui beach in the Changjiang estuary, China. Isobaths display a fractal geometry, with a lower fractal dimension when tides smooth the bathymetry and a higher dimension when waves dominate. Rates of sediment accretion and erosion present a Gaussian distribution driven by tidal and wave action. Episodic extreme wave forcing or frequent land reclamation is responsible for the intermittent adjustment of the estuarine beach bathymetry. After these events the distribution of erosion and accretion becomes power-law, possibly indicating disequilibrium. The fractal dimension of isobaths and the distribution of erosion and deposition rates can therefore be used as metrics to determine the dominant processes in estuarine beaches and whether the system is close to equilibrium or not.

河口边滩广泛存在于全球河口地区，其受到潮汐、波浪与径流作用的多重影响。然而，一直有很少的研究关注这些地貌系统的内在固有特征。利用11套高分辨率水深资料，我们的结果展示了人类活动和自然应力耦合引发长江河口南汇边滩的水深变化。等深线具有分形特征，相对低或高的分维值分别来自于潮流或波浪作用的控制。泥沙淤积和侵蚀速率展示了因潮流和波浪影响的高斯分布。偶尔的极端高能获频繁的土地围垦控制河口边滩间歇性的调整。当河口边滩侵蚀和淤积事件是或解决幂律分布时，河口边滩很可能处于非均衡状态。等深线的分维数和泥沙侵蚀与淤积分布因而可能利用定量判定河口边滩主要的变化过程是否处于或接近均衡。

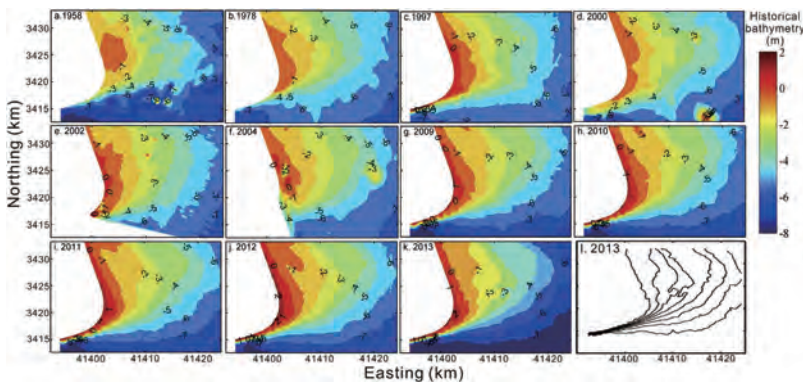


Fig. 2. Distribution of the Nanhui beach bathymetry in different years (a-k is bathymetric distribution in given year, and l is a contours drawn of bathymetric image in 2013).

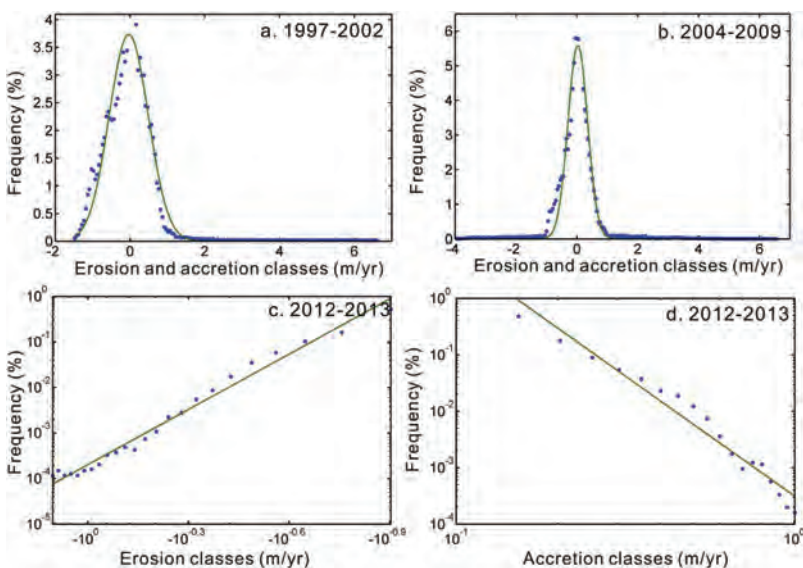


Fig. 5. Frequency of occurrence of erosion and accretion events in different intervals in different years.

Tidal Mixing Sustains a Bottom-Trapped River Plume and Buoyant Coastal Current on an Energetic Continental Shelf

Wu T, Wu H. *Journal of Geophysical Research: Oceans*, 2018, 123:8026-8051.

Conventional wisdoms on river plume dynamics suggest that a down-shelf buoyant coastal current will ultimately be trapped at a specific depth, that is, the trapping depth, as constrained by riverine outflow and offshore bottom Ekman transport. Theoretically, a prerequisite down-shelf current is necessary to form a stable bottom-trapped river plume. In this study an alternative is described by carrying out a modeling study on the Zhe-Min Coastal Current (ZMCC). Buoyant water from the Changjiang River is a major factor driving the ZMCC, as is common in bottom-trapped river plumes; however, the trapping depth is more determined by tidal mixing. When the plume water comes to the sloping topography, strong tidal mixing induces a mixing front, shoreward of which the bottom Ekman layer occupies the entire water column. Such a tidal-induced front maintains a down-shelf frontal current, which is intensified both at the surface due to the thermal wind balance and on the top of bottom boundary layer due to the tidal rectification. Direct wind-induced transport only covers a small fraction of the ZMCC; however, it redistributes the plume water and, thus, affects the coastal current. The tide-induced frontal trapping depth varies much less between seasons than that predicted by previous plume theories. Instead, it fluctuates strongly in the spring-neap cycle. Even in summer when upwelling-favorable winds prevail, the mixing front still sustains a down-shelf coastal current. Intense tidal mixing exists in many coastal waters, which might be an alternative mechanism in forming bottom-trapped river plumes and their associated buoyant coastal current.

河流冲淡水动力学的传统观点认为，受河流径流和底部离岸Ekman输运的限制，向下游传播的浮力沿岸流最终会被捕获在特定等深线之上，这个深度被称为捕获深度。理论上，向下游流动的背景流是形成稳定的底部捕获型冲淡水的前提条件。本文通过对浙闽沿岸流的数值模型研究，为底部捕获型冲淡水的维持提供了另一种动力机制。长江冲淡水是驱动浙闽沿岸流的主要动力因素，这在底部捕获型冲淡水中十分常见，然而浙闽海域长江冲淡水的捕获深度更多地取决于潮汐混合。当长江冲淡水进入倾斜的陆架时，强烈的潮汐混合会形成潮致锋面，在锋面向岸一侧，底部Ekman层充满整个水体。这种潮致锋面在其上驱动了向下游传播的沿岸流。由于热风平衡和潮汐调整，该沿岸流的流速在表层和底边界层顶部增强。浙闽沿岸流中风生流的占比很少，但是风场会影响长江冲淡水的分布，进而对该沿岸流产生影响。潮致锋面捕获深度的季节性变化远远小于理论预测值，相反地，它存在较强的大小潮周期变化。即使在夏季南风盛行的时候，浙闽海域的潮致冲淡水锋面仍可以维持沿岸向下游传播的浮力沿岸流。许多沿岸海域都存在强烈的潮汐混合，本文提出的潮汐混合机制可以为其他地区的底部捕获型冲淡水和浮力沿岸流的形成与维持提供动力解释。

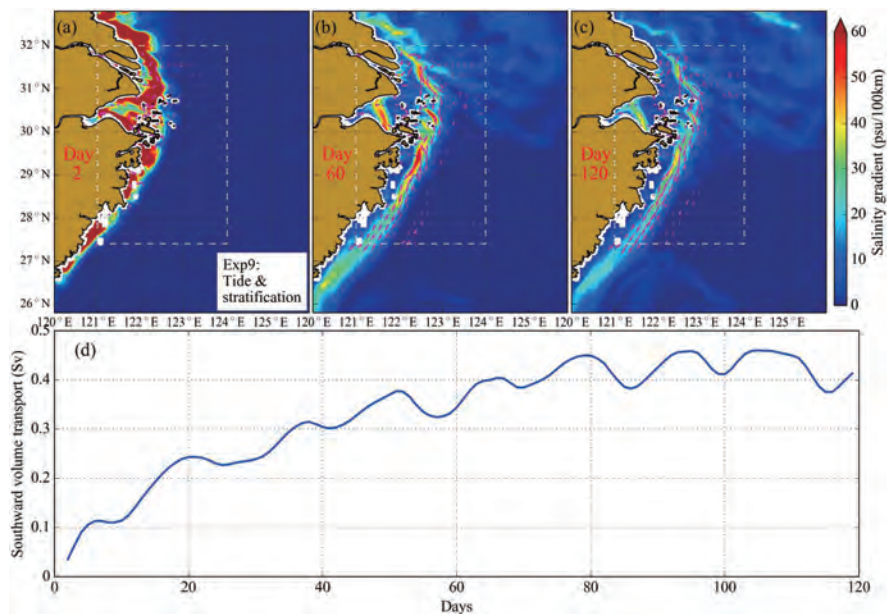


Figure 18. Bottom salinity gradient and residual surface currents in days 2, 60, 120 (a–c) and residual down-shelf volume transport across Section A (d) from Exp9.

Using Multibeam Backscatter Data to Investigate Sediment-Acoustic Relationships

Huang Z, Siwabessy J, Cheng H, et al. *Journal of Geophysical Research: Oceans*, 2018, 123(7):4649-4665.

Sediment properties are known to influence acoustic backscatter intensity. This sediment-acoustic relationship has been investigated previously through using physical geoaoustic models and empirical methods and found to be complex and nonlinear. Here we employ a robust machine-learning statistical model (random forest decision tree) to investigate the most likely nonlinear sediment-backscatter relationships. The analysis uses colocated sediment and acoustic backscatter data (collected from a 300-kHz multibeam sonar system) for 564 locations in four different areas on the Australian margin. Seven sediment grain size properties (%gravel, %sand, %mud, mean grain size, sorting, skewness, and kurtosis) were used to predict the acoustic backscatter responses at individual incidence angles. The modeling results demonstrate the effectiveness of this multivariate predictive approach for the investigation of sediment-acoustic relationship. Thus, we find that for incidence angles between 1° and 41° , the sediment variables explain around 70% of variance in the backscatter intensity. Sediment mud content was found to be the most important sediment variable in the model and has a significant negative relationship with backscatter intensity. Mean grain size was the second ranked sediment variable and found to have a positive relationship with backscatter intensity. The results also show that sediment mud content plays a key role in sorting-backscatter and sand-backscatter relationships. Using only two sediment properties, mud content and mean grain size, together it was possible to largely explain the sediment-acoustic relationship. The strongest backscatter return occurred with medium sediment mud content and large mean grain sizes (or muddy coarse sand).

沉积物属性影响声学背向散射强度，前人曾利用地声学的物理模型和经验模型研究这一沉积物—声学关系，并发现其非常复杂，且为非线性。本文采用一种较为稳健的机器学习的统计模型，即随机决策树模型，分析沉积物—背向散射间可能性最大的非线性关系。数据采用澳洲边缘海四个区域564个站位的沉积物与利用300 kHz多波束声呐系统同步采集的声学背向散射数据，并将砾石含量，砂含量，泥含量，平均粒径，分选度，偏度和峭度等七种沉积物粒度属性作为解释变量，用于预测每个声波束入射角的背向散射强度。模拟结果证明了这种多变量预测方法用于研究沉积物—声学关系的有效性。我们发现当入射角介于 1° 和 41° 时，沉积物变量对背向散射强度变化的影响占了约70%。其中，泥质含量对背向散射强度起着最为重要的显著的负相关关系；平均粒径第二重要，其与背向散射强度之间有着显著的正相关关系。而且，沉积物中泥含量对分选度—背向散射强度和砂含量—背向散射强度间相关关系的预测上起着关键影响。因此，仅用沉积物的泥含量和平均粒径这两种属性，基本上就可以解释沉积物声学特性。返回的背向散射强度最大时，沉积物粒度属性一般为中等泥含量和平均值粒径较大，或为泥质粗砂。

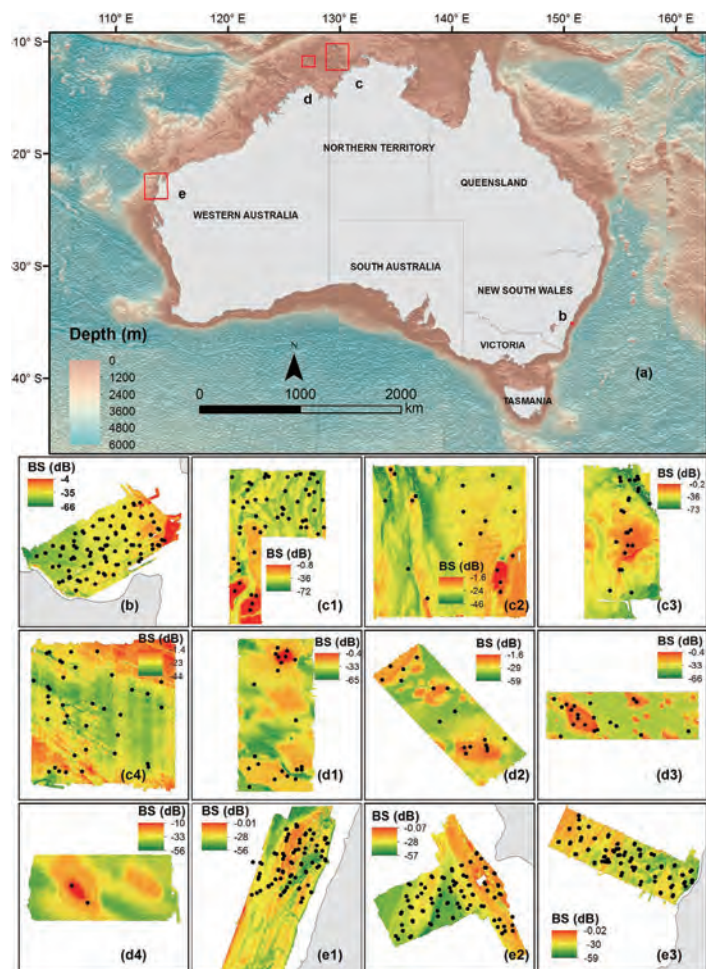


Figure 1. The study areas and the sample locations overlaid on the multibeam backscatter mosaics normalized at 25° incidence angle; (a) the locations of the study areas on the Australian margin; (b) the Jervis Bay survey area; (c1–c4) the four subareas within the Joseph Bonaparte Gulf survey area; (d1–d4) the four subareas within the Oceanic Shoals survey area; (e1–e3) the three subareas within the Carnarvon Shelf survey area.

Formation of Concentrated Benthic Suspension in a Time-Dependent Salt Wedge Estuary

Ge J, Zhou Z, Yang W, et al. *Journal of Geophysical Research Oceans*, 2018, 123(11):8581-8607.

The concentrated benthic suspension (CBS) of mud, as a major contributor of sediment transport in the turbidity maximum of the estuary, is of great challenge to be correctly monitored through field measurements, and its formation mechanism is not well understood. A tripod system equipped with multiple instruments was deployed to measure the near-bed hydrodynamics and sediments in the North Passage of the Changjiang Estuary, with the aim at determining the formation mechanisms of CBS. The measurements detected a significant dominance of high sediment concentration in the near-bed 1-m layer: ~20 g/L at the southern site and ~47 g/L at the northern site. Strong CBS occurred under weak tidal mixing condition and was directly relevant to the sediment-induced suppression of turbulent kinetic energy and the enhanced water stratification due to saltwater intrusion and sediment suspension. During the weak-mixing neap period, the typical thickness of CBS was about 0.2–0.3 m, with a life time of ~2.83 hr (suspended-sediment concentration > 15.0 g/L). Enhanced water stratification reduced vertical mixing and confined the sediment entrainment from the near-bed layer to the upper column. This enhancement was due to the suppression of turbulent kinetic energy as a result of the sediment accumulation in the near-bottom column during the slack water and also due to the appearance of a two-layer salinity structure in the vertical as a result of saltwater intrusion near the bottom. These physical processes worked as a positive feedback loop during the formation of CBS and can be simulated with a process-oriented, one-dimensional vertical CBS model.

河口最大浑浊带区域的近底高浓度泥沙过程对泥沙输运、沉积动力过程影响显著，其观测和模拟都具有较强的挑战性。采用高分辨率多种仪器综合集成的近底三脚架系统观测了长江口最大浑浊带核心北槽区域的近底水沙动力，以分析确定在显著垂向层化背景下河口高浓度泥沙的形成机制。观测及分析表明：长江口北槽区域近底高浓度泥沙在南侧约20 g/L的量级，而在主槽北侧其浓度可达47 g/L的量级，且所有高浓度泥沙主要形成于涨潮-落潮转换期。长江口区域洪季河流输入的淡水与口外的高盐水形成在最大浑浊带形成的显著垂向层化限制了垂向混合，同时，在考虑层化的潮汐混合作用在涨潮-落潮期间也显著减小，从而造成近底层泥沙难以通过潮汐混合达到上层水体。同时，近底层泥沙浓度的逐步增加也在一定程度上增加了垂向层化。结果发现无论主槽南北两侧，在小潮期间都形成了显著的高浓度泥沙，其与小潮期间层化达到最强而潮汐混合作用达到最弱直接相关。基于此动力机制，在FVCOM模型的基础上建立了垂向近底一维高浓度泥沙数值模型，采用北槽近底三脚架观测系统获得的动力要素进行驱动，模拟了近底高浓度泥沙形成过程中在水体-高浓度悬浮层、悬浮层-底床界面上的沉降、悬扬、固结、侵蚀等物理过程的贡献。

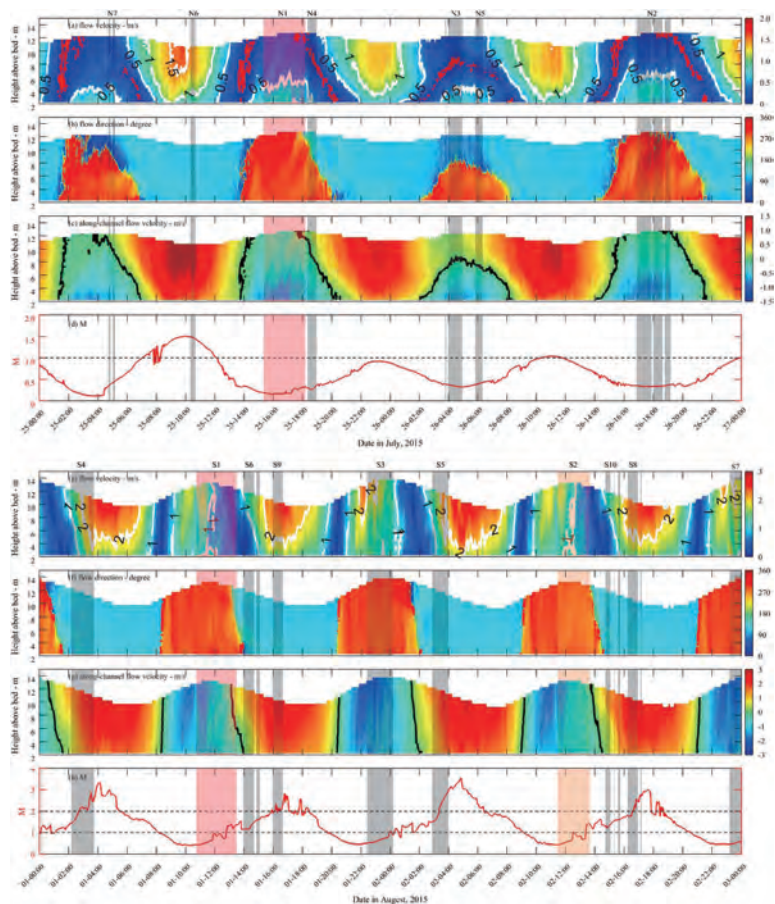


Figure 5. Time series of vertical profiles of (a) flow velocity, (b) flow direction, (c) along-channel flow velocity, and (d) mixing effectiveness parameter during neap tide at site NU. (e–h) Same as Figures 5a–5d, except during spring tide. The shaded regions with labels N1–N7 show the occurrences of concentrated benthic suspension during neap tide, and those with labels S1–S10 indicate the occurrences of concentrated benthic suspension during spring tide.

The chronology of a sediment core from incised valley of the Yangtze River delta: Comparative OSL and AMS ¹⁴C dating

Nian X, Zhang W, Wang Z, et al. *Marine Geology*, 2018, 395:320-330.

Optically stimulated luminescence (OSL) dating has gained increased use in dating deltatic deposits, however, its application can be hindered by the problem of incomplete bleaching. To address this limitation, we test the single-grain OSL method for the first time in the Yangtze River delta. A total of eight OSL and 14 AMS ¹⁴C samples were obtained from a 50.8 m long sediment core from the incised valley of the delta. Quartz extracted from eight OSL samples from the core was first measured with small multi-grain aliquots using medium- (45–63 μm) and coarse-grained (90–125 μm or 150–180 μm) fractions to test the internal consistency of their respective ages. The results showed that four of five medium-grained quartz samples appeared to be well bleached. In contrast, the coarse-grained quartz samples revealed poor bleaching, except for two samples from the delta front facies. Five coarse-grained quartz OSL samples were further analyzed using a single-grain OSL technique. Only 0.5–0.7% of the grains passed the rejection criteria. Single-grain OSL dating is appropriate for age determination of coarse-grained sediments which have been affected by incomplete bleaching. However, it consumes a lot of instrument time. Central and minimum age models (CAM and MAM) were used to calculate the burial age of the samples; MAM ages fit best in the stratigraphic sequence. Small aliquots are recommended as effective in identifying incomplete bleaching for medium- or coarse-grained quartz. A comparison of AMS ¹⁴C dates and OSL ages shows that ¹⁴C values are 1–3 ka older than OSL ages. According to the OSL ages, core SD experienced rapid accumulation 10–8 ka and in the last 2 ka. The former is linked to rapid sea-level rise in early Holocene, while the latter is primarily due to the migration of depo-center towards the core site, rather than entirely increased sediment delivery caused by human activities.

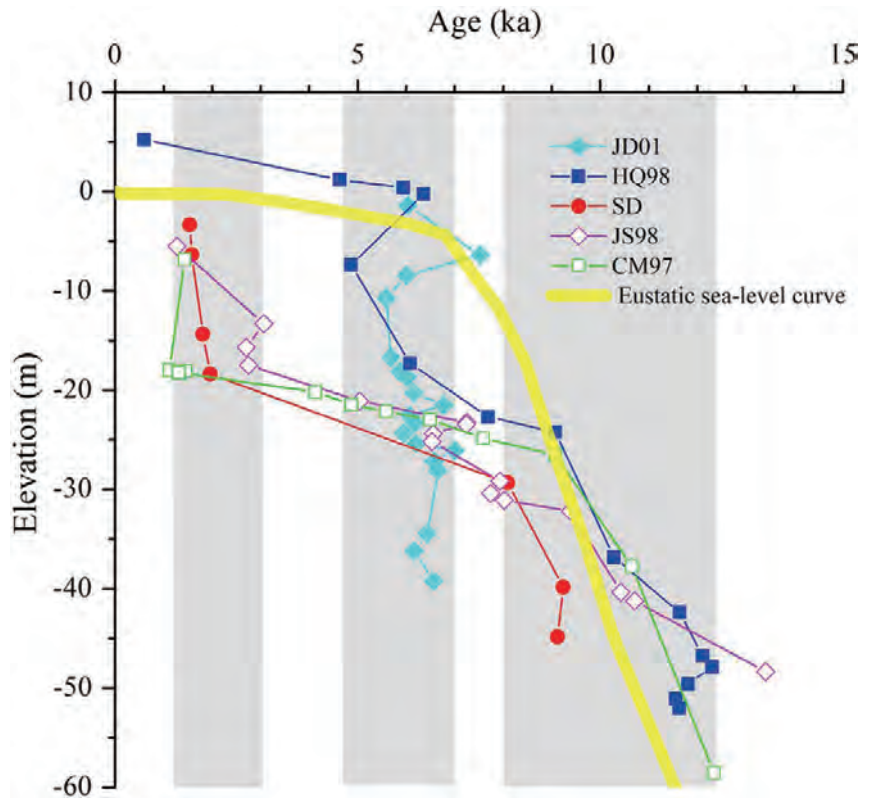


Fig. 8. Age-depth relationships and accumulation curves for cores JD01, HQ98, SD, JS98 and CM97 and a sea-level curve (Lambeck et al., 2014). The grey shaded area: the time period with high accumulation rates.

Optical dating of Holocene sediments from the Yangtze River (Changjiang) Delta, China

Nian X, Zhang W, Wang Z, et al. *Quaternary International*, 2018, 467:251-263.

Establishing a reliable chronology is essential for understanding delta evolution, which is normally performed using radiocarbon (^{14}C) dating and the recently emerging technique of optically stimulated luminescence (OSL). The application of the latter one to the Holocene Yangtze River (Changjiang) Delta deposit is still quite limited. In this study, two 60.9-m-long cores were collected from Taizhou (TZ) and Nantong (NT) within the paleo-incised valley of the Yangtze River, and a total of seven and nine OSL samples were collected from the TZ and NT cores, respectively. In addition, ten accelerator mass spectrometry (AMS) ^{14}C ages of the TZ core were presented with eight AMS ^{14}C ages that were previously obtained from the NT core. The single-aliquot regenerative-dose (SAR) protocol was applied to coarse silt-sized (45-63 μm) and fine sand-sized (90-125 μm) quartz. The results showed that the grains in the 45-63 μm size fractions appeared to be better bleached than those in the 90-125 μm size fractions, and the detection of insufficiently bleached sediments is required in order to obtain accurate age estimates. The ages adopted for the samples range from 3 ka to 9 ka for the TZ core, and from 1 ka to 14 ka for the NT core, which were in general internally coherent within the limits of experimental errors and with respect to their stratigraphic order. The AMS ^{14}C age of the TZ core were significantly older than their OSL ages, while those from the NT core generally showed good agreement with their OSL ages. One should be cautious when using AMS ^{14}C to date deltaic deposits. Based on the OSL ages, two periods of rapid accumulation rates can be found in both cores, which are linked to the rapid sea level rise in early Holocene and migration of delta front facies in late Holocene. These investigations indicate that OSL technique is an effective method with which to date Holocene deltaic deposits, especially in coarse sedimentary layers where organic carbon material is sparse.

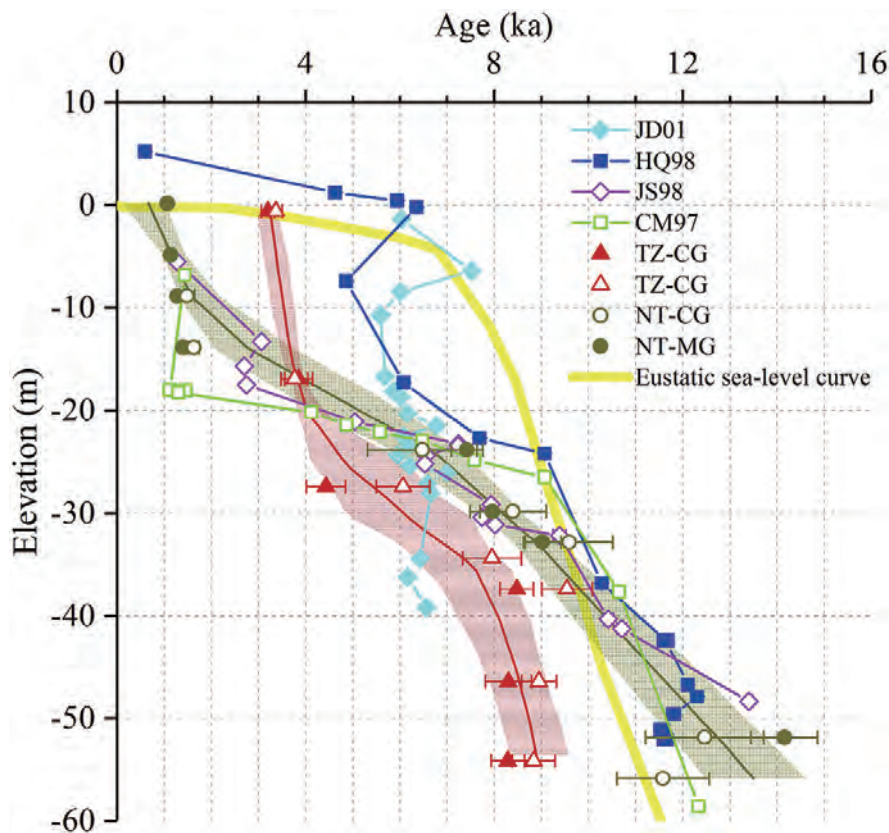


Fig. 8. Age-depth relationships and accumulation curves for cores (TZ and NT) in this study and previous studies (HQ98, JS98 and CM97, Hori et al., 2001, 2002; JD01, Song et al., 2013) and eustatic sea-level curve (Lambeck et al., 2014). Bacon age-depth models of cores TZ and NT were presented (Blaauw and Christen, 2011). The areas filled by the horizontal (TZ) and crossing (NT) lines show the model's 95% probability interval and the central lines represent the single 'best' age-depth model. The weighted mean value of the paired data (two grain-size fractions, in Table 2) was used for age-depth model construction.

Multiple dating approaches applied to the recent sediments in the Yangtze River (Changjiang) subaqueous delta

Wang F, Nian X, Wang J, et al. *The Holocene*, 2018, 28(6):858-866.

The accumulation rate of recent deposits in a delta environment is critical to the study of delta dynamics and their sustainable management. The most commonly used dating approach for recent (<100 years) deposits is based on radionuclide analyses (e.g. ^{210}Pb , ^{137}Cs and $^{239+240}\text{Pu}$), while alternative techniques, such as microplastics dating, are emerging. In this study, a 180-cm sediment core from the Yangtze River (Changjiang) subaqueous delta was dated using multiple techniques, including ^{210}Pb , ^{137}Cs , $^{239+240}\text{Pu}$ geochronology, microplastics content, and optically stimulated luminescence (OSL) dating. The radionuclide profiles show an irregular profile of ^{210}Pb , while $^{239+240}\text{Pu}$ exhibit a clear peak of activity at 74 ± 2 cm, which is linked to the maximum global fallout in 1963. Microplastics were not detected below a depth of 90 cm with maximum counts occurring in the top 16 cm. OSL analysis was conducted on the dominant grain size of the quartz (around 4–11 μm) and the ages were ~60 years older than those derived from ^{210}Pb , ^{137}Cs , $^{239+240}\text{Pu}$, and microplastics analyses. We infer that the relatively old quartz OSL ages are most likely caused by residual OSL signals arising from poorly bleached grains at the time of deposition. The profiles of ^{210}Pb , ^{137}Cs and $^{239+240}\text{Pu}$ activities, microplastics content, and OSL ages indicate a variable sedimentation rate over the last ~200 years reflecting the dynamic nature of delta deposits. This study shows that both OSL and microplastics particles are promising dating tools for recent young deltaic sediments, and their combined use, alongside radionuclide methods, increases the reliability of age determination.

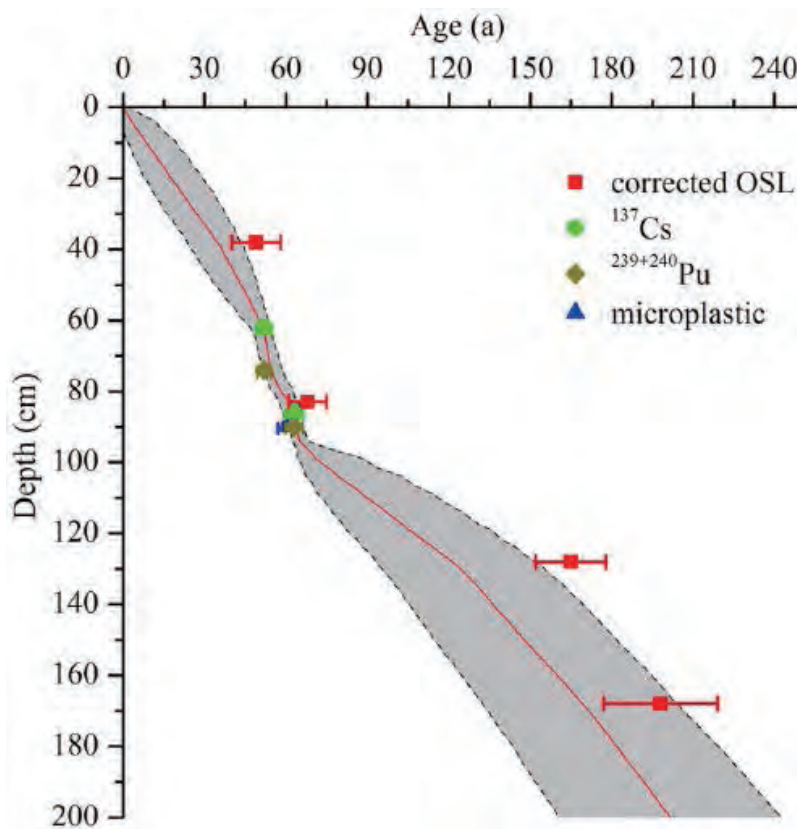


Figure 7. The age–depth model for core A6-6 generated by Bacon (Blaauw and Christen, 2011); gray dotted lines indicate 95% confidence intervals; the red curve shows the single 'best' model based on the weighted mean age for each depth. The age of the top of the core (year of coring, AD 2015) was added into the age–depth model and all the ages were relative to AD 2015 for comparison. Red squares: corrected OSL ages (after subtracting 60 years); green circles: ^{137}Cs ages; dark yellow diamonds: $^{239+240}\text{Pu}$ ages; blue triangles: microplastics age.

A system shift in tidal choking due to the construction of Yangshan Harbour, Shanghai, China

Guo W, Wang X, Ding P, et al. *Estuarine, Coastal and Shelf Science*, 2018, 206(SI):49-60.

Tidal choking is a geometric feature caused by a narrowed channel. Construction of the Yangshan Harbour, Shanghai, China obstructed three key channels and intensively changed the local geometry and topography. In this study nine numerical experiments based on the Finite-Volume Community Ocean Model are conducted to study the project's influence on tidal characteristics. Results show that stronger tidal choking happened at the East Entrance after project, mainly due to the jet induced water-level drop forced by Bernoulli law and the longer and narrower geometry. The stronger tidal choking forces a faster flow and larger tidal energy flux at the choked channel while reducing the tidal amplitude in the Inner Harbour Area (IHA). The scouring on this channel reduces the choking effect but further enlarges tidal energy flux. Moreover, damming the channels decrease the tidal amplitude at the lee side of tidal propagating direction while increasing the amplitude on the stoss side. The dams also decrease the tidal current on both sides, and meanwhile develop two patches with stronger current aside the dam. The project induced changes in tidal characteristics are complex in space, and perturbations in bathymetry increase this complexity. Yangshan Harbour's construction induces little changes in the total tidal energy density in the IHA, but induces obvious changes in the spatial distribution of tidal energy. Although this study is site-specific, the findings may be applicable to tidal dynamics in land reclamation close to open seas, such as the dramatic reclamation of islands in the South China Sea.

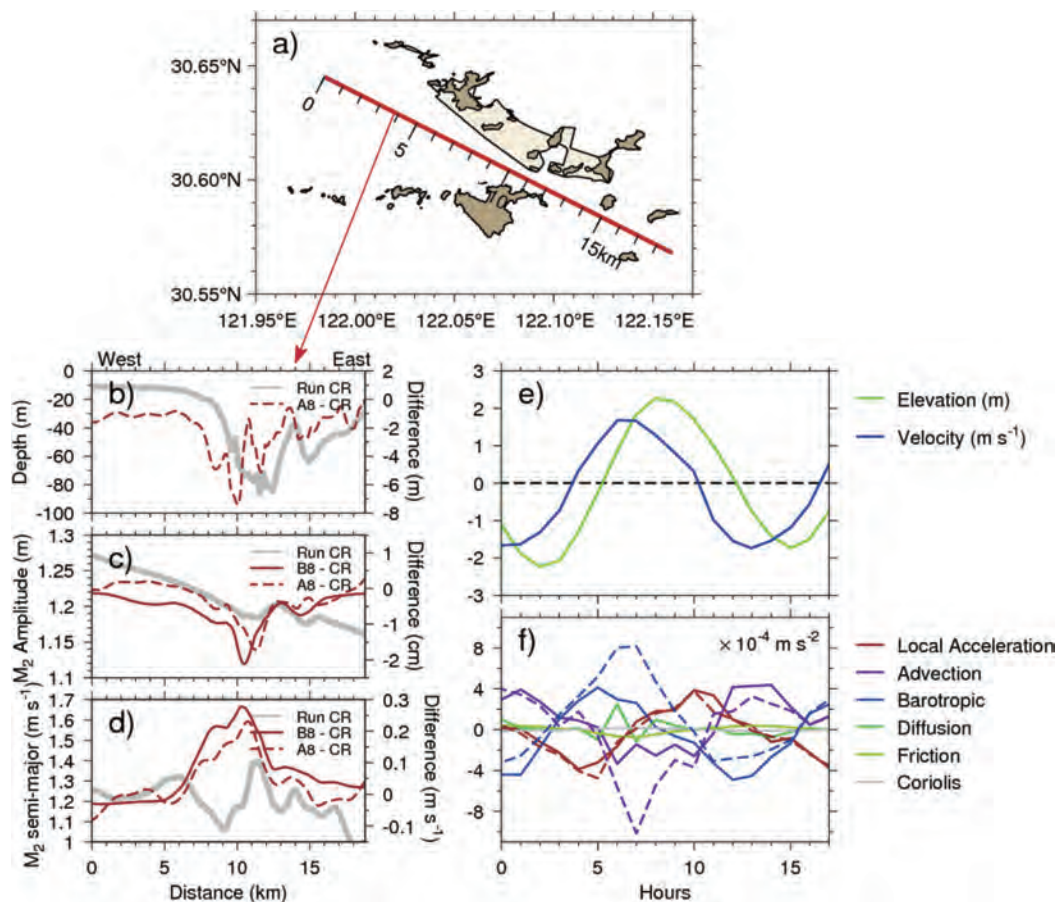


Fig. 7. (a) Location of the cross section for analysis of tidal choking in the East Entrance. The distances relative the west endpoint are labelled. (b), (c) and (d) show the results of depth, M_2 amplitude and the semi-major axis of M_2 current along the cross section shown in (a), respectively. Bold grey lines show the results in Exp. CR; the red solid and dashed lines show the results of Exp B8 e CR and Exp A8 e CR, respectively. (e) The elevation (green) and depth-averaged alongstream velocity (blue) in centre of the East Entrance. (f) The momentum balance (along the cross section shown in Fig. 7a) in centre of the East Entrance (averaged in the segment from 10.5 km to 12 km; solid lines: Exp CR; dash lines: Exp B8). (For interpretation of the references to colour in this figure legend, the reader is referred to the web version of this article.)

Early to Middle Holocene sea level fluctuation, coastal progradation and the Neolithic occupation in the Yaojiang Valley of southern Hangzhou Bay, Eastern China

Liu Y, Sun Q, Fan D, et al. *Quaternary Science Reviews*, 2018, 189:91-104.

The Yaojiang Valley (YJV) of southern Hangzhou Bay was the birthplace of the well-known Hemudu Culture (HC), one of the representatives of Neolithic civilization in eastern China. To explore the magnitude of natural environmental effects on the HC trajectory, the palaeo-embayment setting of the YJV was studied in detail for the first time in terms of 3D Holocene strata supported by a series of new radiocarbon-dated cores. The results indicated that the local relative sea level rose rapidly during the Early Holocene in the YJV, reached its maximum flooding surface ca. 7900 cal yr BP, and then remained stable ca. 7900-7600 cal yr BP. Thereupon, an estuary stretching inland was first formed by marine transgression, and then, it was transformed to an alluvial-coastal plain by regressive progradation. The alluvial plain was initiated in the foothills and then spread towards the valley centre after sea level stabilization ca. 7600 cal yr BP. Accompanying these natural environmental changes, the earliest arrivals of foragers in the valley occurred no later than ca. 7000 cal yr BP. They engaged in rice farming and fostered the HC for approximately two millennia from ca. 7000-5000 cal yr BP as more lands developed from coastal progradation. The rise and development of the HC are closely associated with the sea level-induced landscape changes in the YJV in the Early-Middle Holocene, but the enigmatic exodus of the HC people after ca. 5000 cal yr BP is still contentious and possibly linked with the rapid waterlogging and deterioration of this setting in such a low-lying coastal plain as well as with associated social reasons.

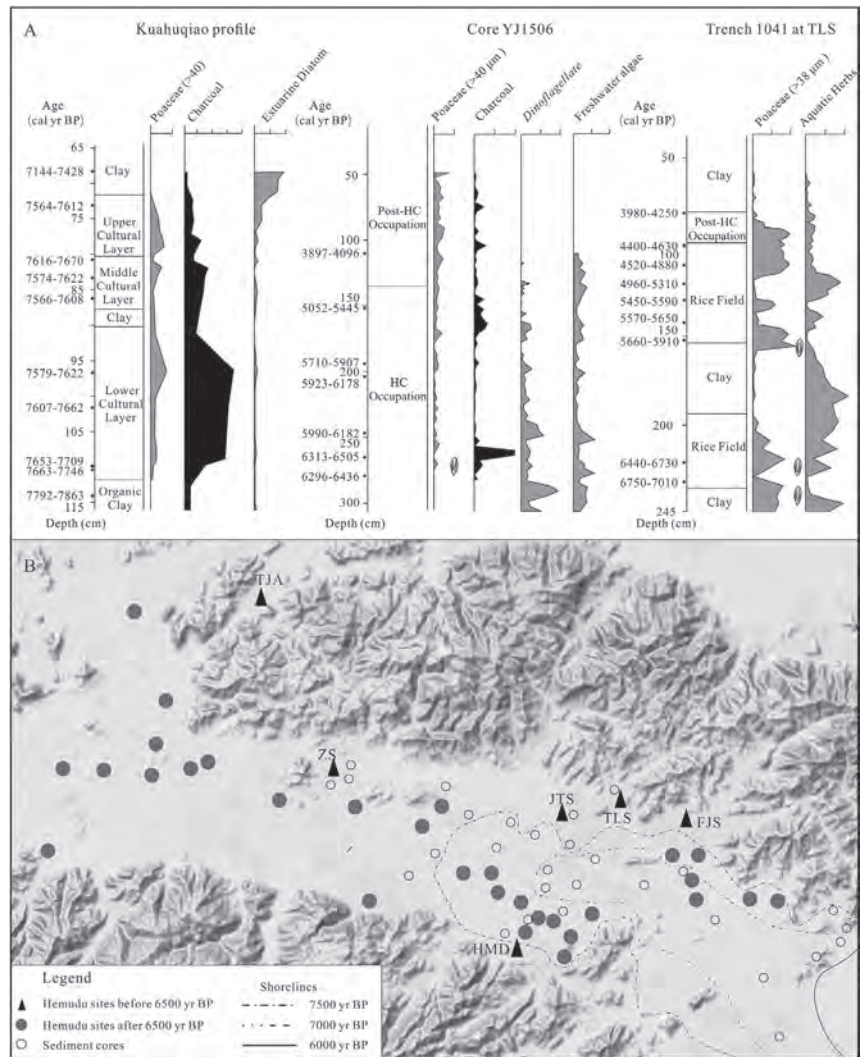


Fig. 9. A) Microfossil evidence showing signs of rice farming activities at the Kuahuqiao (Zong et al., 2007), Hemudu (Liu et al., 2016) and Tianluoshan (Li et al., 2012) sites, B) Human occupations in relation to shoreline migrations in the Yaojiang Valley during 7500-6000 cal yr BP.

Foraminiferal evidence for Holocene environmental transitions in the Yaojiang Valley, south Hangzhou Bay, eastern China, and its significance for Neolithic occupations

Dai B, Liu Y, Sun Q, et al. *Marine Geology*, 2018, 404:15-23.

The transition from a marine-influenced environment to a coastal plain setting during the Early to Middle Holocene was crucial for early human occupation along the eastern China coast. Here, detailed foraminiferal analyses were completed for two sediment cores (YJ1505 and YJ1508) retrieved from the Yaojiang Valley (YJV) along the southern Hangzhou Bay coast of eastern China. Brief environmental changes in the YJV during the Early-Middle Holocene were recovered on the basis of radiocarbon chronology. The assemblages and Detrended Correspondence Analysis (DCA) results of the foraminifera of both cores indicated that the YJV was evidently under a marine influence from 9200 to 7900 cal yr BP; prior to that, it was a fluvial incised valley. The increasing trends in shallow marine foraminifera and the planktonic/benthic foraminifera (P/B) ratio showed that a transgressive period possibly occurred in the valley ca. 9200–7900 cal yr BP, and their following decreases suggested that a rapid regression process occurred thereafter. The disappearance of foraminifera and formation of a peaty layer in core YJ1505 ca. 7600–6500 cal yr BP implied a brief environmental transition to a limnetic wetland setting in the valley centre, which would have been attractive to early human settlers. The disappearance of foraminifera in core YJ1508 at the valley's eastern entrance suggested that most areas of the valley were located far from marine influence after ca. 6250 cal yr BP. Then, the limnetic wetland setting transitioned into a coastal plain environment, attracting more people to the valley. Such a transition in the YJV would have provided more opportunities for ancient people and possibly catalysed the development of the Hemudu culture (HC) for approximately two millennia.

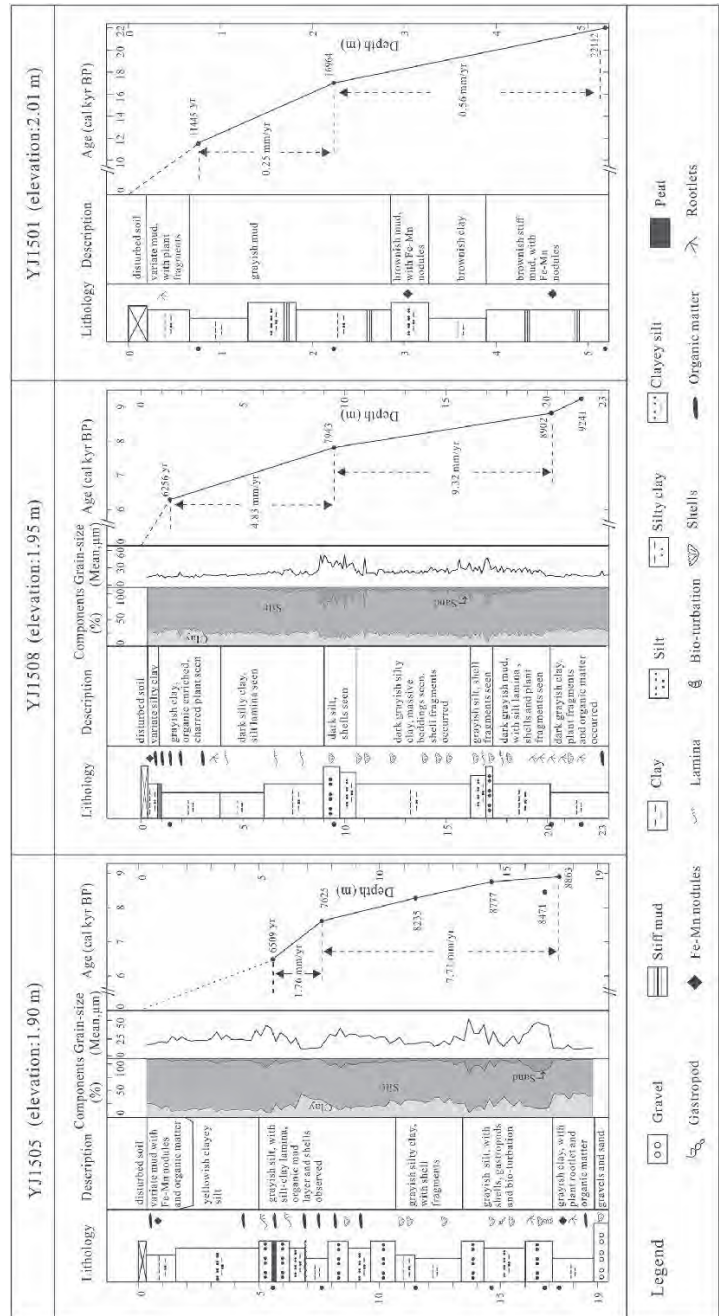


Fig. 2. Lithology and chronology of cores YJ1501, YJ1505, and YJ1508.

Investigation of TLS Intensity Data and Distance Measurement Errors from Target Specular Reflections

Tan K, Zhang W, Shen F, et al. *Remote Sensing*,2018,10:1077.

Terrestrial laser scanners (TLSs) can provide accurate and high-resolution data by measuring the distances (ranges) between the scanned points and the scanner center using time-of-flight or phase-shift-based methods. Distance measurement accuracy is of vital importance in TLSs and mainly influenced by instrument mechanism, atmospheric conditions, scanning geometry, and target surface properties. In general, existing commercial TLSs can achieve millimeter precision. However, significant errors (centimeter and even decimeter levels) beyond the instruments' nominal accuracy exist in distance observations for targets with highly reflective surfaces whose specular reflections are dominant because these reflections can increase the backscattered laser signal power considerably and cause further disorder in the echo detection and recognition by TLS photodetectors. part from distance, the intensity value derived from the backscattered signal and influenced by the same factors as that of the distance measurement errors is recorded by TLSs. A certain link exists between the two instrumental observations. In this study, the anomalous distance measurement errors caused by target specular reflections are explored. The different planar reflective targets scanned by a Faro Focus^{3D} 120 terrestrial scanner are used to experimentally investigate the relationship between the original intensity values and the distance measurement errors. Results imply that the distance measurement errors caused by specular reflections are not as erratic as they ostensibly seem. On the contrary, distance measurement errors are strongly related to the original intensity values. A polynomial can be established to empirically model the relationship between the original intensity data and the distance measurement errors. With use of the original intensity to compensate for the measured distance observations, the point cloud data accuracy can be improved by approximately 55.52%.

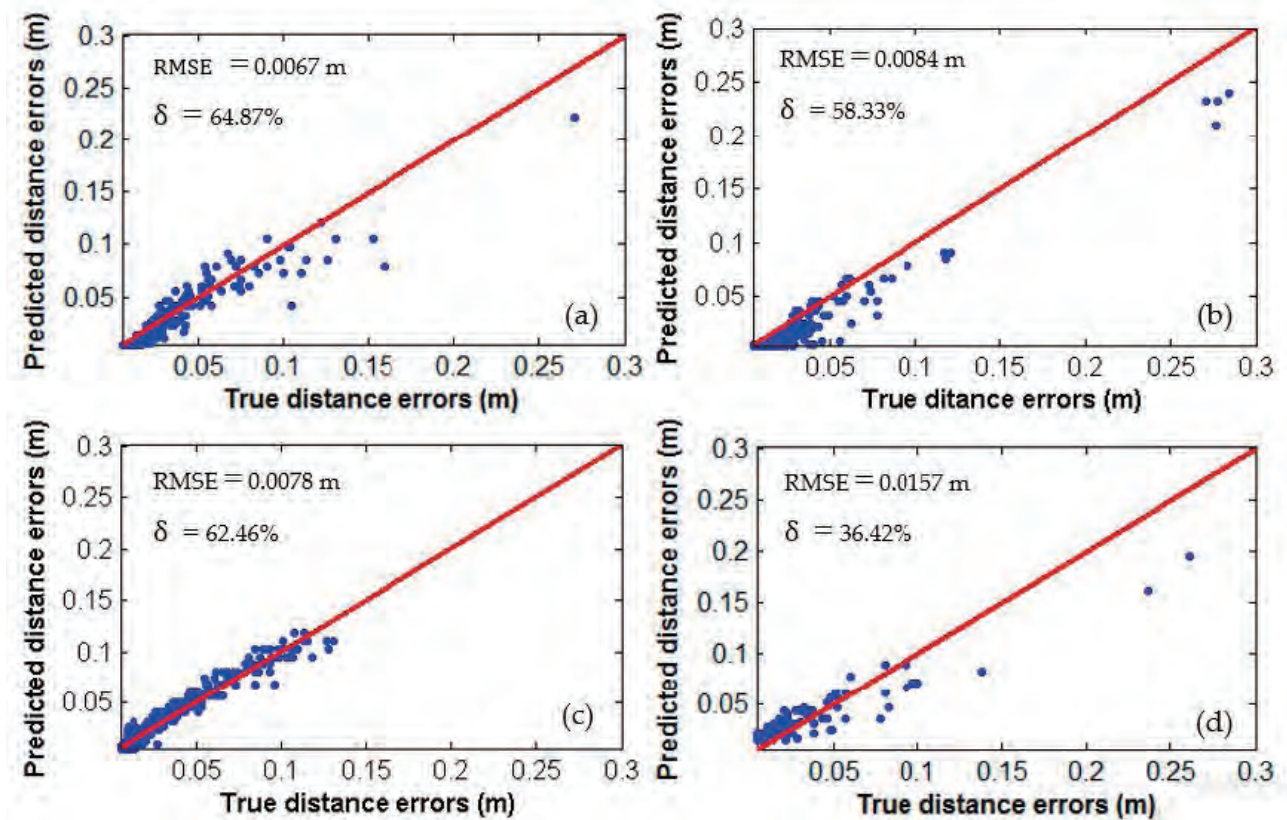


Figure 7. Predicted and true distance errors: (a) polyvinyl chloride sheet; (b) paint steel plate; (c) polished aluminum alloy door; (d) rubber advertising board. The equation of the red lines is $y = x$. RMSE is the root mean square error and δ is a parameter that indicates the degree of distance measurement accuracy improvement.

A study of baroclinic instability induced convergence near the bottom using water age simulations
Zhang W, Hetland R D. *Journal of Geophysical Research Oceans*, 2018, 123(3):1962-1977.

Baroclinic instability of lateral density gradients gives way to lateral buoyancy transport, which often results in convergence of buoyancy transport. Along a sloping bottom, the induced convergence can force upward extension of bottom water. Eddy transport induced convergence at the bottom and the consequent suspended layers of bottom properties are investigated using a three-dimensional idealized model. Motivated by the distinct characteristics of intrusions over the Texas-Louisiana shelf, a series of configurations are performed with the purpose of identifying parameter impacts on the intensity of eddy transport. This study uses the “horizontal slope Burger number” as the predominant parameter; the parameter is functioned with $S_H = SRi^{-1/2} = \delta / Ri$ to identify formation of baroclinic instability, where S is the slope Burger number, δ is the slope parameter, and Ri is the Richardson number, previously shown to be the parameter that predicts the intensity of baroclinic instability on the shelf. Intrusion spreads into the interior abutting a layer that is characterized by degraded vertical stratification; a thickening in the bottom boundary layer collocates with the intrusion, which usually thins at either edge of the intrusion because of a density barrier in association with concentrated isopycnals. The intensity of convergence degrades and bottom tracer fluxes reduce linearly with increased S_H on logarithmic scales, and the characteristics of bottom boundary layer behavior and the reversal in alongshore current tend to vanish.

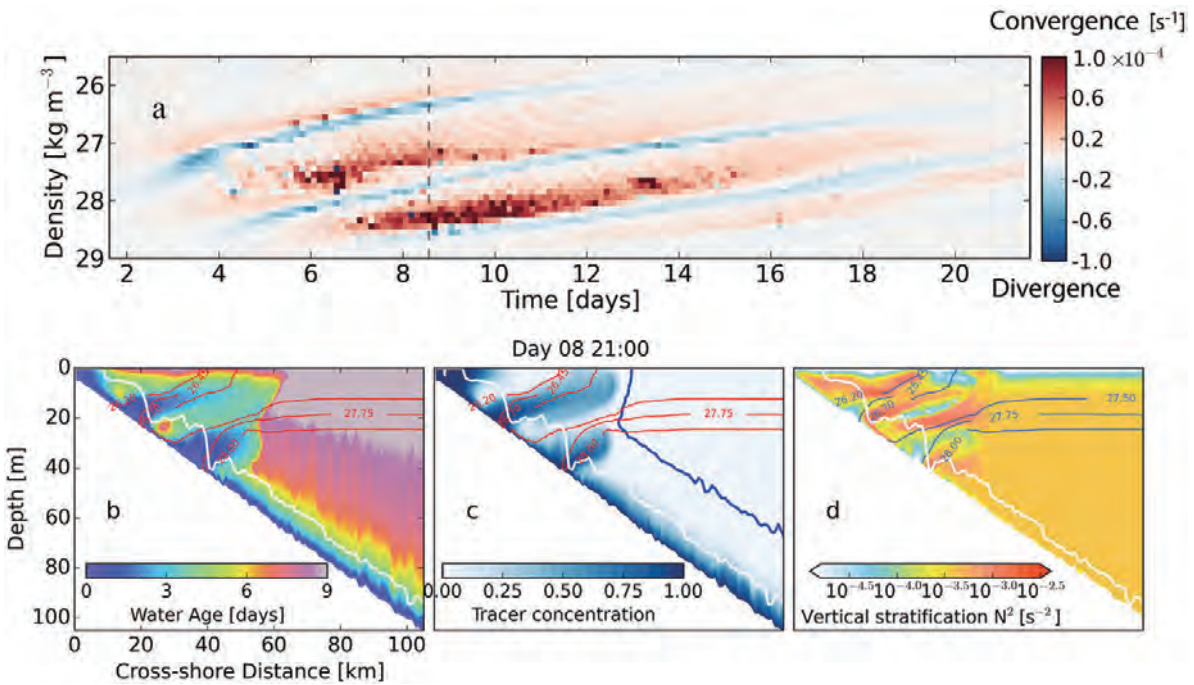


Figure 4. (a) Time series of convergent flow in density coordinates from run 6. Red represents convergence that associated with a net gain of water; blue represents divergence that associated with a net loss of water. Cross-shore section of (b) simulated water age, (c) simulated tracer concentration, and (d) vertical stratification on day 8; the transect is denoted by the red dashed line as shown in Figure 2c. The white lines represent the top of the bottom boundary layer; the blue line in Figure 4c denotes tracer concentration $C_{50.0001}$; and the identical isolines in Figures 4b–4d are density levels.

A modelling approach to assess the effects of atmospheric nitrogen deposition on the marine ecosystem in the Bohai Sea, China

Shou W, Zong H, Ding P, et al. *Estuarine, Coastal and Shelf Science*, 2018, 208:36-48.

Atmospheric deposited nitrogen (AD-N) approximates or exceeds riverine input in many coastal ecosystems, such as the Bohai Sea (BHS) which is one of the most eutrophic coastal waters in China. We construct a three-dimensional (3D) physical-biogeochemical model to understand the influence of atmospheric dissolved inorganic nitrogen (DIN) on the intra- and inter-annual variations of phytoplankton blooms and nutrient dynamics in the BHS. The biological component, which is coupled to the Regional Ocean Modelling System (ROMS), is a simple but widely used Nutrient-Phytoplankton-Zooplankton-Detritus (NPZD) model with eight state variables. The model simulation successfully reproduces the spatial and temporal variations of observed DIN and dissolved inorganic phosphorus (DIP) and the climatological features of phytoplankton biomasses (chlorophyll a), which confirms the major role of air-transported nutrients in controlling standing stocks and nutrient limitations. The modelling results show that the relative contributions of deposited nitrogen to the total DIN in the seawater for the Bohai, Laizhou and Liaodong Bays and Central Bohai Basin reach 84.8%, 49.3%, 37.4% and 44.4% on average, respectively. The relative contribution ratio is approximately 54% for the entire Bohai region, causing a 56.5% increase in the phytoplankton biomass on average. These results also indicate that the effects of AD-N on nutrient and phytoplankton dynamics vary widely in regional areas because of the uneven spatial distribution of nitrogen deposition fluxes and also partially because of the hydrodynamic conditions, shortwave radiation and water temperatures.

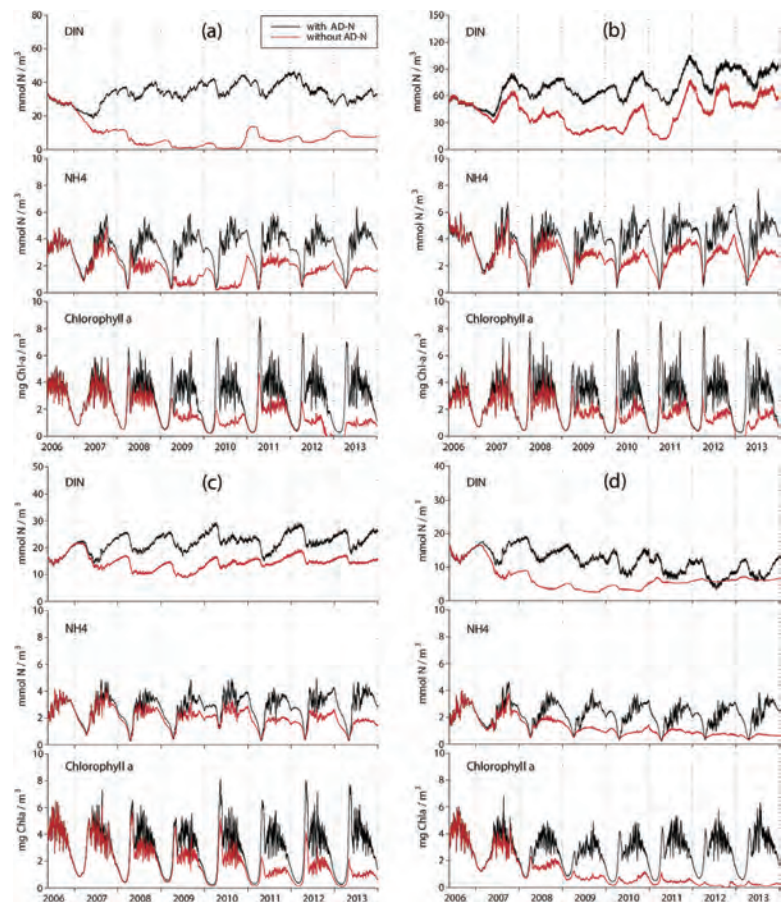


Fig. 6. Modeled DIN, NH₄⁺ and Chl-a in (a) BHB, (b) LZB, (c) LDB and (d) the CBB with (black lines) and without (red lines) atmospheric N deposition from 2006 to 2013. (For interpretation of the references to color in this figure legend, the reader is referred to the Web version of this article.)

河口海岸生态与环境 *Estuarine and Coastal Ecology and Environment*

Reconsideration of the systematics of Peniculida (Protista, Ciliophora) based on SSU rRNA gene sequences and new morphological features of Marituja and Disematostoma

Xu Y, Gao F, Fan X. *Hydrobiologia*, 2018, 806(1):313-331.

Ciliated protists are unicellular eukaryotes that play important roles in aquatic ecosystems. One of the major tasks of ciliate taxonomy is to re-evaluate the systematic confusing taxa using modern methods. In the present study, two peniculid ciliates, *Marituja* cf. *caudata* and *Disematostoma* *minor* collected from east China, were studied using a multi-method approach. New morphological observations supplied additional information for species identification and systematic revision of the order Peniculida. The small subunit ribosomal RNA gene sequences of *M.* cf. *caudata*, *D.* *minor*, and *Frontonia* *terricola* were characterized for the first time and provided new insights into the phylogeny of Peniculida. The family Stokesiidae Roque, 1961, was expanded to include the genera *Disematostoma* and *Marituja* in addition to its type genus *Stokesia*, since the three genera formed a well-supported clade in the phylogenetic analyses. The diagnosis of Stokesiidae was improved to include the newly recognized synapomorphies, i.e., barren kinetosomes on the dorsal side, a ciliated dorsal suture, and the somatic ciliature that can be recognized as transversely oriented circles. Additionally, the systematic relationships of the genera and families of Peniculida were hypothesized. We argue that more diversified morphological features should be considered when assessing diagnostic traits for ciliate taxa during systematic revisions.

本研究对采自长江口崇明东滩湿地的一种罕见纤毛门原生动物的研究。通过结合基于18s rRNA基因序列的系统分析和形态特征分析，我们对Stokesiidae科进行了重新定义。同时我们提出在进行系统修订时，应当考虑更加多样化的形态特征。

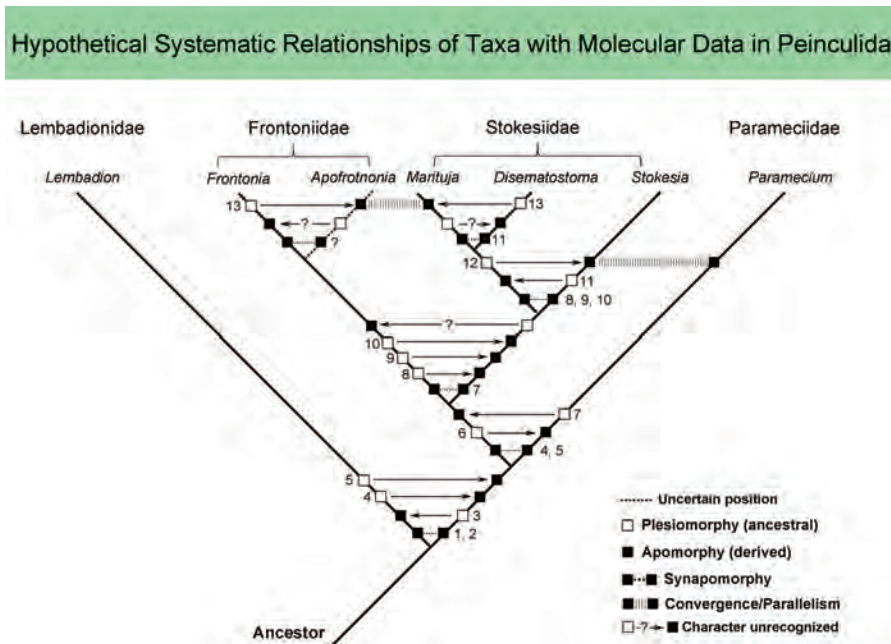


Fig. 9 Hypothetical systematic relationships of Peniculida taxa based on the combined phylogenetic analyses and morphological data. Character states used to separate taxa are listed in Table 3

Microplastics in freshwater river sediments in Shanghai, China: A case study of risk assessment in mega-cities

Peng G, Xu P, Zhu B, et al. *Environmental Pollution*, 2018, 234:448-456.

Microplastics, which are plastic debris with a particle diameter of less than 5 mm, have attracted growing attention in recent years. Its widespread distributions in a variety of habitats have urged scientists to understand deeper regarding their potential impact on the marine living resources. Most studies on microplastics hitherto are focused on the marine environment, and research on risk assessment methodology is still limited. To understand the distribution of microplastics in urban rivers, this study investigated river sediments in Shanghai, the largest urban area in China. Seven sites were sampled to ensure maximum coverage of the city's central districts, and a tidal flat was also included to compare with river samples. Density separation, microscopic inspection and m-FT-IR analysis were conducted to analyze the characteristics of microplastics and the type of polymers. The average abundance of microplastics in six river sediment samples was 802 items per kilogram of dry weight. The abundance in rivers was one to two orders of magnitude higher than in the tidal flat. White microplastic spheres were most commonly distributed in river sediments. Seven types of microplastics were identified, of which polypropylene was the most prevailing polymers presented. The study then conducted risk assessment of microplastics in sediments based on the observed results, and proposed a framework of environmental risk assessment. After reviewing waste disposal related legislation and regulations in China, this study conclude that in situ data and legitimate estimations should be incorporated as part of the practice when developing environmental policies aiming to tackle microplastic pollution.

迄今为止，关于微塑料的生态效应的研究大多集中在室内实验中，缺少对环境介质中微塑料的风险评估的工作。本研究对中国经济发达城市——上海市内的河道沉积物进行了野外采样调查。研究调查了6个河道的沉积物，并采集了1个潮滩的沉积物样品进行对比。通过密度悬浮分离法、显微红外光谱仪的分析，综合比较了微塑料的赋存特性及风险程度。研究发现，七个采样点的所有样品中都存在丰度较高的微塑料，平均丰度达到802件每千克干重。根据人口数量比较区域微塑料污染程度，人口密集地区的微塑料丰度比郊区要高出1-2个数量级。此外，微塑料在不同地区的赋存特征也不尽相同。白色球状微塑料颗粒在河道沉积物中分布最为广泛，而在潮滩中纤维和碎片状的微塑料则占大部分。塑料聚合物分析的结果表明，以聚丙烯(PP)为主要成分的微塑料在数量上占有较大优势。通过对微塑料分布特征的综合分析，进一步了探究城市河道中微塑料的来源。河岸两侧的人类活动、部分未经管控的垃圾处理，导致微塑料大量累积在河道中，最终随河流进入海洋，或沉降于沉积环境中。本研究基于对城市河道沉积物中微塑料的观测结果，对沉积环境中的微塑料生态风险进行了评估，提出了环境风险评估的基本框架，并总结我国的关于废弃物处理的相关立法和法规，旨在为今后治理微塑料污染提供理论支持。科学的实地观测数据和合理的预估推算，是制定管理微塑料污染相关法规的重要基础。未来微塑料的科学研究需要来自不同领域和地区的科学家通力合作，这将有助于我们了解微塑料的分布、来源和归趋。

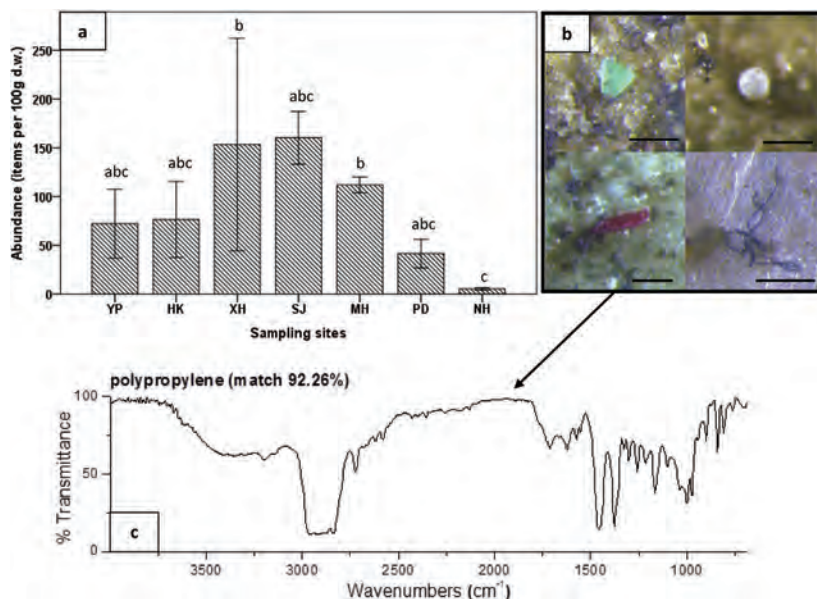


Fig. 2. (a) The average abundance of microplastics per 100 g dry weight sediment in seven sampling sites (error bars indicate standard error of the mean). Bars with the same letter have no significant difference (Mann-Whitney U test, $p < 0.05$). (b) Photos of observed microplastic particles in the shape of fragments, pellets, and fibers, and of various colors. All scale bars indicate 200 μ m. (c) Infrared spectrum of the red fragment particle in 2b, which was identified as polypropylene by m-FT-IR (match 92.26%). (For interpretation of the references to color in this figure legend, the reader is referred to the Web version of this article.)

Native and non-native halophytes resiliency against sea-level rise and saltwater intrusion

Xue L, Li X, Yan Z, et al. *Hydrobiologia*, 2018, 806:47-65.

We quantified the independent impacts of flooding salinity, flooding depth, and flooding frequency on the native species, *Phragmites australis* and *Scirpus mariqueter*, and on the invasive species *Spartina alterniflora* in the Yangtze River Estuary, China. Total biomass of all three species decreased significantly with increasing salinity, but *S. alterniflora* was less severely affected than *P. australis* and *S. mariqueter*. Elevated flooding depth significantly increased their live aboveground biomass of *P. australis* and *S. mariqueter*, while *S. alterniflora* still had high live aboveground biomass and total biomass even at the highest flooding depth. These findings indicated that *S. alterniflora* was more tolerant to experimental conditions than the two native species, and an unavoidable suggestion is the expansion of this non-native species in relation to the native counterparts in future scenarios of increased sea-level and saltwater intrusion. Even so, environmental stresses might lead to significant decreases in total biomass and live aboveground biomass of all three species, which could potentially weaken their ability to trap sediments and accumulate organic matter. However, the relatively high belowground-to-aboveground biomass ratio indicated phenotypic plasticity in response to stressful environmental conditions, which suggests that marsh species can adapt to sea-level rise and maintain marsh elevation.

盐度和淹水变化是影响滨海盐沼植物生长、繁殖和空间分布的关键压力因素，通过调控植物初级生产力和有机质内源输入制约盐沼滩面垂向淤涨。当前，海平面上升和盐水入侵加剧等使盐沼现有盐度和淹水胁迫更为严峻，因此需要通过单因素控制实验来获取盐沼植物对盐度和淹水变化的响应及阈值，作为对野外多因素综合作用的补充。在分析了淹水盐度、深度和频率变化对本地种芦苇、海三棱草，和入侵种互花米草生物量及分配的影响后发现，本地种生物量随淹水盐度和深度增加而下降的程度高于入侵种，均对淹水频率变化无显著响应差异，仅本地种根冠比随淹水盐度增加而显著增加。盐度和淹水胁迫一定程度上会促进互花米草的散布扩张，本地种在高盐环境下倾向于分配更多生物量至地下根系，这对维持盐沼滩面海拔高程更为有利，以应对持续上升的海平面。

Adherence of microplastics to soft tissue of mussels: A novel way to uptake microplastics beyond ingestion

Kolandhasamy P, Su L, Li J, et al. *Science of The Total Environment*, 2018, 610-611:635-640.

Microplastic pollution is recognized as an emerging threat to aquatic ecosystems. One of the main environmental risks associated with microplastics is their bioavailability to marine organisms. Up to date, ingestion has been widely accepted as the sole way for the animals to uptake microplastics. Nevertheless, microplastics have also been found in some organs which are not involved in the process of ingestion. We hypothesize that the animal might uptake microplastics through adherence in addition to ingestion. To test this hypothesis, we collected mussels from the fishery farms, conducted exposure/clearance experiments and analyzed the accumulation of microplastics in specific organs of mussels. Our studies clearly showed the uptake of microplastic in multiple organs of mussels. In the field investigations, we found that the abundance of microplastic by weight but not by individual showed significant difference among organs, and the intestine contained the highest level of microplastics (9.2 items/g). In the uptake and clearance experiment, the accumulation and retention of microfibers could also be observed in all tested organs of mussels including foot and mantle. Our results strongly suggest that

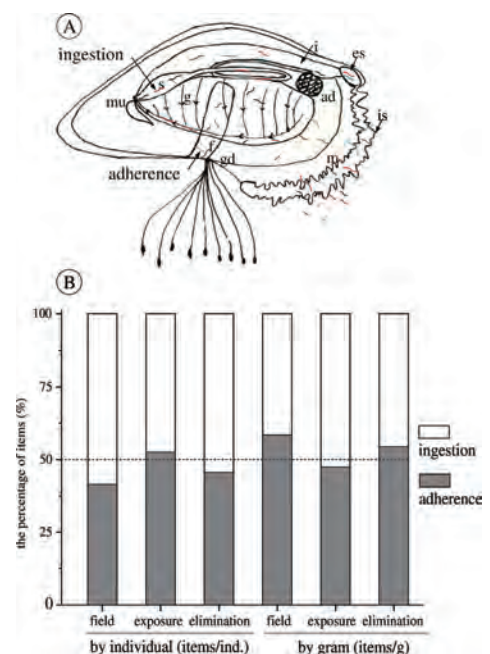


Fig. 5. Ingestion and adherence of microplastics in the mussels. A, outline of the pathway of microplastic ingestion and clearance; B–C, the proportion of ingestion and adherence of microplastics by items/g (B) and by items/individual (C). Gill, intestine and stomach were regarded as being involved in ingestion process, and the rest organs were supposed to be only involved in the adherence process. Abbreviations: ad, adductor tissue; es, exhalant siphon; f, foot; g, gills; gd, gonad; m, mantle skirt; mu, mouth; i, intestine; is, inhalant siphon; s, stomach.

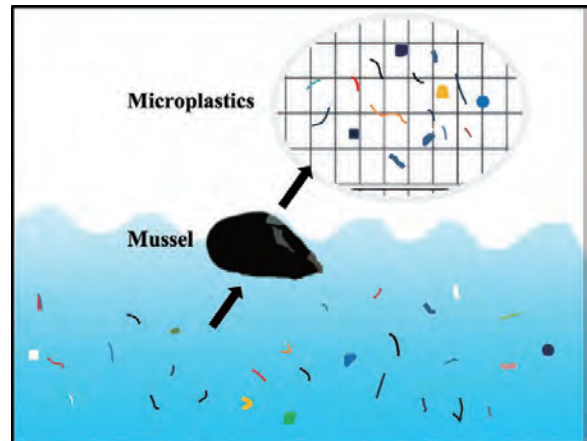
adherence rather than ingestion led to the accumulation of microplastics in those organs which are not involved in ingestion process. To our best knowledge, it is the first time to propose that adherence is a novel way for animals to uptake microplastics beyond ingestion. This new finding makes us rethink about the bioavailability, accumulation and toxicity of microplastics to aquatic animals.

海洋微塑料污染的普遍性和高生物利用度已被人们广泛认知。目前，摄食被认为是生物摄取微塑料的唯一途径。然而，已有研究表明在一些不参与摄入过程的器官中也发现了微塑料。我们假设生物除了摄入塑料外，还可能通过粘附吸收微塑料。为了验证这一假设，我们从水产市场购买健康的贻贝活体，进行暴露/清除实验，并分析了贻贝特定器官中微塑料的积累。结果表明，在贻贝的多个器官中均发现微塑料的存在。野外调查发现贻贝不同器官间微塑料的丰度存在显著差异，其中肠道中微塑料的含量最高(9.2个/g)。暴露/清除实验发现在足部和套膜上也发现了微塑料的积累。因此，本研究结果表明，粘附而非摄入导致了微塑料在那些不参与摄入过程的器官中积累。本研究第一次提出了粘附是生物摄取微塑料的一种新方法。这一新发现让我们重新思考微塑料对水生生物的生物利用度、积累和毒性。

Assessing the relationship between the abundance and properties of microplastics in water and in mussels

Qu X, Su L, Li H, et al. *Science of The Total Environment*, 2018, 621:679-686.

Microplastic pollution is increasingly becoming a great environmental concern worldwide. Microplastics have been found in many marine organisms as a result of increasing plastic pollution within marine environments. However, the relationship between microplastics in organisms and their living environment is still relatively poorly understood. In the present study, we investigated microplastic pollution in the water and the mussels (*Mytilus edulis*, *Perna viridis*) at 25 sites along the coastal waters of China. We also, for the first time, conducted an exposure experiment in parallel on the same site using *M. edulis* in the laboratory. A strong positive linear relationship was found between microplastic levels in the water and in the mussels. Fibers were the dominant microplastics. The sizes of microplastics in the mussels were smaller than those in the water. During exposure experiments, the abundance of microbeads was significantly higher than that of fibers, even though the nominal abundance of fibers was eight times that of microbeads. In general, our results supported positive and quantitative correlations of microplastics in mussels and in their surrounding waters and that mussels were more likely to ingest smaller microplastics. Laboratory exposure experiment is a good way to understand the relative impacts of microplastics ingested by marine organisms. However, significant differences in the results between exposure experiments and field investigations indicated that further efforts are needed to simulate the diverse environmentally relevant properties of microplastics.



微塑料污染已经成为一个世界性的环境污染问题，双壳贝类由于其滤食特性而易于摄食环境中的微塑料。在对我国市售贻贝和东南沿海紫贻贝污染特征调查的基础上，进一步对我国沿海贻贝和牡蛎及其生活的水体中微塑料的污染情况进行调查，发现水体中微塑料的含量在0.68到6.44个/升，紫贻贝体内的微塑料含量在1.52到5.36个/克以及0.77到8.22个/个体。同时，发现水体和贻贝中的微塑料含量具有较强的正相关关系，其相关性不受贻贝品种的影响($p < 0.05$)。该研究表明贻贝可以作为海水环境中微塑料的污染指示种。

为了进一步探索贻贝在组织器官水平上对微塑料的摄入和转运特征，开展了基于贻贝分组织器官的微塑料污染负荷调查以及相应的室内模拟实验。发现不同类型的微塑料不仅能通过通常认为的主动摄入方式（经消化道或呼吸作用）进入生物体内，也有相当部分经被动吸附行为滞留在生物体表面，尤其是腹足部位含量较高。该研究揭示除摄食外，组织粘附是微塑料进入食物链的一条新的途径。

同时，我们选取河蚬作为对象，调查了太湖、鄱阳湖和淀山湖等21个站点河蚬、表层水体和底泥中微塑料的污染特征，结果表明河蚬体内微塑料与底泥中微塑料污染的相关性更为密切。结合运用河蚬室内毒理学暴露的结果，我们提出以河蚬作为淡水系统微塑料污染的指示种。

Using the Asian clam as an indicator of microplastic pollution in freshwater ecosystems

Su L, Cai H, Kolandhasamy P, et al. *Environmental Pollution*, 2018, 234:347-355.

Bioindicators play an important role in understanding pollution levels, bioavailability and the ecological risks of contaminants. Several bioindicators have been suggested for understanding microplastic in the marine environment. A bioindicator for microplastics in the freshwater environment does not exist. In our previous studies, we found a high frequency of microplastic pollution in the Asian clam (*Corbicula fluminea*) in Taihu Lake, China. In the present study, we conducted a large-scale survey of microplastic pollution in Asian clams, water and sediment from 21 sites in the Middle-Lower Yangtze River Basin from August to October of 2016. The Asian clam was available in all sites, which included diverse freshwater systems such as lakes, rivers and estuaries. Microplastics were found at concentrations ranging from 0.3-4.9 items/g (or 0.4-5.0 items/individual) in clams, 0.5-3.1 items/L in water and 15-160 items/kg in sediment. Microfibers were the most dominant types of microplastics found, accounting for 60-100% in clams across all sampling sites. The size of microplastics ranged from 0.021-4.83 mm, and microplastics in the range of 0.25-1 mm were dominant. The abundance, size distribution and color patterns of microplastics in clams more closely resembled those in sediment than in water. Because microplastic pollution in the Asian clam reflected the variability of microplastic pollution in the freshwater environments, we demonstrated the Asian clam as a bioindicator of microplastic pollution in freshwater systems, particularly for sediments.

微塑料污染已经成为一个世界性的环境污染问题，双壳贝类由于其滤食特性而易于摄食环境中的微塑料。在对我国市售贻贝和东南沿海紫贻贝污染特征调查的基础上，进一步对我国沿海贻贝和牡蛎及其生活的水体中微塑料的污染情况进行调查，发现水体中微塑料的含量在0.68到6.44个/升，紫贻贝体内的微塑料含量在1.52到5.36个/克以及0.77到8.22个/个体。同时，发现水体和贻贝中的微塑料含量具有较强的正相关关系，其相关性不受贻贝品种的影响($p < 0.05$)。该研究表明贻贝可以作为海水环境中微塑料的污染指示种。

为了进一步探索贻贝在组织器官水平上对微塑料的摄入和转运特征，开展了基于贻贝分组织器官的微塑料污染负荷调查以及相应的室内模拟实验。发现不同类型的微塑料不仅能通过通常认为的主动摄入方式（经消化道或呼吸作用）进入生物体内，也有相当部分经被动吸附行为滞留在生物体表面，尤其是腹足部位含量较高。该研究揭示除摄食外，组织粘附是微塑料进入食物链的一条新的途径。

同时，我们选取河蚬作为对象，调查了太湖、鄱阳湖和淀山湖等21个站点河蚬、表层水体和底泥中微塑料的污染特征，结果表明河蚬体内微塑料与底泥中微塑料污染的相关性更为密切。结合运用河蚬室内毒理学暴露的结果，我们提出以河蚬作为淡水系统微塑料污染的指示种。

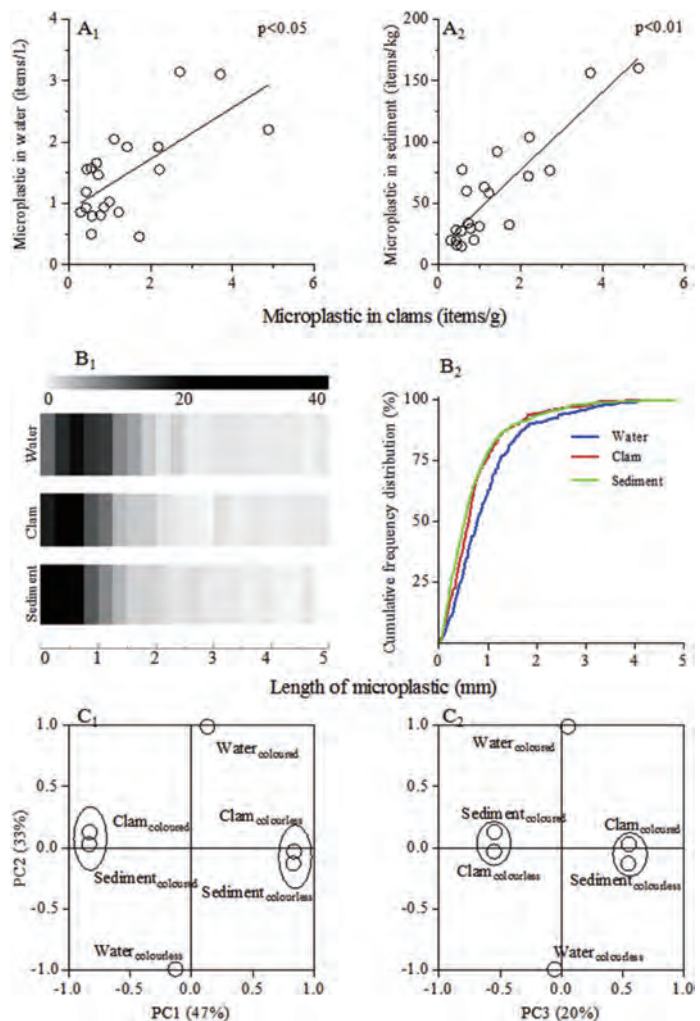


Fig. 5. The relation of microplastics in clams to those in water and sediment. (A) The abundance; (B) The size. The heat map (B1) and the cumulative curve of frequency (B2) were used to show the distribution of microplastic sizes; (C) The color. Principle component analysis was used to interpret the microplastic color patterns. Component loadings for the first and second components (C1) and the second and third component (C2) were plotted. (For interpretation of the references to colour in this figure legend, the reader is referred to the web version of this article.)

Combined effect of water inundation and heavy metals on the photosynthesis and physiology of *Spartina alterniflora*.

Sun X, Xu Y, Zhang Q, et al. *Ecotoxicology and Environmental Safety*, 2018, 153:248-258.

Water samples were collected from the Changjiang Estuary (CE) and adjacent East China Sea (ECS) during two cruises in March 2013 and July 2014 to investigate the distributions and dynamics of dissolved carbohydrate species. The concentrations of surface dissolved organic carbon (DOC) and total dissolved carbohydrates (TCHO) were higher in summer compared with those in spring. The dissolved polysaccharides (PCHO) in surface waters accounted for $65 \pm 14\%$ and $47 \pm 18\%$ of TCHO on average in spring and summer, respectively. The average TCHO/DOC ratio in summer was $17 \pm 5\%$, compared with $11 \pm 3\%$ in spring. DOC and dissolved monosaccharides (MCHO) were significantly correlated with salinity in both seasons, indicating that physical mixing was a major controller of the DOC and MCHO distributions. By contrast, PCHO exhibited greater variations with increasing salinity, which suggest that MCHO and PCHO had different features in the study area. According to principal component analysis, PCHO were significantly correlated with the second principal component "biological factors" and they had the opposite loading with nutrients, especially NO_2^- , which suggest that PCHO were affected greatly by nutrient-related biological processes, such as primary production and bacterial assimilation. By contrast, MCHO were affected mainly by physical factors, especially terrigenous inputs. After comparing the stations with similar salinity along the Changjiang diluted water transport pathways during summer, we observed the obvious production of PCHO and DOC, as well as the consumption of nutrients, which further demonstrated biological impacts on the PCHO concentrations. Furthermore, the increase in PCHO was only half that of DOC, demonstrating the production of other organic matter via the transformation of PCHO, or other biological processes. However, the MCHO concentrations remained constantly high in Changjiang diluted water patches in CE, and appeared to decrease with dilution, suggesting that these molecules persisted rapid microbial turnover. In general, the dynamics of MCHO and PCHO were very different in the study area. MCHO exhibited conservative behavior, whereas PCHO were highly bioactive and influenced greatly by biological factors in the CE and adjacent ECS.

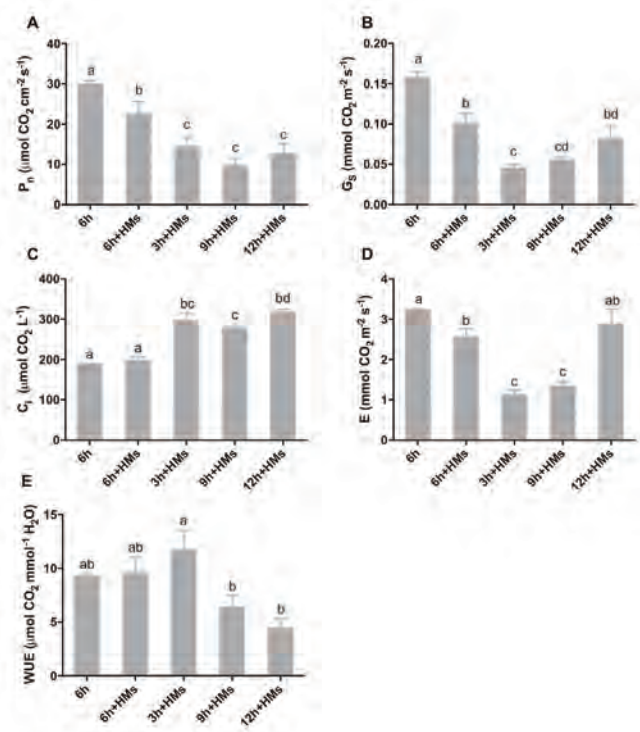


Fig. 4. Effect of different time of water inundation with HMs on (A) P_n , (B) G_s , (C) C_i , (D) E and (E) WUE of *S. alterniflora* (values are mean and SD; for each parameter, data with different letters are significantly different at $P \leq 0.05$).

典型的湿地植物如互花米草等能吸附固化大量的潮滩湿地土壤中的重金属，这种特性使得它们具有一定的植物修复潜力，在一些应用研究中被用来构建人工湿地来处理湿地重金属的污染。潮滩湿地周期性的淹水环境以及人类活动和气候变化等对滩涂地貌高程等的影响，使潮滩湿地土壤的氧化还原，土壤质地，盐度以及有机质等理化特性复杂多变，从而对各种重金属的赋存形态以及其生物有效性产生显著影响，也对重金属在湿地植物中的累积吸收及其毒性效应产生影响。本研究以长江口典型湿地植物互花米草为研究对象，通过温室控制实验研究不同时间淹水（3，6，9，12小时/天）及复合重金属（潮滩环境背景浓度的Cu，Zn，Pb，Cr）复合处理下，互花米草的生理响应特征。作为对照，本研究也采集测定了不同高程潮滩（低、中、高）的互花米草叶片的叶绿素（chl）及丙二醛（MDA）的含量。研究结果表明，20天的淹水及重金属复合处理对互花米草的叶片叶绿素含量未造成显著的影响，在处理第60天时，每天12h的淹水显著降低了叶片叶绿素a（chl_a），叶绿素b（chl_b）以及chl_a/chl_b的比值。净光合

速率 (Pn) 的响应要比叶绿素对淹水和重金属复合处理的响应要敏感的多, 3-12小时/天的淹水和重金属复合处理均显著降低叶片的Pn, 其中9和12小时/天的处理对Pn的抑制最大。淹水时间的延长显著提高了叶片MDA含量, 这与野外采集叶片的MDA随潮位降低而升高的变化一致。主要抗氧化保护酶的活性在短期 (20天) 和长期 (60天) 淹水及重金属复合处理也表现出不同的响应特征, 短期 (20天) 处理下, 植物叶片及根部的过氧化物酶 (POD), 抗坏血酸过氧化物酶 (APx) 以及超氧化物歧化酶 (SOD) 的活性均表现出随淹水时间的延长而升高的趋势。在处理的第60天, 植物叶片的POD和SOD的活性呈现出与20天时相反的变化趋势, 即随着淹水时间的增加而降低, 9-12小时/天的淹水重金属复合处理显著抑制了叶片SOD及POD的活性。通过本研究可知, 互花米草在小于6小时每天的重金属处理下, 从长期来看除了净光合速率受到一定影响之外, 在基本的抗氧化生理上并未受到明显的影响, 表现出一定的淹水和重金属的抗性。

Ecophysiological response of native and exotic salt marsh vegetation to waterlogging and salinity: Implications for the effects of sea-level rise

Li S, Ge Z, Xie L, et al. *Scientific Reports*, 2018, 8(1):2441.

The ecophysiological characteristics of native *Phragmites australis* and exotic *Spartina alterniflora* grown under waterlogging and salinity were investigated to explore their adaptation potential to sea level rise. The seasonal course of phenotypic traits, photosynthetic activity and chlorophyll fluorescence parameters of *P. australis* did not change remarkably under shallow flooding, whereas these variables were sensitive to increasing salinity. Waterlogging exacerbated the negative effects of salinity on shoot growth and photosynthetic activity of *P. australis*, and the combined stresses led to an absence of tassel and reproductive organs. By contrast, *S. alterniflora* performed well under both stresses and showed an obvious adaptation of salt secretion with increasing salinity. Light salinity was the optimal condition for *S. alterniflora*, and the tassel growth, chlorophyll content and fluorescence characters under moderate stresses did not differ notably. The Na⁺ and Cl⁻ concentrations in leaves of both species increased, and the K⁺ content decreased in response to salinity. Under moderate and high saline levels, the ion concentrations in *S. alterniflora* were maintained at relatively consistent levels with increased salt secretion. We expect the degradation of *P. australis* and further colonization of *S. alterniflora* under prolonged flooding and saltwater intrusion from sea level rise on the coastline of China.

滨海湿地植被对潮汐和盐度等水文因子的适应性是决定滩群群落动态的关键因素。芦苇*Phragmites australis*和互花米草*Spartina alterniflora*分别是我国海岸带典型的本土建群种和外来入侵植物。增高淹水对两种植物的生长和光合能力均没有显著影响。然而盐度升高对芦苇的影响显著, 而且淹水和盐度共同作用下加剧抑制了芦苇生长和繁殖器官的发育。相对而言, 盐度对外来物种互花米草生长、光合能力和繁殖器官的影响程度较弱。特别是互花米草具备盐腺, 在高盐度条件下能够析出多余盐分, 调节离子平衡, 体现出较强的生理生态学适应性。在未来海平面上升引起的长期淹水和盐水负荷条件下, 可能引发中国海岸线本土植物的退化和外来种的进一步入侵。

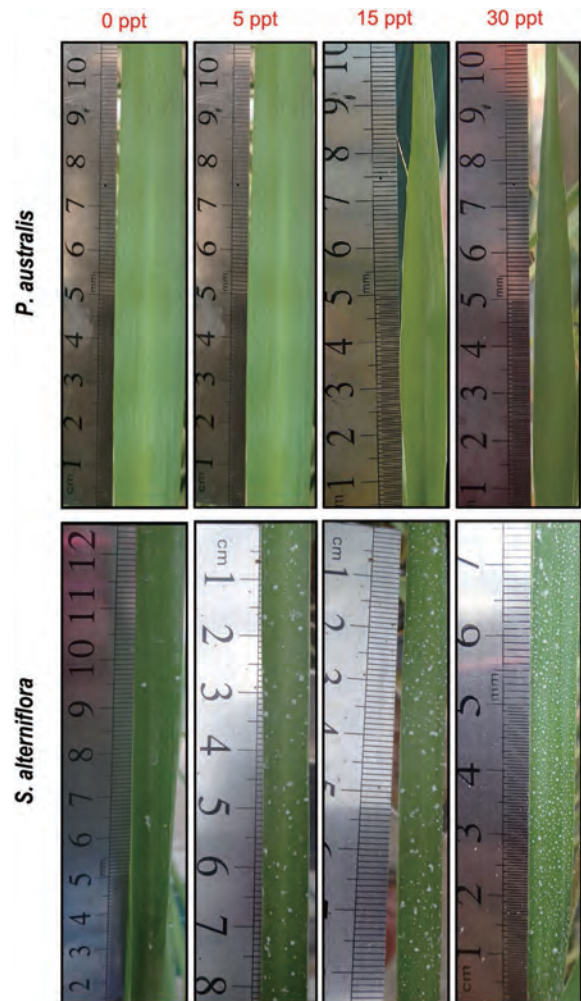


Figure 6. Leaves of *P. australis* (upper panel, no salt secretion) and *S. alterniflora* (bottom panel, distinct salt secretion) subjected to the salinity gradient. The amount of salt secretion was similar between waterlogging treatments. (Photos by S.H.L. and Z.M.G.).

Linkages between the spatial toxicity of sediments and sediment dynamics in the Yangtze River Estuary and neighboring East China Sea

Gao J, Shi H, Dai Z, et al. *Environmental Pollution*, 2018, 233:1138-1146.

NAnthropogenic activities are driving an increase in sediment contamination in coastal areas. This poses significant challenges for the management of estuarine ecosystems and their adjacent seas worldwide. However, few studies have been conducted on how dynamic mechanisms affect the sediment toxicity in the estuarine environment. This study was designed to investigate the linkages between sediment toxicity and hydrodynamics in the Yangtze River Estuary (YRE) area. High sediment toxicity was found in the Yangtze River mouth (Region I), the depocenter of the Yangtze River Delta (Region II), and the southeastern area of the adjacent sea (Region III), while low sediment toxicity was found in the northeastern offshore region (Region IV). A spatial comparison analysis and regression model indicated that the distributed pattern of sediment toxicity was likely related to hydrodynamics and circumfluence in the East China Sea (ECS) shelf. Specifically, high sediment toxicity in Region I may be affected by the Yangtze River Pump (YRP) and the low hydrodynamics there, and high toxicity in Region II can be influenced by the low sediment dynamics and fine sediment in the depocenter. The high sediment toxicity in Region III might be related to the combination of the YRP and Taiwan Warm Current, while the low toxicity in Region IV may be influenced by the local coarse-grained relict sand with strong sediment dynamics there. The present research results further suggest that it is necessary to link hydrodynamics and the spatial behavior of sediment and sediment-derived pollutants when assessing the pollution status of estuarine environments, especially for those mega-estuaries and their neighboring ocean environments with complex waves, tides and ocean currents.

人类活动正在导致海岸带沉积物中污染的增加，从而全球河口生态系统和临近海湾管理面临重要挑战。然而，一直有较少的研究涉及动力机制是如何影响在河口环境泥沙毒性变化。本研究被设计研究长江河口泥沙毒性和水动力之间的耦合关联机制。高的沉积毒性区被发现在长江河口，长江三角洲沉积中心和临近海区的东南离岸区，相对低的沉积毒性区位于长江口北部。空间相关和回归模型表明沉积物毒性区是很可能受水动力和东海海流体系影响。其中，长江口高沉积物毒性可能受长江冲淡水 and 相对低的水动力控制，而沉积中心的高毒性区则受底的沉积动力和高沉降影响。在河口东南部的高沉积毒性主要是和长江冲淡水和台湾暖流共同控制。相对低的沉积物毒性则是受东海陆架残留粗砂和强劲水流作用相关。当前的研究深远的表明，当评估复杂动力作用下的河口环境尤其是巨型河口和临界海湾环境的沉积物污染时，将水动力与泥沙空间行为及泥沙污染直接串联是非常必要的。

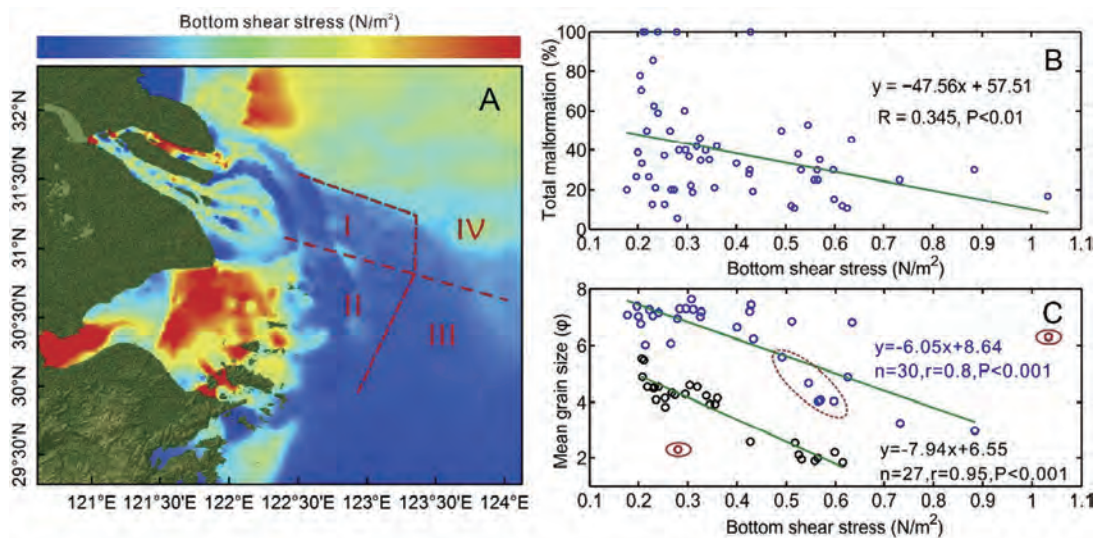


Fig. 8. Bottom shear stress and the sediment dynamic mechanism of sediment toxicity in the Yangtze River Estuary and the neighboring ECS. A. spatial distribution of bottom shear stress; B. correlation between bottom shear stress and percentage of total malformation; C. correlation between bottom shear stress and mean grain size of sediment. The black dots are samples with coarse grain sizes from the relict sand area, while the blue dots (except the ones in the dashed circle) are samples with fine grain sizes from the Yangtze River. Samples within the red circles were excluded when conducting the correlation analysis. (For interpretation of the references to colour in this figure legend, the reader is referred to the web version of this article.)

The role of *ppary* in embryonic development of *Xenopus tropicalis* under triphenyltin-induced teratogenicity

Zhu J, Huang X, Jiang H, et al. *Science of The Total Environment*, 2018, 633:1245-1252.

Evidence has shown that triphenyltin (TPT) triggers severe malformations in *Xenopus tropicalis* embryos, partly due to activation of PPAR γ (peroxisome proliferator activated receptor γ) protein. In the present study, we investigated how abundance of *ppary* and TPT exposure interact and affect *X. tropicalis* embryonic development. We observed *ppary* expression signals appeared in the neural crest and neural fold, as well as in the brain, eyes and spinal cord organs. Both *ppary* overexpression and its Morpholino (MO) knockdown inhibited *pax6* (paired box 6) expression, a marker of eye development, and significantly up- and down-regulated lipid and glucose homeostasis related genes, such as *lpl* (lipoprotein lipase), *slc2a4* (solute carrier family 2 (facilitated glucose transporter), member 4) and *pck1* (phosphoenolpyruvate carboxykinase 1, cytosolic), thus inducing eye phenotypes. Overexpression of *ppary* induced small eye phenotype, while *ppary* MO induced small eye plus turbid eye lens microencephaly and enlarged trunk. In contrast, 5–20 $\mu\text{g Sn/L}$ (stannum/L) TPT exposure reversed some impacts induced by *ppary* overexpression, i.e., no small eye, up-regulation of *pax6* and down-regulation of *ppary*, *lpl*, *slc2a4* and *pck1*. Meanwhile, microinjection of *ppary* MO combined with exposure to 20 $\mu\text{g Sn/L}$ TPT caused 85% mortality. In brief, our work clearly indicates that *ppary* is essential to eye development and inhibition of its expression combined with TPT exposure can be extremely harmful to *X. tropicalis* embryo.

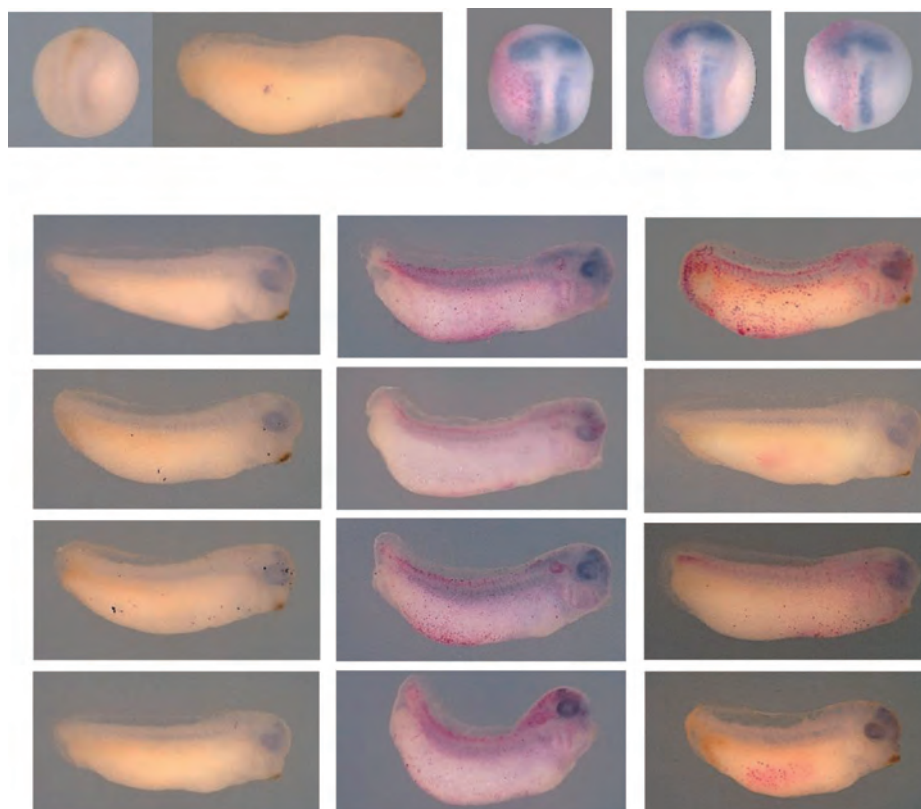


Fig. 5. WISH of *pax6* in *X. tropicalis* embryos following *ppary* misexpression and TPT exposure. (A) In situ hybridization of *pax6* sense probe (control). (B) Embryos were injected at the 2-cell stage with 10 ng standard control MO, and were cultured in 0.1 \times MMR until stage 17 for *pax6* WISH. (C–D) Embryos were injected at the 2-cell stage with 150 pg *ppary* mRNA or 10 ng *ppary* MO, and were cultured in 0.1 \times MMR until stage 17. (E–H) Uninjected embryos were treated with 0, 5, 10, 20 $\mu\text{g Sn/L}$ TPT, and were collected until stage 31. (I–L, M–P) 150 pg *ppary* mRNA or 10 ng *ppary* MO injected embryos were treated with 0, 5, 10, 20 $\mu\text{g Sn/L}$ TPT, and were collected until stage 31. The yellow arrowheads indicate the reduced *pax6* signals. There were 10 embryos per replicate and 3 replicate dishes per group ($n=3$). The confidence ratio is shown in the bottom right of each photo. Scale bar=0.5 mm. (For interpretation of the references to color in this figure legend, the reader is referred to the web version of this article.)

Nutrient input through submarine groundwater discharge in two major Chinese estuaries: the Pearl River Estuary and the Changjiang River Estuary

Liu J, Du J, Wu Y, et al. *Estuarine Coastal & Shelf Science*, 2018, 203:17-28.

In this study, we used a ^{224}Ra mass balance model to evaluate the importance of submarine groundwater discharge (SGD) for the budgets of biogenic elements in two major Chinese estuaries: the Pearl River Estuary (PRE) and the Changjiang River Estuary (CRE). The apparent water age in the PRE was estimated to be 4.8 ± 1.1 days in the dry season and 1.8 ± 0.6 days in the wet season using a physical model based on the tidal prism. In the dry season, the water age in the CRE was estimated to be 11.7 ± 3.0 days using the $^{224}\text{Ra}/^{223}\text{Ra}$ activities ratios apparent age model. By applying the ^{224}Ra mass balance model, we obtained calculations of the SGD flow in the PRE of $(4.5-10) \times 10^8 \text{ m}^3 \text{ d}^{-1}$ ($0.23-0.50 \text{ m}^3 \text{ m}^{-2} \text{ d}^{-1}$) and $(1.2-2.7) \times 10^8 \text{ m}^3 \text{ d}^{-1}$ ($0.06-0.14 \text{ m}^3 \text{ m}^{-2} \text{ d}^{-1}$) in the dry season and wet season, respectively, and the estimated SGD flux was $(4.6-11) \times 10^9 \text{ m}^3 \text{ d}^{-1}$ ($0.18-0.45 \text{ m}^3 \text{ m}^{-2} \text{ d}^{-1}$) in the dry season of the CRE. In comparison with the nutrient fluxes from the rivers, the SGD-derived nutrient fluxes may play a vital role in controlling the nutrient budgets and stoichiometry in the study areas. The large amount of dissolved inorganic nitrogen and phosphorus fluxes together with high N: P ratios into the PRE and CRE would potentially contribute to eutrophication and the occurrence of red tides along the adjacent waters.

作为我国两个大河影响下的河口，珠江口和长江口地区的环境问题一直受到了高度的关注。本研究基于 ^{224}Ra 评估了这两个河口地区SGD及其输送的营养盐对近岸水体的影响。利用 ^{224}Ra 质量平衡模型，得到了输入至珠江口和长江口的SGD通量，其中在枯季，珠江口和长江口SGD通量达到了同期河流流量的(140-320)%和(256-622)%之多，而在珠江口洪季SGD通量为同期珠江流量的(13-29)%；SGD携带的营养盐是珠江口和长江口区域的主要来源，尤其是在更多海水入侵的枯季时期，而且SGD输入的高N:P比值可能会导致珠江口和长江口沿岸水体频繁发生富营养化和赤潮现象。此研究也阐述了SGD对高强度人类活动下河口的生态环境影响。

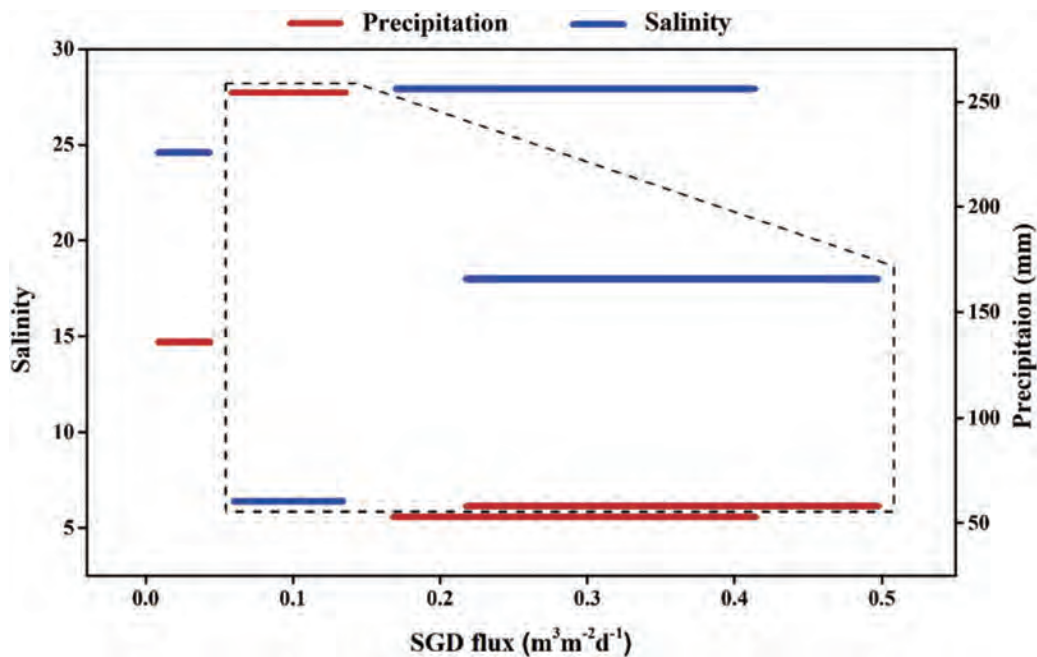


Fig. 6. The relationship between SGD rate ranges and salinity, precipitation in the PRE and CRE. The dashed line represent the SGD flux in the PRE (color figure online).

Stress Responses of Aquatic Plants to Silver Nanoparticles

Yuan L, Richardson C, Ho M, et al. *Environmental Science & Technology*, 2018, 52(5): 2558-2565.

Silver nanoparticles (AgNPs) are increasingly used in consumer products, biotechnology, and medicine, and are released into aquatic ecosystems through wastewater discharge. This study investigated the phytotoxicity of AgNPs to aquatic plants, *Egeria densa* and *Juncus effusus* by measuring physiologic and enzymatic responses to AgNP exposure under three release scenarios: two chronic (8.7 mg, weekly) exposures to either zerovalent AgNPs or sulfidized silver nanoparticles; and a pulsed (450 mg, one-time) exposure to zerovalent AgNPs. Plant enzymatic and biochemical stress responses were assessed using superoxide dismutase (SOD) and peroxidase (POD) activity, malondialdehyde (MDA) concentrations and chlorophyll content as markers of defense and phytotoxicity, respectively. The high initial pulse treatment resulted in rapid changes in physiological characteristics and silver concentration in plant tissue at the beginning of each AgNPs exposure (6h, 36 h, and 9 days), while continuous AgNP and sulfidized AgNP chronic treatments gave delayed responses. Both *E. densa* and *J. effusus* enhanced their tolerance to AgNPs toxicity by increasing POD and SOD activities to scavenge free radicals but at different growth phases. Chlorophyll did not change. After AgNPs exposure, MDA, an index of membrane damage, was higher in submerged *E. densa* than emergent *J. effusus*, which suggested that engineered nanoparticles exerted more stress to submerged macrophytes.

银纳米 (AgNPs) 被广泛地用于生物和医药等领域, 并最终通过废水排放到水生生态系统, 对水生植物产生影响。本研究通过测定两种水生植物 (沉水植物 *Egeria densa* 和挺水植物 *Juncus effusus*) 在三种 AgNPs 释放情景下 (缓释零价 AgNPs、缓释硫化 AgNP 和脉冲式零价 AgNPs) 的生理响应和酶促反应, 研究了 AgNPs 对水生植物的毒性影响。并利用超氧化物歧化酶 (SOD)、过氧化物酶 (POD) 活性、丙二醛 (MDA) 浓度和叶绿素含量作为植物防御和植物毒性的标志物评估植物酶促和生化应激反应。结果表明, 高初始脉冲处理, 在暴露初始阶段 (6h, 36h 和 9 天) 即可导致植物的生理特征和组织中的银浓度快速变化, 而缓释 AgNP 和硫化 AgNP 处理则有延迟效应。两种水生植物 *E. densa* 和 *J. effusus* 都可以通过增加 POD 和 SOD 活性来清除自由基的影响, 从而增强对 AgNPs 毒性的耐受性。AgNPs 处理后, 沉水植物 *E. densa* 体内的 MDA (表征细胞膜受损的指标) 显著高于挺水植物 *J. effusus*, 表明纳米颗粒对沉水植物的影响更大。

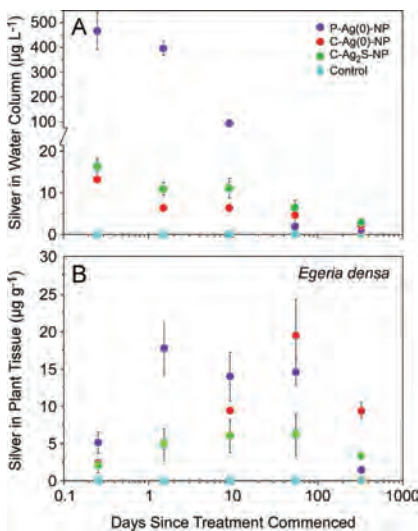


Figure 1. Silver (Ag) concentrations in (A) the water column by pulsed (P) and chronic (C) treatment and days from treatment and (B) *Egeria densa* silver tissue concentrations by treatment and days from treatment. Values are mean \pm SEM for n = 3.

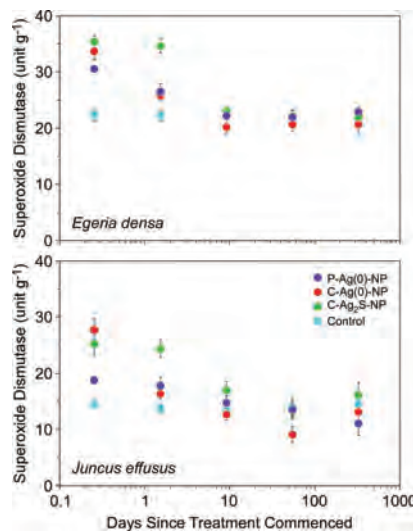


Figure 2. SOD activities in *Egeria densa* and *Juncus effusus* varied by pulsed (P) and chronic (C) treatment and by time. Values are mean \pm SEM for n = 3.

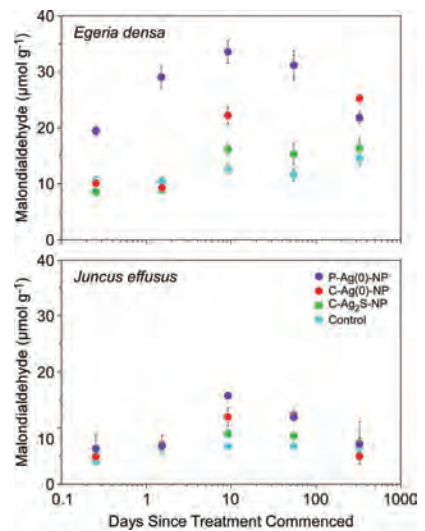


Figure 4. Malondialdehyde (MDA) contents in *Egeria densa* and *Juncus effusus* varied by pulsed (P) and chronic (C) treatment and by time. Values are mean \pm SEM for n = 3.

Functional diversity of benthic ciliate communities in response to environmental gradients in a wetland of Yangtze Estuary, China

Xu Y, Fan X, Warren A, et al. *Marine Pollution Bulletin*, 2018, 127:726-732.

Researches on the functional diversity of benthic ecosystems have mainly focused on macrofauna, and studies on functional structure of ciliate communities have been based only on trophic- or size-groups. Current research was carried out on the changing patterns of classical and functional diversity of benthic ciliates in response to environmental gradients at three sites in a wetland in Yangtze Estuary. The results showed that changes of environmental factors (e.g. salinity, sediment grain size and hydrodynamic conditions) in the Yangtze Estuary induce variability in species composition and functional trait distribution. Furthermore, increased species richness and diversity did not lead to significant changes in functional diversity due to functional redundancy. However, salt water intrusion of Yangtze Estuary during the dry season could cause reduced functional diversity of ciliate communities. Current study provides the first insight into the functional diversity of ciliate communities in response to environmental gradients.

对于底栖生态系统功能多样性的研究一直仅限于大型底栖动物。本研究对长江口湿地的微型底栖动物功能多样性对环境因子自然梯度的响应进行了研究。结果表明盐度、沉积物粒径和水动力条件都会对其群落的物种和功能特征组成产生影响。同时，长江口枯水季的盐水入侵会引起长江口湿地微型底栖动物群落功能多样性的降低。本研究是首次将功能多样性参数应用于微型底栖动物群落的研究中。

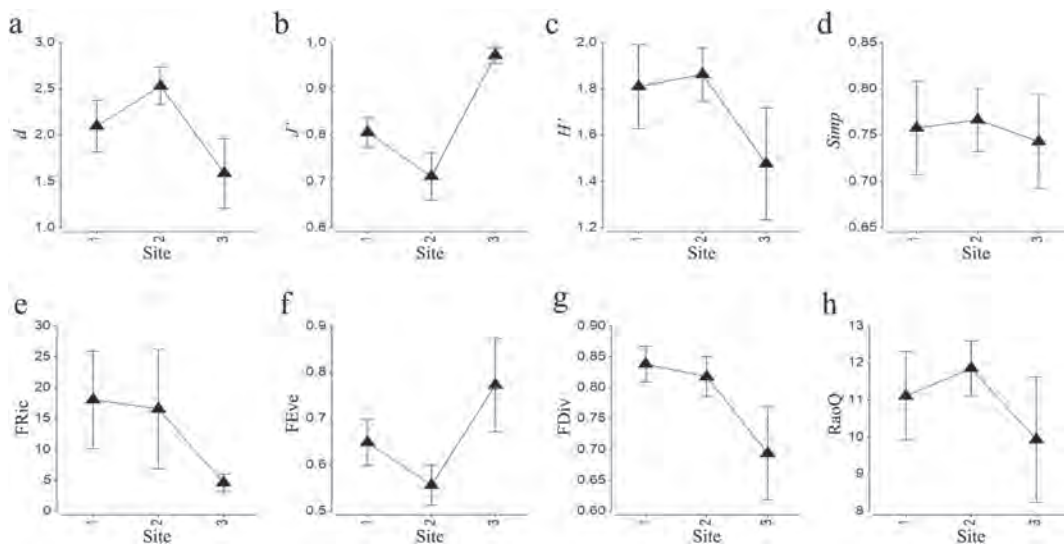


Fig. 5. Means plots of species richness (a), species evenness (b), Shannon-Wiener index (c), Simpson index (d) and functional richness (e), functional evenness (f), functional divergence (g), and Rao's quadratic entropy (h) at the three sampling sites. Error bars denote 95% confidence intervals for those means.

Fusion of Landsat-8/OLI and GOCI Data for Hourly Mapping of Suspended Particulate Matter at High Spatial Resolution: A Case Study in the Yangtze (Changjiang) Estuary

Pan Y, Shen F, Wei X, et al. *Remote Sensing*, 2018, 10(2):158

Suspended particulate matter (SPM) concentrations ($[SPM]$) in the Yangtze estuary, which has third-order bifurcations and four outlets, exhibit large spatial and temporal variations. Studying the characteristics of these variations in $[SPM]$ is important for understanding sediment transport and pollutant diffusion in the estuary as well as for the construction of port and estuarine engineering structures. The 1-h revisit frequency of the Geostationary Ocean Color Imager (GOCI) sensor and the 30-m spatial resolution of the Landsat 8 Operational Land Imager (L8/OLI) provide a new opportunity to study the large spatial and temporal variations in the $[SPM]$ in the Yangtze

estuary. In this study, [SPM] images with a temporal resolution of 1 h and a spatial resolution of 30 m are generated through the product-level fusion of [SPM] data derived from L8/OLI and GOCI images using the Spatial and Temporal Adaptive Reflectance Fusion Model (STARFM). The results show that the details and accuracy of the spatial and temporal variations are maintained well in the [SPM] images that are predicted based on the fused images. Compared to the [SPM] observations at fixed field stations, the mean relative error (MRE) of the predicted SPM is 17.7%, which is lower than that of the GOCI-derived [SPM] (27.5%). In addition, thanks to the derived high-resolution [SPM] with high spatiotemporal dynamic changes, both natural phenomena (dynamic variation of the maximum turbid zone) and human engineering changes leading to the dynamic variability of SPM in the channel are observed.

悬浮颗粒物 (SPM) 浓度在多级分叉河口——长江口的时空分布存在高度变异，研究SPM这一变化特性对于理解河口泥沙运输、污染物扩散以及港口近岸工程建设具有重要意义。尽管静止水色卫星GOCI的1hr重访频率和陆地卫星传感器Landsat-8/OLI (L8/OLI)的30m空间分辨率，为长江口SPM浓度的时空变化研究提供了新的优质数据源，但由于受到传感器时空分辨率的限制，仅依靠单一卫星数据还无法刻画出长江口这一复杂动力河口SPM浓度的高时空变化特性。本研究采用基于STARFM的时空融合方法，对L8/OLI和GOCI反演的SPM浓度进行产品级的融合，生成了同时具有1hr时间分辨率(GOCI) 和30m空间分辨率(OLI)的SPM浓度影像。结果显示，融合后预测的SPM浓度影像保持了良好的时空变化细节和精度，与野外台站OBS观测数据对比，SPM浓度平均相对误差为17.7%，低于GOCI反演的相对误差 (27.5%)。此外，从预测的高分辨率SPM浓度的高时空动态变化，既可以观测到自然现象（最大浑浊带的动态变异现象），也可观测到人类工程对航道动力条件的改变导致SPM浓度的动态变异现象。该研究在不额外增加传感器时空分辨率的情况下，为河口区域尤其是航道内SPM浓度的时空变化研究提供了新的可能。

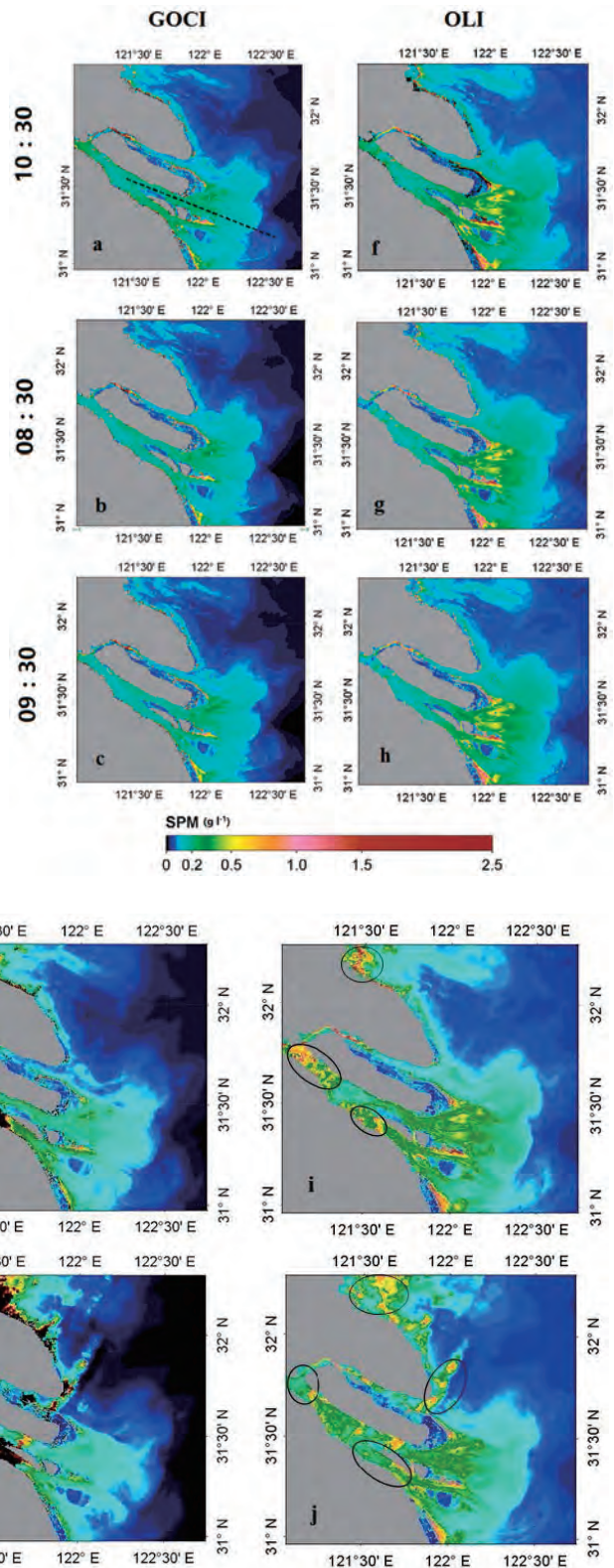


Figure 9. Predicted hourly SPM values at the L8/OLI resolution (g–j) based on one SPM image pair at 10:30 h (a,f) and hourly SPM values retrieved from the GOCI images (08:30 (b), 09:30 (c), 11:30 (d) and 12:30 h (e)) on 29 August 2013 using the Spatial and Temporal Adaptive Reflectance Fusion Model (STARFM) method. No images were predicted for 13:30, 14:30 and 15:30 h because they contained heavy clouds. The dashed black line in (a) is the transect line. The land masks with 1500-m resolution in SeaDAS were used. Black red or black in (d,e), and the black circled areas in (i,j) are clouds.

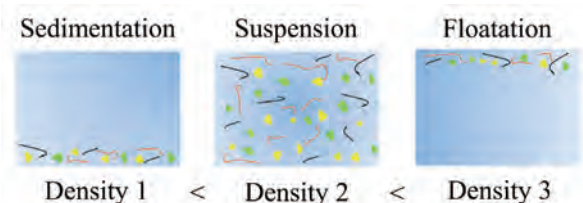
A straightforward method for measuring the range of apparent density of microplastics.

Li L, Li M, Deng H, et al. *Science of The Total Environment*, 2018, 639:367-373.

Density of microplastics has been regarded as the primary property that affect the distribution and bioavailability of microplastics in the water column. For measuring the density of microplastic, we developed a simple and rapid method based on density gradient solutions. In this study, we tested four solvents to make the density gradient solutions, i.e., ethanol (0.8 g/cm³), ultrapure water (1.0 g/cm³), saturated NaI (1.8 g/cm³) and ZnCl₂ (1.8 g/cm³). Density of microplastics was measured via observing the float or sink status in the density gradient solutions. We found that density gradient solutions made from ZnCl₂ had a larger uncertainty in measuring density than that from NaI, most likely due to a higher surface tension of ZnCl₂ solution. Solutions made from ethanol, ultrapure water, and NaI showed consistent density results with listed densities of commercial products, indicating that these density gradient solutions were suitable for measuring microplastics with a density range of 0.8–1.8 g/cm³.

微塑料密度是影响微塑料空间分布及其生物有效性的重要性质。微塑料的密度并不是一成不变的，生产过程中添加剂的不同以及野外环境中塑料老化、微生物的附着等都会导致密度的变化。由于微塑料尺寸小且重量轻，测量微塑料的表现密度仍然是一个巨大的挑战。因此，开发一种简单有效的方法来测定微塑料的密度是必要的。

研究人员利用四种试剂来制作密度梯度溶液，即乙醇（0.8g/cm³），超纯水（1.0g/cm³），饱和NaI（1.8g/cm³）和ZnCl₂（1.8g/cm³），通过观察密度梯度溶液中微塑料的悬浮或沉降状态来测定微塑料的密度。研究发现ZnCl₂溶液的表面张力较高且不稳定，密度测定有很大的不确定性。乙醇，超纯水和NaI是制备密度梯度溶液的最佳选择，适用于测量密度范围为0.8-1.8g/cm³的微塑料。本研究建立的方法为野外和室内表征微塑料提供了有用的工具。



Environmental status assessment using biological traits analyses and functional diversity indices of benthic ciliate communities

Xu Y, Stoeck T, Forster D, et al. *Marine Pollution Bulletin*, 2018, 131:646-654.

In this study, we tested the hypothesis that the functional diversity of benthic ciliates has high potential to monitor marine ecological status. Therefore, we investigated the spatial and temporal variation of functional diversity of benthic ciliates in the Yangtze Estuary during one year using biological traits analyses and functional diversity indices. Traits and community compositions showed clear spatial and temporal variations. Among a variety of biological traits, feeding type and body size emerged as strongest predictable variables. Functional divergence (FDiv) had an advantage over two other functional diversity indices, as well as over classical diversity measures (i.e. richness, evenness, Shannon-Wiener) to infer environmental status. Significant correlations between biological traits, FDiv and environmental variables (i.e. nutrients, temperature, salinity) suggested that functional diversity of benthic ciliates might be used as a bio-indicator in environmental status assessments. Further mandatory researches need to implement functional diversity of ciliates in routine monitoring programs were discussed.

本研究通过研究长江口微型底栖动物群落功能多样性一年的时空变化规律，验证了利用其监测海洋生态环境的假设。结果表明微型底栖动物群落的功能多样性参数（FDiv）相较于物种多样性和其它功能多样性参数在监测环境时具有明显优势。显著性相关分析表明其与氮、磷营养盐等环境因子显著相关，因此具有生物指示的潜力。同时本研究也对如何利用微型底栖动物群落的功能多样性参数进行常规环境监测提出具体方案。

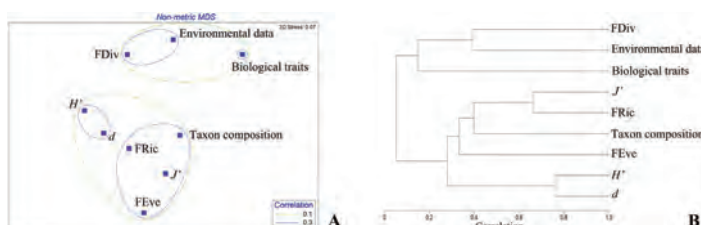


Fig. 4. Second-stage NMDS ordination (A) and clustering analyses (B) of Spearman matrix correlations between every pair of nine resemblance matrices, calculated from environmental data, species abundance, biological traits, three classical diversity indices, and three functional diversity measures. d, species richness; FDiv, functional divergence FEve, functional evenness FRic, functional richness; H', Shannon-Wiener index; J', species evenness.

Microplastics in mussels sampled from coastal waters and supermarkets in the United Kingdom.

Li J, Green C, Reynolds A, et al. *Environmental Pollution*, 2018, 241:35-44.

Global contamination of the marine environment by plastic has led to the discovery of microplastics in a range of marine species, including those for human consumption. In this study, the presence of microplastics and other anthropogenic debris in seawater and mussels (*Mytilus edulis*) from coastal waters of the U.K., as well as supermarket sources, was investigated. These were detected in all samples from all sites with spatial differences observed. Seawater samples taken from 6 locations (in triplicates) displayed 3.5 ± 2.0 debris items/L on average (range: 1.5-6.7 items/L). In wild mussels sampled from 8 locations around the U.K. coastal environment, the number of total debris items varied from 0.7 to 2.9 items/g of tissue and from 1.1 to 6.4 items/individual. For the supermarket bought mussels, the abundance of microplastics was significantly higher in pre-cooked mussels (1.4 items/g) compared with mussels supplied live (0.9 items/g). Micro-FT-IR spectroscopy was conducted on 136 randomly selected samples, with 94 items characterized. The spectra found that 50% of these debris items characterized were microplastic, with an additional 37% made up of rayon and cotton fibers. The microplastic levels detected in the supermarket bought mussels present a route for human exposure and suggests that their quantification be included as food safety management measures as well as for environmental monitoring health measures.

塑料对海洋环境的全球污染导致了微塑料在一系列海洋生物包括供人类食用的物种中的发现。在这项研究中，我们调查了微塑料及其他人为来源物质在英国沿海和超市获得的贻贝 (*Mytilus edulis*) 体内水平。同时也监测了相关海水中水平。海水样品空间差异显著，平均为 3.5 ± 2.0 items/L (范围: 1.5-6.7 items/L)。从8个地点采样的野生贻贝在英国沿海环境中，微塑料总数从0.7到2.9 items/g (1.1至6.4 items/ind)不等。市售贻贝中，预煮贻贝 (1.4 items/g) 的微塑料显著高于鲜活品 (0.9 items/g)。对136个随机选择的样品进行Micro-FT-IR光谱分析，共有94项得到确认。光谱发现，这些个体中50%为微塑料，另外37%由人造丝和棉纤维组成。微塑料在水产品中的发现再次证实了提供了人类接触的途径，同时将来的量化分析手段需要应用于环境和健康风险评估。

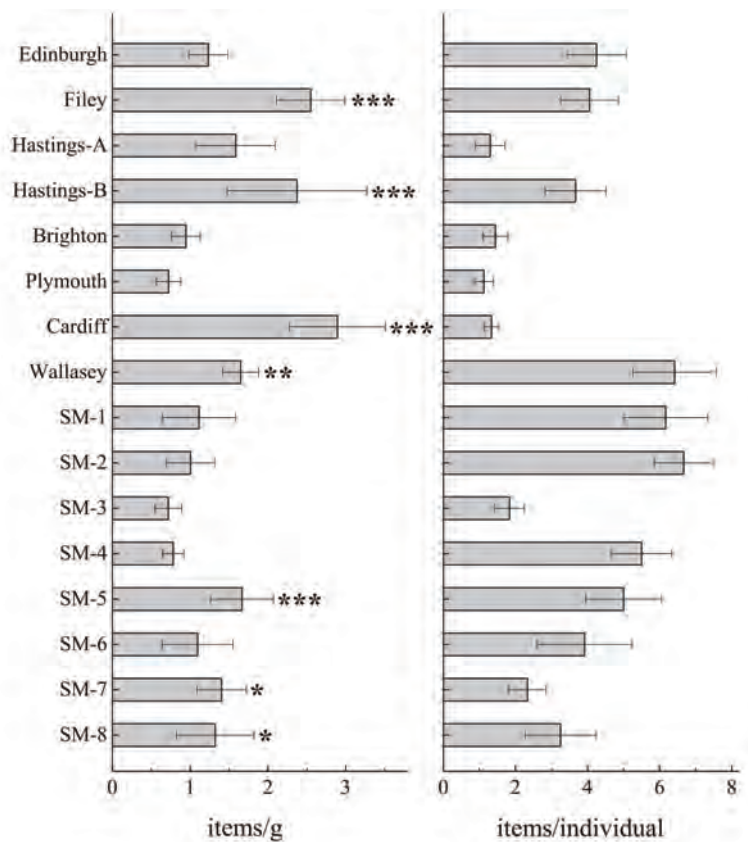


Fig. 3. Abundance of debris items in mussels ($n = 6$). All mussels (coastal and supermarket, SM) contained significantly higher numbers of debris items ($p < 0.001$, with the exceptions of Plymouth, Brighton, Hastings A and Edinburgh (showing no significant difference) compared to the procedural blank. Using Plymouth tissues as 'reference' samples for comparison purposes: the following significance values for seawater samples highlighted are: * $p < 0.05$, ** $p < 0.01$, *** $p < 0.001$. Mussels from SM1- SM4 were bought as live mussels in net bags. SM6-SM8 were frozen/chilled, and SM5 were cooked/frozen/chilled mussels. Using SM3 mussels as a reference sample, SM5, SM7-8 are highlighted as containing significantly high numbers of debris items.

Effects of virgin microplastics on goldfish (*Carassius auratus*).

Jabeen K, Li B, Chen Q, et al. *Chemosphere*, 2018, 213:323-332.

Microplastics (MPs) are abundant in freshwater and marine environments. They are diverse shape and size and are ingested by organisms. In this study, goldfish (*Carassius auratus*) were exposed via diet to three types of virgin MPs material types and shapes including fibers, fragments, and pellets. After six weeks of exposure, various sub-lethal effects, but no mortality, was observed. Fish exposed to plastic showed significant weight loss compared with the control. Fibers were found in the gills, gastrointestinal tract (GIT), and feces were not likely to accumulate in the GIT. Pronounced and severe alterations were found in the livers of fish exposed to fibers. The distal intestine showed more pronounced and severe changes compared to the proximal intestine, likely due to an intake of fibers. The ingestion of fibers caused the highest frequencies of progressive and inflammatory changes in the livers and intestines. This is in accordance with the higher organ index in these organs compared to other taxa. Conversely, fragments and pellets were not ingested but chewed and expelled. Chewing process resulted in damages to the jaws as ranging from slight exfoliation to deep incisions. The highest frequency of regressive and circulatory (e.g., dilated sinusoids) changes was found in fish exposed to fragments, specifically in the upper and lower jaw, and in lower jaw and liver, respectively. Together, these results demonstrate that ingestion and chewing of MPs lead to damages in various organs and tissues of the gastrointestinal system, and suggest that different materials can have drastically different impacts on fish.

微塑料是一种大小、形状和密度等分布不均一的复合污染物，在淡水和海洋环境中含量丰富，易被生物摄食。本论文研究了三种类型的初生源微塑料通过饮食暴露6周对红鲫鱼的毒性效应。结果表明，纤维、碎片和颗粒这三种微塑料不会造成成鱼死亡，但会产生各种亚致死效应。与对照组相比，微塑料暴露组的鱼体重显著减轻。我们观察到红鲫鱼会反复咀嚼微塑料碎片和颗粒最后吐出，但会摄入微塑料纤维，在鳃、肠道和粪便中均有发现，且纤维会导致红鲫鱼肝脏和远端肠道发生严重病变，即高频率的进行性和炎症变化。而微塑料的咀嚼过程造成红鲫鱼上下颌损伤如表皮脱落和很深的切口。总之，这些结果证明红鲫鱼对微塑料的摄入具有选择性，而微塑料的咀嚼和摄入会损害胃肠道系统等器官，且不同形状的微塑料对鱼类的影响也不同。

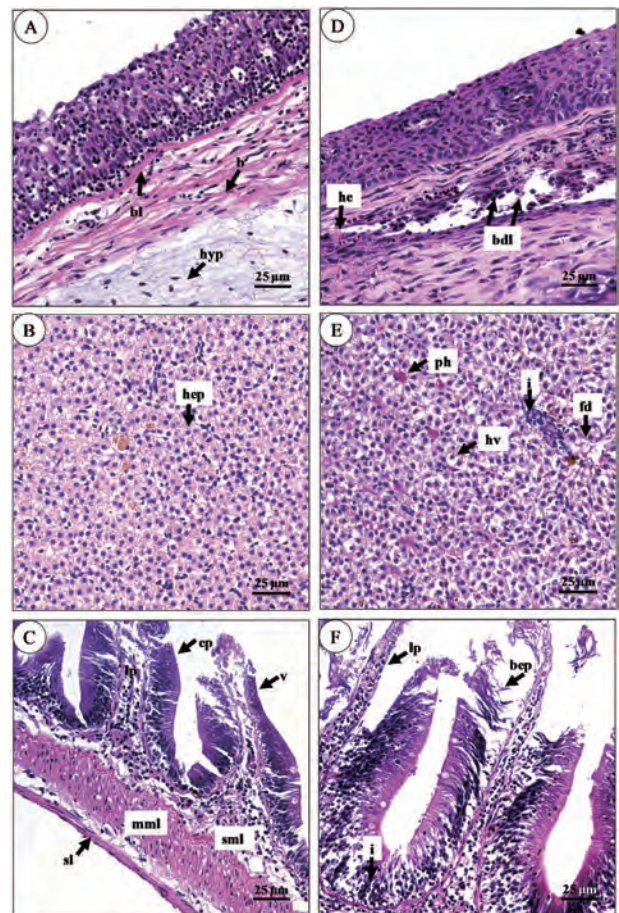


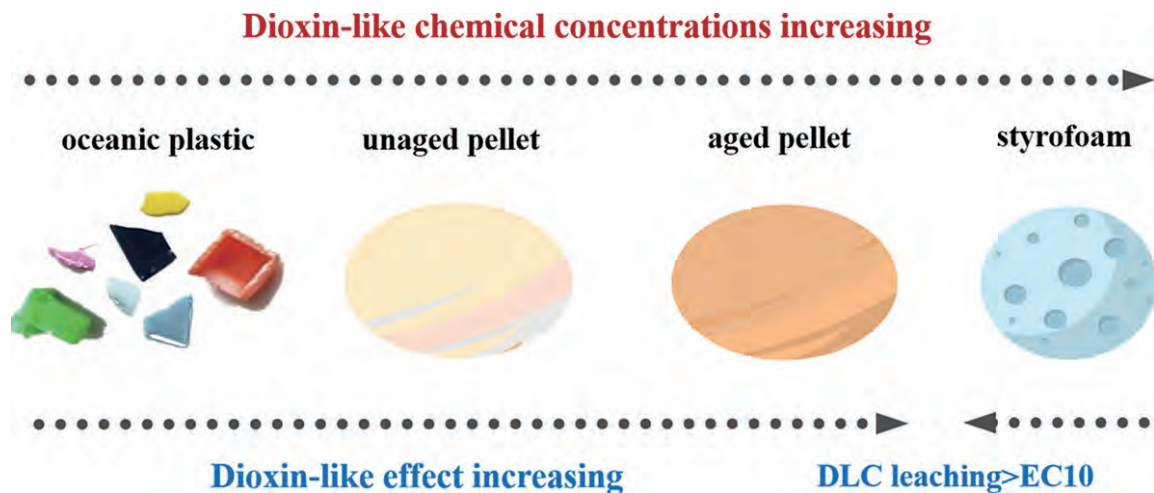
Fig. 4. Microphotographs show the normal structure lower jaw (A), liver (B), and proximal intestine (C) from control group (bl: basal layer, d: dermis, hyp: hypodermis, hep: hepatocytes, v: villus, ep: epithelium, lp: lamina propria, sl: serous layer, mml: muscularis mucosa layer, sml: sub-muscular layer), D: lower jaw from fragment group (he: hemorrhage, bdl: breakage of dermal layer), E: liver from fiber group (ph: passive hyperemia, hv: hydrophic vacuolization, i: infiltration, fd: lipid droplet), F: proximal intestine from fiber group (lp: lamina propria, bep: breakage of epithelium).

Marine microplastics bound dioxin-like chemicals: Model explanation and risk assessment.

Chen Q, Zhang H, Allgeier A, et al. *Journal of Hazardous Materials*, 2018, 364:82-90.

Microplastics have become one of the most pervasive emerging pollutants in the marine environment because of their wide occurrence and high sorption ability for hydrophobic organic contaminants (HOCs). Among the associated HOCs, dioxin-like chemicals (DLCs) can pose severe health risks; however, information on effects of microplastics bound DLCs is lacking. To fill this knowledge gap, this study integrated chemical analysis and in vitro bioassays to elucidate the potential dioxin-like effects of microplastics bound DLCs. Chemical analysis results demonstrated that styrofoams possessed significantly greater DLCs than other coastal or open ocean plastic particles. This was probably due to the presence of additives and greater sorption ability of expanded polystyrene. However, styrofoams did not show as strong dioxin-like effects as predicted by the bioanalysis equivalent model in bioassays. This could be attributed to the decreased DLC bioavailability and increased competition with the presence of styrene oligomers. Besides, bioassay results also demonstrated that aging increased the associated DLC concentrations, since extra sorption from surrounding environment occurred during prolonged retention periods. Finally, it was estimated that the leaching of DLCs could induce dioxin-like effects in marine organisms under 100% (11/11) and 18% (2/11) scenarios for aged pellets and styrofoams through aqueous or dietary exposures.

在本研究中，研究者重点关注了塑料残骸上的一类具有较强生物毒性作用的疏水性有机物，即类二英物质（DLCs）。通过化学分析和生物测试相结合的手段，考察了微塑料上负载的DLCs可能引发的类二英效应。化学分析结果证明：泡沫聚苯乙烯上含有的DLCs含量最高，这可能是由于泡沫聚苯乙烯塑料的添加剂存在和其较强的吸附能力造成的。但是，泡沫聚苯乙烯在生物测试中并没有显示非常强的类二英效应，这主要是由于在苯乙烯多聚体的存在导致的。这些多聚体一方面通过吸附DLCs分子而降低其生物有效性，另一方面这些多聚体自身也是芳烃受体的激活剂，可以和DLCs形成竞争抑制作用。同时生物测试的结果还显示：环境老化作用能够增加DLCs在塑料上的负载量，这主要是由于塑料在老化过程中从周围环境中的额外吸附所致。最后，研究者通过DLCs在不同环境和生物体内的释放情况，预测了11种场景下的潜在毒性风险。



Microplastic risk assessment in surface waters: A case study in the Changjiang Estuary, China

Xu P, Peng G, Su L, et al. *Marine Pollution Bulletin*, 2018, 133:647-654.

The rapid development of plastic industry has resulted in a series of environmental problems caused by microplastics originating from larger plastics. Microplastic pollution risk in surface waters of the Changjiang Estuary was explored based on risk assessment models. The average microplastic concentration was 23.1 ± 18.2 n/100 L. Shape, size, color and composition types of microplastics were examined. The risk assessment models were developed using data on both the concentration and chemical hazard of microplastic polymers. Assessment results indicated that polyvinyl chloride exhibited a critical concern for microplastic risk. Areas around aquaculture farms were regarded as “hotspots” of microplastic pollution due to the accumulation of microplastics and the presence of hazardous microplastic. This risk assessment of microplastics bridged gaps in understanding between field research and policy-making for surface waters. This research provides baseline data for assessing the environmental risk of microplastics in this growing area of research.

海洋微塑料污染的风险不仅仅来源于在环境中的长期积累，还在于微塑料本身作为化学多聚物所具有的化学毒性，本研究在对长江口表层水体中微塑料浓度分布调查的基础上，探索基于丰度和化学性质的微塑料多重环境风险评估。2017年夏季搭乘“润江号”开展长江口海洋微塑料污染调查。长江口及其邻近海域29个站点的表层水体中微塑料的平均浓度为 0.231 ± 0.182 个/升，与世界上其他水体中的浓度相比，处于中等污染水平。由于长江河口动力环境复杂，微塑料的空间分布差异显著。靠近杭州湾处微塑料浓度最高，在离岸较远的水域也出现了微塑料浓度高值。分析空间分布趋势发现，微塑料聚集区域分布与长江冲淡水与台湾暖流的夏季走向相似，今后将着重研究河口动力条件对微塑料分布的影响。同时杭州湾受钱塘江、长江口、东海的多重影响，使得微塑料浓度在此处呈现最高值。对物理特性的研究发现，微塑料的颜色丰富，由于在环境中时间较长，往往褪去表面颜色难以辨认；0.07–1.0 mm 大小的微塑料达到半数以上；除去自然纤维的影响，水体中纤维状微塑料最多。

为全面了解微塑料浓度和多聚物成分的综合影响，本研究引入

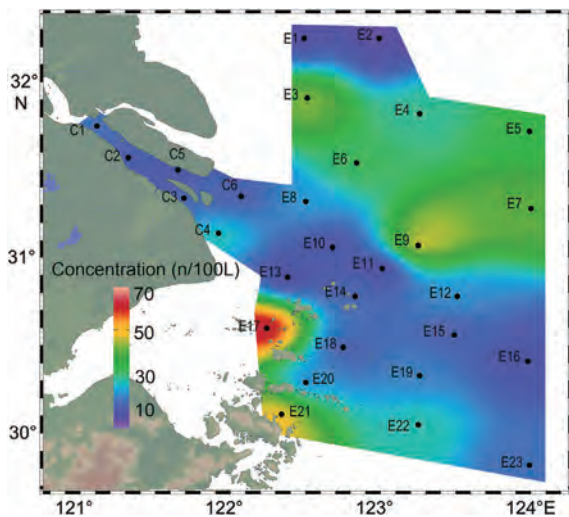


Fig. 2. The distribution of microplastics in surface waters. Areas of low microplastic concentration are represented by blue while areas of high microplastic concentration are shown in red. (For interpretation of the references to color in this figure legend, the reader is referred to the web version of this article.)

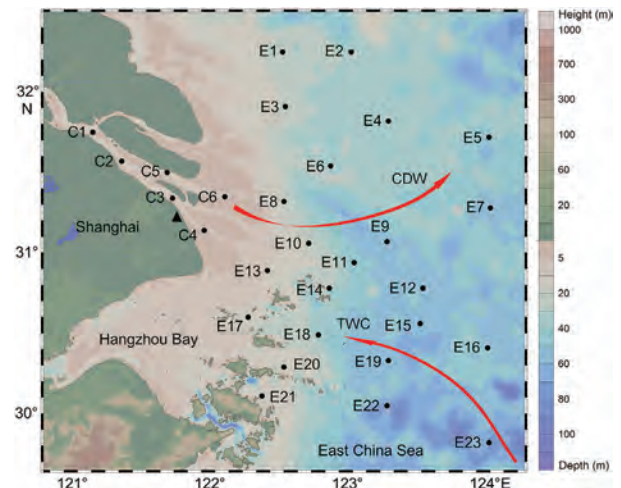


Fig. 1. Location of sampling stations in the Changjiang Estuary and adjacent East China Sea in August 2017. Black circles represent the location of the sampling stations and the Bailonggang Wastewater Treatment Plant is represented by a triangle. Red arrows illustrate current paths (the Changjiang Diluted Water, CDW and the Taiwan Warm Current, TWC) in summer. Land elevation (m) and water depth (m) are shown on the right of the map. (For interpretation of the references to color in this figure legend, the reader is referred to the web version of this article.)

“污染负荷指数”和“多聚物毒性”这两个指标评估微塑料污染风险程度。在本研究的微塑料聚集区内，塑料多聚物的成分主要为聚乙烯（polyethylene，简称PE），丰度占80%以上，在各个站点均有广泛分布。另外，聚氯乙烯（PVC）、聚丙烯（PP）等成分的微塑料也在水体中发现。相比于PE和PP，PVC的化学毒性已被证明是前两者的数千倍，说明高危害性微塑料在环境中即使浓度很低，但长期的累积效应仍然将导致巨大的潜在风险。本研究评估结果表明，微塑料浓度较高区域，污染风险较高，同时，浓度偏低区域由于PVC等高危害多聚物成分含量偏高，其风险也整体偏高。因此，对于海洋微塑料污染的管控，不仅仅聚焦于浓度偏高的“热点”地区，更应该同时兼顾塑料的化学危害性，双重考虑微塑料的空间分布聚集和物理、化学性质，为今后全面评估海洋微塑料污染奠定科学标准。

Microplastics in Small Waterbodies and Tadpoles from Yangtze River Delta, China

Hu L, Chenick M, David E H, et al. *Environmental Science & Technology*, 2018, 52(15):8885-8893.

Although microplastic (MP) pollution in freshwater systems is gaining attention, our knowledge of its distribution in small waterbodies is scarce. Small waterbodies are freshwater habitats to many species, including amphibians, that are vulnerable to MP pollution. This study analyzed the distribution and characteristics of MPs in 25 small waterbodies from the Yangtze River Delta, China. MPs were detected in surface water, sediment, and tadpoles with abundances ranging from 0.48 to 21.52 items L⁻¹, 35.76 to 3185.33 items kg⁻¹, and 0 to 2.73 items individual⁻¹ (0 to 168.48 items g⁻¹), respectively. The dominant shape and polymer of MPs in water and tadpole samples were polyester (PES) fibers, and polypropylene (PP) fibers and fragments were dominant in sediment samples. In addition, MPs were primarily <0.5 mm in length in all samples. Tadpole length was positively correlated to the number of MPs detected. The abundance, shape, and polymer distribution of MPs in tadpoles resembled that of water rather than sediment, suggesting that tadpoles likely take up MPs from the surrounding water. This study demonstrated that MPs are abundant in these small waterbodies and are ingested by resident tadpoles. This may suggest a pathway of MP entry into aquatic and terrestrial food webs.

海洋微塑料污染近年来已在全球范围内被广泛报道，陆源输入被认为是微塑料进入海洋的重要途径。小水体是全球范围内数量最多的淡水水域，不仅物种多样性高，而且与人类生活紧密相关，容易受到人类破坏和微塑料污染。本研究调查了长江下游城市上海和浙江的25个小水体及其栖息物种蝌蚪体内的微塑料污染状况。结果表明，微塑料在水体、沉积物和蝌蚪体内普遍存在，且其丰度并不亚于其他大水域和水生生物。水体和蝌蚪体内的微塑料类型主要是聚酯纤维，而沉积物中聚丙烯纤维和碎片数量相近。此外，样品中的微塑料尺寸集中在小于0.5 mm。微塑料在蝌蚪体内的丰度、形状和聚合物分布与水样中相似而非沉积物，这表明蝌蚪可能是从周围的水体中摄入微塑料进入体内。这项研究表明微塑料在小水体中含量丰富，并可被栖息蝌蚪吸摄入。

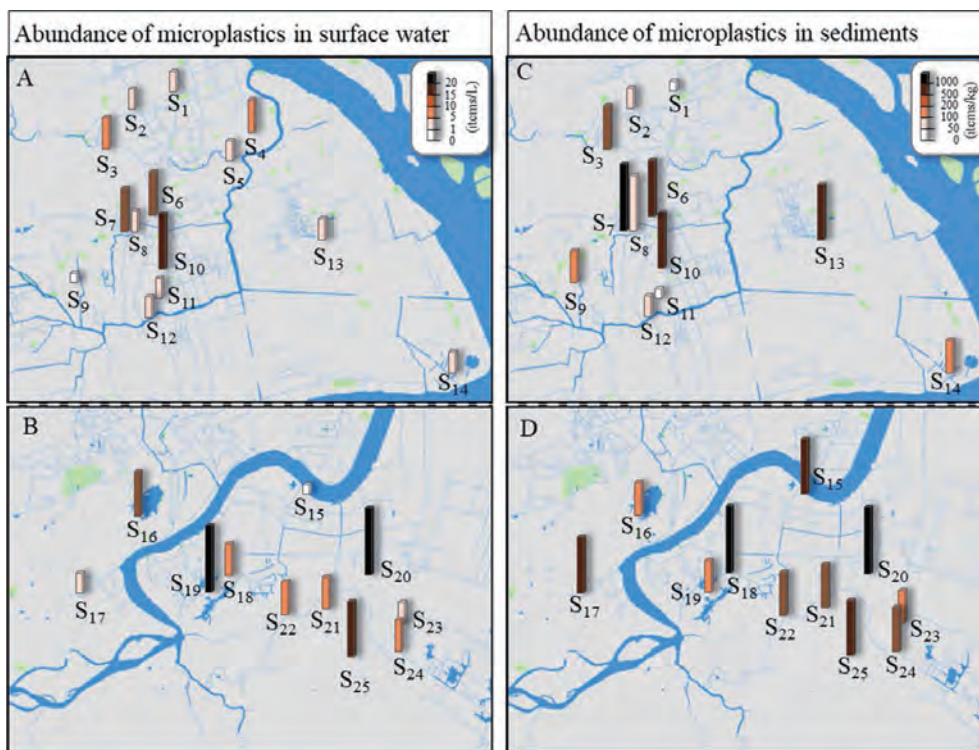


Figure 3. Abundance and spatial distribution of microplastics detected in surface water (A, B) and sediment (C, D) samples collected from Shanghai (A, C) and Zhejiang (B, D). Increasing height and deepening color of bars indicate increasing numbers of items according to the scales in the top right corners of A and C.

Spatial and vertical distribution of ^{129}I and ^{127}I in the East China Sea: Inventory, source and transportation.
Wang J, Fan Y, Liu D, et al. *Science of The Total Environment*, 2018, 652:177-188.

Iodine-129 is useful for tracking water mass movement in the ocean. In this study, the concentration of iodine isotopes in seawater of the East China Sea (ECS) in October 2013 were analyzed to investigate the spatial and vertical distribution of ^{129}I and ^{127}I to understand water mass exchange. Results showed that the $^{129}\text{I}/^{127}\text{I}$ atomic ratios varied with the water mass, with higher values of $(10-20) \times 10^{-11}$ in the coastal regions and lower values of $< 8 \times 10^{-11}$ offshore. Inventories of ^{129}I were estimated to be $(0.23-1.7) \times 10^{12}$ atoms m^{-2} ($n = 18$) in upper 100 m waters, which is comparable to those of other regions without being contaminated by the nuclear accidents or nuclear reprocessing facilities. The total amount of ^{129}I in the ECS water column was estimated to be 88 g in which over 90% is attributed to the oceanic input (e.g., West Pacific) via the Kuroshio Current (KC). The contributions of ^{129}I from Changjiang (Yangtze River) terrestrial watershed ($< 7.5\%$) and atmospheric fallout ($< 2.7\%$) were small. Those from the Fukushima accident were negligible during this investigation. The $^{129}\text{I}/^{127}\text{I}$ ratios versus salinity distribution showed the range and stratification of the Changjiang, Yellow Sea, and KC waters in the ECS. Our study shows that the Changjiang fresh water could be transported to the North Jiangsu coast in October; the Taiwan Warm Current water could intrude to Northern part of the Changjiang Estuary (32°N). Besides, our results suggest that the $^{129}\text{I}/^{127}\text{I}$ profile is useful to indicate the seawater mixing process in ocean marginal systems.

本文通过对2013年10月份采集的东海海水样品中碘同位素的分析，分析了东海碘同位素的来源以及洋流运输。结果显示，近岸区域呈现 $^{129}\text{I}/^{127}\text{I}$ 比值的高值 $(10-20) \times 10^{-11}$ ，离岸区域呈现低值 $< 8 \times 10^{-11}$ 。100米以浅 ^{129}I 的储量为 $(0.23-1.7) \times 10^{12}$ atoms m^{-2} ($n=18$)，与世界上其他没有核污染的区域相当。东海水中总的 ^{129}I 约为88 g，其中90%以上来自外海输入，长江输入贡献较小($< 7.5\%$)，大气沉降贡献可以忽略($< 2.7\%$)。福岛核事故对东海 ^{129}I 的贡献可以忽略。 $^{129}\text{I}/^{127}\text{I}$ 比值和盐度的分布说明东海水团主要受控于长江冲淡水、黄海水和黑潮。本研究结果表明，长江冲淡水在10月份可以输送到江苏沿岸，台湾暖流可以输送到长江口以北 Estuary (32°N)。同时，本研究结果说明 $^{129}\text{I}/^{127}\text{I}$ 的垂向分布可以用于研究边缘海区域海水的混合过程。

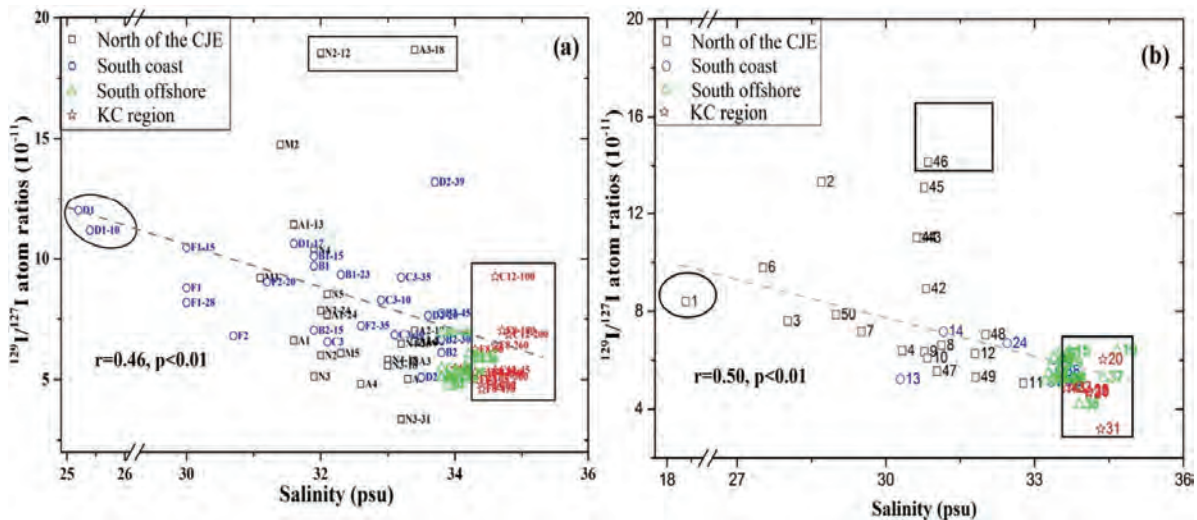


Fig. 6. Distribution of $^{129}\text{I}/^{127}\text{I}$ atom ratios vs. salinity in seawater of the ECS during October (a) and August (b) 2013. CJE represents the Changjiang Estuary.

Using mussel as a global bioindicator of coastal microplastic pollution.

Li J, Lusher A L, Rorchell J M, et al. *Environmental pollution* (Barking, Essex : 1987), 2018, 244:522-533.

The ubiquity and high bioavailability of microplastics have an unknown risk on the marine environment. Biomonitoring should be used to investigate biotic impacts of microplastic exposure. While many studies have used mussels as indicators for marine microplastic pollution, a robust and clear justification for their selection as indicator species is still lacking. Here, we review published literature from field investigations and laboratory experiments on microplastics in mussels and critically discuss the suitability and challenges of mussels as bioindicator for microplastic pollution. Mussels are suitable bioindicator for microplastic pollution because of their wide distribution, vital ecological niches, susceptibility to microplastic uptake and close connection with marine predators and human health. Field investigations highlight a wide occurrence of microplastics in mussels from all over the world, yet their abundance varies enormously. Problematically, these studies are not comparable due to the lack of a standardized approach, as well as temporal and spatial variability. Interestingly, microplastic abundance in fieldcollected mussels is closely related to human activity, and there is evidence for a positive and quantitative correlation between microplastics in mussels and surrounding waters. Laboratory studies collectively demonstrate that mussels may be good model organisms in revealing microplastic uptake, accumulation and toxicity. Consequently, we propose the use of mussels as target species to monitor microplastics and call for a uniform, efficient and economical approach that is suitable for a future largescale monitoring program.

Submarine Groundwater-Borne Nutrients in a Tropical Bay (Maowei Sea, China) and Their Impacts on the Oyster Aquaculture

Chen X, Lao Y, Wang J, et al. *Geochemistry Geophysics Geosystems*, 2018, 19(3): 932-951.

Submarine groundwater discharge (SGD) has been recognized as an important pathway for nutrients into estuaries, coasts, and the adjacent seas. In this study, ^{222}Rn was used to estimate the SGD-associated nutrient fluxes into an aquaculture area in a typical tropical bay (Maowei Sea, China). The SGD into the Maowei Sea during June 2016 was estimated to be $0.36 \pm 0.33 \text{ m d}^{-1}$ and was associated with SGD-derived dissolved inorganic nitrogen (DIN), dissolved inorganic phosphorus (DIP), and dissolved silicon (DSi) fluxes (mol d^{-1}) of $(4.5 \pm 5.5) \times 10^6$, $(5.3 \pm 9.1) \times 10^4$, and $(9.4 \pm 9.3) \times 10^6$, respectively. The SGD-derived nutrients (i.e., DIN, DIP, and DSi) were more than 1.9, 0.9, and 3.6 times the amounts in the local river input and served as dominant sources in the nutrient

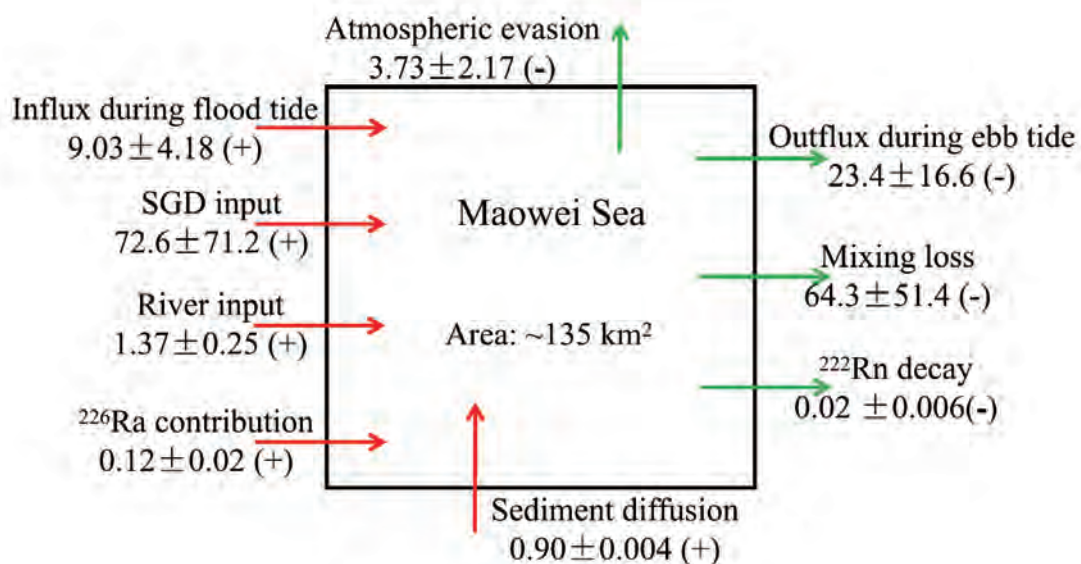


Figure 7. The ^{222}Rn sources (+) and sinks (-) (all in $\text{Bq m}^{-2} \text{ h}^{-1}$) during June 2016 in the Maowei Sea (here the SGD input is a conservative estimate and the others are mean values).

budgets in the Maowei Sea. Moreover, the N/P ratios in the SGD around the Maowei Sea were high (mean: 64), and these ratios likely exceeded the environmental self-purification capacity, thereby enhancing the biomass and changing the phytoplankton community structure. Therefore, SGD processes with derived nutrients may affect the biogeochemical cycles and marine ecological environment in the Maowei Sea. Furthermore, the N/P ratios (~67) in oysters are very close to those in the SGD in the Maowei Sea; this coincidence suggests that the high N/P ratios in the SGD are likely to be one of the most important sources that support oyster aquaculture, which might weaken the burden of water eutrophication in the Maowei Sea.

海底地下水排放 (SGD) 是营养盐等生源要素进入河口和近岸海域的一个重要途径。本文利用 ^{222}Rn 的质量平衡模型估算了茅尾海SGD携带的营养盐通量, SGD输送至茅尾海的溶解无机氮 (DIN)、溶解无机磷 (DIP) 和溶解硅 (DSi) 通量分别为 $(6.5 \pm 10.2) \times 10^2$, $(1.0 \pm 2.1) \times 10^3$ 和 $(6.4 \pm 7.4) \times 10^2 \text{ mol m}^{-2} \text{ d}^{-1}$, 发现SGD输送的DIN、DIP和DSi分别是茅尾海当地河流输送1.9、0.9和3.9倍, 因此, SGD输送的营养盐是茅尾海营养盐的主要来源。此外我们也发现茅尾海沿岸地下水中的N/P比 (64) 很高, 大量的含有高N/P比的营养盐通过SGD进入茅尾海可能会超过环境自净能力, 使得茅尾海生物量增加, 进而改变浮游植物群落结构。因此, SGD输送的营养盐可能会影响茅尾海海域的生物地球化学循环和海洋生态环境。此外, 我们的研究也发现茅尾海牡蛎体内的N/P比 (~67) 与茅尾海SGD中的N/P比非常接近, 这表明SGD中高N/P比的营养盐可能是支持牡蛎养殖最重要的来源, 因此, 合理的牡蛎养殖可能会削弱茅尾海水体富营养化的负担。

Table 3
The DIN and DIP Budgets During June 2016 in the Maowei Sea

| Sources and sinks | DIN flux (mol month^{-1}) | Percentage to total DIN sources/sinks (%) | DIP flux (mol month^{-1}) | Percentage to total DIP sources/sinks (%) |
|------------------------------------|---|---|---|---|
| <i>Sources</i> | | | | |
| SGD input | 1.3×10^8 | 50.2 | 1.6×10^6 | 23.6 |
| River input | 6.9×10^7 | 25.7 | 1.8×10^6 | 26.7 |
| Sewage outfall | 3.9×10^7 | 14.4 | 2.8×10^6 | 42.0 |
| Diffusion from sediment | 1.9×10^7 | 7.1 | 2.8×10^5 | 4.1 |
| Aquaculture | 3.1×10^6 | 1.1 | 2.2×10^5 | 3.3 |
| Atmospheric deposition | 3.9×10^6 | 1.5 | 1.8×10^4 | 0.3 |
| <i>Sinks</i> | | | | |
| Mixing loss | 8.8×10^7 | 32.7 | 2.0×10^6 | 30.1 |
| Absorption by primary productivity | 3.4×10^7 | 12.8 | 2.1×10^6 | 32.0 |
| Organic debris deposition | 6.3×10^6 | 2.3 | 5.4×10^4 | 0.8 |
| Mangrove absorption | 2.9×10^6 | 1.1 | 1.4×10^5 | 2.0 |
| Harvest from aquaculture | 1.4×10^8 | 51.1 | 2.3×10^6 | 35.0 |

Spatiotemporal Variation of the Quality, Origin, and Age of Particulate Organic Matter Transported by the Yangtze River (Changjiang)

Wu Y, Eglinton T I, Zhang J, et al. *Journal of Geophysical Research: Biogeosciences*, 2018, 123(9):2908-2921.

Information on the age dynamics of particulate organic matter (POM) in large river systems is currently sparse and represents an important knowledge gap in our understanding of the global carbon cycle. Here we examine variations in organic geochemical characteristics of suspended sediments from the Changjiang (Yangtze River) system collected between 1997 and 2010. Higher particulate organic carbon content (POC%) values were observed in the middle reach, especially after 2003, and are attributed to the increase of in situ (aquatic) primary production associated with decreased total suspended matter concentrations. Corresponding $\Delta^{14}\text{C}$ values from depth profiles taken in 2009 and 2010 indicate spatial and temporal variations in POC sources within the basin. Two isotopic mass balance approaches were explored to quantitatively apportion different sources of Changjiang POM. Results indicate that contributions of biomass and pre-aged soil organic matter are dominant, regardless of hydrological conditions, with soil-derived organic carbon comprising 17–56% of POC based on a Monte Carlo three-end-member mixing model. In contrast, binary mixing model calculations suggest that up to 80% of POC (2009 samples only) derived from biospheric sources. The emplacement of the Three Gorges Dam and resulting trapping of sediment from the upper reach of the watershed resulted in a modification of POM ^{14}C ages in the reservoir. With the resulting decline in sediment load and increase in the proportion of modern POC in the lower reach, these changes in POM flux and composition of the Changjiang have significant implications for downstream carbon cycle processes.

关于大型河流系统中颗粒有机物(POM)年龄的时空分布特征的信息目前很少,这是我们对全球碳循环理解中的一个重要知识缺口。本文研究了1997年至2010年长江水系悬浮沉积物的有机地球化学特征变化。其中长江中游特别是2003年以后,颗粒态有机碳含量(POC%)较高,这是由于原地(水生)初级生产力的增加与总悬浮物浓度的降低有关。2009年和2010年采集的深度剖面相应的 ^{14}C 值显示了盆地内POC源的时空变化。并定量分析了不同来

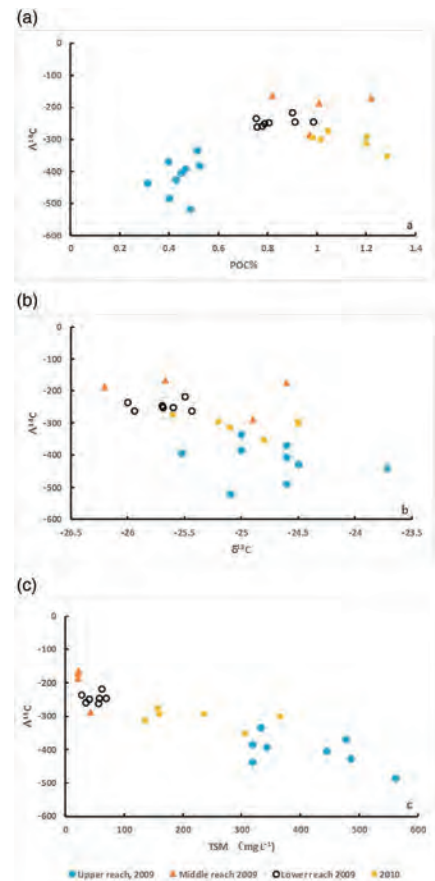


Figure 4. Relationships between radiocarbon contents of suspended particulate organic carbon (POC; $\Delta^{14}\text{C}$ values, ‰) with (a) POC%, (b) POC stable carbon isotope composition ($\delta^{13}\text{C}$, ‰), and (c) total suspended matter (TSM; mg/L) of TSM samples of the Changjiang. Different color symbols correspond to samples from the upper (blue), middle (orange), and lower (gray) reaches in 2009 and from the middle and lower (yellow) reaches in 2010.

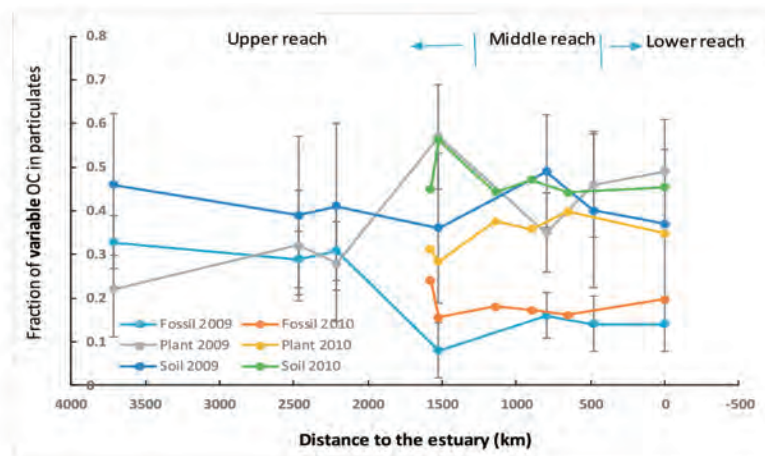


Figure 7. Results from model calculations for mean proportions of modern biomass (orange symbols), pre-aged soil (gray symbols), and fossil organic carbon (OC; blue symbols) in the Changjiang; error bar was illustrated for each point based on model calculations.

源的贡献比例。结果表明,无论水文条件如何,生物贡献和老化土壤有机质的贡献都占主导地位,其中土壤有机碳占POC的17-56%。相比之下,二元混合模型计算表明,高达80%的POC(仅2009年的样品)来自生物圈源。长江三峡水利枢纽工程的运行以及由此产生上游沉积物的沉积导致了水库中POM ^{14}C 年龄的变化。随着下游泥沙量的减少和现代有机颗粒物比例的增加,颗粒物通量和长江有机质成分的变化对下游碳循环过程有着重要的影响。

Ocean fronts construct spatial zonation in microfossil assemblages

Liu D, Wang Y, Wang Y, et al. *Global Ecology and Biogeography*, 2018, 27(10):1225-1237.

Aim: Integration of macroecology and palaeoecology is an important trend in understanding rapidly changing marine ecosystems. However, the spatial mismatch between these two data types has led to difficulties in interpretation, particularly for short-lived phytoplankton and their microfossils. Fronts are narrow transition zones between distinct water masses and play an essential role in partitioning phytoplankton assemblages in the ocean. Whether they also delimit microfossil assemblages deposited at the sea floor is unclear. We examined the correlation between quasi-stationary mesoscale fronts and the spatial distribution of microfossils (diatoms, dinoflagellates and silicoflagellates) in the Bohai, Yellow and East China Seas, to establish a causal link between microfossil assemblages and the factors controlling pelagic species assemblages on continental shelves.

宏观生态学和古生态学的整合是认识快速变化的海洋生态系统的重要趋势。然而，这两种数据类型之间的空间不匹配，导致了数据分析解释上的困难，特别是对于寿命较短的浮游植物及其微体化石来说。锋面是不同水团之间的窄过渡带，在海洋浮游植物群落的划分中起着至关重要的作用。但目前对于锋面是否也可以划分海底沉积物中的微体化石群落尚不清楚。本文采用2003-2015年卫星海表面温度梯度分析法确定了渤海、黄海和东海的锋面位置，并通过对126处表层沉积物中共计345种进行双向指示种分析，对微体化石群落进行了分类，确定了10个主要锋面和4个主要微体化石群落类型。对锋面、微体化石群落类型、海温、盐度和营养盐的空间格局分析表明，锋面将微体化石群落按水团的物理化学特征划分为不同的类型。研究结果为解释沉积柱状样数据及其与宏观生态环境数据的整合提供了可能性。

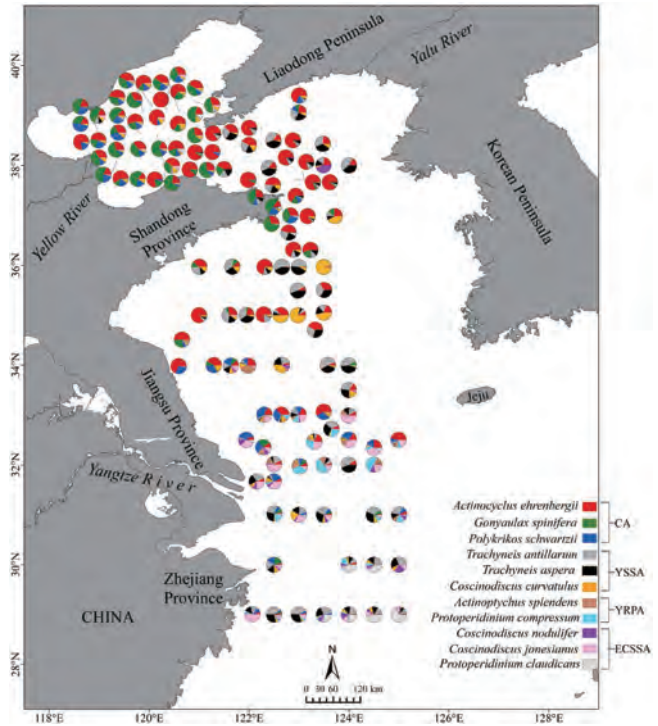


FIGURE4 The spatial distribution of representative species in each microfossil assemblage weighted by a two-way indicator species analysis (TWINSpan) [Colour figure can be viewed at wileyonlinelibrary.com]

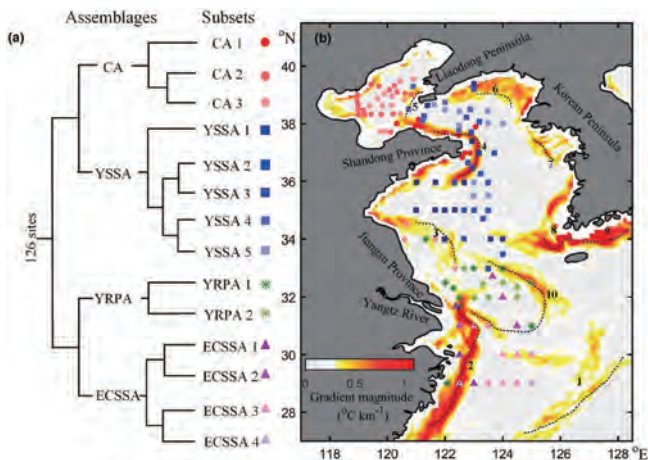


FIGURE3(a) Classification of microfossil assemblages from a two-way indicator species analysis (TWINSpan; CA = Coastal Assemblage; ECSSA = East China Sea Shelf Assemblage; YRPA = Yangtze River Plume Assemblage; YSSA = Yellow Sea Shelf Assemblage). (b) Geographical map of microfossil assemblages coupled with front patterns [Colour figure can be viewed at wileyonlinelibrary.com]

Impacts of coastal reclamation on wetlands: Loss, resilience, and sustainable management

Wu W, Yang Z, Tian B, et al. *Estuarine, Coastal and Shelf Science*, 2018, 210:153-161.

Coastal wetlands are some of the most valuable ecosystems on Earth because they provide many ecological services for coastal security. However, these wetlands are seriously threatened by accelerated climate change and intensive anthropogenic activities. To understand the impacts of land reclamation on landscape change of coastal wetlands and the long-term effects of disturbances of coastal wetlands on their sustainable management, we used time-series Landsat imagery with an object-oriented classification and Digital Shoreline Analysis System to map wetland changes within a reclaimed area in the Pudong District (PD), in Shanghai, China. Our analysis indicated that from 1989 to 2013, 19,793.4 ha of coastal wetlands have been changed to inland wetlands enclosed by a seawall and dike since 1989, thereby cutting off the exchange of sediment and water flux between the wetlands and the coastal ocean. Subsequently, under the increasing threats of anthropogenic activities, the wetland ecosystem collapsed sharply, in a transformation chain of inland wetland (fresh swamp), artificial wetland (agriculture and aquaculture wetland), and non-wetland (urban land). Under this explosive utilization following coastal reclamation, only 8.9% of natural wetlands remain in the reclaimed area, which has experienced an average annual wetland loss rate of 3.8% over the past 24 years. More than 80% of the wetlands have been developed for agricultural, industrial, and urban land uses, leading to an enormous loss of associated ecological services—benefits arising from the ecological functions provided by wetland ecosystems, thereby undermining the coastal protection these wetlands provided. Nevertheless, considerable regeneration of wetlands occurred because of their inherent resilience. This paper addresses the importance of maintaining a balance between economic growth and coastal ecological protection for sustainable management. It proposes a strategy for how ecosystem-based land planning and ecological engineering should be applied to ensure the effective and sustainable management of living shorelines so that the benefits of healthy ecological functions accrue to coastal ecosystems.

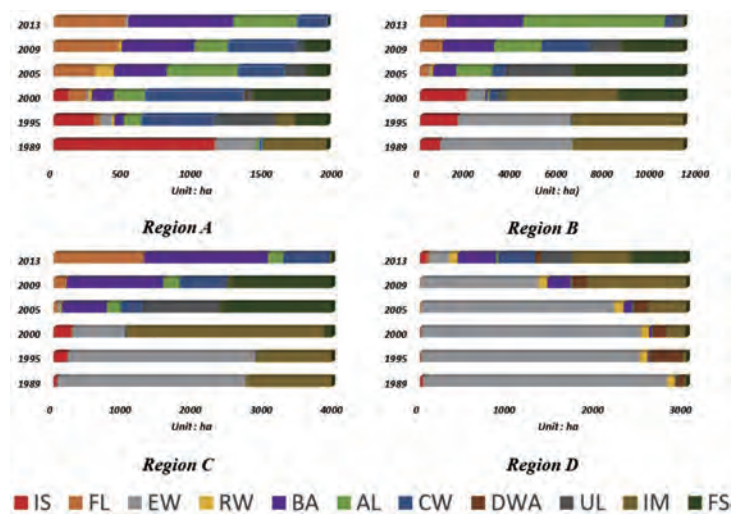


Fig. 3. Dynamic proportion of different land covers in four parts of reclaimed wetland. The types of landscape include intertidal saltmarsh (IS), forest land (FL), estuarine water (EW), riverine wetland (RW), built-up area (BA), agriculture land (AL), constructed wetland (CW), deep water area (DWA), unused land (UL), intertidal mudflat (IM), and freshwater swamp (FS).



Fig. 3. Dynamic proportion of different land covers in four parts of reclaimed wetland. The types of landscape include intertidal saltmarsh (IS), forest land (FL), estuarine water (EW), riverine wetland (RW), built-up area (BA), agriculture land (AL), constructed wetland (CW), deep water area (DWA), unused land (UL), intertidal mudflat (IM), and freshwater swamp (FS).

中国沿海围填海工程实施，造成了生态类型的转换和河口湿地景观结构改变，圈围后土地利用方式主要表现为滨海湿地-淡水沼泽湿地-农业用地-建成区模式转变。人类干预不断加强，原有系统提供生态系统服务功能价值不断降低。为缓解区域经济发展和海岸生态安全之间的矛盾，需要在土地改造利用强度和湿地再生速度之间寻找到一个平衡点，提出一种基于生态系统恢复力的土地利用政策，实现区域湿地资源的可持续发展和管理，以应对全球气候变化和人类活动影响下的河口三角洲转型过程。本研究采用长时间序列的Landsat卫星遥感影像数据，基于面向对象

图像分析方法和技术，以上海南汇东滩为例，研究近三十年来海岸带围垦强度，围垦区土地利用和景观变化过程，探明高强度海岸围垦工程实施后，河口地区生态与环境转型特点和发展变化规律。结果表明：在1989-2013年间，研究区内仅留存8.9%的自然湿地，年损失率达到3.8%，超过80%的湿地被改造成为农业用地、工业用地和城镇居住用地，造成湿地系统及其所提供的海岸保护功能的严重丧失。研究系统揭示了区域内滨海湿地生态系统高强度人类活动影响下的演化过程，区域土地利用变化的转化方式以及湿地生态系统的退化路径。

Mapping the conservation priority of migratory shorebird habitat on a dynamic deltaic coast

Zhang T, Tian B, Bo S, et al. *Estuarine, Coastal and Shelf Science*, 2018, 212:219-232.

Shorebird habitat degradation and loss due to high-intensity disturbances from human activities and the negative effects of global climate change in coastal deltas have led to the need to identify and designate priority areas for conservation with different levels of protection. We have proposed an integrated framework and model for the management of priority shorebird habitats in dynamic coastal delta zones (MPH-DC) based on a fuzzy spatial assessment model that incorporates habitat importance and disturbance analyses. By evaluating the relationships between shorebird populations and key ecological habitats, 19 structural factors, including land cover type, vegetation structure, terrain, potential human influence and natural interference, were derived from multi-temporal optical and radar remotely sensed imagery and incorporated into the index system to evaluate habitat conservation priority levels for Charadriidae and Anatidae in the Changjiang estuary, a typical coastal habitat that currently faces enormous challenges but is not yet under dynamic conservation priority management at a large spatial-temporal scale. The use of the MPH-DC framework proved to be effective for evaluating the spatial distribution and conservation priority of habitats in dynamic coastal deltas and for rapidly identifying regions where restoration and priority adjustment are needed, thus enriching broad-scale integrated ecosystem management solutions for coastal deltaic zones.

由于高强度的人类活动干扰以及全球气候变化对海岸三角洲的负面影响，滨海水鸟栖息地不断退化和损失，亟需确定不同保护级别的保护优先区域。基于模糊空间评价模型，我们提出了耦合生境重要性和干扰性分析的动态海岸三角洲地区栖息地的MPH-DC综合管理框架。长江口作为一个典型的海岸生境，目前面临着巨大的挑战，但尚未在较大的时空尺度上进行栖息地的动态保护及优先管理。本文从光学和雷达多源遥感数据中提取了19个结构因子（包括土地覆盖类型、植被结构、地形、潜在的人类影响和自然干扰等）来评价滨海水鸟种群与主要生境要素之间的关系，通过构建评价指标体系确定长江口鹈类和雁鸭类的生境保护优先级别。MPH-DC管理框架的提出有助于快速评估动态海岸三角洲栖息地的空间分布，高效确定不同生境的保护优先权，明确需要优先恢复和调整的区域，进一步丰富了海岸三角洲地区生态系统的综合管理解决方案

The specific criteria and strategies for the overlay analysis.

| Strategy | HI | HD | HP | The description of MPH |
|----------|-------------------|------------------------|----|---------------------------------------|
| 1 | High (≥ 5) | Low (≤ 3) | N | Potential protected areas |
| 2 | High (≥ 5) | High (≥ 5) | Y | Intense active protected areas |
| 3 | Low (≤ 3) | Low (≤ 3) | Y | Enhancement and restoration areas |
| 4 | Low (≤ 3) | Very high (≥ 7) | Y | Adjustment and close monitoring areas |

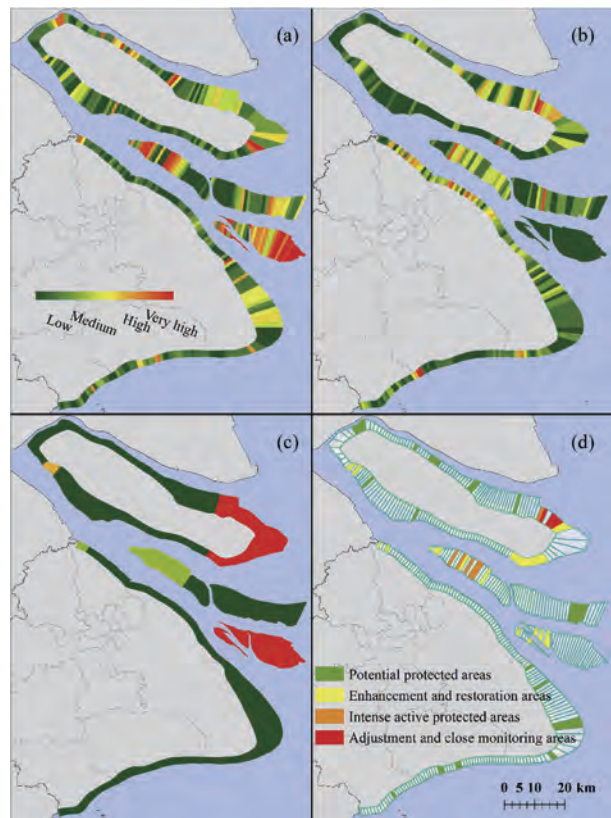


Fig. 6. Map of (a) habitat importance, (b) habitat disturbance, (c) habitat protection level and (d) overlay analysis results for four management strategies.

Transient hypoxia extent off Changjiang River Estuary due to mobile Changjiang River plume

Zhang W, Wu H, Zhu Z. *Journal of Geophysical Research-oceans*, 2018.

Observed oxygen concentrations collected at discrete locations during research cruises were conventionally used to estimate spatial extents of bottom low-oxygen/hypoxia. Yet observed oxygen concentrations were often not quantitatively representative of spatial patterns in instantaneous oxygen concentrations in coastal oceans, especially when the bottom hypoxia was transient. Over the Changjiang River estuary and its adjacent sea, research cruises could easily be longer than the time scale of variability of bottom hypoxia extent. The Changjiang River plume is extremely mobile due to changes in wind magnitude and direction, and the redistribution of this freshwater cap strongly regulates vertical stratification on which bottom hypoxia formation depends. A high-resolution ecosystem model was developed, which successfully reproduced observed temperature, salinity, and bottom oxygen concentration. This model suggested fast response of bottom oxygen to vertical stratification evolution (generally ~6–50 hr) and a transient spatial extent of summer bottom hypoxia off the Changjiang River estuary. Comparisons between observed and modeled oxygen concentrations implied that the hypoxic area calculated from dissolved oxygen at discrete locations often had possible errors and the estimated magnitude of hypoxic area which depended on the chronological order of observations. Therefore, it is risky to estimate the spatial extent of hypoxic area based on observations exclusively, and the relevant quantification of annual hypoxia area trend is also questionable. Integration of quasi-simultaneous observations is required to advance the understanding of oxygen dynamics, to minimize observational uncertainties. The development of skillful ecosystem models that profit from ample observations and have the power to reproduce dissolved oxygen is indispensable.

研究人员通常通过走航观测收集离散站点点的溶解氧数据，进而估计海底低氧或缺氧区的空间范围。然而，这样的观测结果往往无法定量地表现近海海洋中瞬时的溶解氧浓度空间分布，难以捕捉海底缺氧这种短暂性事件。在长江河口及其邻近海域，走航观测的时间跨度往往超过海底缺氧事件的时间尺度。由于风速和风向的变化，长江冲淡水极易发生摆动，而冲淡水的分布形势控制着缺氧区形成所依赖的垂向层化的分布。本文开发了一套高分辨率生态系统数值模式，该模式的模拟结果与实测的温度、盐度和底部溶解氧浓度都有较好的匹配。模式结果表明，底部溶解氧对垂向层化的变化响应迅速（大约6-50小时），而夏季长江口外底部缺氧区扩展态势的变化也十分迅速。通过对走航观测数据和模式模拟结果，本文发现通过离散站点点走航观测获取的溶解氧数据计算的缺氧区面积通常存在误差，并且估算结果取决于站点观测的时间顺序。因此，仅基于观测结果来估算缺氧区的空间范围是有风险的，由此估计的缺氧区变化趋势是存在问题的。因此，为了更好地研究溶解氧的变化趋势，减小观测中的不确定性，研究人员需要进行准同步观测。与此同时，开发与实测结果相符、能够准确模拟溶解氧的生态系统模式也必不可少。

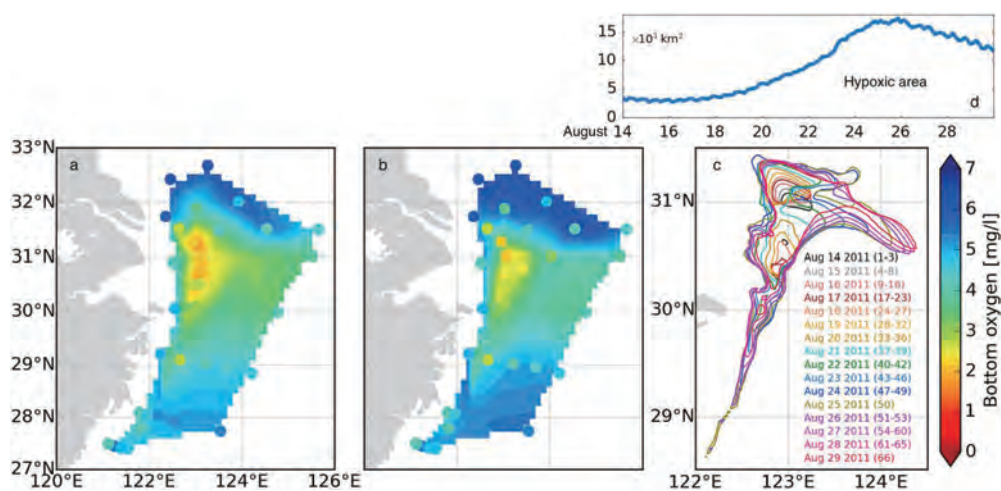


Figure 10. (a) Modeled bottom dissolved oxygen corresponding to cruise 1, this is identical to Figure 3d; (b) modeled bottom dissolved oxygen associated with the reversed chronological order, observed oxygen is superimposed for both; (c) plan-view (3-hourly output averaged to daily) and (d) time series (3-hourly) of modeled bottom hypoxic area over the date range of cruise 1.

Gut microbial diversity in two insectivorous bats: Insights into the effect of different sampling sources

Wu H, Xing Y, Sun H, et al. *MicrobiologyOpen*, 2018:e00670.

The gut microbiota is now known as a key factor in mammalian physiology and health. Our understanding of the gut microbial communities and their effects on ecology and evolution of their hosts is extremely limited in bats which represent the second largest mammalian order. In the current study, gut microbiota of three sampling sources (small intestine, large intestine, and feces) were characterized in two sympatric and insectivorous bats (*Rhinolophus sinicus* and *Myotis altarium*) by high-throughput sequencing of the V3-V4 region of the 16S rRNA gene. Combining with published studies, this work reveals that Gammaproteobacteria may be a dominant class in the whole Chiroptera and Fusobacteria is less observed in bats although it has been proven to be dominant in other mammals. Our results reveal that the sampling source influences alpha diversity of the microbial community in both studied species although no significant variations of beta diversity were observed, which support that fecal samples cannot be used as a proxy of the microbiota in other gut regions in wild animals.

肠道微生物与哺乳动物的生理和健康密切相关。我们对于肠道微生物及它们对宿主生态和进化方面的影响都知之甚少，尤其是在翼手目动物中。本研究通过扩增和分析16S rRNA基因的 V3-V4区序列，比较了两种同域分布的食虫蝙蝠在大肠、小肠和粪便中肠道微生物的组成差异。研究表明，不同的取样来源对肠道微生物多样性的研究有着较大影响，而只选取粪便来代表整个生物个体的微生物多样性存在一定的片面性。

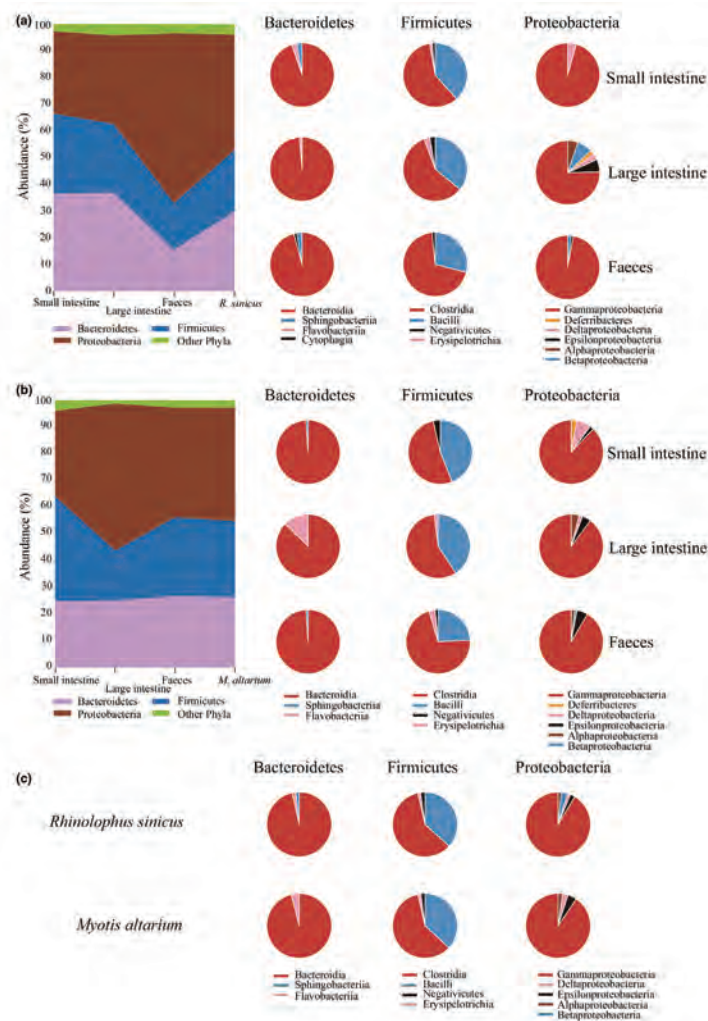


Figure 2. Bacteria community composition and relative abundance at the phyla and class levels in (a) *R. sinicus* and (b) *M. altarium*. (c) Pie charts show relative abundances of bacterial classes with an abundance of > 1% in three dominated phyla in *R. sinicus* and *M. altarium*

Iron plaque formation and heavy metal uptake in *Spartina alterniflora* at different tidal levels and waterlogging conditions

Xu Y, Sun X, Zhang Q, et al. *Ecotoxicology and environmental safety*, 2018, 153:91-100.

Tidal flat elevation in the estuarine wetland determines the tidal flooding time and flooding frequency, which will inevitably affect the formation of iron plaque and accumulations of heavy metals (HMs) in wetland plants. The present study investigated the formation of iron plaque and HM's (copper, zinc, lead, and chromium) accumulation in *S. alterniflora*, a typical estuarine wetland species, at different tidal flat elevations (low, middle and high) in filed and at different time (3, 6, 9, 12 h per day) of waterlogging treatment in greenhouse conditions. Results showed that the accumulation of copper, zinc, lead, and chromium in *S. alterniflora* was proportional to the exchangeable fraction of these metals in the sediments, which generally increased with the increase of waterlogging time, whereas the formations of iron plaque in roots decreased with the increase of waterlogging time. Under field conditions, the uptake of copper and zinc in the different parts of the plants generally increased with the tidal levels despite the decrease in the metals' exchangeable fraction with increasing tidal levels. The formation of iron plaque was found to be highest in the middle tidal positions and significantly lower in low and high tidal positions. Longer waterlogging time increased the metals' accumulation but decreased the formation of iron plaque in *S. alterniflora*. The binding of metal ions on iron plaque helped impede the uptake and accumulation of copper and chromium in *S. alterniflora*.

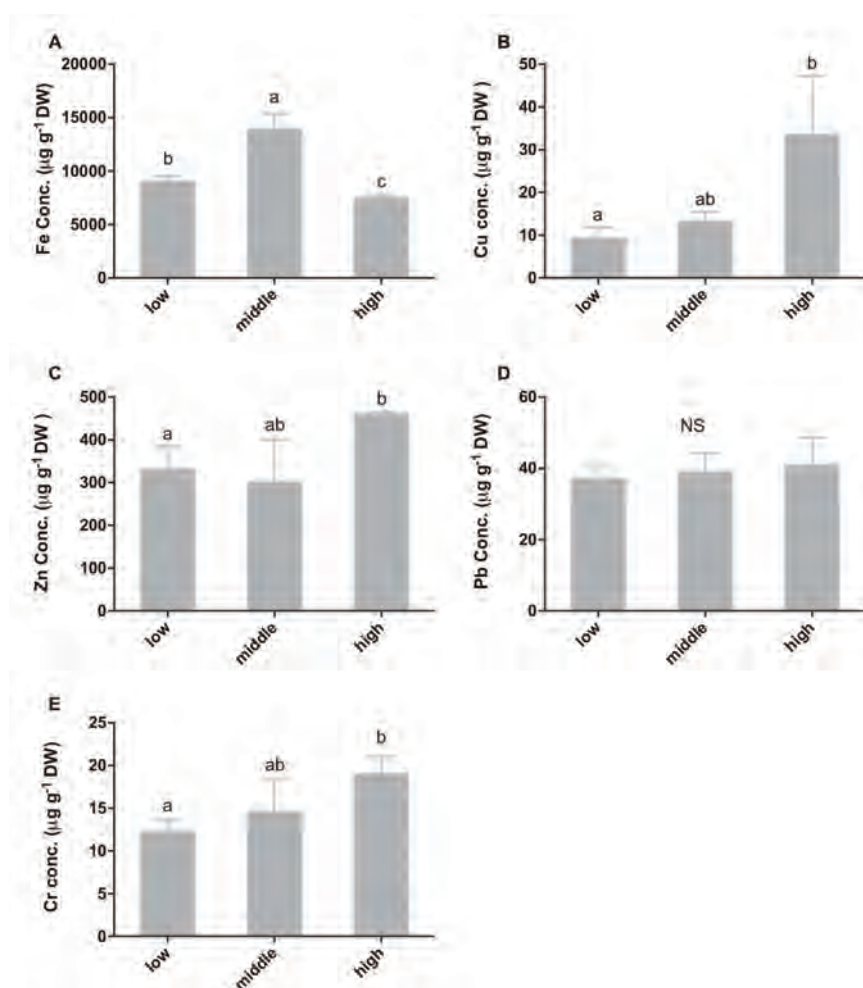


Fig. 2. Sediment physiochemical characteristics along different tidal levels. (A) clay content (%); (B) silt content; (C) MD (µm); (D) Salinity (‰); (E) TOM (%); (F) Eh (values are mean and SD; for each parameter, data with different letters are significantly different at $P \leq 0.05$).

潮滩湿地由于其独特的水文条件及沉积物的理化特征承接并累积大量重金属污染物。互花米草作为河口典型的湿地植物，在重金属的生物地球化学循环中扮演着重要作用。根表铁膜的形成是湿地植物的特有现象，铁膜的形成对湿地植物营养元素的吸收利用以及重金属的迁移转化都起到一定的作用。潮滩湿地周期性的潮汐浸淹决定了湿地土壤的氧化还原特征也周期性发生变化，滩涂高程也决定了潮滩植物的淹水时间和淹水频率，这些因素必然影响湿地植物的铁膜产生以及重金属在土壤中的生物有效性，也会对重金属在植物体内的累积迁移产生影响。本研究对比研究了野外不同潮滩高程（光滩，低，中，高潮滩）和室内不同时间淹水（3，6，9，12小时/日）和重金属复合处理下互花米草铁膜的形成和主要重金属（Cu，Zn，Pb，Cr）在互花米草中的吸收转运。结果表明，不同潮滩高程土壤中的Cu和Zn的含量随着高程的增加而增加，而Cr的含量在潮位最低的光滩含量最高，土壤Pb含量在各潮位无显著性差异。土壤Pb和Cr弱酸可提取态的含量随高程的增加而降低。土壤Cu和Zn弱酸可提取态的含量在各潮位没有明显差异，然而弱酸可提取态与土壤总重金属含量的比值随高程的增加而降低。四种重金属均主要积累于互花米草根，其次为茎，叶片中最少。在各潮位中，高潮位的互花米草根和茎中Cu的含量明显高于中低潮位的，叶片Cu的含量则在各潮位中无显著性差异；高程变化对互花米草各个部位中Zn的含量无显著影响；根部Pb和Cr的含量在低潮滩最高，然而茎和叶片的Pb、Cr含量在各潮位没有显著差异。室内不同淹水时间控制实验结果表明，Cu在根和茎中的含量随淹水时间的增加而减少，而不同的淹水时间处理对Zn在叶片和茎中含量影响不显著，根部和叶片Cr和Pb的含量随淹水时间的增加而显著增加。以上结果与野外实验的结果基本一致。本研究用DCB提取法研究了互花米草根系铁膜的含量和铁膜中结合重金属的情况，结果显示，野外中潮滩根表铁膜含量最高，而高潮滩最低。铁膜中Cu和Zn的含量随高程的升高而显著降低，而Pb和Cr的含量则随高程无明显变化规律。不同时间淹水的控制实验结果显示，每日6小时淹水处理下铁膜含量最高，而12小时淹水铁膜含量最低，铁膜中Cu含量在不同淹水时间下呈现与铁膜类似的变化规律，而铁膜中Zn、Pb、Cr的含量变化皆随淹水时间的增加而增加。

Table 2
Accumulations of Cu, Zn, Pb and Cr in different plant parts 60 days after different time of waterlogging treatments (metals concentration in each plant parts with different letters indicate they are significantly different at the level of $P \leq 0.05$, no letter appended if the data is not significantly different).

| Heavy metals conc. ($\mu\text{g g}^{-1}\text{DW}$) | Plant part | 6 h | 3 h + 2HM | 6 h + 2HM | 9 h + 2HM | 12 h + 2HM |
|--|------------|---------------------------|------------------------------|-----------------------------|-----------------------------|------------------------------|
| Cu | Root | 15.76 ± 1.46 ^b | 91.89 ± 20.51 ^a | 78.64 ± 17.91 ^a | 84.64 ± 14.24 ^a | 102.61 ± 14.66 ^a |
| | Stem | 15.62 ± 3.60 | 17.88 ± 2.98 | 22.03 ± 5.65 | 20.87 ± 9.17 | 17.73 ± 4.02 |
| | Leaf | 8.13 ± 1.24 ^a | 8.36 ± 0.19 ^a | 18.75 ± 6.01 ^b | 13.45 ± 3.78 ^{ab} | 18.92 ± 6.40 ^b |
| Zn | Root | 21.95 ± 8.74 ^d | 91.81 ± 19.62 ^b | 163.16 ± 8.74 ^c | 248.87 ± 7.77 ^a | 230.41 ± 8.74 ^a |
| | Stem | 34.20 ± 2.15 ^c | 86.74 ± 19.50 ^{abc} | 86.02 ± 15.15 ^{bc} | 144.08 ± 29.09 ^a | 115.00 ± 29.31 ^{ab} |
| | Leaf | 26.50 ± 5.70 ^a | 70.96 ± 23.96 ^a | 148.59 ± 21.39 ^b | 142.20 ± 22.78 ^b | 138.51 ± 7.01 ^b |
| Pb | Root | 1.39 ± 0.04 ^e | 1.99 ± 0.54 ^c | 3.76 ± 0.27 ^d | 5.55 ± 0.27 ^b | 7.82 ± 0.09 ^a |
| | Stem | 0.77 ± 0.23 ^c | 0.87 ± 0.45 ^{bc} | 1.08 ± 0.12 ^{bc} | 2.34 ± 0.75 ^a | 1.89 ± 0.08 ^{ab} |
| | Leaf | 0.31 ± 0.02 ^b | 0.62 ± 0.28 ^b | 0.90 ± 0.19 ^{ab} | 1.64 ± 0.59 ^a | 1.66 ± 0.11 ^a |
| Cr | Root | 2.00 ± 0.97 ^c | 4.63 ± 0.65 ^{bc} | 8.03 ± 2.99 ^b | 4.48 ± 0.13 ^{bc} | 8.76 ± 0.13 ^a |
| | Stem | 0.77 ± 0.27 ^a | 1.19 ± 0.30 ^{ab} | 2.01 ± 0.71 ^b | 1.36 ± 0.14 ^{ab} | 2.19 ± 0.54 ^b |
| | Leaf | 1.57 ± 0.58 ^a | 2.51 ± 0.50 ^{ab} | 3.49 ± 0.28 ^{ab} | 4.80 ± 1.85 ^b | 5.01 ± 1.75 ^b |

Submarine Groundwater Discharge-Derived Carbon Fluxes in Mangroves: An Important Component of Blue Carbon Budgets?

Chen X, Zhang F, Lao Y, et al. *Journal of Geophysical Research: Oceans*, 2018, 123(9):6962-6979.

Mangroves are blue carbon systems characterized by high soil carbon storage and sequestration. Soil carbon losses via groundwater or pore water pathways are potentially important yet poorly understood components of mangrove carbon budgets. Here we quantified submarine groundwater discharge (SGD) and associated dissolved inorganic carbon (DIC) and organic carbon (DOC) fluxes into a mangrove-dominated tropical bay (Maoweï Sea) using a radon (^{222}Rn) mass balance model. The SGD fluxes in Maoweï Sea were estimated to be 4.9×10^7 (0.36 ± 0.33 m/day) and 2.6×10^7 m³/day (0.20 ± 0.18 m/day) for the wet and dry seasons, respectively, implying that SGD may respond to precipitation. The SGD-derived DIC and DOC fluxes ($\text{mol}\cdot\text{m}^{-2}\cdot\text{day}^{-1}$) in the wet season (DIC: 0.70 ± 0.82 ; DOC: 0.31 ± 0.30) were higher than those in the dry season (DIC: 0.25 ± 0.24 ; DOC: 0.25 ± 0.23). These SGD-derived carbon fluxes exceed local river inputs and constituted >70% of the total DIC and DOC input into the bay. If scaled up to the global weighted mangrove area in combination with data from other 32 study sites, carbon fluxes via SGD into mangroves may be equivalent to 29–48% of the global riverine input into the ocean. Therefore, we suggest that SGD is a major component of coastal carbon budgets and that accounting for SGD helps to reduce uncertainties in mangrove blue carbon budgets.

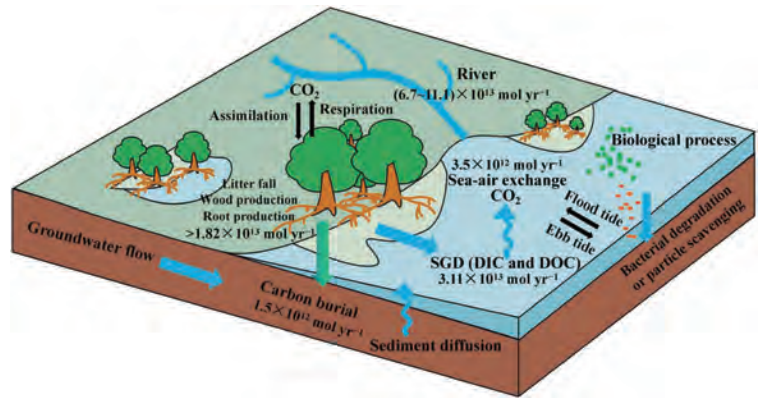


Figure 8. Schematic diagram for biogeochemical processes of mangrove blue carbon including estimated global SGD carbon fluxes (modified from Bouillon et al., 2008; Gao et al., 2016). SGD = submarine groundwater discharge.

以我国典型热带北部湾红树林生境茅尾海为例，利用氡 (Rn-222) 质量平衡模型量化了该区的海底地下水排放 (SGD)，和相关的溶解无机碳 (DIC) 和有机碳 (DOC) 通量。在雨季和旱季，茅尾海的SGD通量估计分别为 4.9×10^7 m³/day (0.36 ± 0.33 m/day) 和 2.6×10^7 m³/day (0.20 ± 0.18 m/day)。雨季中SGD携带的DIC和DOC通量 (DIC: 0.70 ± 0.82 mol·m²·day⁻¹; DOC: 0.31 ± 0.30 mol·m²·day⁻¹) 高于旱季 (DIC: 0.25 ± 0.24 mol·m²·day⁻¹; DOC: 0.25 ± 0.23 mol·m²·day⁻¹)。这些SGD衍生的碳通量超过当地河流输入，占进入海湾的DIC和DOC总量的70%以上。将其他32个研究点的数据扩大到全球并加权红树林面积，定量评估了通过SGD进入红树林的碳通量可能相当于全球河流输入海洋碳通量的29-48%。阐明了海底地下水排放的碳是近岸红树林湿地碳收支的重要组成部分，弥补了先前红树林蓝碳收支计算中缺失的部分。

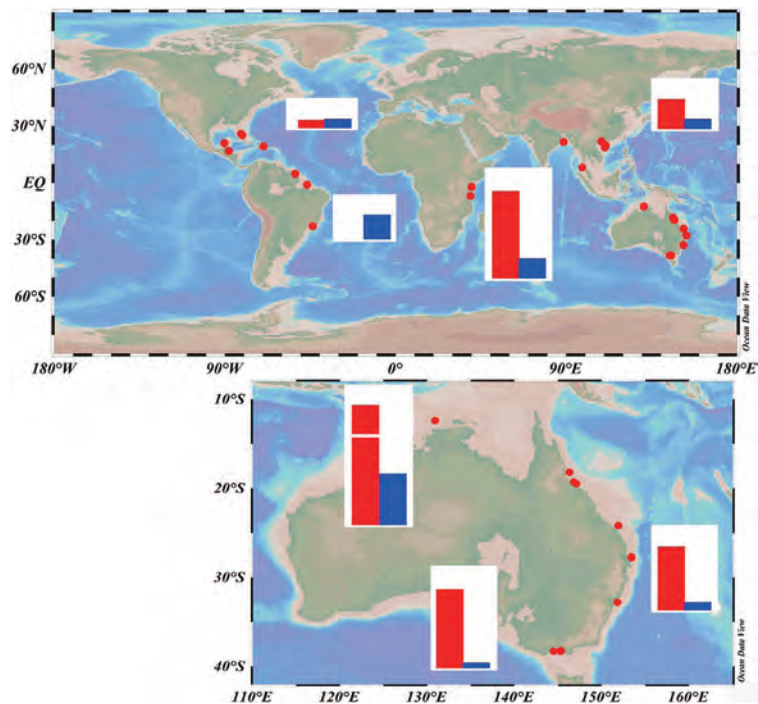


Figure 7. Global research cases (red dots) for dissolved carbon input via SGD in mangrove ecosystems. The red and blue bars represent the DIC and DOC fluxes ($\text{mol}\cdot\text{m}^{-2}\cdot\text{day}^{-1}$) from SGD in different mangrove areas around the world, respectively. The number represents an average of research cases showed in Table 4. We used the SGD rate (10 cm/day) of Mauritius Island (Povinec et al., 2012) closest to the number 18 and 19 as the SGD rate in Africa. SGD = submarine groundwater discharge; DIC = dissolved inorganic carbon; DOC = dissolved organic carbon.

In situ and satellite observations of phytoplankton size classes in the entire continental shelf sea, China
Sun X, Shen F, Liu D, et al. *Journal of Geophysical Research: Oceans*, 2018, 123(5):3523-3544.

Phytoplankton size classes (PSCs) is of great significance for exploring marine ecological and biogeochemical processes. Remote sensing of PSCs has been successfully applied to open oceans; however, it is still quite limited for optically complex coastal oceans. In this study, the entire continental shelf sea of China including Bohai Sea (BS), Yellow Sea (YS), and East China Sea (ECS) characterized by distinctive turbid waters and impacted by plumes of large world-class river (the Changjiang River) was taken as an example of turbid coastal ocean for remotely sensed spatial-temporal distributions of PSCs. In situ data were collected from cruises during April to June in 2014 and an improved algorithm for PSCs retrieval was proposed. PSCs derived from GOCI (Geostationary Ocean Color Imager) images revealed that microplankton was dominant in the BS, the YS, and the nearshore ECS and nanoplankton distributed widely in the entire study area, while picoplankton mainly distributed in the offshore ECS in April, which was consistent with in situ investigation and related to environmental factors. Validation indicated that the improved algorithm provided a more accurate estimation of PSCs, with the root mean square error (RMSE) between estimated and measured size-fractionated concentrations been 0.774, 0.257, and 0.142 mg m⁻³ for micro, nano, and picoplankton, respectively. Diurnal variations of PSCs were mainly affected by tidal currents and light intensity depending on different water types. These illustrated that remote sensed spatial distributions as well as diurnal variations of PSCs are effective in turbid continental shelf seas of China.

浮游植物粒级 (PSCs) 对探索海洋生态、生物地球化学过程有着重要的意义。目前, 遥感反演PSCs已被广泛应用于大洋水体, 但对于光学性质较为复杂的近岸水体的应用仍十分有限。本研究以浑浊的、受大河影响的中国东大陆架边缘海, 即渤海、黄海和东海为研究区域, 开展遥感反演PSCs时空分布的研究。基于2014年4月至6月现场采集的数据, 我们提出了一个改进的反演PSCs的遥感算法。GOCI影像反演得到的结果显示, 小型浮游植物主要分布在渤海水域, 黄海水域, 和东海的近岸水域; 微型浮游植物在研究区域内的分布较广; 微微型浮游植物主要分布在东海的外海水域, 与实际调查结果相一致, 主要受到环境因素的影响。验证结果显示, 改进的算法能够提高反演PSCs的精度, 小型、微型、微微型浮游植物的遥感反演浓度和实测浓度的均方根误差分别是0.774, 0.257和0.142mg m⁻³。PSCs在不同水域的日变化主要是受到潮汐和光照强度的影响。这些结果表明, 在浑浊的近岸水域进行遥感反演PSCs的空间变化和日变化有效的。

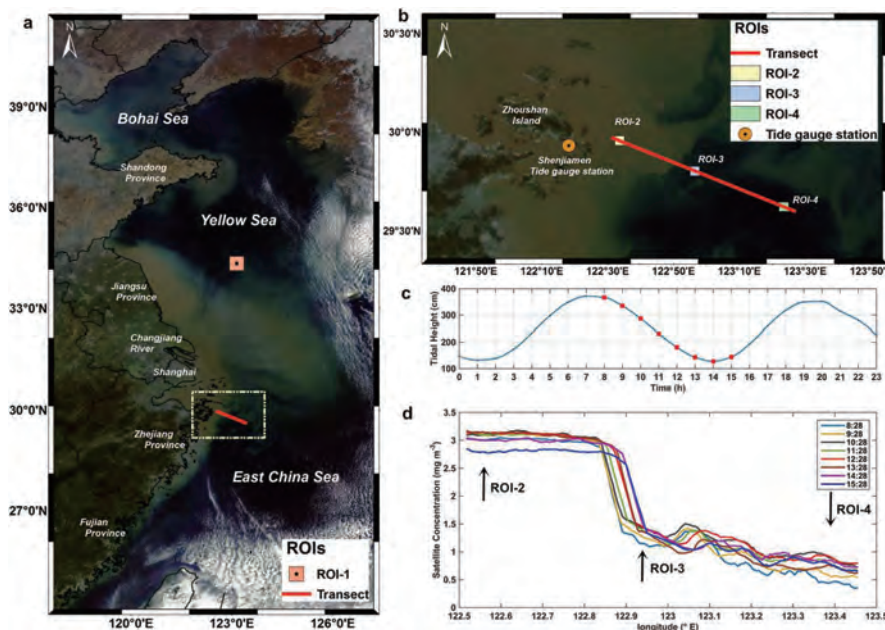


Figure 7. A transect and four regions of interest (ROIs) utilized in diurnal variation (a, b). The base map is a three-band composite true color image acquired at 10:28 (local time, red: Band 6, green: Band 4, blue: Band 2). (c) Tide height from Shenjiamen tide gauge station on 7 April 2013, the red squares represent hourly imaging time of GOCI images. (d) Diurnal variation of GOCI-derived chlorophyll-a concentration of the transect.

Ecophysiological linkage of nitrogen enrichment to heavily silicified diatoms in winter

Liu D, Glibert P M. *Marine Ecology Progress Series*, 2018, 604:51-63.

Over recent decades, increased anthropogenic nitrogen and reduced land-based loading of silica in many coastal waters have asymmetrically changed the nitrogen:silica ratios. These changes have contributed to shifts in phytoplankton assemblages from diatoms to nondiatoms, as well as increases in the frequency and magnitude of non-diatom harmful algal blooms. Here we show a subtle and counterintuitive change in diatom assemblage, i.e. heavily silicified diatoms significantly increased in winter after nitrogen enrichment, based on paleoecological and contemporary seasonal water column data from 2 eutrophic bays in the Yellow Sea. The heavily silicified diatom *Paralia sulcata* showed an increasing trend over time in parallel with nitrogen enrichment, which was associated with low temperature, and low dissolved inorganic nitrogen: phosphorus, high dissolved nitrogen:silica, and low ammonium:nitrate ratios on a seasonal basis. Applying recent insights regarding diatom nitrogen metabolism and its putative urea cycle, a physiological mechanism linking nitrogen, carbon, and silica metabolism is suggested to explain the phenomenon of increased silicification under winter conditions at the cellular level. Winter sequestration of silica in *P. sulcata* valves also has biogeochemical consequences, including a weakening of the silica pump and a slowing of biogenic silica dissolution, thereby reducing the availability of silica for further diatom growth in subsequent seasons and increasing the window of opportunity for summer growth of non-diatom harmful algal bloom species.

近几十年来, 人类活动导致许多沿海水域氮含量升高, 而陆源硅的输入量减少, 使得氮硅比显著升高。这种变化导致浮游植物群落由硅藻向非硅藻的转变, 并造成非硅藻有害藻华频率和数量的增加。本文根据黄海2个富营养化海湾的古生态学和现代海水数据, 揭示了硅藻群落的一种微妙的、违反直觉的变化, 即冬季氮富集后, 重度硅化硅藻出现显著增加。重度硅化硅藻具槽帕拉藻随时间的推移, 与氮富集呈现出同步增长的趋势, 同时与季节性的低温、低氮磷比、高氮硅比和低氨氮硝氮比有关。基于最近关于硅藻氮代谢及其假设的尿素循环的见解, 提出了一种连接氮、碳和硅代谢的生理机制, 以在细胞水平上解释冬季的环境条件下硅化作用增加的现象。冬季封存在具槽帕拉藻的硅也存在生物地球化学效应, 包括削弱硅泵和减缓生物硅溶解, 从而减少随后季节硅藻生长可利用的硅, 并为夏季非硅藻有害藻华种的生长提供机会。

Fig. 8. Conceptual diagram of the seasonal succession of phytoplankton and corresponding rates of BSi dissolution under (a) pre-eutrophic conditions and (b) nutrient-enriched conditions. Note that in the pre-enrichment state, winter diatoms are more diverse, silica dissolution is more rapid, and the proportional accumulation of non-diatoms during the warmer months is relatively lower. In the eutrophic condition, more heavily silicified diatoms dominate in winter, prolonging the period of BSi dissolution and cycling, enhancing the period for nondiatoms to accumulate during the warmer months

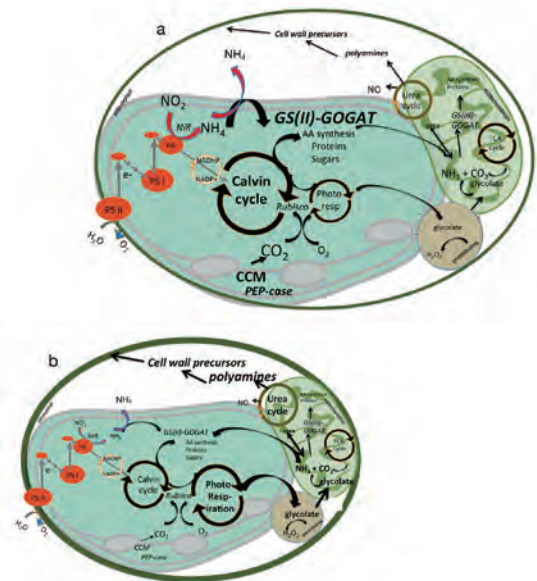
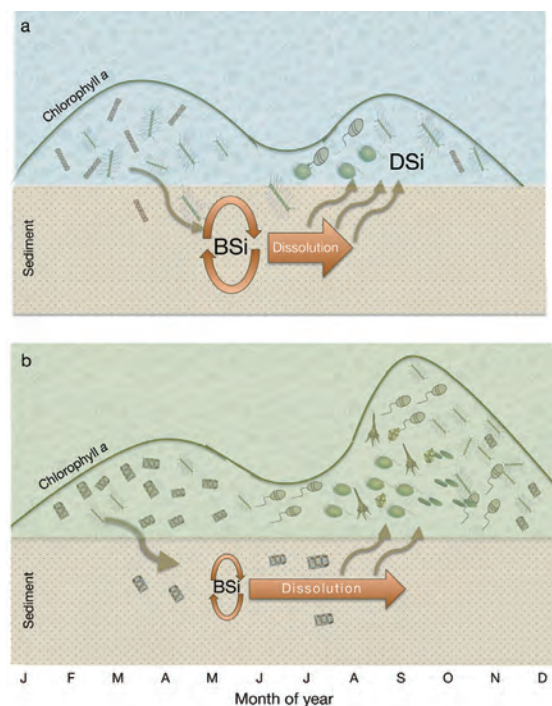


Fig. 7. Conceptual schematics of (a) a typical diatom and (b) a smaller, more heavily silicified diatom, showing the electron transport of photosynthesis, the coupling to the Calvin cycle and photorespiration and the urea cycle and its link to cell wall precursor formation. Note that in the heavily silicified case, photorespiration is higher, as is export of glycolate to the peroxisome and urea cycle cell wall precursor formation. Figure modified and reproduced from Glibert et al. (2016) based on a creative commons license



Dynamical Response of Changjiang River Plume to a Severe Typhoon With the Surface Wave-Induced Mixing

Zhang Z, Wu H, Yin X, et al. *Journal of Geophysical Research: Oceans*, 2018.

Typhoons (or hurricanes) are the most energetic atmospheric forcing acting on coastal waters. Here in this study, we investigated the response of the summertime Changjiang River plume to a typical typhoon, Chan-hom (1509), with a combination of field observation and numerical simulation. Surface wave-induced mixing was considered in the model configuration. The results showed that the typical offshore-extending summer Changjiang River plume completely disappeared under the influence of typhoon wind. Instead, it extended southward along the Zhejiang and Fujian (Zhe-Min) coast as a typical wintertime Changjiang River plume. The along-shelf plume extension lasted for extra ~10 days after the typhoon passage, until another strong weather event came. The competition between wind-driven current and buoyancy-driven current dominated the recovery of the Changjiang River plume. Through calculation, we found that the freshwater transported to the Zhe-Min Coastal Water reached $\sim 4.7 \times 10^{10} \text{ m}^3$ as influenced by typhoon Chan-hom, which was $\sim 5\%$ of the total Changjiang River discharge in 2015 or $\sim 12\%$ of the total dry season Changjiang River discharge (October-April) when the majority of Changjiang River plume extended to Zhe-Min Coastal Water. The remote sensing data of chlorophyll- α from Geostationary Ocean Color Imager also showed that significant algal bloom occurred when the southward extending Changjiang River plume retreated. Surface wave-induced mixing caused by typhoon wind was found to be important in destroying the vertical plume stratification and elongating the recovery processes from the typhoon influence.

台风（或飓风）是作用于沿岸海域最剧烈的大气强迫。结合现场观测和数值模拟，本文研究了夏季长江冲淡水对典型台风案例——灿鸿（第1509号台风）的响应。在模型配置中，本文将波浪混合也考虑其中。结果表明，在台风的影下，长江冲淡水典型的夏季离岸扩展形态完全消失。相反的，它沿着浙闽海域向南延伸，这与冬季长江冲淡水的扩展形态类似。在台风过境后，这种冲淡水的沿岸扩展形态持续了约10天，直至另一场强烈的天气事件发生。风生流和浮力沿岸流之间的竞争主导了长江冲淡水的恢复过程。本文通过计算发现，在台风灿鸿的影响下，输运至浙闽海域的淡水总量多达 $4.7 \times 10^{10} \text{ m}^3$ ，这约占2015年长江总径流量的5%或枯季长江径流量的12%。GOCI的叶绿素- α 遥感数据也显示，当长江冲淡水向南扩展的态势减弱时，浙闽海域发生了藻类爆发事件。此外，台风引起的波浪混合破坏了冲淡水的垂向层化，延长了冲淡水的恢复过程。

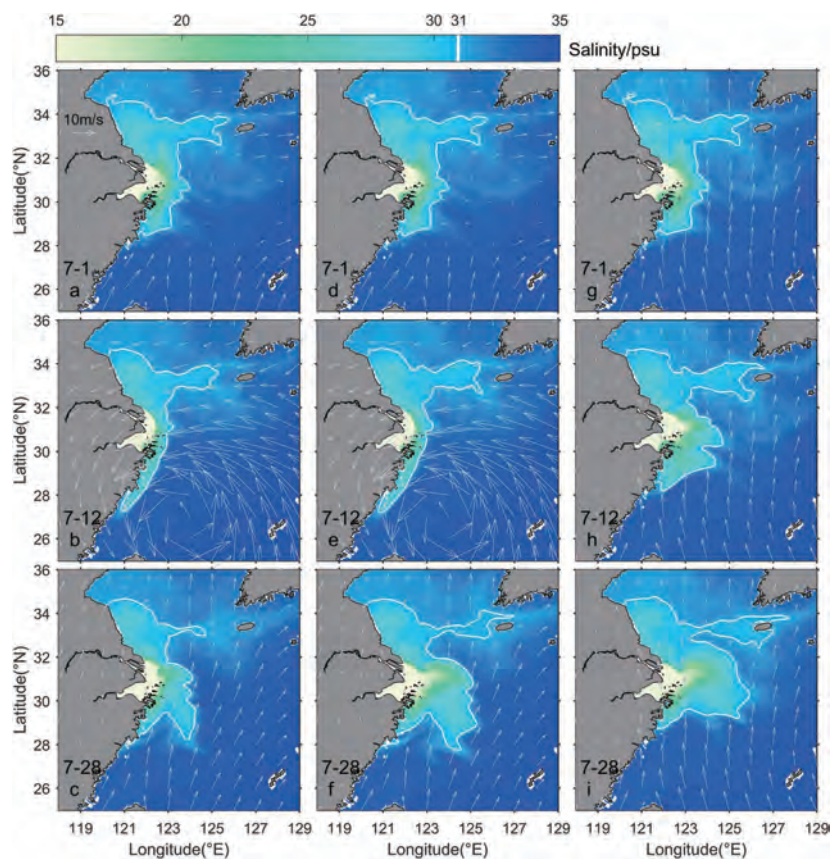
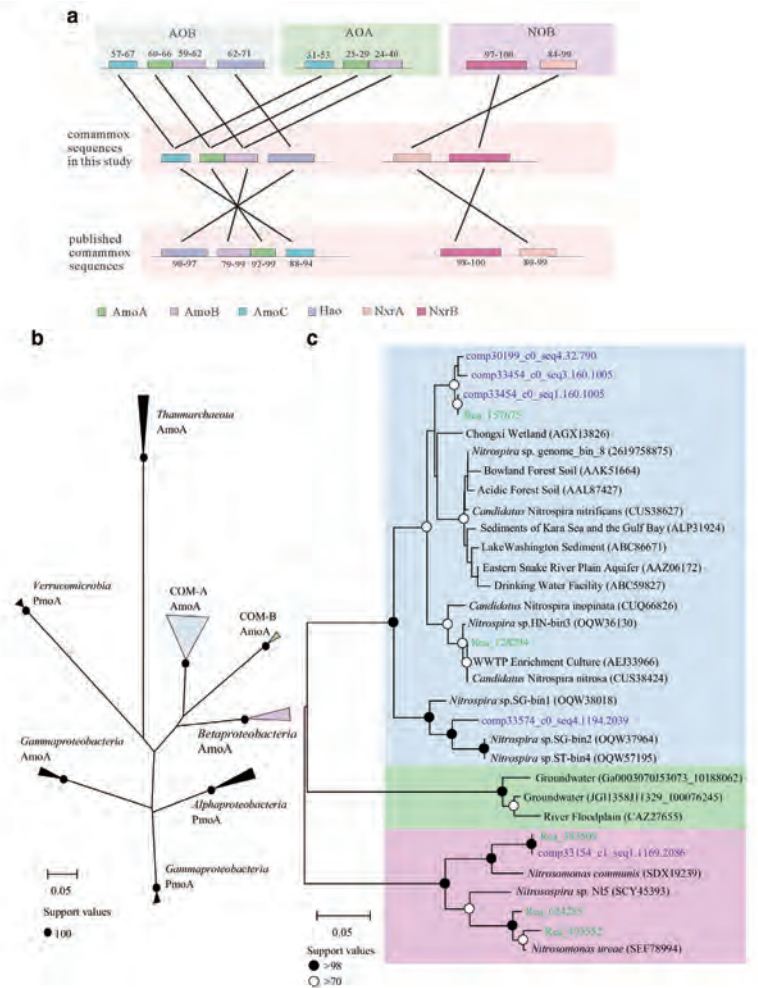


Figure 4. Modeled surface salinity in Exp1 (a-c), Exp2 (d-f), and Exp3 (g-i) before (1 July), during (12 July), and after (28 July) the passage of typhoon Chan-hom. psu = practical salinity unit.

Evidence for complete nitrification in enrichment culture of tidal sediments and diversity analysis of clade a comammox *Nitrospira* in natural environments.

Yu C, Hou L, Zheng Y, et al. *Applied Microbiology and Biotechnology*, 2018.

Complete ammonia oxidizers (comammox), as novel microbial communities, are predicted to play an important role in the nitrogen cycle. Here we reported the presence of complete nitrification in tidal sediments and examined the diversity and abundance of comammox in natural ecosystems. Metagenome and metatranscriptome of the enrichment culture from tidal sediments harbored the genes of comammox. Near-complete comammox AmoA/B/C- and Hao-like sequences showed close relationships to the known comammox (with sequence identity from 79 to 99%) rather than classical betaproteobacterial ammonia-oxidizing bacteria (β -AOB) (57 to 66%) and ammonia-oxidizing archaea (AOA) (24 to 38%). To analyze the diversity of comammox in natural environments, a new primer set targeting clade A comammox *Nitrospira* (COM-A) amoA genes was designed based on sequences obtained in this study and sequences from published database. In silico evaluation of the primers showed the high coverage of 89 and 100% in the COM-A amoA database. Application of the primers in six different ecosystems revealed their strong availability. Community composition of COM-A suggested a relatively higher diversity than β -AOB in similar environments. Quantification results showed that COM-A amoA genes accounted for about 0.4–5.6% in total amoA genes. These results provide novel insight into our perception of the enigmatic comammox and have significant implications for profound understanding of complex nitrification process.



目前，河口地区全程氨氧化微生物（comammox）的菌群多样性、丰度及潜在活性还不清楚。本研究以长江河口为主要研究区域，通过富集培养证明了长江口潮滩沉积物中comammox的存在，深入分析了富集物 comammox 的种群结构和基因表达模式，并基于富集所得的 comammox 基因序列设计了特异性引物，用于研究河口环境中 comammox 菌群多样性及其丰度。PCR扩增子克隆测序和实时荧光定量PCR分析结果，显示河口生态系统沉积物中comammox群落组成相近，不同于湖泊、河流等沉积环境的群落组成。河口沉积环境中comammox的丰度为 $3.50 \times 10^5 - 1.56 \times 10^6$ copies g^{-1} ，占样品中amoA拷贝量的0.4% - 5.6%。研究结果表明了自然环境中comammox较高的多样性，并从amoA基因丰度的角度评估了comammox在硝化过程中不可忽略的贡献。环境样品中comammox群落多样性主要取决于沉积物 NH_4^+ 浓度，而盐度、pH、沉积物含水率、总有机碳等理化因子的影响不显著。关于河口自然环境中 comammox 种群多样性的研究结果暗示了 comammox 在氮循环过程中的重要作用。

Nitrogen fixation in surface sediments of the East China Sea: Occurrence and environmental implications

Wang R, Li X, Hou L, et al. *Marine pollution bulletin*, 2018, 137:542-548.

Sediment nitrogen fixation and associated functional gene in the East China Sea were investigated using nitrogen-isotope tracing and molecular techniques. Potential rates of nitrogen fixation were detected, with values of 0.06–5.51 nmol N g⁻¹ h⁻¹. Abundance of functional gene (nifH) ranged from 0.36×10⁶ to 5.39×10⁷ copies g⁻¹. Nitrogen fixation rates were not related to the abundance of nifH gene but to temperature, salinity, sulfide, iron and C/N, indicating that the sediment properties rather than microbial abundance dominated the nitrogen fixation. It is also estimated that sediment nitrogen fixation annually contributed about 3.43×10⁵ to 3.10×10⁷ tons nitrogen to the East China Sea, which accounted for 8.2–22.6% of the total inorganic nitrogen input. Overall, this study highlights the importance of benthic nitrogen fixation in controlling nitrogen budget in the East China Sea and improves our knowledge on nitrogen cycling in the coastal marine environments.

本研究利用同位素示踪和分子生物学技术，测定了东海沉积物固氮过程速率及相关功能微生物丰度。分析结果显示，潜在的沉积物固氮速率为0.06–5.51 nmol N g⁻¹ h⁻¹，功能微生物基因（nifH）丰度为0.36 × 10⁶-5.39 × 10⁷ copies g⁻¹。统计分析发现，东海沉积物固氮速率与nifH基因丰度无显著相关性，而与沉积物温度、盐度、硫化物、碳氮原子比有关，反映了沉积物理化特征是影响沉积物固氮速率时空分布格局的重要因素。此外，根据沉积物固氮速率的时空变化特征，估算了研究区域内沉积物的年固氮量约为3.43 × 10⁵-3.1 × 10⁷吨，占总无机氮输入量的8.2-22.6%。研究结果反映了沉积物固氮过程在调控氮收支平衡的重要性，提升了对河口近海氮循环过程的认识。

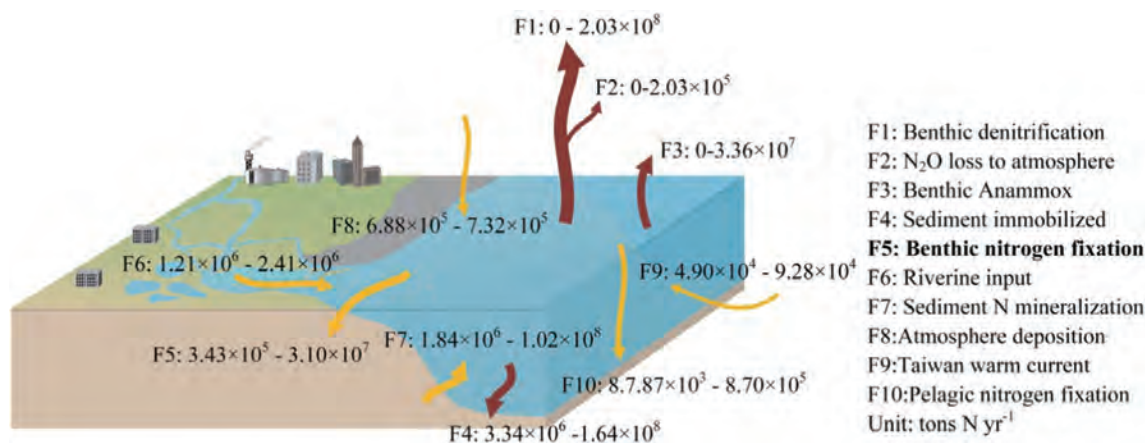


Fig. 5. General fluxes of nitrogen sources and sinks in the East China Sea. The area assigned for calculation is 7.7×10⁵ km². The yellow and brown arrows represent the possible nitrogen sources and sinks, respectively. (For interpretation of the references to colour in this figure legend, the reader is referred to the web version of this article.)

Shifts in the Community Dynamics and Activity of Ammonia-Oxidizing Prokaryotes Along the Yangtze Estuarine Salinity Gradient

Gao J, Hou L, Zheng Y, et al. *Journal of Geophysical Research: Biogeosciences*, 2018, 123(11):3458-3469.

Ammonia oxidation, the first and rate-limiting step in nitrification, plays a critical role in the nitrogen cycle. However, the links between the dynamics of ammonia-oxidizing communities and ecosystem processes along the estuarine salinity gradient remain uncertain. In this study, we examined the diversity, abundance, and community structure of ammonia-oxidizing prokaryotes, and the potential nitrification rates along the Yangtze estuarine salinity gradient. Phylogenetic analysis showed that the predominant ammonia-oxidizing bacteria (AOB) and ammonia-oxidizing archaea (AOA) fell within the *Nitrosospira* and *Nitrosopumilus* clusters, respectively. The AOB *amoA* gene abundance (4.67×10^5 to 3.90×10^7 copies per gram of dry sediment) outnumbered AOA (5.14×10^4 to 8.88×10^6 copies per gram of dry sediment). The potential nitrification rates varied between 0.13 and $0.63 \mu\text{g N}\cdot\text{g}^{-1}\cdot\text{day}^{-1}$ and related only to AOA *amoA* gene abundance. Salinity had significant effects on AOA *amoA* gene abundance, nitrification rates, and the community structure of ammonia-oxidizing prokaryotes. Principal coordinate analysis showed that the AOB *amoA* gene clones derived from the middle- and high-salinity regions behaved as a cohesive group, while all the low-salinity clone libraries were grouped together. Moreover, the distribution of AOA communities showed a distinct salinity differentiation. Overall, this study improves the understanding of the dynamic shifts in ammonia-oxidizing microorganisms in the Yangtze Estuary.

氨氧化过程作为硝化反应的第一步和限速步骤，在氮素生物地球化学循环中起到非常重要的作用。然而，氨氧化群落动态对河口盐度梯度的响应机制尚不清楚。本研究探究了长江口典型盐度断面硝化细菌（AOB）与古菌（AOA）的多样性、丰度、菌群结构以及硝化速率的变化特征。系统发育分析结果表明，AOB和AOA的优势菌群分别为 *Nitrosospira* 和 *Nitrosopumilus*。沉积物中AOB *amoA* 基因丰度 (4.67×10^5 - 3.90×10^7 copies g^{-1}) 高于AOA *amoA* 基因 (5.14×10^4 - 8.88×10^6 copies g^{-1})。研究区内硝化速率介于0.13-0.63 $\mu\text{g N g}^{-1} \text{d}^{-1}$ 之间，且仅与AOA *amoA* 基因丰度显著相关。在所有监测的环境因子中，盐度对AOA *amoA* 基因丰度、硝化速率以及氨氧化微生物菌群组成均具有显著的影响。菌群结构空间差异聚类分析，发现AOA *amoA* 基因克隆文库在低、中、高盐度区均呈现出明显的差异；而来自中盐度和高盐度区沉积物的AOB菌群与低盐度区也有明显的差异。本研究为进一步认识河口氨氧化过程的微生物驱动机制提供了新的见解。

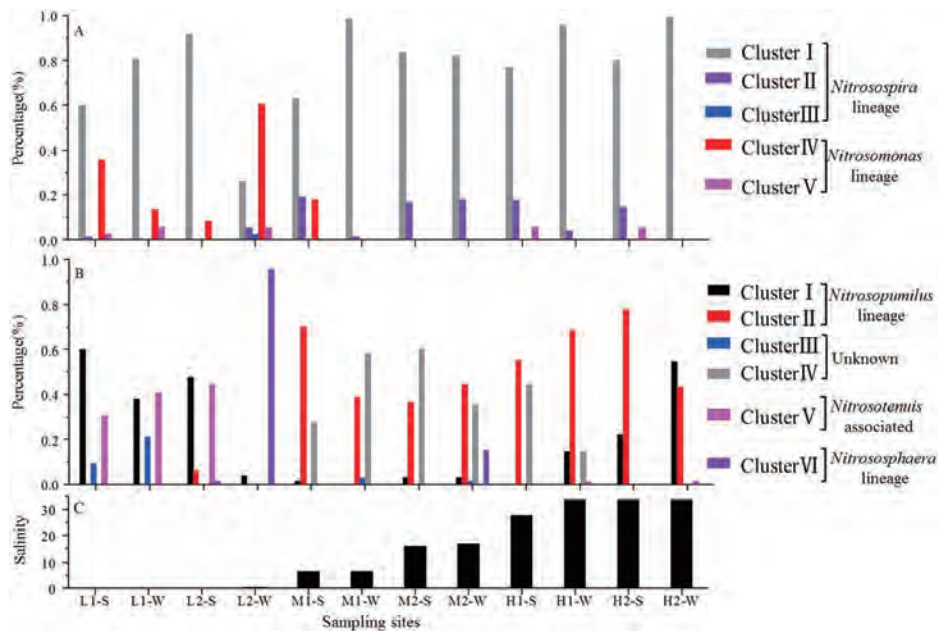


Fig. 4. The composition of (a) ammonia-oxidizing bacteria and (b) ammonia-oxidizing archaea communities along the (c) salinity gradient of the Yangtze Estuary. L, M, and H represent low, middle, and high salinity, respectively. S and W represent summer and winter samples, respectively.

Nitrogen fixation in the intertidal sediments of the Yangtze Estuary: Occurrence and environmental implications

Hou L, Wang R, Yin G, et al. *Journal of Geophysical Research: Biogeosciences*, 2018, 123(3):936-944.

Nitrogen fixation is a microbial-mediated process converting atmospheric dinitrogen gas to biologically available ammonia or other molecules, and it plays an important role in regulating nitrogen budgets in coastal marine ecosystems. In this study, nitrogen fixation in the intertidal sediments of the Yangtze Estuary was investigated using nitrogen isotope tracing technique. The abundance of nitrogen fixation functional gene (*nifH*) was also quantified. The measured rates of sediment nitrogen fixation ranged from 0.37 to 7.91 nmol N g⁻¹ hr⁻¹, while the abundance of *nifH* gene varied from 2.28 × 10⁶ to 1.28 × 10⁸ copies g⁻¹ in the study area. The benthic nitrogen fixation was correlated closely to the abundance of *nifH* gene and was affected significantly by salinity, pH, and availability of sediment organic carbon and ammonium. It is estimated that sediment nitrogen fixation contributed approximately 9.3% of the total terrigenous inorganic nitrogen transported annually into the Yangtze estuarine and coastal environment. This result implies that the occurrence of benthic nitrogen fixation acts as an important internal source of reactive nitrogen and to some extent exacerbates nitrogen pollution in this aquatic ecosystem.

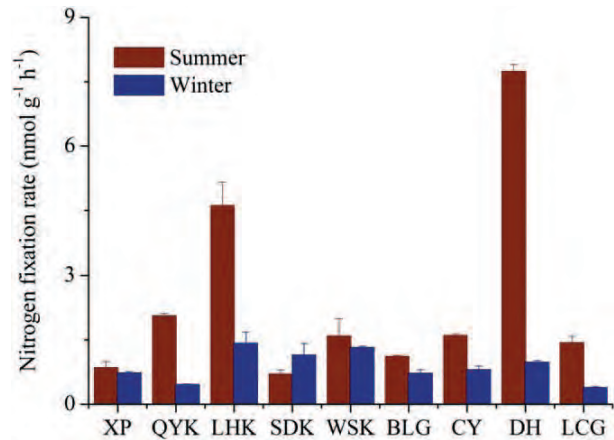


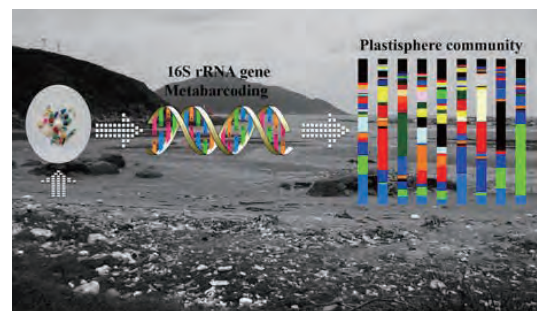
Figure 2. Nitrogen fixation rates in the intertidal sediments of the Yangtze Estuary. The vertical bar denotes standard deviation of triplicate samples.

微生物固氮过程可把大气中的惰性氮转化为生物可利用性氮，在调控河口、近海氮的收支平衡扮演重要功能。本研究利用氮同位素示踪技术，分析了长江口潮滩湿地固氮过程速率及其环境调控因素。研究表明，沉积物固氮速率在0.37-7.91 nmol N g⁻¹ hr⁻¹之间；固氮速率与固氮功能微生物菌群丰度呈显著正相关关系，并且受盐度、酸碱度、沉积物有机质和氨氮等环境因子的调控。此外，估算结果显示长江口沉积物年固氮量约占河流无机氮输入通量的9.3%，反映底栖沉积物固氮是一个重要的活性氮来源，可进一步加剧河口海岸生态系统的氮污染。

Microplastic-associated bacterial assemblages in the intertidal zone of the Yangtze Estuary

Jiang P, Zhao S, Zhu L, et al. *Science of The Total Environment*, 2018, 624:48-54.

Plastic trash is common in oceans. Terrestrial and marine ecosystem interactions occur in the intertidal zone where accumulation of plastic frequently occurs. However, knowledge of the plastic-associated microbial community (the plastisphere) in the intertidal zone is scanty. We used high-throughput sequencing to profile the bacterial communities attached to microplastic samples from intertidal locations around the Yangtze estuary in China. The structure and composition of plastisphere communities varied significantly among the locations. We found the taxonomic composition on microplastic samples was related to their sedimentary and aquatic origins. Correlation network analysis was used to identify keystone bacterial genera (e.g. Rhodobacterales, phingomonadales and Rhizobiales), which represented important microbial associations within the plastisphere community. Other species (i.e. potential pathogens) were considered as hitchhikers in the plastic attached microbial communities. Metabolic pathway analysis suggested adaptations of these bacterial assemblages to the plastic surface-colonization lifestyle. These adaptations included reduced “cell motility” and greater “xenobiotics biodegradation and metabolism.” The findings illustrate the diverse microbial assemblages that occur on microplastic and increase our understanding of plastisphere ecology.



Spatial and vertical distribution of radiocesium in seawater of the East China Sea

Zhao L, Liu D, Wang J, et al. *Marine Pollution Bulletin*, 2018, 128:361-368.

The ^{137}Cs activity in surface water of the East China Sea (ECS) was $0.66\text{--}1.36\text{ Bq m}^{-3}$ during May of 2011. The low activities were observed in the Changjiang Estuary and Zhejiang-Fujian coast and high activities were observed in the south offshore and Kuroshio Current pathway, suggesting that the influence from the current system in the ECS. The ^{134}Cs were undetectable ($< 0.03\text{ Bq m}^{-3}$) and the contribution of the Fukushima accident to ECS is estimated to be below 3%; hence it is negligible during the investigation period. Using the vertical profiles of ^{137}Cs in the ECS, the mass balance is obtained, which suggests that the oceanic input dominates the ^{137}Cs source in the ECS. ^{137}Cs is potentially useful to trace water mass movement in the ECS. Our study provides comprehensive baseline of ^{137}Cs in the ECS for evaluation of the possible influence of the nuclear power plants in the future.

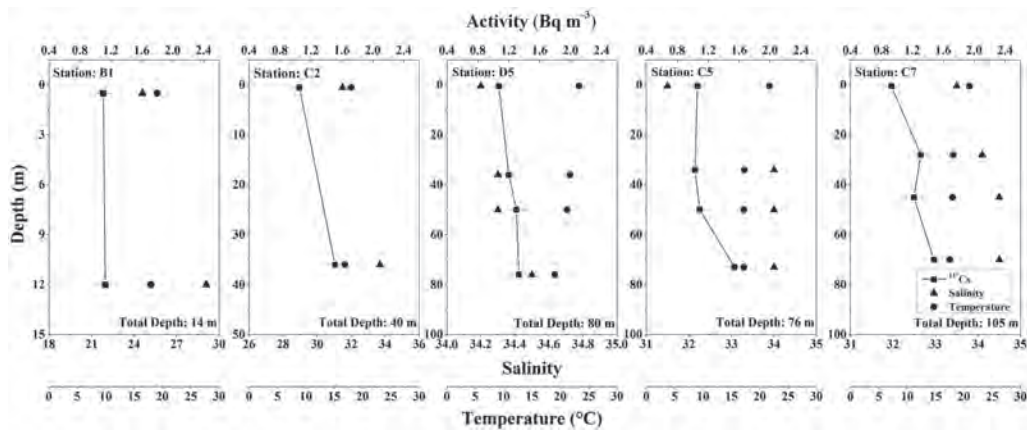


Fig. 4. Vertical profiles of ^{137}Cs activity (squares) at shallow column, temperature (circles) and salinity (triangles) at five typical stations in the ECS.

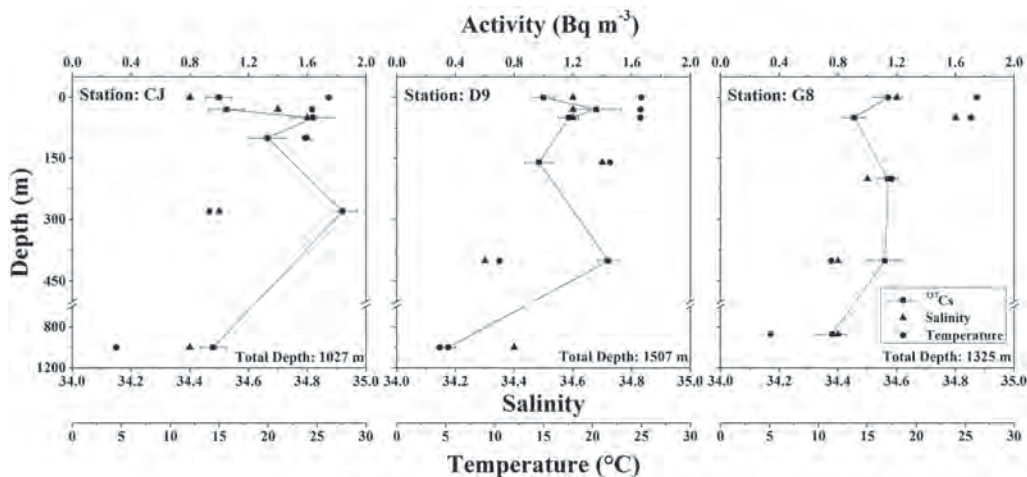


Fig. 5. Vertical profiles of ^{137}Cs activity (squares) at deep water column, temperature (circles) and salinity (triangles) at three typical stations in the ECS.

Bacterial community structure in response to environmental impacts in the intertidal sediments along the Yangtze Estuary, China

Guo X, Lu D, Niu Z, et al. *Marine Pollution Bulletin*, 2018, 126:141-149.

This study was designed to investigate the characteristics of bacterial communities in intertidal sediments along the Yangtze Estuary and their responses to environmental factors. The results showed that bacterial abundance was significantly correlated with salinity, SO_4^{2-} and total organic carbon, while bacterial diversity was significantly correlated with SO_4^{2-} and total nitrogen. At different taxonomic levels, both the dominant taxa and their abundances varied among the eight samples, with Proteobacteria being the most dominant phylum in general. Cluster analysis revealed that the bacterial community structure was influenced by river runoff and sewerage discharge. Moreover, SO_4^{2-} , salinity and total phosphorus were the vital environmental factors that influenced the bacterial community structure. Quantitative PCR and sequencing of sulphate-reducing bacteria indicated that the sulphate reduction process occurs frequently in intertidal sediments. These findings are important to understand the microbial ecology and biogeochemical cycles in estuarine environments.

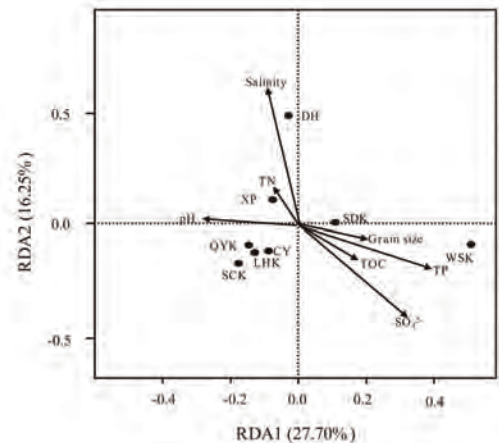


Fig. 5. Redundancy discriminant analysis (RDA) biplot of the distribution of bacterial communities with environmental factors along the Yangtze Estuary.

Distinguishing Cyanobacterial Bloom From Floating Leaf Vegetation in Lake Taihu Based on Medium-Resolution Imaging Spectrometer (MERIS) Data

Zhu Q, Li J, Zhang F, et al. *IEEE Journal of Selected Topics in Applied Earth Observations and Remote Sensing*, 2018, 11(1):34-44.

Based on field measurements of water surface reflectance spectra in Lake Taihu, we construct a model for distinguishing between cyanobacterial bloom and floating leaf vegetation by combining a chlorophyll spectral index with a baseline of phycocyanin. In situ R_{rs} measurements validation results show that this model performs well in distinguishing cyanobacterial bloom from floating leaf vegetation in Lake Taihu. We apply this model to 52 remote sensing images from the Medium-Resolution Imaging Spectrometer (MERIS) from 2003 to 2011. Using two different accuracy evaluation methods, we find an average recognition accuracy of more than 80% for cyanobacterial bloom and floating leaf vegetation when using optimal index thresholds. Using an average index threshold to extract cyanobacterial bloom and floating leaf vegetation from the images, the relative accuracies are 78.8% and 74.6%, respectively. If more efficiency is desired, these average thresholds can be used, which is convenient for batch processing and automated extraction of cyanobacterial bloom and floating leaf vegetation from remote sensing data. The overall distribution of cyanobacterial bloom and floating leaf vegetation in Lake Taihu from 2003 to 2011 is determined by overlapping the distribution maps from individual images, and the results of our analysis are consistent with previously published results. In addition, our analysis shows that this model is immune to perturbations from thin clouds and aerosols.

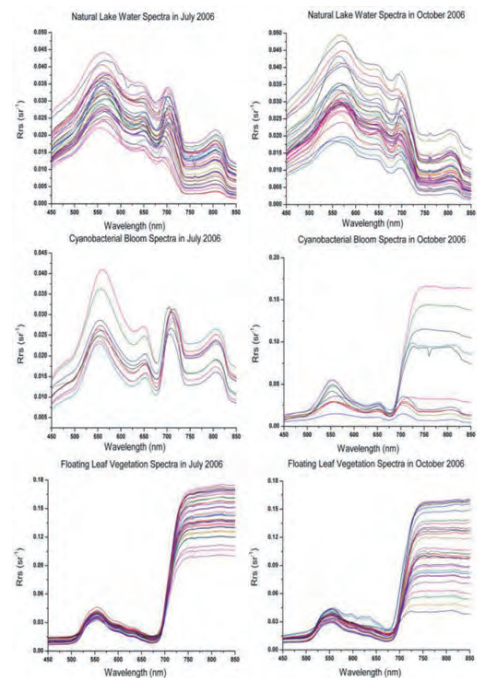


Fig. 2. Remote sensing reflectance spectra of natural lake water, cyanobacterial bloom and floating leaf vegetation in Lake Taihu in July 2006 (left side of picture) and October 2006 (right side of picture).

The effects of flue gas desulfurization gypsum (FGD gypsum) on P fractions in a coastal plain soil

He K, Li X, Dong L. *Journal of Soils and Sediments*, 2018, 18(3):804-815.

Purpose In order to explore the possibility of using FGD gypsum in controlling P loss due to agricultural runoff, the effects of FGD gypsum on the P fraction were studied in the Yangtze River Delta coastal plains. The field experiments were conducted to identify (1) different application rates of FGD Gypsum to the P losses and (2) formation of Ca-P complexes in the soil in response to FGD gypsum applications.

Materials and methods The field experiments consisted four rates of FGD gypsum (0, 15, 30, and 45 t/ha) in triplicate. FGD gypsum was obtained from a coal burning power plant. The B“S” multi-point sampling method was used to collect samples of the uppermost soil interval in July and December of 2015. The total phosphorus (TP) in soil and plants was determined using the sulfuric acid-perchloric acid digestion method. The available phosphorus (AP) was determined using the sodium bicarbonate extraction-molybdenum-antimony anti-spectrophotometric method. The soluble reactive phosphorus (SRP) in the soil leachate was determined using the molybdenum-antimony anti-spectrophotometric method. The Visual MINTEQ 3.0 model was used to simulate the forms and distribution of the P fractions in the soil solution.

Results and discussion The results indicated that the soil P fractions changed with application rates of FGD gypsum while the total soil P showed no significant change. The concentrations of SRP in the leachate also decreased in average of 27.5, 41.9, and 54.5%, respectively, with increasing FGD gypsum rates. The amounts of Ca₂-P, Ca₈-P, and Ca₁₀-P of the calcium phosphates in the soil were significantly increased over the ranges of 44.3–68.6, 34.1–70.1, and 7.4–17.2%, while soil AP concentrations decreased. Visual MINTEQ modeling confirmed the speciation and fractionation of Ca-P compounds under the coastal plain soil conditions. The field experiments also showed that FGD gypsum applications did not affect the absorption of P by the vegetation.

Conclusions Experiments indicated that FGD gypsum has been shown to react with P in soil, resulting in decrease of AP and SRP and formation of insoluble Ca-P compounds and thereby decreasing the potential of P losses with surface runoff. FGD gypsum appears to be a more viable soil amendment than commercially mined gypsum to potentially achieve reductions in P losses and eutrophication of receiving waters.

Effects of sediment disturbance regimes on *Spartina* seedling establishment: Implications for salt marsh creation and restoration

Cao H, Zhu Z, Balke T, et al. *Limnology & Oceanography*, 2018, 63(2):647-659.

Seedling establishment is an important process relevant for the restoration of salt marsh within the framework of sustainable coastal defense schemes. Recent studies have increasingly highlighted how the short-term (i.e., the day-to-day) sediment dynamics can form major bottlenecks for seedling establishment. Until recently, studies on quantifying the threshold values of such short-term sediment dynamics for marsh seedlings remain rare. As accretion/erosion trends and dynamics may differ greatly under global change, we study the effects of short-term sediment disturbance-regimes on seedling establishment of two globally distributed foundation species: *Spartina alterniflora* and *Spartina anglica*. Seedlings with different disturbance-free periods were exposed to a set of different accretion/erosion-regimes in the laboratory. Seedling survival appeared to be much more sensitive to erosion than accretion, seedlings with short disturbance-free periods were more sensitive than seedlings with longer ones, and *S. alterniflora* was more sensitive than *S. anglica*. Seedlings were less sensitive to gradual changes in sediment height (accretion/erosion) than to abrupt changes where time for morphological adjustment is lacking. Critical erosion depth (the maximum erosion that seedlings are able to withstand) was shown to mainly depend on sedimentation history. Our results confirm that the establishment of *Spartina* seedlings requires a flooding disturbance-free “window of opportunity” and that sediment disturbances affect their survival both directly and via morphological adjustment. These results provide fundamental insights into seedling establishment that can be used for designing engineering measures to create suitable conditions and enable marsh creation/restoration for nature goals or as part of coastal defense schemes under global change.

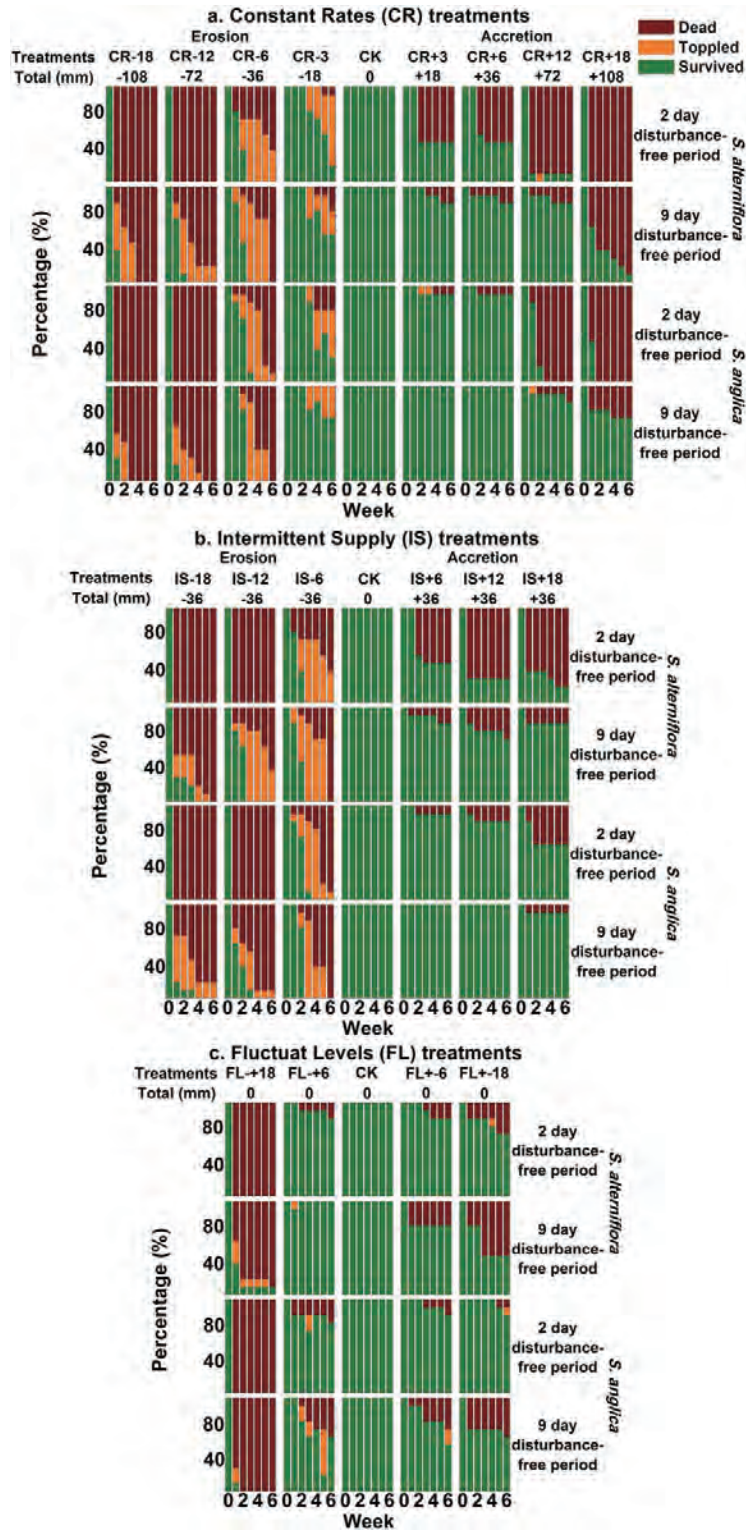
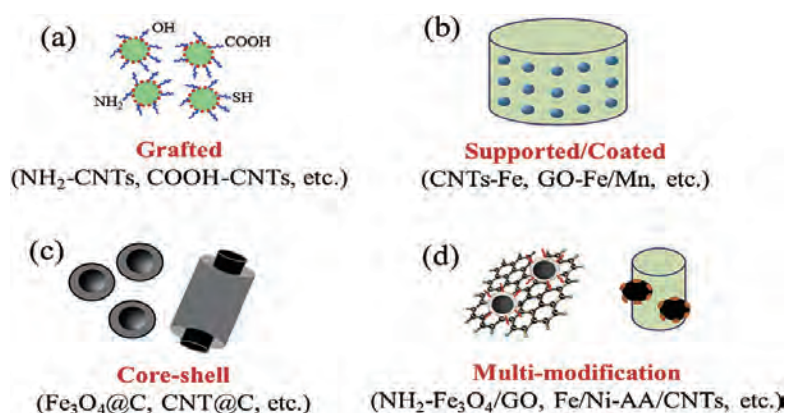


Fig. 3. Percentage of surviving, toppled and dead seedlings during the mesocosm experiments. (a) CR treatment groups, (b) IS treatment groups, and (c) FL treatment groups.

A review of functionalized carbon nanotubes and graphene for heavy metal adsorption from water: Preparation, application, and mechanism

Xu J, Cao Z, Zhang Y, et al. *Chemosphere*, 2018, 195:351-364.

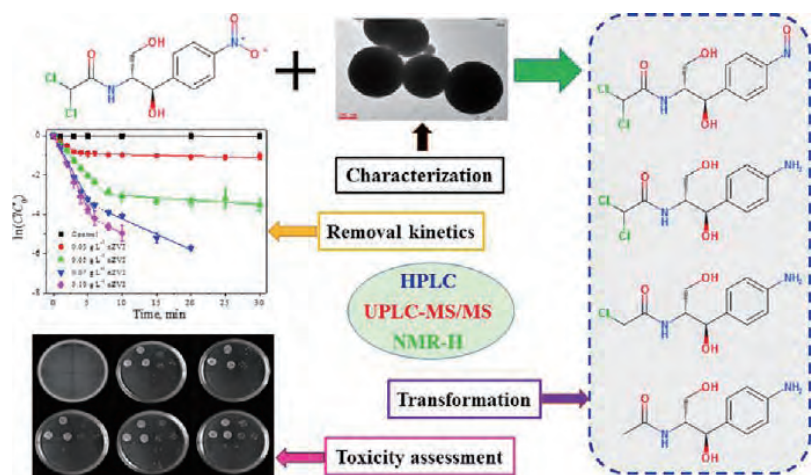
Carbon-based nanomaterials, especially carbon nanotubes and graphene, have drawn wide attention in recent years as novel materials for environmental applications. Notably, the functionalized derivatives of carbon nanotubes and graphene with high surface area and adsorption sites are proposed to remove heavy metals via adsorption, addressing the pressing pollution of heavy metal. This critical review assesses the recent development of various functionalized carbon nanotubes and graphene that are used to remove heavy metals from contaminated water, including the preparation and characterization methods of functionalized carbon nanotubes and graphene, their applications for heavy metal adsorption, effects of water chemistry on the adsorption capacity, and decontamination mechanism. Future research directions have also been proposed with the goal of further improving their adsorption performance, the feasibility of industrial applications, and better simulating adsorption mechanisms.



Insight into the kinetics and mechanism of removal of aqueous chlorinated nitroaromatic antibiotic chloramphenicol by nanoscale zero-valent iron

Liu X, Cao Z, Yuan Z, et al. *Chemical Engineering Journal*, 2018, 334:508-518.

Nanoscale zero-valent iron (nZVI) is very efficient in removing chlorinated nitroaromatic antibiotic chloramphenicol (CAP) from different waters including DI water, surface water, groundwater, and seawater. The corrosion of nZVI and product distribution after reaction in these water matrices were also investigated. Based on the identification of four main reduction products via HPLC, UPLC-MS/MS, and NMR-H spectrums, a more detailed pathway of CAP degradation by nZVI was proposed than ever reported. The two O atoms on the NO₂ group were successively



reduced first, and then two Cl atoms were removed via dechlorination. The process of CAP removal could be divided into two stages according to the pseudo-first-order kinetic model. A total of 97.0% of 0.30 mM CAP was rapidly removed by 1.8 mM nZVI in the first stage (6 min) with a surface-area-normalized reaction rate of 1.13 L min⁻¹ m⁻². Notably, after reaction with nZVI, the antibacterial activity of the CAP solution was greatly reduced. This study demonstrates that nZVI is a promising alternative to remediate CAP-contaminated water to reduce the antibiotic selection pressure of the environment.

Field-Based Evidence for Microplastic in Marine Aggregates and Mussels: Implications for Trophic Transfer

Zhao S, Ward J E, Danley M, et al. *Environmental Science & Technology*, 2018, 52(19):11038-11048.

Marine aggregates incorporate particles from the environment, including microplastic (MP). The characteristics of MP in aggregates and the role of aggregates in linking MP with marine organisms, however, are poorly understood. To address these issues, we collected aggregates and blue mussels, *Mytilus edulis*, at Avery Point, CT, and analyzed samples with microspectrometers. Results indicate that over 70% of aggregates sampled harbored MP (1290 ± 1510 particles/ m^3). Fifteen polymer types were identified, with polypropylene, polyester and synthetic-cellulose accounting for 44.7%, 21.2% and 10.6%, respectively, of the total MP count. Over 90% of MP in aggregates were $\leq 1000 \mu m$, suggesting that aggregations are a sink for this size fraction. Although size, shape, and chemical type of MP captured by mussels were representative of those found in aggregates, differences in the sizes of MP in pseudofeces, feces and digestive gland/gut were found, suggesting size-dependent particle ingestion. Over 40% of the MP particles were either rejected in pseudofeces or egested in feces. Our results are the first to identify a connection between field-collected marine aggregates and bivalves, and indicate that aggregates may play an important role in removing MP from the ocean surface and facilitating their transfer to marine food webs.

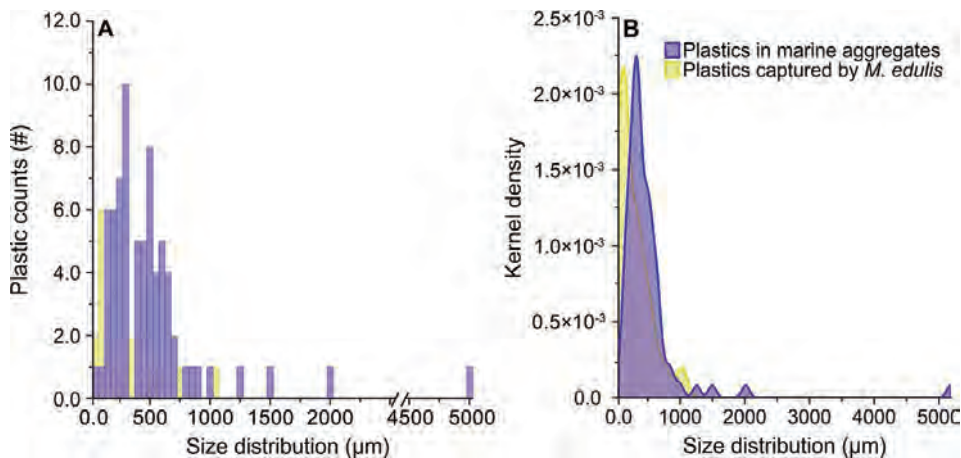


Figure 4. Distribution of plastic counts versus size (A) and its kernel-density estimation (B) for MP in samples of marine aggregates and *M. edulis*.

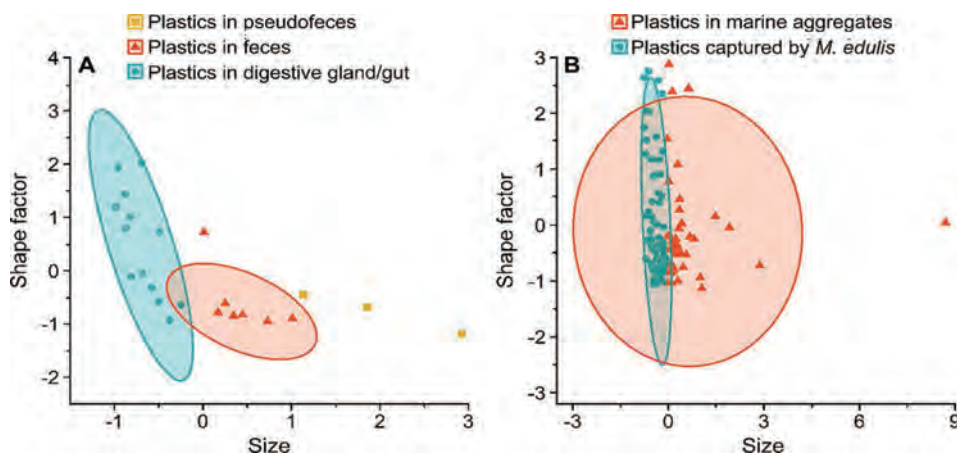


Figure 5. Clustering using a k-medoids algorithms depicting the relationships of MP, based on size and shape factors, in (A) pseudofeces, feces and digestive-gland/gut samples of *M. edulis*; and (B) marine aggregates and *M. edulis* samples.

Dissolved Lead in the East China Sea with Implications for Impacts of Marg Seas on the Open Ocean Through Cross-Shelf Exchange

Jiang S, Zhang J, Zhang R, et al. *Journal of Geophysical Research Oceans*, 2018, 123(8):6004-6018.

The distribution of lead (Pb) in the ocean is influenced by human activities. During a cruise in the East China Sea (ECS) in August 2013, we investigated six representative stations and gave the first systematic description of dissolved lead (DPb) distributions after the phasing out of leaded gasoline in China. The DPb concentration in the ECS ranged from 23.8 to 96.7 pmol/kg, with the highest concentrations observed at the surface of the middle shelf, while the lowest concentrations were determined to be in deep samples collected at the shelf break. Vertical profiles of DPb vary with geographic locations, seawater turbidity, hypoxic conditions, atmospheric deposition, and hydrographic regimes. As one of the most important western boundary currents, Kuroshio receives an additional 10–20 pmol/kg of DPb from the ECS shelf through a cross-shelf exchange process, and approximately $(1.1\text{--}1.7) \times 10^9$ g/yr of DPb was exported through the shelf break area, which will directly join the North Pacific circulation based on a preliminary box model. In addition, the ECS shelf exported another 1.4×10^9 g/yr of DPb from the Tsushima/Korea Strait, which has the potential to influence the northwestern Pacific Ocean as well as the Sea of Japan/East Sea. A residence time of 2–3 months for DPb in the ECS was inferred.

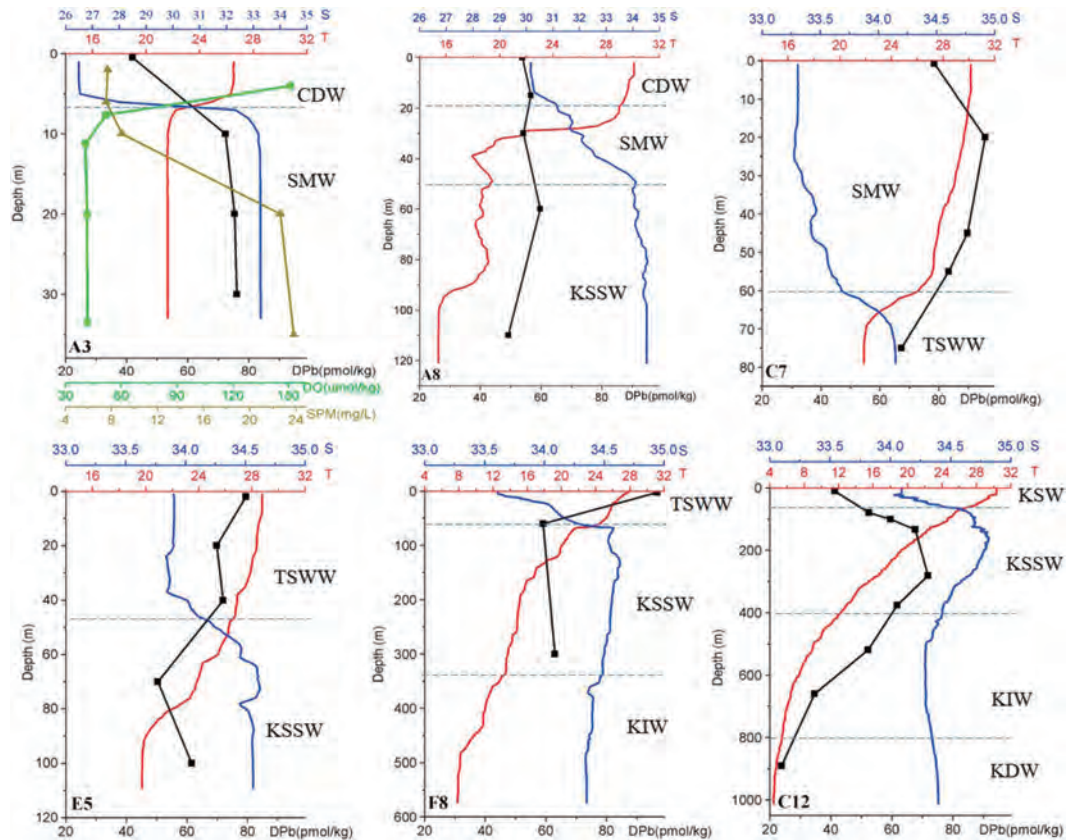


Figure 4. Vertical profiles of salinity, temperature and DPb concentration of individual stations; dissolved oxygen, and suspended particulate matter were collected only for Station A3.

交流与合作

Academic Communications & Cooperations

实验室积极开展国际交流与合作，目前承担了政府间国际科技创新合作重点专项项目“水环境的高光谱及多源高分辨率光学遥感研究”、“应对转型中的河口三角洲”、“中美大河三角洲侵蚀灾害与应对策略比较研究”；国家自然科学基金-重点国际（地区）合作研究项目“高浊度河口航道回淤及滩槽系统响应研究”、“早-中全新世长江与尼罗河三角洲环境演变异同及早期农业文明对比研究”及“长江河口最大浑浊带的动力沉积过程对大型工程的自适应机理研究”等国际合作项目7项。

SKLEC is actively involved in international communications and cooperation. SKLEC is currently in charge of 7 international cooperation projects, including the intergovernmental international scientific and technological innovation cooperation special program “Hyperspectral and multi-mission high resolution optical remote sensing of aquatic environments” “Coping with deltas in transition” “Comparative study on erosion hazards and coping strategies in river deltas between China and America” and NSFC international (regional) cooperation and communication program: “Navigation to a resilient estuary – morphological interactions between navigation channel and estuary”, “A comparative study between the Yangtze and Nile delta: the similarity and discrepancy of the early-middle Holocene environmental evolution and early agricultural civilization” and “Natural versus anthropogenically driven behavior of hydrodynamics and sediment dynamics in estuarine delta networks, application to the Yangtze Estuary Delta” and so on.

2018年实验室接待国内外学者、专家来室合作研究与学术交流160多人次。85人次参加国际学术会议并进行学术交流，其中邀请报告（含大会报告）17次。主/承办11次国际会议及1次国内学术研讨会。2018年实验室共举办学术报告40多场次。

More than 160 scholars visited SKLEC in 2018. SKLEC researchers attended international conferences for 85 person-times, including 17 plenary lectures and invited talks. In 2018, SKLEC hosted 11 international conferences and 1 national conference. More than 40 lectures were given in SKLEC in total.

在研国际合作项目进展

Progress of International Cooperation Projects

国家自然科学基金委员会与荷兰科学研究组织、英国研究理事会合作研究项目：长江河口最大浑浊带的动力沉积过程对大型工程的自适应机理研究(2017.06-2021.12)

Trilateral Cooperation Project of NSFC, Netherlands Organization for Scientific Research (NWO), and Research Councils UK (RCUK): Natural versus anthropogenically driven behavior of hydrodynamics and sediment dynamics in estuarine delta networks, application to the Yangtze Estuary Delta (2017.06-2021.12)

由我室牵头的国家自然科学基金委(NSFC)、荷兰科学研究组织(NWO)及英国研究理事会(RCUK)合作研究项目“长江河口最大浑浊带的动力沉积过程对大型工程的自适应机理”，本年度组织了4次现场多个定点水文泥沙和纵横断面水文泥沙、溶解氧、叶绿素、水下微地貌等的走航测量，采集多个水样和底质样品，收集社会经济数据。参与4次国家自然科学基金项目共享航次ADCP和CTD数据。分析发现在气候变暖、海平面上升和流域及河口工程建设持续影响下，长江河口从最大浑浊带直至潮区界潮动力增强；近期长江河口最大浑浊带河道含沙量受其流域来沙锐减和河口工程影响并不明显；基于Delft3D建立了长江口平面二维和垂向分层的三维水沙数值模型，其应用k- ϵ 模型考虑紊流、谢才公式计算底部摩擦，探讨了密度层化和悬浮泥沙对紊动场的抑制效应及其模化方法；发明一种宽量程和动态最佳分辨率测量含沙量的实现方法和装置；完成水动力垂直二维解析模型的求解，采用新的线性化方法将涡粘性系数以及底部滑移系数线性化，并通过模型解计算每条河道的涡粘性系数与底部滑移系数；提出基于二维解析模型的最大浑浊带泥沙捕集物理机制和寒潮期间强风对长江口北支盐水入侵的影响，以及应对海平面上升的上海地区洪水保险政策。已发表标注论文4篇(第一标注)，出版专著1部；已完成投稿论文10篇；申请发明专利2项、实用新型专

利2项、软件著作权2项。一次国际学术大会报告，一次国际会议邀请报告。

This is a trilateral cooperation project of NSFC, Netherlands Organization for Scientific Research (NWO), and Research Councils UK (RCUK), which is hosted by East China Normal University. It focus on the natural versus anthropogenically driven behavior of hydrodynamics and sediment dynamics in the Yangtze estuary. In 2018, historical data collections and four cruises of field measurements of water level, society and economics, suspended sediment concentration (SSC) and bed sediments, dissolved oxygen, chlorophyll, bathymetry were made. Four more shared NSFC cruises were involved in for the data collection of ADCP and CTD. The data analysis results show an intensifying tidal dynamics along the main channels from the estuarine turbidity maxima (ETM) to the tidal limit while a minor fluctuation of SSC within the ETM with the combined impacts of the climate warming induced sea level rise and human interventions in the river basin and estuary. A two-dimensional and vertical stratified three-dimensional numerical model of hydrodynamics and sediment dynamics in the Yangtze estuary established using Delft3D. The bottom friction is calculated by k- ϵ model considering turbulence and Chezy coefficient. The depression effect of density stratification and suspended sediment on turbulent field and its modelling method discussed. A new method and device for measuring SSC with wide range and dynamic optimal resolution invented. The solution of vertical two-dimensional analytical model of hydrodynamics completed using a new linearization method to linearize the eddy viscosity coefficient and bottom slip coefficient. The eddy viscosity coefficient and bottom slip coefficient of each individual channel in the Yangtze estuary calculated by the model solution. The physical mechanism of sediment entrapment in ETM based on two-dimensional analytical model, the effect of strong wind on saltwater intrusion in the Northern Branch of the Yangtze estuary during cold wave, and flood insurance policy to cope with the sea level rise in Shanghai proposed. Four annotated papers and one book have been published (the first annotation) and ten manuscripts have been submitted. Two patents of invention and two software copyrights applied.

学术会议 Workshop & Conference

第二届海洋微塑料污染与控制国际学术研讨会

The Second International Symposium on Marine Microplastic Pollution and Control

4月24日，由我校河口海岸学国家重点实验室、海洋塑料研究中心主办，联合国教科文组织政府间海洋学委员会西太分委会和国家海洋局协办的“第二届海洋微塑料污染与控制国际学术研讨会”在校开幕。二十余名国内外知名专家学者在为期三天的研讨会中带来了精彩的学术报告，并和与会专家一起围绕海洋微塑料在海洋中的来源和归趋、海洋微塑料运输数值模型、海洋微塑料与化学污染物的相互作用、微塑料对海洋生物的生态效应、公民科学家参与解决海洋垃圾问题及海洋微塑料防治措施等议题进行探讨交流。

The 2nd symposium is organized by the State Key Laboratory of Estuarine and Coastal Research and the Plastic Marine Debris Research Center (PMDRC), East China Normal University, co-

organized by Intergovernmental Oceanographic Commission Sub-Commission for the Western Pacific, and the State Oceanic Administration of China. More than 70 famous experts and scientists from 7 different countries joined the symposium. They discussed four key topics of microplastic research: 1) Occurrence and fate of microplastics in the marine environment; 2) Microplastics interacting with biological and chemical contaminants; 3) Influences of microplastics on the marine biota; 4) Citizens science and possible solutions/remediation measure for marine microplastics.



2018年华东师范大学海外青年科学家论坛—海洋科学分论坛

2018 International Forum for Outstanding Oversea Young Scholars in marine science



4月28日，华东师范大学2018年海外青年科学家论坛——海洋科学分论坛在我校中山北路校区办公楼小礼堂召开。来自美国、英国、加拿大、澳大利亚、新加坡的10名海外青年学者参加论坛。此次论坛所涉及学科领域广泛，主要包括：河口海岸沉积动力学与海岸工程、河口水文过程演变、滨海湿地碳循环、海岸生物地球化学、极地生态系统演变、全新世海平面变化等。会上，青年学者详细介绍了学术经历、研究领域、最新科研进展以及未来发展计划。与会专家就科学研究与成果应用、科学研究与国家战略的结合、科学研究与团队合作等问题与青年学者进行了详细交流，并给青年学者提出了一些积极建议。

The 2018 International Forum for Outstanding Oversea Young Scholars in marine science was

held on 28, April in ECNU. 10 oversea young scholars joined this forum and gave talks on physical oceanography, oceanographically remote sensing, marine ecosystem, marine geology and ocean chemistry. This forum provided a platform to enhance the exchange between SKLEC and oversea young scholars.

国家重点研发计划政府间国际科技创新合作重点专项“应对转型中的河口三角洲”项目启动会

Kick off meeting of the Joint Research Project between China and the Netherlands 'Coping with Deltas in Transition' was held in ECNU

2018年5月15-16日，国家重点研发计划政府间国际科技创新合作重点专项“应对转型中的河口三角洲”项目启动会及学术研讨会在华东师范大学举行。该项目是由中国科技部(MOST)和荷兰皇家科学院(KNAW)联合发起的政府间科技合作项目，意在确立中国与荷兰长期的科学战略合作关系。中荷双方就项目的实施工作进行了研讨和交流，项目组围绕项目建议书中的四个主要子课题开展了主题演讲和讨论，并就项目工作重点、研究任务分工、合作交流方式等进行了磋商。



The kick-off meeting of the joint research project 'Coping with Deltas in Transition', which is the Intergovernmental cooperation on science and technology innovation of the National Key Research and Development Program, was held at East China Normal University during May 15-16, 2018. This project is supported by the Programme Strategic Scientific Alliances (PSA) between China and the Netherlands and funded by MOST and KNAW, with the vision of establishing a new framework of long-term scientific cooperation with mutual benefit to the Netherlands and China. The Chinese and Dutch colleagues had fruitful discussion on the project during the kick-off meeting. Major outputs of the meeting include clarification of future research and collaborative subjects, exchange of students and scholars, and ideas of joint field work.

“海洋生物地球化学与西太平洋生物圈可持续化发展”国际研讨会

The 8th China-Japan-Korea IMBeR Symposium and Training Course

9月17-19日，“海洋生物地球化学与西太平洋生物圈可持续发展”国际研讨会议暨第八届中-日-韩“海洋生物圈整合研究”研讨会在我校图书馆报告厅举行。会议由我校河口海岸学国家重点实验室、中国海洋生态系统研究计划（China GLOBEC-IMBeR）和IMBeR区域项目办公室联合主办。来自日本、韩国、泰国、印度、巴基斯坦、斯里兰卡、马来西亚、加拿大和中国等国家和地区的近30家海洋科研机构及大学的100余名代表参会，大会围绕主题集中探讨了气候变化和人类活动影响下西太平洋地区生态系统所承载的压力及其可持续化发展问题。



The 8th China-Japan-Korea IMBeR Symposium and Training Course (IMBeR CJK 2018) was held from September 17 to 19 in 2018 at the East China Normal University (ECNU) in Shanghai, China, with the focus on Marine Biogeochemical Sciences for the Sustainability of the West Pacific Biosphere. The State Key Laboratory of Estuarine and Coastal Research (SKLEC) & ECNU, China GLOBEC-IMBeR project and IMBeR Regional Project Office co-hosted the event. IMBeR CJK 2018 attracted over 100 delegates including scientists, young researchers and students from almost 30 marine scientific research institutions and universities, which were from China, Japan, Korea, Thailand, India, Pakistan, Sri Lanka, Malaysia and Canada.

大河三角洲国际研讨会在上海召开 International Symposium for Mega Deltas

大河三角洲国际研讨会于2018年10月15-16日在上海召开。会议主办方为华东师范大学河口海岸学国家重点实验室。会议邀请了来自11个国家从事大河三角洲研究的20余位顶级科学家。各国专家分别汇报全球13个大河三角洲概况和最新研究成果。与会专家从海洋视角探讨了大河三角洲面临问题的根源，以及多学科、多方位的综合解决方案。



International symposium for mega deltas organized by SKLEC was held in Shanghai during October 15 to 16 in 2018. More than 20 mega deltas scientists were invited to the symposium. They presented their latest research progress and discussed 1) Solutions to the various problems identified ; 2) Management strategies for sustainable support to economic and social development; 3) Formulate a SCOR Working Group application draft to continue the research in the near future.

第二届西太地区海洋微塑料学术研讨会在校举行 WESTAPC 2ND Microplastic Workshop

10月15-17日，由联合国教科文组织政府间海洋学委员会西太分委会主办，河口海岸学国家重点实验室、海洋塑料研究中心承办的“第二届西太地区海洋微塑料学术研讨会”在校召开。来自日本、韩国、泰国、中国、印度尼西亚等亚太九个国家的海洋塑料污染问题研究领域的国际知名教授和专家学者等50余人参加本次研讨会。与会专家和学者围绕微塑料相关问题进行探讨和交流。相互交流了西太国家相关研究的最新进展，总结了第一届西太微塑料研讨会以来建立的海滩沉积物中微塑料监测标准化方法指南，汇报了西太各国海滩微塑料监测试点站位的监测结果，对即将开展的海水、海洋生物微塑料监测工作组的方法标准化工作提出了具体要求，并制定了未来亟待开展的相关海洋微塑料研究行动计划。



The 2nd WESTPAC Workshop on Distribution, Source, Fate and Impacts of Marine Microplastics in Asia and the Pacific was held from 15-17 October in Shanghai, China, with great support from State Key Laboratory of Estuarine and Coastal Research, East China Normal University. More than 50 renowned scientists and participants from 9 countries took part in the workshop. The first day was dedicated to a mini symposium focused on 1) Flux, distribution, and fate; 2) Impacts on biota and marine ecosystems and 3) Research and monitoring methods, model development, risk assessment. The following workshop dealt with progress reports on each

country following last year's workshop, finalization of guidelines on sampling and analysis of microplastics in the sediment, water and biota, and related action plans in the following year.

邀请报告

Invited Presentations at International Conferences & Workshops

2018年实验室有85人次参加国际学术会议并进行学术交流，其中邀请报告14次，大会报告3次。

Members of SKLEC attended international conferences for more than 80 person-times, including 14 invited talks and 3 plenary lectures.

WÜnnemann Bernd, International Research Training Programme as a tool for enhanced cooperation-*International Research Training Group TransTIP*, February, Germany

LI Daoji, Progress of Microplastic Marine Debris Research in China-*The Second International Symposium on Marine Microplastics Pollution and Control*, April, China

LI Daoji, Progress of Marine Microplastic Research in China-*The 4th International Conference on Environmental Pollution and Health*, May, China

HOU Lijun, Nitrogen dynamics in estuarine and coastal wetlands-*The 4th International Conference on Environmental Pollution and Health*, May, China

WANG Yaping, Drag reduction caused by suspended sediment in the coast-ocean bottom boundary layer: a case study-*International workshop on Sediment Dynamics*, July, China

LI Daoji, Advance Scientific Knowledge and develop research capacity on microplastics -*Monitoring and Assessment of Plastics and Microplastics in the Coastal and Open Ocean Environment: Regional Expert Consultation*, July, Thailand

CHENG Heqin, Mapping Sea Level Rise Behavior in an Estuarine Delta System: A Case Study along the Shanghai Coast-*World Summit on Climate Change and Global Warming*, June, France

LI Daoji, Progress and Prospect of Marine Microplastic Research in China-*Eco Forum Global Annual Conference Guiyang*, July, China

LI Daoji, Progress and Prospect of Marine Microplastic Research in China-*UK-Chian Plastic Waste Collaboration Forum*, July, China

LI Daoji, Progress and Prospect of Microplastic Marine Debris Research in China-*APEC Workshop on Innovative Marine Debris Solutions*, July, China

TANG Jianwu, Reconciling the relationship between solar induced fluorescence and photosynthesis by upscaling leaf to canopy scales Ecological- *Society of America annual meeting*, August, USA

TANG Jianwu, Carbon dynamics during the restoration process of a salt marsh in Massachusetts- *International Blue Carbon Policy and Scientific Working Group Annual Meeting*, August, China

WANG Yaping, Sediment transport and geomorphology in the southern Yellow Sea: in-situ measurements and modelling-*Mainland-Hong Kong Joint Workshop: Challenges in Sustainable Coastal Observation and Experiments in a Rapidly Changing Environment*, September, China

LI Daoji, Scientific Basis for Supporting Future Government-*"An Ocean of Opportunities"Norway-China Business Summit*, October, China

GAO Shu, Planning and Producing a Special Issue; Examples for Marine Geology - *9th International Conference on Asian Marine Geology (ICAMG-9) Session W04*, October, China

GAO Shu, Why mega deltas matter: A general introduction - *International Symposium for Mega Deltas*, October, China

WANG Yaping, The influence of bio-physical processes on sediment transport over tidal flat-*Sediment Dynamics of Estuaries and Muddy Coasts, November*, China

专家学者来访 Visiting Scholars

2018年实验室接待境外专家、学者来室合作研究与学术交流160多人次。
In 2018, more than 160 scholars visited SKLEC.

List of Visiting Scholars

| 专家 Visiting Scholar | 单位 Affiliation | 备注 Remark |
|-------------------------|---|--|
| Agung Dhamar Syakti | Raja Ali Haji Maritime University, Indonesia | |
| Ahmad Al Karim | Maritime Affairs, Bangladesh | |
| Alaa Salem | Kafrelsheikh University, Egypt | 海外高层次专家 Oveasea High-Level Expert |
| Alfonse Dubi | University of Dar es Salaam, Tanzania | |
| Alison Spodek Keimowitz | Vassar College, USA | |
| Andelka Plenković-Mora | University of Zagreb, Croatia | |
| Andrés Cózar Cabañas | Universidad de Cádiz, Spain | |
| Andrew Rose | South Cross University, Australia | |
| Anil Premaratne | National Aquatic Resources and Research Development Agency, Sri Lanka | |
| Anja Scheffers | South Cross University, Australia | |
| Anthony L. Andrady | North Carolina State University, USA | |
| Atsuhiko Isobe | Kyushu University, Japan | |
| Bas van Maren | Delft University of Technology, the Netherlands | 中荷项目成员 Member of Joint Research Project between China and the Netherlands |
| Baskaran Mark | Wayne State University, USA | |
| Bayden Russell | University of Hongkong | |
| Bert van Bavel | Norwegian Institute for Water Research, Norway | |
| Bram van Prooijen | Delft University of Technology, the Netherlands | 中荷项目成员 Member of Joint Research Project between China and the Netherlands |
| Brian Finlayson | The University of Melbourne, Australia | |
| Bruce Glavovic | Massey University, New Zealand | |
| Carina Lackman | Aachen University, Germany | |
| Chan Joo Jang | Korea Institute of Ocean Science & Technology, South Korea | |

| 专家 Visiting Scholar | 单位 Affiliation | 备注 Remark |
|--------------------------|---|--|
| Chao Chen | Boise State Univ, USA | |
| Charles A. Nittrouer | University of Washington, USA | |
| Christian Joshua Sanders | Southern Cross University, Australia | |
| Christopher Bruce Craft | Indiana University, USA | |
| Corinna Schrum | Helmholtz-Zentrum Geesthacht Center for Materials and Coastal Research, Germany | |
| Corry Yanti Manullang | Center for Deep Sea Research, Indonesia | |
| Daphne van der Wal | Royal Netherlands Institute for Sea Research, the Netherlands | 中荷项目成员 Member of Joint Research Project between China and the Netherlands |
| David J. Esteban | Vassar College, USA | |
| Deeptha Amarathunga | National Aquatic Resources Research & Development Agency, Sri Lanka | |
| Deping Cao | Nanyang Technological University, Singapore | |
| Dirk Jan Walstra | Deltares, the Netherlands | 中荷项目成员 Member of Joint Research Project between China and the Netherlands |
| Donald Forbes | Bedford Institute of Oceanography, Dartmouth, NS, Canada | |
| Quirijn Lodder | Rijkswaterstaat, the Netherlands | 中荷项目成员 Member of Joint Research Project between China and the Netherlands |
| Duong Thanh Nghi | Institute of Marine Environment and Resources, Vietnam | |
| Edward Anthony | Université Aix-Marseille, France | |
| Elizabeth Wastson | Drexel University, USA | |
| Faming Wang | University of Chicago, USA | |
| Geofrey Felix Kalumuna | University of Dar es Salaam, Tanzania | |
| Gi Hoon Hong | Korea Institute of Ocean Science and Technology, South Korea | 海外高层次专家 Overseas High-Level Expert |
| Han Winterwerp | Delft University of Technology, the Netherlands | 中荷项目成员 Member of Joint Research Project between China and the Netherlands |
| Heath Kelsey | University of Maryland, USA | |
| Henner Hollert | Aachen University, Germany | |

| 专家 Visiting Scholar | 单位 Affiliation | 备注 Remark |
|-------------------------|---|--|
| Hideshige Takada | Tokyo University of Agriculture and Technology, Japan | |
| Hiroaki Saito | The University of Tokyo, Japan | |
| Hongxia Xiao | Aachen University, Germany | |
| Huan Feng | Montclair State University, USA | |
| Huib de vriend | Delft University of Technology, the Netherlands | 中荷项目成员 Member of Joint Research Project between China and the Netherlands |
| Huibert Eduard de Sward | Utrecht University, the Netherlands | 海外高端专家 Foreign High-end Experts |
| Ian Thomas | University of Melbourne, Australia | |
| Ian Townend | Southampton University, UK | |
| Irina Chubarenko | Shirshov Institute of Oceanology, Russian Academy of Sciences, Russia | |
| Isaac Santos | Southern Cross University, Australia | |
| J. Evan Ward | University of Connecticut, USA | |
| Jaap Kwadijk | Deltares, the Netherlands | |
| Jackson Isdory | University of Dar es Salaam, Tanzania | |
| James Liu | Sun Yat-sen University, Taiwan (China) | |
| James Morris | University of South Carolina, USA | |
| Jeffrey R. Walker | Vassar College, USA | |
| Jeremy Reiman | Louisiana State University, USA | |
| Jianping Gan | The Hong Kong University of Science and Technology, Hong Kong (China) | |
| Jing Tao | Dalhousie University, Canada | |
| John Claydon | IMBeR International Project Office | |
| John Keesing | The Commonwealth Scientific and Industrial Research Organization, Australia | |
| Josip Tica | University of Zagreb, Croatia | |
| Kam-biu Liu | Louisiana State University, USA | |

| 专家 Visiting Scholar | 单位 Affiliation | 备注 Remark |
|-----------------------------|---|--|
| Karline Soetaert | Royal Netherlands Institute for Sea Research, the Netherlands | 中荷项目成员 Member of Joint Research Project between China and the Netherlands |
| Lynette Ying | National University of Singapore, Singapore | |
| Makino Mitsutaku | National Research Institute of Fisheries Science, Japan | |
| Manousos Valyrakis | University of Glasgow, UK | |
| Marcel Stive | Technische Universiteit Delft, the Netherlands | |
| Mark Baskaran | Wayne State University, USA | |
| Martin Le Tissier | Futureearth Coasts | |
| MaryAnn Cunningham | Vassar College, USA | |
| Masao Ishii | Japan Meteorological Agency, Japan | |
| Md Shahadat Hossain | University of Chittagong, Bangladesh | |
| Merle Sowman | University of Cape Town, South Africa | |
| Method Samwel Semion | University of Dar es Salaam, Tanzania | |
| Milena Zic Fuchs | Croatian Academy of Science and Art, Croatia | |
| Mislav Ježi | Croatian Academy of Science and Art, Croatia | |
| Moritz Muller | Swinburne University of Technology Sarawak Campus, Malaysia | |
| Nachapa Saransuth | UNESCO/IOC Regional Office for the Western Pacific (WESTPAC) | |
| Narumol Kornkanitnan | Department of Marine and Coastal Resources, Thailand | |
| Nicole Khan | Nanyang Technological University, Singapore. | |
| Nils Andersen | Universität Bremen, Germany | |
| Noor Ahmed Kalhor | National Institute of Oceanography, Pakistan | |
| Pan Shunqi | Cardiff University, UK | |
| Patricia Marguerite Glibert | University of Maryland Center for Environment Science, USA | |
| Paul Liu | North Carolina State University, UK | |
| Pengcheng Eang | Dalhousie University, Canada | |

| 专家 Visiting Scholar | 单位 Affiliation | 备注 Remark |
|--------------------------|--|--|
| Penjai Somphongchaiyakul | Chulalongkorn University, Thailand | 开放基金 Open research |
| Peter Herman | Delft University of Technology, the Netherlands | 中荷项目成员 Member of Joint Research Project between China and the Netherlands |
| Peter Wieringa | Delft University of Technology, the Netherlands | 中荷项目成员 Member of Joint Research Project between China and the Netherlands |
| Phaothep Cherdsukjai | Phuket Marine Biological Center, Thailand | |
| Pichai Sonchaeng | Burapha University, Thailand | |
| Qiang Yao | Louisiana State University, USA | |
| Qinghua Ye | Deltares, the Netherlands | |
| Roxane Maranger | University of Montreal, Canada | |
| Samina Kidwai | National Institute of Oceanography, Pakistan | |
| Samuel J. Bentley | Louisiana State University, USA | |
| Sayedur Chowdhury | University of Chittagong, Bangladesh | |
| Seung- Kyu Kim | Incheon National University, South Korea | |
| Shen Jian | Virginia institute of marine science, USA | |
| Sheng-Yuan Teng | National Taiwan Ocean University, Taiwan(China) | |
| Shunqi Pan | Cardiff University, UK | |
| Singae Yoo | Institute of Ocean Science and Technology, South Korea | |
| Siu Ngan Nina Lam | Louisiana State University, USA | |
| Somkiat Khokiattiwong | Phuket Marine Biological Center, Thailand | |
| Somkiat Khokiattiwong | Department of Marine and Coastal Resources, Thailand | |
| Stefan Aarninkhof | Delft University of Technology, the Netherlands | |
| Stefan Aarninkhof | Delft University of Technology, the Netherlands | |
| Stephen E. Darby | Southampton University, UK | |

| 专家 Visiting Scholar | 单位 Affiliation | 备注 Remark |
|--------------------------------|---|--|
| Steven L. Goodbred Jr. | Vanderbilt University, USA | |
| Suchana Chavanich | Chulalongkorn University, Thailand | |
| Supakij Suttiruengwong | Silpakorn University, Thailand | |
| Suvaluck Satumanatpan | Mahidol University, Thailand | |
| T N Sabiqah Tuan Anuar | Universiti Malaysia Terengganu, Malaysia | |
| Takashi Ohmura | Environmental Engineer related Administration, Japan | |
| Thamasak Yeemin | Ramkhamhaeng university, Thailand | |
| Thomas Larson | Max Planck Institute, Germany | |
| Timothy Shaw | Nanyang Technological University, Singapore. | |
| Tom Ysebaert | Royal Netherlands Institute for Sea Research, the Netherlands | 中荷项目成员 Member of Joint Research Project between China and the Netherlands |
| Ulo Mander | Tartu University, Estonia | 海外高端专家 Foreign High-end Experts |
| Valerie Cummins | University College Cork, Ireland | |
| Venugopalan Ittekkot | Leibniz Center for Topical Marine Ecology, Germany | 华东师范大学荣誉教授 Honorary professor of ECNU |
| Vladimir Bermanec | University of Zagreb, Croatia | |
| Vo Tran Tuan Linh | Department of Hydro-Geo Chemistry, Institute of Oceanography, Vietnam | |
| Wang Bo | Louisiana State University, USA | |
| Wang Zhengbing | Delft University of Technology, the Netherlands | |
| Waqar Ahmed | National Institute of Oceanography, Pakistan | |
| Weifeng Zhang | Woods Hole Oceanographic Institution, USA | |
| Wenxi Zhu | The Intergovernmental Oceanographic Commission for the Western Pacific (UNESCO IOC/WESTPAC) | |
| Wenxi Zhu | UNESCO/IOC Regional Office for the Western Pacific (WESTPAC) | |
| Willard S. Moore | South Carolina State University, USA | |
| William Andey Lazaro Anangisye | University of Dar es Salaam, Tanzania | |
| Won Joon Shim | Korea Institute of Ocean Science and Technology, South Korea | |

| 专家 Visiting Scholar | 单位 Affiliation | 备注 Remark |
|------------------------|---|--|
| Xiang Gao | Ocean Policy Research Institute, The Sasakawa Peace Foundation, Japan | |
| Yijun Xu | Louisiana State University, USA | |
| Yingming Wang | Christian-Albrecht-Universitaet zu Kiel, Germany | |
| Yinji Li | Tokai University, Japan | |
| Yu Zhou | Vassar College, USA | |
| Yusof Shuaib Ibrahim | Universiti Malaysia Terengganu, Malaysia | |
| Zainal Arifin | Indonesian Institute of Sciences, Indonesia | |
| Zhaohui Wang | Woods Hole Oceanographic Institution, USA | |
| Zheng Guangming | National Oceanic and Atmospheric Administration, USA | |
| Zheng Jian | National Institute of Radiological Sciences, Japan | |
| Zhengbing Wang | Delft University of Technology, the Netherlands | 中荷项目成员 Member of Joint Research Project between China and the Netherlands |
| Zhixuan Feng | Woods Hole Oceanographic Institution, USA | |
| Zhong Peng | Fugro GB Marine Ltd., UK | |
| Zulfigar Yasin | Universiti Sains Malaysia, Malaysia | |

开放基金

SKLEC Research Fund

2018年, 实验室在研开放基金课题37项, 共370.8万元, 其中, 新增开放基金课题11项, 共88万元。

There were 37 on-going projects that were funded by SKLEC with a total of 3.71 million RMB in 2018. Eleven new projects were approved in 2018 with a funding total of 0.88 million RMB.

2018年河口海岸学国家重点实验室设立开放基金课题 Research Fund Projects in 2018

| 姓名 Name | 课题名称 Title | 单位 Affiliation |
|-----------------------|--|---|
| 王龙升 WANG Longsheng | 长江三角洲全新世不同粒径沉积物磁性特征及其对古环境变化的响应 Magnetic Properties of the Holocene Sediments with Different Grain sizes and the response for paleoenvironmental changes in the Yangtze River Delta | 鲁东大学 Lu Dong University |
| 边昌伟 BIAN Changwei | 风浪环境下海底边界层湍混合过程及其对沉积物输运影响的研究 Study on turbulent mixing and its influence on sediment transport of the bottom boundary layer in wavy environment | 中国海洋大学物理海洋教育部重点实验室 Key Laboratory of Physical Oceanography, MOE, CHINA |
| 于谦 YU Qian | 低角度沙波形成演化机制研究 Formation and evolution mechanisms of low-angle sand dunes | 南京大学 Nan Jing University |
| 马小川 MA Xiaochuan | 山东半岛沿岸流域近百年以来重金属沉积记录及其对黄河入海通量变化的响应 Records of heavy metal in the area of Shandong Coastal Current in the past hundred years and their responses to the flux variation of Yellow River | 中国科学院海洋研究所 Institute of Oceanology, Chinese Academy of Sciences |
| 张衡 ZHANG Heng | 长江口盐沼湿地亚生境对虾虎鱼类优势种栖息方式的影响机制 Influence mechanism of selection for the Gobies' dominant species using the sub habitats of salt marsh in the Yangtze River Estuary | 中国水产科学研究院东海水产研究所 East China Sea Fisheries Research Institute, CAFS |
| Isaac Santos | Groundwater and carbon pump in the mangrove ecosystems in China and Australia' s coast | Southern Cross University, Australia |
| Henner Hollert | The Health Risk Assessment of Organic Pollutants on Microplastics | RWTH Aachen University, Germany |
| 张亚娟 ZHANG Yajuan | 长江河口湿地丛枝菌根真菌物种多样性及其对互花米草入侵的生态响应研究 The Species Diversity of Arbuscular Mycorrhizal Fungi and Ecological Response to Spartina alterniflora Invasion in Yangtze River Estuary | 河北大学 He Bei University |
| 蔡华阳 CAI Huayang | 长江与珠江磨刀门河口余水位形成变化机制 Mechanism governing the generation and development of residual water level in the Yangtze estuary and the Modaomen estuary in the Pearl River | 中山大学 Sun Yat-Sen University |
| Alfonse Dubi | Towards Sustainable Fresh Water Supply For Dar es Salaam City and Estuarine Vicinity of the Ruvu River, Tanzania | University of Dar es Salaam, Tanzania |
| 沈晓腾 SHEN Xiaoteng | 层化河口悬浮颗粒物的絮凝机理及其粒径分布 Flocculation processes and the particle size distributions of suspended particles in stratified estuaries | 比利时荷语区鲁汶大学 Katholieke Universiteit Leuven |

论文专著

List of Peer Reviewed Publications

2018年，实验室在国内外重要刊物上发表学术论文223篇，其中国际刊物175篇，国内重要刊物48篇；出版中文著作2部，参与编写出版英文专著4部。

In 2018, 223 peer-reviewed papers and book were published, among which 175 were published in international journals, 48 in national journals. Eight SKLEC members published 4 chapters of English books and 2 Chinese books.

国际刊物发表论文列表

List of International Peer Reviewed Publications

- [1] Bai M, Zhu L, An L, et al. Estimation and prediction of plastic waste annual input into the sea from China[J]. *Acta Oceanologica Sinica*, 2018, 37(11):26-39.
- [2] Breitburg D, Levin L, Oschlies A, et al. Declining oxygen in the global ocean and coastal waters[J]. *Science*, 2018.
- [3] Cai L, Hu L, Shi H, et al. Effects of inorganic ions and natural organic matter on the aggregation of nanoplastics[J]. *Chemosphere*, 2018, 197:142-151.
- [4] Cao H, Zhu Z, Balke T, et al. Effects of sediment disturbance regimes on *Spartina* seedling establishment: Implications for salt marsh creation and restoration[J]. *Limnology & Oceanography*, 2018, 63(2):647-659.
- [5] Chen D, Ye G, Gao W, et al. Ecological response of *Casuarina equisetifolia* to environmental stress in coastal dunes in China[J]. *Journal of Forest Research*, 2018, 23(3):173-182.
- [6] Chen L, Zhang P, Shang W, et al. Enrichment culture of electroactive microorganisms with high magnetic susceptibility enhances the performance of microbial fuel cells[J]. *Bioelectrochemistry*, 2018, 121:65-73.
- [7] Chen Q, Reisser J, Cunsolo S, et al. Pollutants in Plastics within the North Pacific Subtropical Gyre[J]. *Environmental Science & Technology*, 2018, 52(2): 446-456.
- [8] Chen Q, Zhang H, Allgeier A, et al. Marine Microplastics Bound Dioxin-like Chemicals: Model Explanation and Risk Assessment[J]. *Journal of Hazardous Materials*, 2018, 364:82-90.
- [9] Chen T, Ryves D B, Wang Z, et al. Mid- to late Holocene geomorphological and hydrological changes in the south Taihu area of the Yangtze delta plain, China[J]. *Palaeogeography Palaeoclimatology Palaeoecology*, 2018, 498:127-142.
- [10] Chen X, Lao Y, Wang J, et al. Submarine Groundwater-Borne Nutrients in a Tropical Bay (Maowei Sea, China) and Their Impacts on the Oyster Aquaculture[J]. *Geochemistry Geophysics Geosystems*, 2018, 19(3): 932-951.
- [11] Chen X, Zhang F, Lao Y, et al. Submarine groundwater discharge-derived carbon fluxes in mangroves: An important component of blue carbon budgets?[J]. *Journal of Geophysical Research: Oceans*, 2018, 123(9):6962-6979.
- [12] Chen Y, Zhu J. Observation and simulation of 2-methylisoborneol in the Qingcaosha Reservoir, Changjiang estuary[J]. *Journal of Oceanology and Limnology*, 2018, 36(5):1586-1596.

- [13] Chen Y, Zhu J. Reducing eutrophication risk of a reservoir by water replacement: a case study of the Qingcaosha reservoir in the Changjiang Estuary[J]. *Acta Oceanologica Sinica*, 2018, 37(6):23-29.
- [14] Cheng H, Chen J, Chen Z, et al. Mapping Sea Level Rise Behavior in an Estuarine Delta System: A Case Study along the Shanghai Coast[J]. *Engineering*, 2018, 4(1):156-163.
- [15] Cheng L, Zhou J, Cheng J. Bioaccumulation, tissue distribution and joint toxicity of erythromycin and cadmium in Chinese mitten crab (*Eriocheir sinensis*) [J]. *Chemosphere*, 2018, 210:267-278.
- [16] Dai B, Liu Y, Sun Q, et al. Foraminiferal evidence for Holocene environmental transitions in the Yaojiang Valley, south Hangzhou Bay, eastern China, and its significance for Neolithic occupations[J]. *Marine Geology*, 2018, 404:15-23.
- [17] Dai Z, Fagherazzic S, Gao S, et al. Scaling properties of estuarine beaches[J]. *Marine Geology*, 2018,404:130-136.
- [18] Dai Z, Mei X, Darby S E, et al. Fluvial sediment transfer in the Changjiang (Yangtze) river-estuary depositional system[J]. *Journal of Hydrology*, 2018, 566:719-734.
- [19] Du J, Shen J, Park K, et al. Worsened physical condition due to climate change contributes to the increasing hypoxia in Chesapeake Bay[J]. *Science of The Total Environment*, 2018, 630:707-717.
- [20] Du Y, Gao S, Liu X, et al. Meiofauna and nematode community characteristics indicate ecological changes induced by geomorphic evolution: A case study on tidal creek systems[J]. *Ecological Indicators*, 2018, 87:97-106.
- [21] Fan Y, Chen S, Zhao B, et al. Monitoring tidal flat dynamics affected by human activities along an eroded coast in the Yellow River Delta, China[J]. *Environmental Monitoring and Assessment*, 2018, 190(7):396.
- [22] Fan Y, Chen S, Zhao B, et al. Shoreline dynamics of the active Yellow River delta since the implementation of Water-Sediment Regulation Scheme: A remote-sensing and statistics-based approach[J]. *Estuarine, Coastal and Shelf Science*, 2018, 200:406-419.
- [23] Gao J, Hou L, Zheng Y, et al. Shifts in the community dynamics and activity of ammonia-oxidizing prokaryotes along the Yangtze estuarine salinity gradient[J]. *Journal of Geophysical Research: Biogeosciences*, 2018, 123(11):3458-3469.
- [24] Gao J, Shi H, Dai Z, et al. Linkages between the spatial toxicity of sediments and sediment dynamics in the Yangtze River Estuary and neighboring East China Sea[J]. *Environmental Pollution*, 2018, 233:1138-1146.
- [25] Gao L, Zhou Z, Reyes A V, et al. Yields and characterization of dissolved organic matter from different aged soils in northern Alaska[J]. *Journal of Geophysical Research: Biogeosciences*, 2018, 123:2035-2052.
- [26] Ge J, Zhou Z, Yang W, et al. Formation of Concentrated Benthic Suspension in a Time-Dependent Salt Wedge Estuary[J]. *Journal of Geophysical Research Oceans*, 2018, 123(11):8581-8607.
- [27] Ge Y , Liang S, Gui X, et al. Optimizing landslide susceptibility mapping in the Kongtong District, NW China: Comparing the subdivision criteria of factors[J]. *Geocarto International*, 2018, doi: 10.1080/10106049.2018.14998161.
- [28] Guo C, He Q, Van Prooijen B, et al. Investigation of flocculation dynamics under changing hydrodynamic forcing on an intertidal mudflat[J]. *Marine Geology*, 2018, 395:120-132.

- [29] Guo L, Matthew B, Sanders B F, et al. Tidal asymmetry and residual sediment transport in a short tidal basin under sea level rise[J]. *Advances in Water Resources*, 2018, 121: 1-8.
- [30] Guo L, Su N, Zhu C, et al. How have the river discharges and sediment loads changed in the Changjiang River basin downstream of the Three Gorges Dam?[J]. *Journal of Hydrology*, 2018, 560:259-274.
- [31] Guo W, Wang X, Ding P, et al. A system shift in tidal choking due to the construction of Yangshan Harbour, Shanghai, China[J]. *Estuarine, Coastal and Shelf Science*, 2018, 206(SI):49-60.
- [32] Guo X, Liu X, Niu Z, et al. Seasonal and spatial distribution of antibiotic resistance genes in the sediments along the Yangtze Estuary, China[J]. *Environmental Pollution*, 2018, 242(A):576-584.
- [33] Guo X, Lu D, Niu Z, et al. Bacterial community structure in response to environmental impacts in the intertidal sediments along the Yangtze Estuary, China[J]. *Marine Pollution Bulletin*, 2018, 126:141-149.
- [34] Guo X, Yang Y, Lu D, et al. Biofilms as a sink for antibiotic resistance genes (ARGs) in the Yangtze Estuary[J]. *Water Research*, 2018, 129:277-286.
- [35] He K, Li X, Dong L. The effects of flue gas desulfurization gypsum (FGD gypsum) on P fractions in a coastal plain soil[J]. *Journal of Soils and Sediments*, 2018, 18(3):804-815.
- [36] Hou L, Wang R, Yin G, et al. Nitrogen fixation in the intertidal sediments of the Yangtze Estuary: Occurrence and environmental implications[J]. *Journal of Geophysical Research: Biogeosciences*, 2018, 123(3):936-944.
- [37] Hu L, Chenick M, David E H, et al. Microplastics in Small Waterbodies and Tadpoles from Yangtze River Delta, China[J]. *Environmental Science & Technology*, 2018, 52(15):8885-8893.
- [38] Huang X, Liu S, Liu Z, et al. Impact of zinc oxide nanoparticles and ocean acidification on antioxidant responses of *Mytilus coruscus*[J]. *Chemosphere*, 2018, 196:182-195.
- [39] Huang X, Wang X, Li X, et al. Distribution Pattern and Influencing Factors for Soil Organic Carbon (SOC) in Mangrove Communities at Dongzhaigang, China[J]. *Journal of Coastal Research*, 2018, 34(2):434-442.
- [40] Huang Z, Siwabessy J, Cheng H, et al. Using Multibeam Backscatter Data to Investigate Sediment-Acoustic Relationships[J]. *Journal of Geophysical Research: Oceans*, 2018, 123(7):4649-4665.
- [41] Jabeen K, Li B, Chen Q, et al. Effects of virgin microplastics on goldfish (*Carassius auratus*)[J]. *Chemosphere*, 2018, 213:323-332.
- [42] Ji H, Chen S, Pan S, et al. Morphological variability of the active Yellow River mouth under the new regime of riverine delivery[J]. *Journal of Hydrology*, 2018, 564:329-341.
- [43] Jia J, Gao J, Cai T, et al. Sediment accumulation and retention of the Changjiang (Yangtze River) subaqueous delta and its distal muds over the last century[J]. *Marine Geology*, 2018, 401:2-16.
- [44] Jia J, Yang , Cai T, et al. On the sediment age estimated by ²¹⁰Pb dating: probably misleading “prolonging” and multiple-factor-caused “loss” [J]. *Acta Oceanologica Sinica*, 2018, 37(6):30-39.
- [45] Jiang C, Chen S, Pan S, et al. Geomorphic evolution of the Yellow River Delta: Quantification of basin-scale natural and anthropogenic impacts[J]. *Catena*, 2018, 163:361-377.
- [46] Jiang H, Liu D, Song X, et al. Response of phytoplankton assemblages to nitrogen reduction in the Laizhou Bay, China[J]. *Marine Pollution Bulletin*, 2018, 136:524-532.
- [47] Jiang P, Zhao S, Zhu L, et al. Microplastic-associated bacterial assemblages in the intertidal zone of the

Yangtze Estuary[J]. *Science of The Total Environment*, 2018, 624:48-54.

- [48] Jiang S, Zhang J, Zhang R, et al. Dissolved Lead in the East China Sea With Implications for Impacts of Marginal Seas on the Open Ocean Through Cross-Shelf Exchange[J]. *Journal of Geophysical Research Oceans*, 2018, 123(8):6004-6018.
- [49] Jin R, Ji F, Lin H, et al. The synthesis of Zr-metal-organic framework functionalized magnetic graphene nanocomposites as an adsorbent for fast determination of multi-pesticide residues in tobacco samples[J]. *Journal of Chromatography A*, 2018, 1577:1-7.
- [50] Kolandhasamy P, Su L, Li J, et al. Adherence of microplastics to soft tissue of mussels: A novel way to uptake microplastics beyond ingestion[J]. *Science of The Total Environment*, 2018, 610-611:635-640.
- [51] Lei L, Liu M, Song Y, et al. Polystyrene (nano) microplastics cause size -dependent neurotoxicity, oxidative damages and other adverse effects in *Caenorhabditis elegans*. [J]. *Environmental Science-Nano* 2018, 5(8):2009-2020.
- [52] Lei L, Wu S, Lu S, et al. Microplastic particles cause intestinal damage and other adverse effects in zebrafish *Danio rerio* and nematode *Caenorhabditis elegans*[J]. *Science of The Total Environment*, 2018, 619-620:1-8.
- [53] Li G, Gao S, Wang Y, et al. Sediment flux from the Zhoushan Archipelago, eastern China[J]. *Journal of Geographical Sciences*, 2018, 28(4):387-399.
- [54] Li H, Dai S, Ouyang Z, et al. Multi-scale temporal variation of methane flux and its controls in a subtropical tidal salt marsh in eastern China[J]. *Biogeochemistry*, 2018, 137(1-2):163-179.
- [55] Li H, Ma L, Lin L, et al. Microplastics in oysters *Saccostrea cucullata* along the Pearl River Estuary, China[J]. *Environmental Pollution*, 2018, 236:619-625.
- [56] Li J, Green C, Reynolds A, et al. Microplastics in mussels sampled from coastal waters and supermarkets in the United Kingdom[J]. *Environmental Pollution*, 2018, 241:35-44.
- [57] Li J, Lusher A L, Rorchell J M, et al. Using mussel as a global bioindicator of coastal mic ssel as a global bioindicator of coastal mi roplastic pollution.[J]. *Environmental pollution (Barking, Essex : 1987)*, 2018, 244:522-533.
- [58] Li L, Li M, Deng H, et al. A straightforward method for measuring the range of apparent density of microplastics[J]. *Science of The Total Environment*, 2018, 639:367-373.
- [59] Li L, Pohl C, Ren J, et al. Revisiting the biogeochemistry of arsenic in the Baltic Sea: Impact of anthropogenic activity.[J]. *Science of The Total Environment*, 2018, 613-614:557-568.
- [60] Li R, Yu Q, Wang Y, et al. The relationship between inundation duration and *Spartina alterniflora* growth along the Jiangsu coast, China[J]. *Estuarine, Coastal and Shelf Science*, 2018, 213:305-313.
- [61] Li S, Ge Z, Xie L, et al. Ecophysiological response of native and exotic salt marsh vegetation to waterlogging and salinity: Implications for the effects of sea-level rise[J]. *Scientific Reports*, 2018, 8(1):2441.
- [62] Li X, Bellerby R, Craft C, et al. Coastal wetland loss, consequences, and challenges for restoration[J]. *Anthropocene Coasts*, 2018, 1:1-15.
- [63] Li Y, Jia J, Zhu Q, et al. Differentiating the effects of advection and resuspension on suspended sediment concentrations in a turbid estuary[J]. *Marine Geology*, 2018, 403:179-190.

- [64] Liao W, Fan X, Zhang Q, et al. Morphology and Phylogeny of Two Novel Ciliates, *Arcanisutura chongmingiensis* n. gen. n. sp. and *Naxella paralucida* n. sp. from Shanghai, China[J]. *Journal of Eukaryotic Microbiology*, 2018, 65(1):48-60.
- [65] Liu D, Glibert P M. Ecophysiological linkage of nitrogen enrichment to heavily silicified diatoms in winter[J]. *Marine Ecology Progress Series*, 2018, 604:51-63.
- [66] Liu D, Wang Y, Wang Y, et al. Ocean fronts construct spatial zonation in microfossil assemblages[J]. *Global Ecology and Biogeography*, 2018, 27(10):1225-1237.
- [67] Liu J T, Hsu R T, Yang R J, et al. A comprehensive sediment dynamics study of a major mud belt system on the inner shelf along an energetic coast[J]. *Scientific Reports*, 2018, 8(1):4229.
- [68] Liu J, Du J, Wu Y, et al. Nutrient input through submarine groundwater discharge in two major Chinese estuaries: The Pearl River Estuary and the Changjiang River Estuary[J]. *Estuarine Coastal & Shelf Science*, 2018, 203:17-28.
- [69] Liu M, Lu S, Song Y, et al. Microplastic and mesoplastic pollution in farmland soils in suburbs of Shanghai, China[J]. *Environmental Pollution*, 2018, 242:855-862.
- [70] Liu X, Cao Z, Yuan Z, et al. Insight into the kinetics and mechanism of removal of aqueous chlorinated nitroaromatic antibiotic chloramphenicol by nanoscale zero-valent iron[J]. *Chemical Engineering Journal*, 2018, 334:508-518.
- [71] Liu X, Chen J, Maher B A, et al. Connection of the proto-Yangtze River to the East China Sea traced by sediment magnetic properties[J]. *Geomorphology*, 2018, 303:162-171.
- [72] Liu Y, Sun Q, Fan D, et al. Early to Middle Holocene sea level fluctuation, coastal progradation and the Neolithic occupation in the Yaojiang Valley of southern Hangzhou Bay, Eastern China[J]. *Quaternary Science Reviews*, 2018, 189:91-104.
- [73] Lou Y, Mei X, Dai Z, et al. Evolution of the mid-channel bars in the middle and lower reaches of the Changjiang (Yangtze) River from 1989 to 2014 based on the Landsat satellite images: impact of the Three Gorges Dam[J]. *Environmental Earth Sciences*, 2018, 77(10):394.
- [74] Lu Z, Fan W, Li S, et al. Large-eddy simulation of the influence of a wavy lower boundary on the turbulence kinetic energy budget redistribution[J]. *Journal of Oceanology and Limnology*, 2018, 36(4):1178-1188.
- [75] Luo Y, David D, Kevin R, et al. Saturation of water reflectance in extremely turbid media based on field measurements, satellite data and bio-optical modelling[J]. *Optics Express*, 2018, 26(8):10435-10451.
- [76] Lv J, Wang Y. Multi-scale analysis of heavy metals sources in soils of Jiangsu Coast, Eastern China[J]. *Chemosphere*, 2018, 212:964-973.
- [77] Lv J, Yu Y. Source identification and spatial distribution of metals in soils in a typical area of the lower Yellow River, eastern China[J]. *Environmental Science and Pollution Research*, 2018, 25:21106-21117.
- [78] Lv J. Multivariate receptor models and robust geostatistics to estimate source apportionment of heavy metals in soils[J]. *Environmental pollution*, 2018, 244:72-83.
- [79] Lyu H, Zhu J. Impact of the bottom drag coefficient on saltwater intrusion in the extremely shallow estuary[J]. *Journal of Hydrology*, 2018, 557:838-850.
- [80] Marks L, Salem A, Welc F, et al. Holocene lake sediments from the Faiyum Oasis in Egypt: a record of

- environmental and climate change[J]. *Boreas*, 2018, 47(1):62-79.
- [81] Mei X, Dai Z, Darby S E, et al. Modulation of Extreme Flood Levels by Impoundment Significantly Offset by Floodplain Loss Downstream of the Three Gorges Dam[J]. *Geophysical research letters*, 2018, 45(7):3147-3155.
- [82] Mei X, Dai Z, Tang Z, et al. Impacts of historical records on extreme flood variations over the conterminous United States[J]. *Journal of Flood Risk Management*, 2018, 11(1):S359-S369.
- [83] Mei X, Dai Z, Wei W, et al. Secular bathymetric variations of the North Channel in the Changjiang (Yangtze) Estuary, China, 1880–2013: causes and effects[J]. *Geomorphology*, 2018, 303:30-40.
- [84] Mei X, Du J, Dai Z, et al. Decadal sedimentation in China's largest freshwater lake, Poyang Lake[J]. *Geochemistry, Geophysics, Geosystems*, 2018, 19(8):2384-2396.
- [85] Mwijage A P, Shilla D A, Machiwa J F, et al. Important organic matter sources and trophic pathway for the nutrition of *Hilsa kelee* (Cuvier, 1829) and *Valamugil buechanani* (Bleeker, 1853) in Pangani macro-tidal estuary, Tanzania[J]. *Chemistry and Ecology*, 2018, 34(10): 941-963.
- [86] Nian X, Zhang W, Wang Z, et al. Optical dating of Holocene sediments from the Yangtze River (Changjiang) Delta, China[J]. *Quaternary International*, 2018, 467:251-263.
- [87] Nian X, Zhang W, Wang Z, et al. The chronology of a sediment core from incised valley of the Yangtze River delta: Comparative OSL and AMS ¹⁴C dating[J]. *Marine Geology*, 2018, 395:320-330.
- [88] Nie J, Feng H, Witherell B B, et al. Causes, Assessment, and Treatment of Nutrient (N and P) Pollution in Rivers, Estuaries, and Coastal Waters[J]. *Current Pollution Reports*, 2018, 4(2):154-161.
- [89] Niu Z, Pan H, Guo X, et al. Sulphate-reducing bacteria (SRB) in the Yangtze Estuary sediments: Abundance, distribution and implications for the bioavailability of metals[J]. *Science of The Total Environment*, 2018, 634:296-304.
- [90] Pan Y, Shen F, Wei X, et al. Fusion of Landsat-8/OLI and GOCI Data for Hourly Mapping of Suspended Particulate Matter at High Spatial Resolution: A Case Study in the Yangtze (Changjiang) Estuary[J]. *Remote Sensing*, 2018, 10(2):158
- [91] Peng G, Xu P, Zhu B, et al. Microplastics in freshwater river sediments in Shanghai, China: A case study of risk assessment in mega-cities[J]. *Environmental Pollution*, 2018, 234:448-456.
- [92] Peng Y, Liu D, Wang Y, et al. Analyzing biases of nitrogen contents and $\delta^{15}\text{N}$ values arising from acidified marine sediments with different CaCO_3 concentrations[J]. *Acta Oceanologica Sinica*, 2018, 37(8):1-5.
- [93] Qu X, Su L, Li H, et al. Assessing the relationship between the abundance and properties of microplastics in water and in mussels[J]. *Science of The Total Environment*, 2018, 621:679-686.
- [94] Selemani J R, Zhang J, Muzuka A N N, et al. Nutrients' distribution and their impact on Pangani River Basin's ecosystem – Tanzania[J]. *Environmental Technology*, 2018, 39(6):702-716.
- [95] Shan X, Shi X, Clift P D, et al. Carbon isotope and rare earth element composition of Late Quaternary sediment gravity flow deposits on the mid shelf of East China Sea: Implications for provenance and origin of hybrid event beds[J]. *Sedimentology*, 2018, doi.org/10.1111/sed.12561.
- [96] Shi S, Cheng H, Xuan X, et al. Fluctuations in the tidal limit of the Yangtze River estuary in the last decade[J]. *Science China Earth Sciences*, 2018, 61(8):1136-1147.

- [97] Shou W, Zong H, Ding P, et al. A modelling approach to assess the effects of atmospheric nitrogen deposition on the marine ecosystem in the Bohai Sea, China[J]. *Estuarine, Coastal and Shelf Science*, 2018, 208:36-48.
- [98] Su L, Cai H, Kolandhasamy P, et al. Using the Asian clam as an indicator of microplastic pollution in freshwater ecosystems[J]. *Environmental Pollution*, 2018, 234:347-355.
- [99] Sun X, Shen F, Liu D, et al. In situ and satellite observations of phytoplankton size classes in the entire continental shelf sea, China[J]. *Journal of Geophysical Research: Oceans*, 2018, 123(5):3523-3544.
- [100] Sun X, Xu Y, Zhang Q, et al. Combined effect of water inundation and heavy metals on the photosynthesis and physiology of, *Spartina alterniflora*[J]. *Ecotoxicology and Environmental Safety*, 2018, 153:248-258.
- [101] Tan K, Zhang W, Shen F, et al. Investigation of TLS Intensity Data and Distance Measurement Errors from Target Specular Reflections[J]. *Remote Sensing*, 2018, 10:1077.
- [102] Tang J, Ye S, Chen X, et al. Coastal blue carbon: Concept, study method, and the application to ecological restoration[J]. *Science China Earth Sciences*, 2018, 61(6):637-646.
- [103] Valiela I, Liu D, Lioret J, et al. Stable isotopic evidence of nitrogen sources and C4 metabolism driving the world's largest macroalgal green tides in the Yellow Sea[J]. *Scientific Reports*, 2018, 8:17437.
- [104] Wang F, Nian X, Wang J, et al. Multiple dating approaches applied to the recent sediments in the Yangtze River (Changjiang) subaqueous delta[J]. *The Holocene*, 2018, 28(6):858-866.
- [105] Wang G, Liu Y, Chen J, et al. Magnetic evidence for heavy metal pollution of topsoil in Shanghai, China[J]. *Frontiers of Earth Science*, 2018, 12(1):125-133.
- [106] Wang G, Wang J, Xia X, et al. Nitrogen removal rates in a frigid high-altitude river estimated by measuring dissolved N_2 and N_2O [J]. *Science of The Total Environment*, 2018, 645:318-328.
- [107] Wang J, Dai Z, Mei X, et al. Immediately downstream effects of Three Gorges Dam on channel sandbars morphodynamics between Yichang-Chenglingji Reach of the Changjiang River, China[J]. *Journal of Geographical Sciences*, 2018, 28(5):629-646.
- [108] Wang J, Fan Y, Liu D, et al. Spatial and vertical distribution of ^{129}I and ^{127}I in the East China Sea: Inventory, source and transportation[J]. *Science of The Total Environment*, 2018, 652:177-188.
- [109] Wang J, Zhang W, Baskaran M, et al. Fingerprinting Sediment Transport in River-Dominated Margins Using Combined Mineral Magnetic and Radionuclide Methods[J]. *Journal of Geophysical Research: Oceans*, 2018, 123(8): 5360-5374.
- [110] Wang L, Zhou Y, Shen F. Suspended sediment diffusion mechanisms in the Yangtze Estuary influenced by wind fields[J]. *Estuarine, Coastal and Shelf Science*, 2018, 200:428-436.
- [111] Wang R, Li X, Hou L, et al. Nitrogen fixation in surface sediments of the East China Sea: Occurrence and environmental implications[J]. *Marine pollution bulletin*, 2018, 137:542-548.
- [112] Wang Z, Ryves D B, Lei S, et al. Middle Holocene marine flooding and human response in the south Yangtze coastal plain, East China[J]. *Quaternary Science Reviews*, 2018, 187:80-93.
- [113] Wang Z, Saito Y, Zhan Q, et al. Three-dimensional evolution of the Yangtze River mouth, China during the Holocene: impacts of sea level, climate and human activity[J]. *Earth-Science Reviews*, 2018, 185:938-955.
- [114] Wei T, Wang Z, Chen J, et al. Non-flood season neap tides in the Yangtze estuary offshore: Flow mixing

- processes and its potential impacts on adjacent wetlands[J]. *Physics and Chemistry of the Earth, Parts A/B/C*, 2018, 103(SI):127-139
- [115] Wu F, Cui S, Sun M, et al. Combined effects of ZnO NPs and seawater acidification on the haemocyte parameters of thick shell mussel *Mytilus coruscus*[J]. *Science of The Total Environment*, 2018, 624:820-830.
- [116] Wu H, Gu J, Zhu P. Winter Counter Wind Transport in the Inner Southwestern Yellow Sea[J]. *Journal of Geophysical Research Oceans*, 2018, 123(1):411-436.
- [117] Wu H, Wu T, Bai M. Mega Estuarine Constructions Modulate the Changjiang River Plume Extension in Adjacent Seas[J]. *Estuaries and Coasts*, 2018, 41(5):1234-1252.
- [118] Wu H, Xing Y, Sun H, et al. Gut microbial diversity in two insectivorous bats: Insights into the effect of different sampling sources[J]. *MicrobiologyOpen*, 2018:e00670.
- [119] Wu S, Lei L, Liu M, et al. Single and mixture toxicity of strobilurin and SDHI fungicides to *Xenopus tropicalis* embryos[J]. *Ecotoxicology and Environmental Safety*, 2018, 153:8-15.
- [120] Wu T, Wu H. Tidal Mixing Sustains a Bottom-Trapped River Plume and Buoyant Coastal Current on an Energetic Continental Shelf[J]. *Journal of Geophysical Research: Oceans*, 2018, 123:8026-8051.
- [121] Wu W, Yang Z, Tian B, et al. Impacts of coastal reclamation on wetlands: Loss, resilience, and sustainable management[J]. *Estuarine, Coastal and Shelf Science*, 2018, 210:153-161.
- [122] Wu Y, Eglinton T I, Zhang J, et al. Spatiotemporal Variation of the Quality, Origin, and Age of Particulate Organic Matter Transported by the Yangtze River (Changjiang)[J]. *Journal of Geophysical Research: Biogeosciences*, 2018, 123(9):2908-2921.
- [123] Wünnemann B, Yan D, Andersen N, et al. A 14 ka high-resolution $\delta^{18}\text{O}$ lake record reveals a paradigm shift for the process-based reconstruction of hydroclimate on the northern Tibetan Plateau[J]. *Quaternary Science Reviews*, 2018, 200:65-84.
- [124] Xie D, Pan C, Gao S, et al. Morphodynamics of the Qiantang Estuary, China: Controls of river flood events and tidal bores[J]. *Marine Geology*, 2018, 406:27-33.
- [125] Xie W, He Q, Wang X, et al. Role of mudflat-creek sediment exchanges in intertidal sedimentary processes[J]. *Journal of Hydrology*, 2018, 567:351-360.
- [126] Xie Z, Li X, Zhang Y, et al. Accelerated expansion of built-up area after bridge connection with mainland: A case study of Zhujiajian Island[J]. *Ocean & Coastal Management*, 2018, 152:62-69.
- [127] Xiong J, Wang Y, Gao S, et al. On estimation of coastal wave parameters and wave-induced shear stresses[J]. *Limnology and Oceanography Methods*, 2018, 16(9):594-606.
- [128] Xiong X, Zhang K, Chen X, et al. Sources and distribution of microplastics in China's largest inland lake - Qinghai Lake[J]. *Environmental Pollution*, 2018, 235:899-906.
- [129] Xu J, Cao Z, Zhang Y, et al. A review of functionalized carbon nanotubes and graphene for heavy metal adsorption from water: Preparation, application, and mechanism[J]. *Chemosphere*, 2018, 195:351-364.
- [130] Xu J, Kiorboe T. Toxic dinoflagellates produce true grazer deterrents[J]. *Ecology*, 2018, 99(10):2240-2249.
- [131] Xu P, Peng G, Su L, et al. Microplastic risk assessment in surface waters: A case study in the Changjiang Estuary, China[J]. *Marine Pollution Bulletin*, 2018, 133:647-654.

- [132] Xu Y, Fan X, Warren A, et al. Functional diversity of benthic ciliate communities in response to environmental gradients in a wetland of Yangtze Estuary, China[J]. *Marine Pollution Bulletin*, 2018, 127:726-732.
- [133] Xu Y, Gao F, Fan X. Reconsideration of the systematics of Peniculida (Protista, Ciliophora) based on SSU rRNA gene sequences and new morphological features of *Marituja* and *Disematostoma*[J]. *Hydrobiologia*, 2018, 806(1):313-331.
- [134] Xu Y, Stoeck T, Forster D, et al. Environmental status assessment using biological traits analyses and functional diversity indices of benthic ciliate communities[J]. *Marine Pollution Bulletin*, 2018, 131:646-654.
- [135] Xu Y, Sun X, Zhang Q, et al. Iron plaque formation and heavy metal uptake in *Spartina alterniflora* at different tidal levels and waterlogging conditions[J]. *Ecotoxicology and environmental safety*, 2018, 153:91-100.
- [136] Xue H, Wang Z, Hua Y, et al. Molecular signatures and functional analysis of beige adipocytes induced from in vivo intra-abdominal adipocytes[J]. *Science Advances*, 2018, 4(7):eaar5319.
- [137] Xue L, Li X, Yan Z, et al. Native and non-native halophytes resiliency against sea-level rise and saltwater intrusion[J]. *Hydrobiologia*, 2018, 806:47-65.
- [138] Xue L, Li X, Zhang Q, et al. Elevated salinity and inundation will facilitate the spread of invasive *Spartina alterniflora* in the Yangtze River Estuary, China[J]. *Journal of Experimental Marine Biology & Ecology*, 2018, 506:144-154.
- [139] Yan D, Wünnemann, B, Zhang Y, et al. Response of lake-catchment processes to Holocene climate variability: Evidences from the NE Tibetan Plateau[J]. *Quaternary Science Reviews*, 2018, 201:261-279.
- [140] Yang H, Yang S, Meng Y, et al. Recent coarsening of sediments on the southern Yangtze subaqueous delta front: A response to river damming[J]. *Continental Shelf Research*, 2018, 155:45-51.
- [141] Yang H, Yang S, Xu K, et al. Human impacts on sediment in the Yangtze River: A review and new perspectives[J]. *Global and Planetary Change*, 2018, 162:8-17.
- [142] Yang Z, Cheng H, Cao Z, et al. Effect of Riverbed Morphology on Lateral Sediment Distribution in Estuaries[J]. *Journal of Coastal Research*, 2018, 34(1):202-214.
- [143] Ye L, Zhang R, Sun Q, et al. Hydrochemistry of the meltwater streams on Fildes Peninsula, King George Island, Antarctica[J]. *Journal of Oceanology and Limnology*, 2018, 36(6):2181-2193.
- [144] Yu C, Hou L, Zheng Y, et al. Evidence for complete nitrification in enrichment culture of tidal sediments and diversity analysis of clade a comammox *Nitrospira* in natural environments[J]. *Applied Microbiology and Biotechnology*, 2018, 102(21):9363-9377.
- [145] Yu P, Zhong X, Zhou Y. Impact of Model Resolution on Radar Imaging of Underwater Sand Waves[J]. *Journal of Coastal Research*, 2018, 34(1):114-121.
- [146] Yu Y, Mei X, Dai Z, et al. Hydromorphological processes of Dongting Lake in China between 1951 and 2014[J]. *Journal of Hydrology*, 2018, 562:254-266.
- [147] Yuan L, Richardson C, Ho M, et al. Stress Responses of Aquatic Plants to Silver Nanoparticles[J]. *Environmental Science & Technology*, 2018, 52(5): 2558-2565.
- [148] Yuan Z, Liu D, Keesing J K, et al. Paleoecological evidence for decadal increase in phytoplankton biomass off northwestern Australia in response to climate change[J]. *Ecology and Evolution*, 2018, 8(4):2097-2107.

- [149] Zhang J, Zhu Z, Mo W, et al. Hypoxia and nutrient dynamics affected by marine aquaculture in a monsoon-regulated tropical coastal lagoon[J]. *Environmental Monitoring and Assessment*, 2018, 190(11):656.
- [150] Zhang K, Shi H, Peng J, et al. Microplastic pollution in China's inland water systems: A review of findings, methods, characteristics, effects, and management[J]. *Science of The Total Environment*, 2018, 630:1641-1653.
- [151] Zhang M, Townend I, Cai H, et al. The influence of seasonal climate on the morphology of the mouth-bar in the Yangtze Estuary, China[J]. *Continental Shelf Research*, 2018, 153:30-49.
- [152] Zhang T, Tian B, Bo S, et al. Mapping the conservation priority of migratory shorebird habitat on a dynamic deltaic coast[J]. *Estuarine, Coastal and Shelf Science*, 2018, 212:219-232.
- [153] Zhang W, Dong C, Hutchinson S M, et al. Recent Applications of Mineral Magnetic Methods in Sediment Pollution Studies: a Review[J]. *Current Pollution Reports*, 2018, 4(1):1-7.
- [154] Zhang W, Hetland R D. A Study of Baroclinic Instability Induced Convergence Near the Bottom Using Water Age Simulations[J]. *Journal of Geophysical Research Oceans*, 2018, 123(3):1962-1977.
- [155] Zhang W, Wu H, Zhu Z. Transient hypoxia extent off Changjiang River Estuary due to mobile Changjiang River plume[J]. *Journal of Geophysical Research-oceans*, 2018, 10.1029/2018JC014596.
- [156] Zhang X, Ha B, Wang S, et al. The earliest human occupation of the high-altitude Tibetan Plateau 40 thousand to 30 thousand years ago[J]. *Science*, 2018, 362:1049-1051.
- [157] Zhang X, Lin C, Dalrymple R W, et al. Use of the Cone Penetration Testing (CPT) method to interpret late Quaternary tide-dominated successions: a case study from the eastern China coastal plain[J]. *Continental Shelf Research*, 2018, 161:49-57.
- [158] Zhang X, Zhang Q, Yang A, et al. Incorporation of Microbial Functional Traits in Biogeochemistry Models Provides Better Estimations of Benthic Denitrification and Anammox Rates in Coastal Oceans[J]. *Journal of Geophysical Research: Biogeosciences*, 2018, 123(10): 3331-3352.
- [159] Zhang Y, Yang K, Du J, et al. Chemical characterization of fractions of dissolved humic substances from a marginal sea—a case from the Southern Yellow Sea[J]. *Chinese Journal of Oceanology & Limnology*, 2018, 36(2):238-248.
- [160] Zhang Z, Wu H, Yin X, et al. Dynamical Response of Changjiang River Plume to a Severe Typhoon With the Surface Wave-Induced Mixing[J]. *Journal of Geophysical Research: Oceans*, 2018, doi:10.1029/2018JC014266.
- [161] Zhao B, Yan X, Wang Z, et al. Sedimentary evolution of the Yangtze River mouth (East China Sea) over the past 19,000 years, with emphasis on the Holocene variations in coastal currents[J]. *Palaeogeography, Palaeoclimatology, Palaeoecology*, 2018, 490:431-449.
- [162] Zhao J, Guo L, He Q, et al. An analysis on half century morphological changes in the Changjiang Estuary: Spatial variability under natural processes and human intervention[J]. *Journal of Marine Systems*, 2018, 181:25-36.
- [163] Zhao L, Liu D, Wang J, et al. Spatial and vertical distribution of radiocesium in seawater of the East China Sea[J]. *Marine Pollution Bulletin*, 2018, 128:361-368.
- [164] Zhao S, Ward J E, Danley M, et al. Field-based Evidence for Microplastic in Marine Aggregates and Mussels: Implications for Trophic Transfer[J]. *Environmental Science & Technology*, 2018, 52(19):11038-11048.

- [165] Zheng B, Li Y, Li J, et al. Impact of tropical cyclones on the evolution of the monsoon-driven upwelling system in the coastal waters of the northern South China Sea[J]. *Ocean Dynamics*, 2018, 68(2):223-237.
- [166] Zheng S, Cheng H, Shi S, et al. Impact of anthropogenic drivers on subaqueous topographical change in the Datong to Xuliujing reach of the Yangtze River[J]. *Science China Earth Sciences*, 2018, 61(7):940-950.
- [167] Zheng S, Xu Y, Cheng H, et al. Assessment of bridge scour in the lower, middle, and upper Yangtze River estuary with riverbed sonar profiling techniques.[J]. *Environmental Monitoring & Assessment*, 2018, 190(1):15.
- [168] Zheng S, Xu Y, Cheng H, et al. Riverbed erosion of the final 565 kilometers of the Yangtze River (Changjiang) following construction of the Three Gorges Dam[J]. *Scientific Reports*, 2018, 8(1):11917.
- [169] Zhong X, Dong P, Chen S. Large-scale shoreline undulations and role of self-organization processes[J]. *Current Science*, 2018, 115(4):729-738.
- [170] Zhong Y, Li Y, Wu X, et al. Morphodynamics of a tidal ridge system in the southwestern Yellow Sea: HF radar study[J]. *Estuarine, Coastal and Shelf Science*, 2018, 206:27-37.
- [171] Zhu J, Huang X, Jiang H, et al. The role of ppar γ in embryonic development of *Xenopus tropicalis* under triphenyltin-induced teratogenicity.[J]. *Science of The Total Environment*, 2018, 633:1245-1252.
- [172] Zhu L, He Q, Shen J. Modeling lateral circulation and its influence on the along-channel flow in a branched estuary[J]. *Ocean Dynamics*, 2018, 68(2):177-191.
- [173] Zhu P, Wu H, et al. Origins and transports of the low-salinity coastal water in the southwestern Yellow Sea[J]. *Acta Oceanologica Sinica*, 2018, 37(4):1-11.
- [174] Zhu Q, Li J, Zhang F, et al. Distinguishing Cyanobacterial Bloom From Floating Leaf Vegetation in Lake Taihu Based on Medium-Resolution Imaging Spectrometer (MERIS) Data[J]. *IEEE Journal of Selected Topics in Applied Earth Observations and Remote Sensing*, 2018, 11(1):34-44.
- [175] Zhu X, Zhang R, Wu Y, et al. The Remobilization and Removal of Fe in Estuary—A Case Study in the Changjiang Estuary, China[J]. *Journal of Geophysical Research Oceans*, 2018, 123(4):2539-2553.

国内刊物发表论文列表

List of Chinese Peer Reviewed Publications

- [1] 白雨, 赵世焯, 彭谷雨, 等. 城市污水处理过程中微塑料赋存特征[J]. *中国环境科学*, 2018, 38(5):1734-1743.
- [2] 陈启晴, 杨守业, Henner, 等. 微塑料污染的水生生态毒性与载体作用[J]. *生态毒理学报*, 2018, 13(1):16-30.
- [3] 陈小华, 钱晓雍, 李小平, 等. 洱海富营养化时间演变特征(1988-2013年)及社会经济驱动分析[J]. *湖泊科学*, 2018, 30(1):70-78.
- [4] 陈莹璐, 张玉柱, 谭子辉, 等. MS2000和LS13320激光粒度仪测定沉积物粒度结果的差异[J]. *中山大学学报(自然科学版)*, 2018, 57(4):48-55.
- [5] 高成志, 郑崇伟. SWAN模式对西行台风所致台风浪的模拟分析[J]. *哈尔滨工程大学学报*, 2018, 39(07):1158-1164.
- [6] 高永强, 高磊, 朱礼鑫, 等. 长江口及其邻近海域悬浮颗粒物浓度和粒径的时空变化特征[J]. *海洋学报*, 2018, 40(3):62-73.
- [7] 贺坤, 李小平, 徐晨, 等. 烟气脱硫石膏对滨海盐渍土的改良效果[J]. *环境科学研究*, 2018, 31(3):547-554.

- [8] 黄芳, 黄亮, 张国森. 东海表层沉积物中多环芳烃的分布特征及来源解析[J]. 地球与环境, 2018, 46(1):50-58.
- [9] 姜会超, 王玉珏, 李佳蕙, 等. 莱州湾营养盐空间分布特征及年际变化趋势[J]. 海洋通报, 2018, 37(4):411-423.
- [10] 柯科腾, 葛建忠, 丁平兴. 长江口北槽近底高质量浓度泥沙形成关键机制分析[J]. 海洋科学进展, 2018, 36(4):560-569.
- [11] 李昶, 邓兵, 汪福顺, 等. 三峡库区草堂河库湾水动力特征[J]. 水利水电科技进展, 2018, 38(2):49-56.
- [12] 李高聪, 高抒, 高建华. 全新世以来亚洲七个主要河口三角洲的生长极限[J]. 海洋地质与第四纪地质, 2018, 38(1):11-22.
- [13] 李国平, 朱建荣. 2015-2017年枯季长江河口青草沙水库盐水入侵分析[J]. 华东师范大学学报: 自然科学版, 2018, 2:160-169.
- [14] 栗文静, 雷少, 王张华, 等. 浙江大榭史前制盐遗址人工土台的堆土特征及来源分析[J]. 古地理学报, 2018, 20(6):1102-1112.
- [15] 刘健辉, 姜锋, 陈杰, 等. 中国典型河流沉积物石英释光性质初探及其物源指示意义[J]. 高校地质学报, 2018, 24(1):88-96.
- [16] 栾华龙, 柯科腾, 葛建忠, 等. 长江口规划工程影响下的咸潮入侵数值模拟[J]. 海洋科学进展, 2018, 36(4):525-539.
- [17] 吕建树, 何华春. 江苏海岸带土壤重金属来源解析及空间分布[J]. 环境科学, 2018, 39(6):2853-2864.
- [18] 年小美, 张卫国. 光释光技术在我国海岸晚第四纪沉积测年中的应用[J]. 第四纪研究, 2018, 38(3):573-586.
- [19] 苏国宾, 陈沈良, 许从亮, 等. 基于GF-1影像的黄河口潮滩高程定量反演[J]. 海洋地质前沿, 2018, 34(11):1-9.
- [20] 田原原, 陈沈良, 袁庆. 旅游海滩管理云平台的研究与设计[J]. 海洋通报, 2018, 37(1):25-32.
- [21] 唐剑武, 叶属峰, 陈雪初, 等. 海岸带蓝碳的科学概念、研究方法以及在生态恢复中的应用[J]. 中国科学:地球科学, 2018(6).
- [22] 王杰, 戴志军, 魏稳, 等. 基于LiDAR观测的长江河口南汇南滩近期动力地貌研究[J]. 海洋与湖沼, 2018, 49(4):756-768.
- [23] 王景, 任景玲, 王召伟, 等. 珠江口和南海北部海水中的总溶解无机As[J]. 海洋环境科学, 2018, 37(1):48-54.
- [24] 王利花, 周云轩. 大通站水沙关系演变驱动因素分析[J]. 吉林大学学报(地球科学版), 2018, 48(1):226-233.
- [25] 王淑平, 程和琴, 郑树伟, 等. 近期长江与鄱阳湖汇流河段冲淤变化与微地貌特征[J]. 泥沙研究, 2018, 43(3):15-20.
- [26] 王淑平, 程和琴, 郑树伟, 等. 近期长江张家洲南水道强冲刷机理与趋势分析[J]. 长江流域资源与环境, 2018, 27(9):2070-2077.
- [27] 吴电明, 夏玉玲, 侯立军, 等. 土壤亚硝酸气体(HONO)排放过程及其驱动机制[J]. 中国生态农业学报, 2018, 26(2):190-194.
- [28] 徐夕博, 吕建树, 吴泉源, 等. 基于PCA-MLR和PCA-BPN的莱州湾南岸滨海平原土壤有机质高光谱预测研究[J]. 光谱学与光谱分析, 2018, 38(8):2556-2562.
- [29] 许宇田, 童春富. 长江口九段沙湿地海三棱草生物量分配特征及其影响因子[J]. 生态学报, 2018, 38(19):7034-7044.
- [30] 薛成凤, 贾建军, 高抒, 等. 中小河流对长江水下三角洲远端泥沉积的贡献:以椒江和瓯江为例[J]. 海洋学报, 2018, 40(05):75-89.
- [31] 薛莲, 李秀珍, 闫中正, 等. 盐度和淹水对长江口潮滩盐沼植物碳储量的影响[J]. 生态学报, 2018, 38(9):2995-

3003.

- [32] 杨世伦, 吴秋原, 张赛赛, 等. 崇明海岸湿地现状及其在生态岛建设中的作用[J]. 上海国土资源, 2018, 39(3):34-37.
- [33] 杨万伦, 道付海, 栾华龙, 等. 长江口洪季南北槽落潮分流分沙比观测研究[J]. 华东师范大学学报: 自然科学版, 2018, 2:170-180.
- [34] 杨文卿, 孙立广, 杨仲康, 等. 南澳宋城: 被海啸毁灭的古文明遗址[J]. 科学通报2018, 63, doi: 10.1360/N972018-00740
- [35] 尤迪, 童春富, 吴逢润. 枯季长江口南汇东滩潮间带盐沼湿地冲淤变化对大型底栖动物功能群的影响[J]. 海洋学报, 2018, 40(8):63-78.
- [36] 游博文, 张国安, 李一鸣, 等. 近30年来长江口北支及口外沉积特征及输移趋势[J]. 长江流域资源与环境, 2018, 27(10):2328-2338.
- [37] 于元赫, 吕建树, 王亚梦. 黄河下游典型区域土壤重金属来源解析及空间分布[J]. 环境科学, 2018, 39(6):2865-2874.
- [38] 俞怡, 王锦龙, 黄德坤, 等. 海水中¹³¹I的快速检测技术[J]. 核化学与放射化学, 2018, 50(5):317-323.
- [39] 岳凯凯, 邓兵, 何荣, 等. 长江中下游悬浮物稀土元素地球化学特征及其对三峡工程的响应[J]. 地球与环境, 2018, 46(3):288-295.
- [40] 张家豪, 周丰年, 程和琴, 等. 多模态传感器系统在河槽边坡地貌测量中的应用[J]. 测绘通报, 2018, 3:102-107.
- [41] 张家豪, 周丰年, 程和琴, 等. 基于多模态传感器系统的长江下游窝崩边坡稳定性分析[J]. 自然灾害学报, 2018, 27(1):155-162.
- [42] 张晶晶, 刘东艳, 孙慧慧, 等. 液质联用技术在测定浮游植物色素与粒级分类中的应用[J]. 海洋通报, 2018, 37(2):158-164.
- [43] 张霞, 林春明, 杨守业, 等. 晚第四纪钱塘江下切河谷充填物物源特征[J]. 古地理学报, 2018, 20(5):877-892.
- [44] 张元, 童春富. 长江口盐沼湿地无齿螳臂相手蟹 (*Chiromantes dehaani*) 胃含物特征与取食偏好[J]. 生态学杂志, 2018, 37(7):2059-2066.
- [45] 郑崇伟. 21世纪海上丝绸之路:风能资源详查[J]. 哈尔滨工程大学学报, 2018, 39(1):16-22.
- [46] 郑树伟, 程和琴, 石盛玉, 等. 长江大通至徐六泾水下地形演变的人为驱动效应[J]. 中国科学:地球科学, 2018, 48(5):112-122.
- [47] 朱建荣, 白凤朋. 引江济淮工程对长江口咸潮入侵的影响研究[J]. 三峡生态环境监测, 2018, 3(3):60-65.
- [48] 朱晓桐, 衣俊, 强丽媛, 等. 长江口潮滩表层沉积物中微塑料的分布及沉降特点[J]. 环境科学, 2018, 39(5):2067-2074.

专著、章节

Books and Chapters

- [1] Du J, Shi B, Li J, Wang Y. Muddy Coast off Jiangsu, China: physical, ecological, and anthropogenic processes. In book: Sediment Dynamics of Chinese Muddy Coasts and Estuaries: Physics, Biology and Their Interactions, Elsevier, 2018, Chapter 3:25-49.
- [2] Gao S. Geomorphology and sedimentology of tidal flats. In book: Coastal wetlands: an ecosystem integrated approach (second edition). Elsevier 2018, Chapter10: 359-381.
- [3] Liu D, Zhou M. Green Tides of the Yellow Sea: Massive Free-Floating Blooms of *Ulva prolifera*. In book: Global Ecology and Oceanography of Harmful Algal Blooms, Springer, 2018.
- [4] Zhao S, Zhu L, Gao L, Li D. Limitations for Microplastic Quantification in the Ocean and Recommendations for Improvement and Standardization. In book: Microplastic Contamination in Aquatic Environments, Elsevier, 2018, Chapter 2:27-29.
- [5] 高抒. 《走向蓝色海洋》, 中国文史出版社, 2018.
- [6] 汤臣栋, 马强, 葛振鸣. 《上海崇明东滩鸟类国家级自然保护区科学研究》, 高等教育出版社, 2018.

获奖与专利 Awards & Patents

Innovation prize in marine science technology

由我室程和琴教授领衔完成的科研成果“长江口海平面上升对上海城市安全影响及其应对关键技术研究”荣获2018年度上海市水务海洋科学技术奖二等奖。

The project entitled “Research on the impact of rising sea level on the city security and key adaptive technologies” awarded the second prize of Shanghai Marine Science and Technology Award in 2018.

该项目由华东师范大学河口海岸学国家重点实验室牵头，联合校内城市与区域科学学院、生态与环境科学学院和上海市水务局及其所属的上海市水务规划设计研究院等上海市涉水相关研究与管理机构，首次定量评估了2011-2030年三峡大坝及河口重大工程对上海相对海平面上升的贡献，将IPCC第一至第五次评估报告有关海平面上升的气候变暖、构造沉降和城市开采地下水等3个原因扩展至5个原因。揭示了近期长江口相对海平面上升导致长江潮区界洪季上移82 km，枯季上移220 km，致使长江中下游干流河槽侵蚀性地貌显著发育；近百年来长江口北港、北槽和南槽三个入海汊道拦门沙向下游移动，其在未来相对海平面上升与来沙持续减少叠加作用下将向陆方向移动；上海沿海侵蚀型岸滩发育，滩底刷深约1.0 m，海平面上升将引起岸线后退2-7%，提出了构建盐沼—牡蛎礁生态工程的应对措施。模拟分析了人口增长、来沙减少和海平面上升等因子叠加下长江口水源地水资源量、供水安全风险，研制海平面上升背景下长江口水源地供水安全模型和预警系统；提出了应对海平面上升的近、中、远期上海行动指南。该项目出版专著1部，发表论文42篇，获得软件著作权1项。成果已应用于《上海市海塘规划(2011-2020年)》(沪府[2013]88号文)和国家防总《长江口咸潮应对工作预案》(国汛[2015]1号文)、上海市国土规划部门《上海市地面沉降防治管理条例》等重要文件的制定和长江口深水航道治理上，也已应用于上海市政府其他有关部门和单位应对海平面上升以尽早防御防汛、供水、交通等涉水灾害，有力保障了上海市涉水公共安全，经济与社会效益显著且巨大。

This project is hosted by SKLEC, and in collaboration with the School of Urban and Regional Science and School of Ecological and Environmental Sciences of East China Normal University, and Shanghai Water Authority, Shanghai Water Planning Design and Research Institute. The research team quantitatively assessed for the first time the contribution of the Three Gorges Dam and major estuarine engineering projects to Shanghai's relative sea level rise (SLR) by 10-16 cm in 2011-2030. This contribution expanded two more behaviors of local SLR in the Yangtze estuary from conventional three as climate warming, tectonic subsidence and urban groundwater exploitation reported in the first to fifth IPCC assessment report. To cope with these five SLR behaviors, five natural and anthropogenic behaviors of tidal limit, morphology of riverbed and tidal flat, fresh water supply and guidelines for urban action obtained. They were by the data analysis of historical and field measured records of water level, population, depth, flow velocity, sediments and morphology by using sophisticated instruments in our SKLEC as ADCP, SeaBat 7125 multibeam sonar, Riegl-VZ-4000 terrestrial laser scanner, Edgetech-3100p sub-bottom profiler along main channels from the estuarine front to the Three Gorges Dam. Firstly, tidal limit had moved 82 km upstream wards in flood season and 220 km in dry season for past decade. The migration resulted in the significant development of erosive geomorphology in the middle and lower reaches of the Yangtze River. Secondly, the mouth bars had moved downstream wards in three main channels of North Channel, North Passage and South Passage except the North Branch for past hundred years. Nevertheless, the simulation results of the Boolean network model display these mouth bars will move upstream wards. Thirdly, the eroded tidal flat along the Shanghai coast have been well-developed, closure depth increase 1 m, the coastline will retreat by 2-7%, and consequently, the construction of salt marsh-oyster reef ecological engineering to cope with the future SLR has been proposed to the local government of Shanghai. Fourthly, a fresh water supply security model was constructed and an early warning system explored in the Shanghai area. Fifthly, a short-, medium- and long-term Shanghai Action Guidelines to cope with SLR put forward. Published a book, 42 papers, and a software copyright.

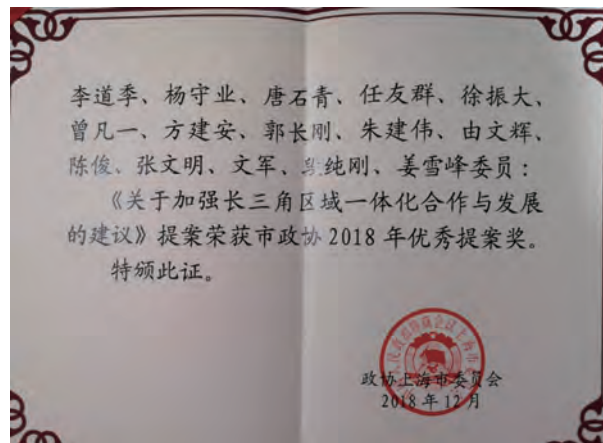
The above results used into the formulation of important urban planning of local or central government as Shanghai Seawall Planning (2011-2020) by Shanghai Water Authority [2013], (No. 88 Shanghai Government) and

Pre-arranged Plan for Salt Tide in Yangtze Estuary (No. 1 of State Flood Control and Drought Relief Headquarters [2015]). They also used to the Regulations on Land Subsidence Prevention and Control in Shanghai City by Shanghai Urban Planning and Land Resources Bureau, adopted by the Shanghai Municipal People's Congress and the regulation of Deep Waterway in the Yangtze Estuary. They also effectively guarantee the public safety of Shanghai's water-related activities with remarkable economic and social benefits.

Excellent Proposal Award

由我室李道季教授领衔的政协委员提案“关于加强长三角区域一体化合作与发展的建议”荣获上海市政协2018年优秀提案奖。

The proposal entitled “Suggestions on strengthening the regional integration cooperation and development of the Yangtze River delta” was awarded the Excellent Proposal Award by Shanghai CPPCC in 2018.



发明专利 Invention Patent

2018年度，实验室获批2项发明专利。
In 2018, SKLEC was authorized 2 National Invention Patents.

| 专利名称 Patent Name | 发明人 Inventor | 专利号 Patent Number |
|--------------------------|-------------------|----------------------|
| 一种基于膜入口质谱仪分析溶解态氮同位素含量的方法 | 侯立军; 刘敏; 尹国宇; 郑艳玲 | ZL 2013 1 0369577.5 |
| 一种连续提取沉积物样品中各形态硫的实验装置 | 瞿建国; 徐桂茹 | ZL 2015 1 0898993.3 |



实用新型专利 National Utility Model Patent

2018年度，实验室获批4项实用新型专利。
In 2018, SKLEC was authorized 4 National Utility Model Patents.

| 专利名称 Patent Name | 发明人 Inventor | 专利号 Patent Number |
|---------------------|--|----------------------|
| 一种多功能悬沙浓度标定系统 | 张文祥; 程武风; 朱琴; 章啸程; 苏国宾 张赛赛; 顾靖华; 胡进; 张丹; 崔贺 赵中豪; 陈晴; 沈裕莘 | ZL 2017 2 1812644.6 |
| 用于三维激光扫描系统的定位标靶装置 | 谢卫明; 何青; 王宪业; 郭磊城; 顾靖华 张迨 | ZL 2018 2 0723359.5 |
| 一种室内用滤纸法过滤水样悬浮物的装置 | 张丹; 张文祥 | 201820474650.3 |
| 一种批量制备小体积滤液样品的装置 | 崔莹 | 201820514958.6 |



标准制定 Standard establishment

我室唐剑武教授获得全国海洋标准化技术委员会2018年自然资源（海洋领域）标准制定项目，标准名称为“蓝碳生态系统碳库规模调查与评估技术规程 盐沼”，标准级别HYT，标准体系所述领域为蓝碳。

The standard setting project named “Carbon pool scale survey and assessment technical specification in blue carbon ecosystems•salt marsh” was awarded by the national technical committee on Marine standardization of China in 2018.

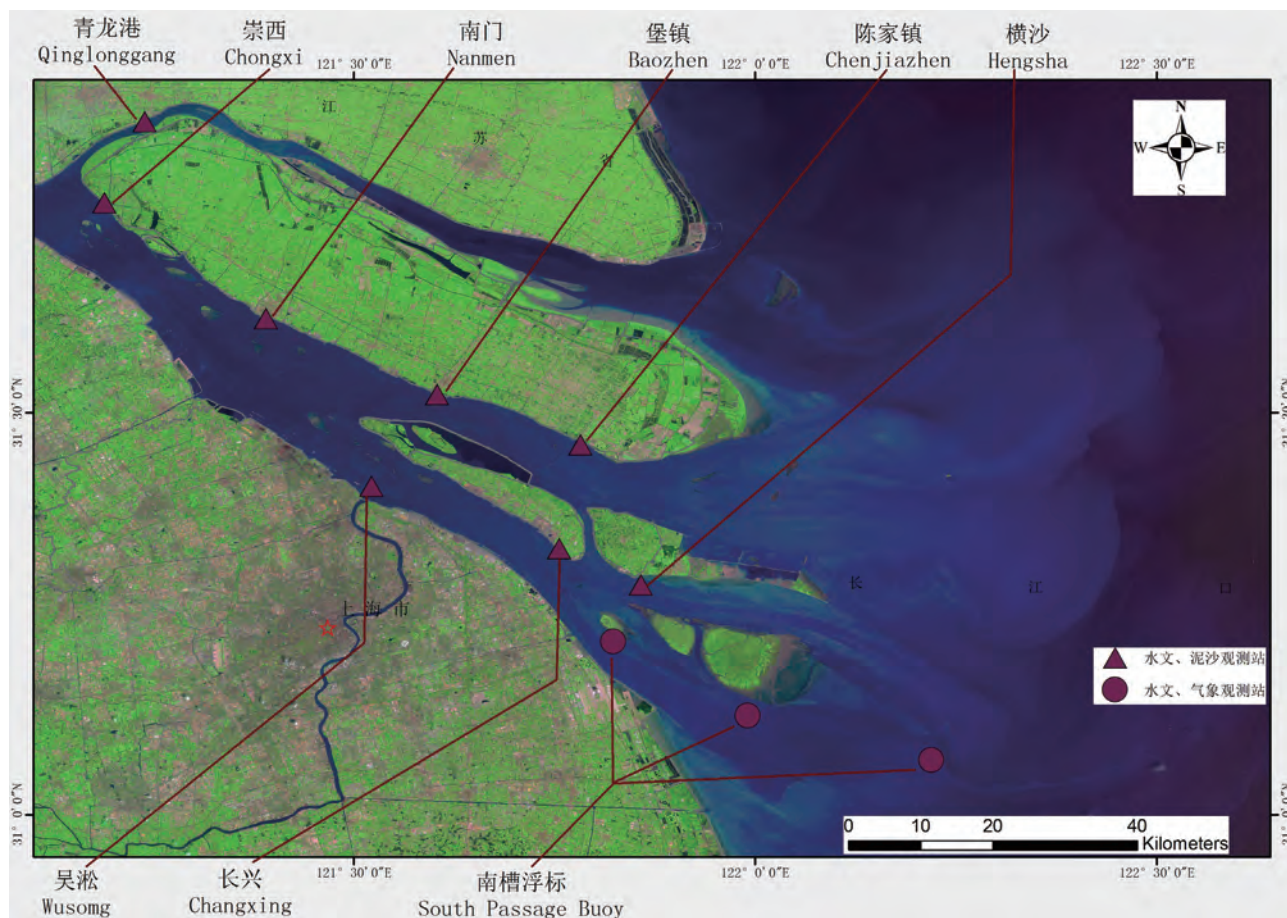


| 序号 | 项目编号 | 标准名称 | 级别 | 制修订 | 负责起草单位 | 计划完成年限 | 标准体系所属领域 | 标准化指导人员 |
|----|--------------|--------------------------------|------|-----|------------------|--------|----------|---------|
| 57 | 2018100104-T | 海洋经济融合数据库建设规范 | HY/T | 制定 | 国家海洋信息中心 | 2020 | 海洋信息化 | 张燕珠 |
| 58 | 2018100105-T | 海洋数据共享目录规范格式 | HY/T | 制定 | 国家海洋信息中心 | 2020 | 海洋信息化 | 陈方芳 |
| 59 | 2018100106-T | 海洋应用软件集成 接口标准 | HY/T | 制定 | 国家海洋信息中心 | 2020 | 海洋信息化 | 陈方芳 |
| 60 | 2018100107-T | 海洋应用软件集成 身份认证技术规范 | HY/T | 制定 | 国家海洋信息中心 | 2020 | 海洋信息化 | 陈方芳 |
| 61 | 2018100108-T | 海洋生态企业数据模型规范 | HY/T | 制定 | 国家海洋信息中心 | 2020 | 海洋信息化 | 张燕珠 |
| 62 | 2018100109-T | 海洋生物信息元数据 | HY/T | 制定 | 国家海洋信息中心 | 2020 | 海洋信息化 | 陈方芳 |
| 63 | 2018100133-T | 蓝碳生态系统碳库评估技术规范 盐沼 | HY/T | 制定 | 华东师范大学 | 2020 | 蓝碳 | 陈 华 |
| 64 | 2018100134-T | 海洋资源生物碳库评估调查与评估技术规范 大型绿藻（短丝藻类） | HY/T | 制定 | 中国水产科学研究院黄海水产研究所 | 2020 | 蓝碳 | 陈 华 |
| 65 | 2018100135-T | 海洋资源生物碳库评估调查与评估技术规范 贝类（贻贝类） | HY/T | 制定 | 中国水产科学研究院黄海水产研究所 | 2020 | 蓝碳 | 真 华 |
| 66 | 2018100136-T | 海洋资源生物碳库评估调查与评估技术规范 红树林 | HY/T | 制定 | 江苏省海洋水产研究所 | 2020 | 蓝碳 | 陈 华 |
| 67 | 2018100137-T | 海洋资源生物碳库评估调查与评估技术规范 藻类 | HY/T | 制定 | 中国水产科学研究院黄海水产研究所 | 2020 | 蓝碳 | 真 华 |

平台设施与野外观测 Facilities & Field Observations

平台与设施 Facilities

实验室现有水文观测站包括崇明环岛水文站，包括横沙、长兴、堡镇、南门、崇西、永隆以及南槽3个浮标站。
The hydrological observation stations, including coastal stations such as Hengsha, Changxing, Baozhen, Nanmen, Chongxi, Yonglong and three buoys stations in the Southern Channel.



长江河口水文观测站分布图
Hydrological Stations in the Yangtze River Estuary

崇明遥感观测平台

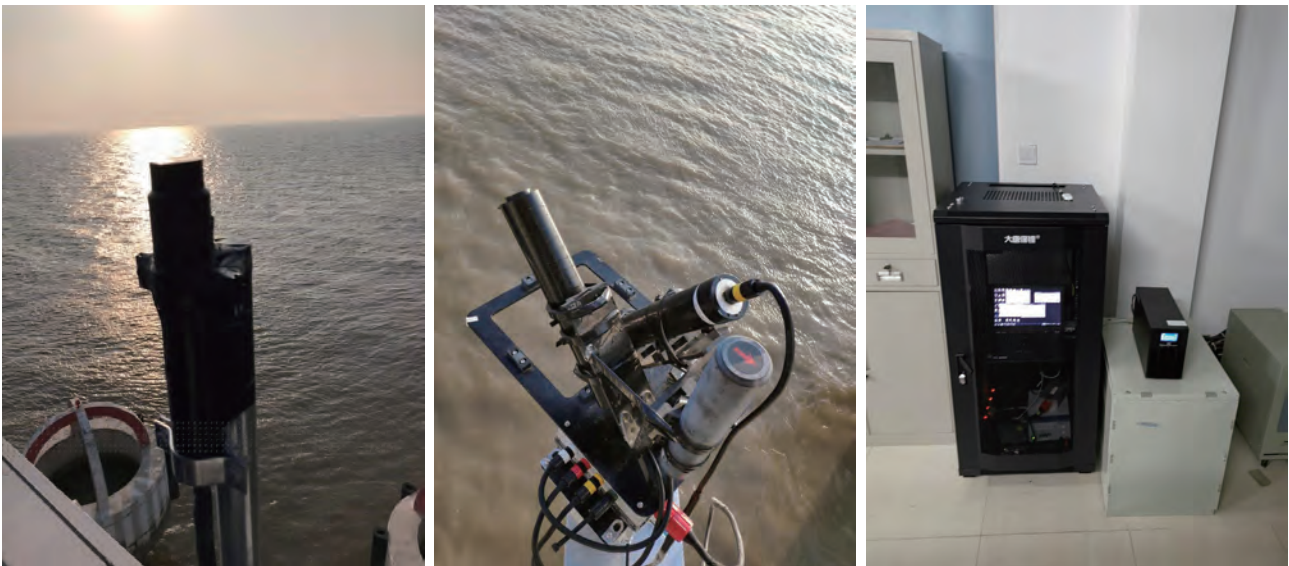
Remote sensing observation platform in Chongming

为获取河口区域长时间序列水质参数光学定量反演产品以及卫星遥感大气校正算法的开发与验证，我室在崇明堡镇水文站布设太阳跟踪式高光谱数据采集系统。

The remote sensing observation platform was set up by SKLEC in Baozhen hydrological observation station, in order to get optical quantitative inversion products of water quality parameters in long time series, and develop/validate related atmospheric correction algorithms for satellite remote sensing in estuary region.

太阳跟踪式高光谱数据采集系统由数据采集系统，自动跟踪装置以及计算机三部分组成。数据采集系统主要用于采集水体与天空光的辐射信息，自动跟踪装置用于水体光学信息采集时传感器探头与太阳相对方位的调整，计算机负责相关软件控制，数据远程传输以及处理分析。

There are three parts of solar tracking hyperspectral data acquisition system: data acquisition system, automatic tracking device and computer. The data acquisition system is mainly used to collect the radiation information of water and sky light, the automatic tracking device is used to adjust the relative azimuth between the sensor probe and the sun when collecting optical information of water, the computer is responsible for related software control, data remote transmission, data processing and analysis.



太阳跟踪式高光谱数据采集系统
Solar tracking hyperspectral data acquisition system

九段沙蓝碳监测系统

Jiuduansha blue carbon observation systems

实验室在九段沙湿地国家级自然保护区建成两座自有产权含叶绿素荧光（SIF）、二氧化碳/水（CO₂/H₂O）及甲烷（CH₄）的一体化‘蓝碳’实时观测塔站。

SKLEC established two blue carbon observation systems including SIF, CO₂/H₂O and CH₄ in Jiuduansha Wetland Nature Reserve of China.

LI-7500A开路式CO₂/H₂O涡度相关测量系统主要用于近地气层的瞬时三维风速脉动、温度脉动、H₂O脉动和CO₂脉动及CO₂通量、H₂O通量、显热通量、空气动量通量等地表与大气之间的物质与能量交换通量及磨擦风速等微气象特征量。

LI-7500A Open Path CO₂/H₂O Analyzer is a high speed, high precision, non-dispersive infrared gas analyzer that accurately measures densities of carbon dioxide and water vapor in turbulent air structures. With the eddy covariance

technique, these data are used in conjunction with sonic anemometer air turbulence data to determine the fluxes of CO_2 and H_2O .

Biomet101能量平衡系统（生物气象辅助传感器系统）主要用于净辐射四分量、光合有效辐射、降雨量、空气温度、空气相对湿度、土壤温度、土壤湿度、土壤热通量。Biomet101 system (biological and meteorological measurements) is mainly used to measure shortwave (upward and downward) and longwave (upward and downward) radiation, photosynthetically active radiation, precipitation, air temperature, relative humidity, soil temperature, soil moisture, and soil heat flux.

LI-7700甲烷分析仪重量轻，功耗低，高频响应，用于获取描述生态系统 CH_4 通量所必需的 CH_4 密度数据，是美国LI-COR公司历时4年研发测试后推出的全球第一款开路式甲烷测定设备。

LI-7700 Open Path CH_4 Analyzer makes in-situ measurement of methane density with the resolution, speed, and stability required for the eddy covariance technique.

高性能微型光谱仪QE-PRO用于测定盐沼植被冠层日光诱导叶绿素荧光（SIF）。

The Optical spectrometer QE-PRO is used to measure canopy scale solar-induced chlorophyll fluorescence of saltmarshes.



九段沙上沙野外全天候观测塔站，主要植被类型为芦苇



九段沙下沙野外全天候观测塔站，主要植被类型为互花米草

崇明东滩Argus视频观测系统 Argus video observation system

崇明东滩Argus海岸视频监测平台，是以27米高铁塔为搭载平台，集成多路高分辨率视频成像单元、网络传输单元、数据存储单元及图像处理系统，是集数据获取和分析的一体化实时监测平台。Argus平台获取海岸带实时视频图片数据，通过计算机视觉算法获取水边线、波浪、地貌和植被等关键参数，相比于传统海岸带监测手段，能有效减小自然条件对监测调查过程的影响，且无人值守，是极端天气条件下海岸带湿地监测的一种有效方式。为地貌学、水动力学及生态学等学科提供高时间分辨率、高空间分辨率和高精度的基础数据，也为潮滩演化机理和模型构建提供可靠的数据支撑。



Argus系统设计图

主要新增科研设备 (20万元以上) New Instruments for Field Survey

| 设备名称 Equipment | 型号 Type | 管理人员 Manager |
|-------------------|--------------|-----------------|
| 图形服务工作站 | DELL R7910 | 田波 |
| 视频存储阵列 | EMC 5400 | 田波 |
| Precon痕量气体预浓缩装置 | Precon | 侯立军 |
| 岩心切割机 | * | 张丹 |
| 温度梯度培养箱 | GRD1 | 侯立军 |
| 海底微地貌仪 | Model 2001 | 贾建军 |
| 平面型高纯锗探测器 | BE3830 | 杜金洲 |
| 井型高纯锗探测器 | GSW275L | 杜金洲 |
| 厌氧培养箱 | MP50-HS-SC | 侯立军 |
| 傅里叶显微红外光谱仪 | * | 施华宏 |
| 显微拉曼光谱仪 | * | 施华宏 |
| 河口锋面湍流观测设备 | MSS90 | 吴辉 |
| 便携式土壤呼吸测量系统 | SOILBOX-FMS | 童春富 |
| 盐度计 | 8400B | 张丹 |
| 现场激光粒度仪 | LISST 200X | 张文祥 |
| CO2监测系统 | * | Richard |
| 硝酸盐分析仪 | SUNA V2 | Richard |
| 新型数字流式细胞摄像系统 | Flowcam 8400 | Richard |
| 侵蚀微观实验系统 | UGEMS | 王宪业 |

野外调查 Field Observations

基金委长江口共享航次项目“长江口科学考察实验研究”2018年度野外调查 NSFC Public Cruise Fund “Scientific Observation on the Yangtze River Estuary” Observation in 2018

3月3日~3月21日、7月4~7月22日、10月9日~10月25日，国家自然科学基金委海洋科学共享航次“长江口科学考察实验研究”（航次编号：NORC2018-03）分别圆满完成冬季、夏季和秋季三个航段的野外作业内容。

Three cruises of NSFC Public Cruise Fund “Scientific Observation on the Yangtze River Estuary” in winter, summer and autumn were successfully completed.

本次调查由中国科学院海洋研究所“科学三号”和“创新二”号联合执行，中国科学院海洋研究所于仁成、王云峰、孔凡洲，华东师范大学张卫国、邓兵和浙江海洋大学李博分别担任现场首席科学家。国内涉海高校和海洋机构的78名科考队员参加了航次。

The cruises were jointly carried out by "Kexue No.3" and "Chuangxin No. 2" of Institute of Oceanology, Chinese Academy of Sciences (CAS). YU Rencheng, WANG Yunfeng, and KONG Fanzhou from Institute of Oceanology, CAS, ZHANG Weiguo and DENG Bing from East China Normal University, and LI Bo from Zhejiang Ocean University were the chief scientists in the field. There were 78 scientific staff attended the cruises.

此次考察项目包括物理海洋、海洋地质、海洋化学、海洋生物等内容。在科考队员的精心计划和船方的积极配合下，本航次安全、高效地完成任务书中断面和站位的观测与采样，同时还增做了一条33海里长测线的下切河谷浅剖与旁扫

声纳断面调查。

The observation of physical oceanology, marine geology, marine chemistry, and marine biology was covered. Along with the stations and sections in the project specification, one cross section survey about 33 nautical mile were carried.

张经院士研究团队执行东印度航次科考任务

Prof. ZHANG Jing's team carried out "Scientific Observation on the East Indian Ocean" cruise

3月，张经院士带领他的5位研究生弟子参加了“2018年国家自然科学基金委东印度洋共享航次”。本航次计划航时83天，航程约13000海里，设计综合站位100个。张经团队共计完成了痕量元素表层及剖面采样、溶解态铅的含量、铅在该海域的分布、行为的因素及其源、汇分析等多方面的计划任务。

In March, Prof. ZHANG Jing and five graduate students carried out "Scientific Observation on the East Indian Ocean" cruise which was funded by the NSFC. The cruise finished 100 stations, with a total of 83 days working at sea, and sailing about 13,000 nautical miles. During the cruise, multifaceted tasks such as trace elements sampling, the amount of dissolved lead, distribution and behavior of Lead were covered.



张经和他的学生们

人才培养 Student Programs

2018年实验室在读研究生307人，其中博士研究生140人，硕士研究生167人。
There are 307 postgraduate students in SKLEC, including 140 Ph.D. students and 167 M.Sc. students.

学位授予 Degrees Offered

硕士学位：自然地理学；物理海洋学；海洋化学；海洋生物学；海洋地质；生态学；环境科学；港口、海岸及近海工程

M.Sc. Programs: Physical Geography; Physical Oceanography; Marine Chemistry; Marine Biology; Marine Geology; Ecology; Environmental Science; Port Coastal and Offshore Engineering

博士学位：自然地理学；河口海岸学；物理海洋学；海洋化学；海洋生物学；海洋地质；生态学；环境科学

Ph.D. Programs: Physical Geography; Estuarine and Coastal Science; Physical Oceanography; Marine Chemistry; Marine Biology; Marine Geology; Ecology; Environmental Science

入学新生与毕业学生 The Freshmen and Graduates

2018年实验室共招收研究生90人，其中博士生37人（含留学生4人），硕士生53人；招收的博士生中直博生14人、硕博连读6人。2018年共毕业69人，其中博士生22人（含留学生2人），硕士生47人（含留学生1人），杨海飞、张家豪、罗浩、曲晓芸、王峰被评为2018年上海市优秀毕业生。

90 students were enrolled in 2018, including 37 Ph.D. and 53 M.Sc. students. 69 students graduated in 2018, including 22 Ph.D. and 47 M.Sc. students. YANG Haifei, ZHANG Jiahao, LUO Hao, QU Xiaoyun, WANG Feng were honored as Outstanding Graduate Student of Shanghai.

博士毕业生 List of Ph.D. Graduates

自然地理学/Physical Geography

| 姓名 Name | 导师 Supervisor | 毕业论文题目 Thesis | 就业单位 Employment |
|---------------------|---------------------|---|--|
| 郑斌鑫 ZHENG Binxin | 李九发 LI Jiufa | 台湾海峡及邻近海域未登陆台风激发的陆架陷波及水体输运过程 Coastal-trapped waves and water transport along the coast of Taiwan Strait and the adjacent sea caused by no-landfall typhoons | 自然资源部第三海洋研究所 Third Institute of oceanography, Ministry of Natural Resources |
| 魏稳 WEI Wen | 戴志军 DAI Zhijun | 长江河口边滩多时间尺度动力地貌过程 Multi-time-scale morphodynamics of the Changjiang estuarine marginal shoal | 华东师范大学 East China Normal University |
| 葛灿 GE Can | 张卫国 ZHANG Weiguo | 长江口-东海内陆架沉积物磁性特征及其指示意义 Magnetic properties of sediments in the Yangtze Estuary and adjacent inner shelf of the East China Sea and their environmental implications | 浙江省水利河口研究院 Zhejiang Institute of Hydraulics & Estuary |

| 姓名 Name | 导师 Supervisor | 毕业论文题目 Thesis | 就业单位 Employment |
|---------------------|-----------------------|--|--|
| 赖晓鹤 Lai Xiaohu | 陈中原 Chen Zhongyuan | 三峡建坝后河床冲刷过程与机理及其对入海泥沙通量的影响和预测 The process and mechanism of river channel erosion below Three Gorges Dam - its effect and prediction to sediment load into the sea | 福建省三明市委组织部 Organizatin Department of CPC Sanming Municipal Committee, Fujian Province |
| 郑树伟 Zheng Shuwei | 程和琴 Cheng Heqin | 长江汉口至吴淞口河槽冲淤与微地貌演变对人类活动的自适应行为研究 Adaptive behavior of channel morphodynamics and micro-geomophology evolution under human activities from Hankou to Wusongkou reach of the Yangtze River | 山东师范大学 Shandong Normal University |

地图学与地理信息系统/ Cartography and Geographical Information System

| 姓名 Name | 导师 Supervisor | 毕业论文题目 Thesis | 就业单位 Employment |
|-------------------|------------------|---|---|
| 潘燕群 Pan Yanqun | 沈芳 Shen Fang | 浑浊水体大气校正方法及典型水色参数的遥感反演研究 Studies on atompseric correction methods and remote sensing inversions of typical ocean color parameters over turbid waters | 加拿大魁北克大学里穆斯基分校 Université du Québec à Rimouski |

河口海岸学/Estuarine and Coastal Science

| 姓名 Name | 导师 Supervisor | 毕业论文题目 Thesis | 就业单位 Employment |
|--------------------|----------------------|--|---|
| 寿玮玮 Shou Weiwei | 丁平兴 Ding Pingxing | 大气沉降对渤海营养盐的贡献及生态效应 Contribution of Atompseric Deposition to the Nutrients and Its Ecological Effects in the Bohai | 浙江贵仁信息科技股份有限公司 Zhejiang Keepsoft Information and Technology Corp., Ltd. |
| 朱磊 Zhu Lei | 何青 He Qing | 河势变化下河口环流结构及变异研究 Alteration of estuarine circulation under the influence of morphological evolution | 中山大学 Sun Yat-sen University |
| 谢卫明 Xie Weiming | 何青 He Qing | 高浊度河口潮滩动力地貌过程及植被影响研究 Study on morphodynamic processes and the influence of vegetation in a high-turbidity estuarine tidal flat | 黄河水利科学研究院 Yellow River Institute of Hydraulic Research |
| 王晓娜 Wang Xiaona | 吴莹 Wu Ying | 光谱与色谱技术结合示踪溶解有机物在长江—东海的组成、来源及转化 Combined spectrum and chromatographic technique to trace the sources, compositions and transformations of dissolved organic matter in Changjiang-East China Sea continuum | |
| 郭超 Guo Chao | 何青 He Qing | 粘性泥沙絮凝沉降过程与控制机制研究 Cohesive sediment flocculation and settling processes and the controlling mechanisms | 长江水利委员会长江科学院 Changjiang River Scientific Research Institute of Changjiang Water Resources Commission |

| 姓名 Name | 导师 Supervisor | 毕业论文题目 Thesis | 就业单位 Employment |
|---------------------|----------------------|---|--|
| 夏凉 Xia Liang | 周俊良 Zhou Junliang | 药物类污染物对斑马鱼胚胎形态、行为和基因表达的生态毒理效应研究 Ecotoxicity of several pharmaceutical pollutants on embryo morphology, behavior and genetic expression in zebrafish | 艾本德（上海）国际贸易有限公司 Eppendorf Lab Technologies (Shanghai) Co., Ltd. |
| 李翔宇 Li Xiangyu | 朱建荣 Zhu Jianrong | 层化水体中的悬沙输运—长江口资料分析与数值模拟 Suspended Sediment Transport in Stratified Waters: Field Observation and Numerical Simulation of the Changjiang Estuary | 中山大学 Sun Yat-sen University |
| 陈义中 Chen Yizhong | 朱建荣 Zhu Jianrong | 青草沙水库富营养化生态动力学模式研发 Research on ecological dynamics model of Qingcaosha Reservoir eutrophication | 上海市环境科学研究院 Shanghai Academy of Environmental Sciences |
| 杨海飞 Yang Haifei | 杨世伦 Yang Shilun | 长江及其水下三角洲沉积物的沿程格局和近期变化 The spatial patterns and recent changes of the sediments in the Yangtze River and its subaqueous delta | 长江水利委员会长江口水温水资源勘测局 Changjiang River Estuary Bureau of Hydrology and Water Resources Survey, Changjiang Water Resources Commission |
| 程琳 Cheng Lin | 周俊良 Zhou Junliang | 典型污染物对成年中华绒螯蟹的短期生态毒理效应及作用机理研究 The ecotoxicological effects and mechanism of representative contaminants on adult Chinese mitten crab (<i>Eriocheir sinensis</i>) | 上海市农业科学院 Shanghai Academy of Agricultural Sciences |
| 罗志发 Luo Zhifa | 朱建荣 Zhu Jianrong | 长江口及其邻近海域泥沙输运及其动力机制 The sediment transport and its mechanism in changjiang estuary and its adjacent waters | 广东省水利水电科学研究院 Guangdong Research Institute of Water Resources and Hydropower |
| 衣俊 Yi Jun | 程金平 Cheng Jinping | 潮滩沉积物微生物群落表征及其对污染物的响应研究 Analysis of microbial community in intertidal wetlands and study of their responses to pollutants | |

生态学/Ecology

| 姓名 Name | 导师 Supervisor | 毕业论文题目 Thesis | 就业单位 Employment |
|-----------------|---------------------|--|--|
| 贺坤 He Kun | 李小平 Li Xiaoping | 烟气脱硫石膏控制平原河网地区农业面源磷流失的研究 Influence of Flue Gas Desulfurization Gypsum on Phosphorus Loss of Agricultural Non-point Source Pollution in Plain River Network Area | 上海应用技术大学 Shanghai Institute of Technology |
| 王恒 Wang Heng | 张利权 Zhang Liquan | 河口湿地时空动态及其影响因子的尺度效应 The spatio-temporal dynamics of estuarine wetlands and the scaling effects of the influencing factors | 中山大学 Sun Yat-sen University |

环境科学/Environmental Science

| 姓名 Name | 导师 Supervisor | 毕业论文题目 Thesis | 就业单位 Employment |
|-------------------------|--------------------|---|--|
| SELEMANI JUMA RAJABU | 张经 Zhang Jing | 坦桑尼亚潘加尼河流域水体影响因素：水量及水质对人类及水生生态系统健康的影响 Factors influencing water of Pangani River Basin, Tanzania: implication of water quality and quantity for human and aquatic ecosystem health | 坦桑尼亚曼德拉非洲科学技术研究院 Nelson Mandela African Institution of Science and Technology, Tanzania |
| JABEEN KHALIDA | 施华宏 Shi Huahong | 中国近海和淡水鱼体内微塑料的研究 Characteristics of microplastics in fish from coastal and fresh waters of China | |

硕士毕业生List of M.Sc. Graduates

自然地理学/Physical Geography

| 姓名/Name | 导师/Supervisor | 姓名/Name | 导师/Supervisor |
|-------------------|--------------------|------------------|--------------------|
| 朱栾/Zhu Luan | Richard Bellerby | 王杰/Wang Jie | 戴志军/Dai Zhijun |
| SHEASHAA HADEER | 陈中原/Chen Zhongyuan | 王淑平/Wang Shuping | 李占海/Li Zhanhai |
| 葛芳/Ge Fang | 周云轩/Zhou Yunxuan | 杨孟毅/Yang Mengyi | 蒋雪中/Jiang Xuezhong |
| 李一鸣/Li Yiming | 张国安/Zhang Guoan | 于亚文/Yu Yawen | 戴志军/Dai Zhijun |
| 田原原/Tian Yuanyuan | 陈沈良/Chen Shenliang | | |

物理海洋学/Physical Oceanography

| 姓名/Name | 导师/Supervisor | 姓名/Name | 导师/Supervisor |
|------------|---------------|-------------------|---------------|
| 白玫/Bai Mei | 吴辉/Wu Hui | 汪永超/Wang Yongchao | 沈芳/Shen Fang |

海洋化学/Marine Chemistry

| 姓名/Name | 导师/Supervisor | 姓名/Name | 导师/Supervisor |
|----------------|---------------|----------------|---------------|
| 李昶/Li Chang | 邓兵/Deng Bing | 岳凯凯/Yue Kaikai | 邓兵/Deng Bing |
| 曹梦莉/Cao Mengli | 吴莹/Wu Ying | 李明/Li Ming | 吴莹/Wu Ying |

海洋生物学/ Marine Biology

| 姓名/Name | 导师/Supervisor | 姓名/Name | 导师/Supervisor |
|-------------------|---------------|------------------|---------------|
| 高永强/Gao Yongqiang | 高磊/Gao Lei | 江沛霖/Jiang Peilin | 李道季/Li Daoji |

海洋地质/ Marine Geology

| 姓名/Name | 导师/Supervisor | 姓名/Name | 导师/Supervisor |
|-----------------|----------------|-------------------|--------------------|
| 代斌/Dai Bin | 孙千里/Sun Qianli | 杨钦川/Yang Qinchuan | 陈庆强/Chen Qingqiang |
| 刘健辉/Liu Jianhui | 陈静/Chen Jing | 姚振兴/Yao Zhenxing | 陈庆强/Chen Qingqiang |

生态学/Ecology

| 姓名/Name | 导师/Supervisor | 姓名/Name | 导师/Supervisor |
|---------------|------------------|-----------------|--------------------|
| 张元/Zhang Yuan | 童春富/Tong Chunfu | 王峰/Wang Feng | 刘权兴/Liu Quanxing |
| 吴昊楠/Wu Haonan | 毛秀光/Mao Xiuguang | 王琰/Wang Yan | 童春富/Tong Chunfu |
| 费蓓莉/Fei Beili | 葛振鸣/Ge Zhenming | 邢宇彤/Xing Yutong | 毛秀光/Mao Xiuguang |
| 李诗华/Li Shihua | 袁琳/Yuan Lin | 徐艳/Xu Yan | 闫中正/Yan Zhongzheng |

| | | | |
|-----------------|--------------------|-----------|-----------------|
| 李伟/Li Wei | 袁琳/Yuan Lin | 尤迪/You Di | 童春富/Tong Chunfu |
| 孙秀丽/Sun Xiangli | 闫中正/Yan Zhongzheng | | |

环境科学/Environmental Science

| 姓名/Name | 导师/Supervisor | 姓名/Name | 导师/Supervisor |
|----------------|-------------------|------------------|-------------------|
| 操珍/Cao Zhen | 周俊良/Zhou Junliang | 余晨笛/Yu Chendi | 侯立军/Hou Lijun |
| 刘雪/Liu Xue | 周俊良/Zhou Junliang | 俞怡/Yu Yi | 张芬芬/Zhang Fenfen |
| 曲晓芸/Qu Xiaoyun | 施华宏/Shi Huahong | 朱晓桐/Zhu Xiaotong | 程金平/Cheng Jinping |

港口、海岸及近海工程/Port, Coastal and Offshore Engineering

| 姓名/Name | 导师/Supervisor | 姓名/Name | 导师/Supervisor |
|-----------------|-----------------|------------------|-----------------|
| 李远/Li Yuan | 李占海/Li Zhanhai | 王浩斌/Wang Haobin | 杨世伦/Yang Shilun |
| 艾威/Ai Wei | 李茂田/Li Maotian | 王梦寒/Wang Menghan | 王宪业/Wang Xianye |
| 陈钢/Chen Gang | 程和琴/Cheng Heqin | 张家豪/Zhang Jiahao | 程和琴/Cheng Heqin |
| 陈思明/Chen Siming | 王宪业/Wang Xianye | 朱平/Zhu Ping | 吴辉/Wu Hui |
| 沈逸/Shen Yi | 何青/He Qing | | |

公派留学

Oversea Study Supported by China Scholarship Council

2018年，实验室共有19位学生获公派留学资格，赴美国、英国、澳大利亚、荷兰等国家接受联合培养，其中5位学生为我室2018年新申请获批的国家留学基金委“创新型人才国际合作培养项目”资助。

Nineteen students were supported by China Scholarship Council scholarships to study abroad (USA, UK, Australia, the Netherlands, etc.), among which 5 were supported by CSC International Cooperative Program for Innovative Talents (ICIT).

联合培养/Ph.D. Degree to be Offered Jointly with SKLEC

| 姓名 Name | 国内导师 Supervisor | 申报国别/地区 Country/Region | 留学单位 Oversea institute | 备注 Remarks |
|----------------------|----------------------|---------------------------|--|-------------------------------|
| 湛玉剑 Zhan Yujian | 周云轩 Zhou Yunxuan | 荷兰 the Netherlands | 代尔夫特理工大学/Delft University of Technology | 创新人才项目，双学位/ICIT, Dual Diploma |
| 周在扬 Zhou Zaiyang | 丁平兴 Ding Pingxing | 荷兰 the Netherlands | 代尔夫特理工大学/Delft University of Technology | 创新人才项目，双学位/ICIT, Dual Diploma |
| 张雨宁 Zhang Yuning | 何青 He Qing | 荷兰 the Netherlands | 代尔夫特理工大学/Delft University of Technology | 创新人才项目，双学位/ICIT, Dual Diploma |
| 彭谷雨 Peng Guyu | 李道季 Li Daoji | 挪威 Norway | 罗格斯大学/Rutgers University | 创新人才项目/ICIT |
| 李双双 Li Xiaoshuang | Richard Bellerby | 挪威 Norway | 水环境研究所/Norwegian Institute for Water Research | 创新人才项目/ICIT |
| 李亚南 Li Yanan | 杜金洲 Du Jinzhou | 美国 USA | 伍兹霍尔海洋研究所/Woods Hole Oceanographic Institution | |
| 陈小刚 Chen Xiaogang | 杜金洲 Du Jinzhou | 澳大利亚 Australia | 南十字星大学/Southern Cross University | |

| | | | |
|------------------------|-----------------------|-------------------|--|
| 蒋硕 Jiang Shuo | 张经 Zhang Jing | 美国 USA | 麻省理工学院/Massachusetts Institute of Technology |
| 吕行行 Lv Hanghang | 朱建荣 Zhu Jianrong | 英国 UK | 利物浦大学/University of Liverpool |
| 蒋杰 Jiang Jie | 何青 He Qing | 美国 USA | 威廉玛丽学院/College of William & Mary |
| 姬泓宇 Ji Hongyu | 陈沈良 Chen Shenliang | 英国 UK | 卡迪夫大学/Cardiff University |
| 赵小双 Zhao Xiaoshuang | 陈中原 Chen Zhongyuan | 澳大利亚 Australia | 墨尔本大学/The University of Melbourne |
| 王龙 Wang Long | 王张华 Wang Zhanghua | 新加坡 Singapore | 南洋理工大学/Nanyang Technological University |
| 张淼 Zhang Miao | 吴莹 Wu Ying | 德国 Germany | 亥姆霍兹慕尼黑研究中心-德国环境健康研究中心/Helmholtz Zentrum München - German Research Center for Environmental Health |
| 孙雪融 Sun Xuerong | 沈芳 Shen Fang | 英国 UK | 普利茅斯海洋实验室/Plymouth Marine Laboratory |
| 强丽媛 Qiang Liyuan | 程金平 Cheng Jinping | 美国 USA | 新泽西州立罗格斯大学/Rutgers, The State University of New Jersey |
| 牛文蕾 Niu Wenlei | 王张华 Wang Zhanghua | 新加坡 Singapore | 南洋理工大学 Nanyang Technological University |
| 王硕 Wang Shuo | 王张华 Wang Zhanghua | 美国 USA | 马里兰大学东海岸分校/University of Maryland Eastern Shore |
| 徐韦 Xu Wei | 程和琴 Cheng Heqin | 美国 USA | 路易斯安纳州立大学/Louisiana State University |

海外研修 Overseas Visiting

2018年，实验室有4位同学赴美国、荷兰进行交流访学。

Three students went abroad (USA, the Netherlands) as visiting students.

| 姓名/Name | 访学单位/Visiting institute | 起止时间/Date |
|--------------------|--|-----------------|
| 高娟 Gao Juan | 美国莱特州立大学 Wright State University, USA | 2017.11-2018.01 |
| 赵旋琪 Zhao Xuanqi | 美国路易斯安那州立大学 Louisiana State University, USA | 2018.09-2019.08 |
| 赵丽侠 Zhao Lixia | 荷兰皇家海洋研究院 Royal Netherlands Institute for Sea Rese, the Netherlands | 2018.10-2019.10 |
| 张婷 Zhang Ting | 美国威廉玛丽学院 College of William & Mary, USA | 2018.10-2019.03 |

研究生科研成果

Research Outputs Contributed by Graduate Students

2018年研究生发表第一作者论文85篇，占实验室第一作者论文总数的65%，其中SCI/SCIE论文62篇（I区文章2篇，II区文章29篇），占实验室第一作者SCI/SCIE论文的61%。实验室学生中有17人次参加国际学术会议，其中7人做口头报告。

The graduate students published 85 papers as first authors, among which 62 papers were published in SCI/SCIE journals. Seventeen (17) students attended international conferences with 7 oral presentations.

公众服务

Outreach

5月26日，实验室开展了主题为“‘一带一路’与河口海岸”公众开放日活动，活动吸引了80多位社会各界人士积极参与，包括在校大学生，研究生，退休教师，公司白领等。

On May 26, 2018, SKLEC Public Open Day attracted more than 80 visitors including university teachers, students and workers.

为促进优秀大学生之间的思想交流，扩大河口海岸学国家重点实验室在国内相关院校中的影响力，提高实验室研究生生源质量，由我校研究生院主办、河口海岸学国家重点实验室承办的“2018年河口海岸学优秀大学生夏令营”于2018年7月9日至12日在我校举行。通过高校推荐和河口海岸学国家重点实验室的选拔，共有来自国内二十多所高校的34名大学生参加本次夏令营。

Under the guidance of East China Normal University, SKLEC hosted Excellent Students' Summer School of Estuarine and Coastal Science during July 9-12, 2018. According to recommendation from universities and SKLEC's selection, finally, there were 34 excellent students that participated in the programme.

7月26日，实验室与中国航海博物馆签署合作协议，未来双方将根据协议内容互通有无，在多个领域开展深入的交流与合作，力求积极响应国家科技创新与科学普及发展战略，更好地推进河口海岸科学知识的传播。

On July 26, 2018, SKLEC signed the MOU with China Maritime Museum.

8月20-21日，荷兰代尔夫特理工大学本科生夏令营访问了河口海岸学国家重点实验室。李秀珍教授讲解了我室的发展历史及对国家和地方做出的贡献，介绍了相关的学科知识，并带领他们访问了我校崇西湿地科学实验站和崇明东滩湿地公园。

Undergraduate students of the Delft University of Technology visited SKLEC from the 20th August, 2018. Professor LI Xiuzhen introduced some information about SKLEC.

11月17-18日，实验室应邀参加了上海自然博物馆的“科学家面对面”活动，实验室钟强强和张雨宁两位博士研究生同学，代表实验室携手向公众介绍了放射性核素在近岸海洋-大气-水环境中的应用科学研究成果，引起了现场中学生的浓厚兴趣。

In November, 2018, SKLEC attended the “Talk to Scientists” event hosted by the Shanghai Museum of Natural History. Doctoral students ZHONG Qiangqiang and ZHANG Yuning attended the event.

海洋科学（含港口、海岸及近海工程）学位评定分委员会

主任：高抒

副主任：何青、杜金洲

委员：高磊、贾建军、李道季、刘东艳、汪亚平、吴辉

Marine Science (including Port Coastal and Offshore Engineering) Committee for Academic Degree Assessment

Chair: Gao Shu

Deputy Chair: He Qing, Du Jinzhou

Members: Gao Lei, Jia Jianjun, Li Daoji, Liu Dongyan, Wang Yaping, Wu Hui

研究队伍 Research Staff

2018年，重点实验室引进研究人员22人，现有固定人员93人（其中研究人员83人，技术人员7人，管理人员3人）。
Twenty two research members joined SKLEC in 2018. There are 93 fulltime members, including 83 academic research members, 7 technical members and 3 administrative members.

固定人员 Faculty and Staff

教授 Professors

| 姓名 Title | 研究专长 Research Interest | Email |
|---------------------------|---|---|
| 陈 静 Dr. Chen Jing | 第四纪地质学 Quaternary Geology | jchen@geo.ecnu.edu.cn |
| 陈庆强 Dr. Chen Qingqiang | 海洋沉积学；环境与生物地球化学 Marine Sedimentology; Environmental Geochemistry & Biogeochemistry | qqchen@sklec.ecnu.edu.cn |
| 陈沈良 Dr. Chen Shenliang | 海岸动力地貌；三角洲侵蚀与脆弱性 Coastal Morphodynamics; Delta Erosion and Vulnerability | slchen@sklec.ecnu.edu.cn |
| 陈中原 Dr. Chen Zhongyuan | 河流-三角洲沉积地貌过程；水文地貌过程；环境考古 River-Delta Sedimentological and Geomorphological Processes; Geoarchaeology | z.chen@sklec.ecnu.edu.cn |
| 程和琴 Dr. Cheng Heqin | 河口海岸动力沉积学；工程地貌与环境；海岸带管理 Estuarine and Coastal Dynamic Sedimentation; Engineered Morphodynamics and Environment; Integrated Coastal Management | hqch@sklec.ecnu.edu.cn |
| 戴志军 Dr. Dai Zhijun | 河口海岸动力地貌 Estuarine and Coastal Morphodynamics | zjdai@sklec.ecnu.edu.cn |
| 丁平兴 Dr. Ding Pingxing | 潮滩动力学及数值模型；波-流与泥沙运输 Coastal Dynamics and Numerical Modeling; Sediment Transport by Waves and Currents; | pxding@sklec.ecnu.edu.cn |
| 董宏坡 Dr. Dong Hongpo | 海洋微生物分子生态；海洋微生物适应环境的分子基础；海洋微生物参与元素循环的过程和机理 Molecular Ecology of Marine Microorganisms; Molecular Foundation of Marine Microorganisms for Environmental Adaptation; Processes and Mechanisms of Marine Microorganisms Involved in Biogeochemical Cycles | hpdong@sklec.ecnu.edu.cn |
| 杜金洲 Dr. Du Jinzhou | 同位素海洋学；环境放射化学 Oceanography of Isotopes; Environmental Radiochemistry | jzdu@sklec.ecnu.edu.cn |
| 高 抒 Dr. Gao Shu | 海洋沉积动力学 Marine Sediment Dynamics | sgao@sklec.ecnu.edu.cn shugao@nju.edu.cn |

| 姓名 Title | 研究专长 Research Interest | Email |
|---------------------------|--|---|
| 何青 Dr. He Qing | 河口海岸水动力学; 河口海岸泥沙运动学 Estuarine and Coastal Hydrodynamics; Estuarine and Coastal Sediment Transport | qinghe@sklec.ecnu.edu.cn |
| 葛振鸣 Dr. Ge Zhenming | 气候变化与生态系统碳过程; 生态模型; 湿地生态学 Climate Change & Ecosystem Carbon-process; Ecological Model; Wetland Ecology | zmge@sklec.ecnu.edu.cn |
| 侯立军 Dr. Hou Lijun | 环境地理学; 环境地球化学 Environmental Geography; Environmental Geochemistry | ljhou@sklec.ecnu.edu.cn |
| 贾建军 Dr. Jia Jianjun | 河口海岸沉积动力过程、记录与地貌效应; 海洋空间资源 管理的支撑技术 Estuarine and coastal sediment dynamics and morphology; Techniques supporting marine spatial resources management; | jjjia@sklec.ecnu.edu.cn |
| 姜晓东 Dr. Jiang Xiaodong | 浮游动物适应与进化 Adaptation and Evolution of Zooplankton | xdjiang@bio.ecnu.edu.cn |
| 李超 Dr. Li Chaoj | 发育生物学 Developmental Biology | cli1@biochem.umass.edu |
| 李道季 Dr. Li Daoji | 生物海洋学; 河口和近岸海域生态系统 Biological Oceanography; Estuarine and Coastal Ecosystem | daojili@sklec.ecnu.edu.cn |
| 李秀珍 Dr. Li Xiuzhen | 景观生态学; 湿地生态学; 遥感与地理信息系统应用 Landscape Ecology; Wetland Ecology; Application of Remote Sensing and GIS | xzli@sklec.ecnu.edu.cn |
| 刘东艳 Dr. Liu Dongyan | 海洋藻类生态学 Marine Algae Ecology | dyliu@sklec.ecnu.edu.cn |
| 刘权兴 Dr. Liu Quanxing | 系统生态学 Systems Ecology | qxliu@sklec.ecnu.edu.cn |
| Dr. Richard Bellerby | 海洋生物地球化学循环 Marine Biogeochemical Cycles | Richard.Bellerby@niva.no richard@sklec.ecnu.edu.cn |
| 沈芳 Dr. Shen Fang | 河口近岸水色遥感; 遥感技术与GIS综合应用 Coast / Ocean Colour Remote Sensing; Integrated Applications of GIS and Remote Sensing Technology | fshen@sklec.ecnu.edu.cn |
| 施华宏 Dr. Shi Huahong | 生态毒理学; 生物监测; 环境与健康 Ecotoxicology; Biomonitoring; Environment and Health | hhshi@des.ecnu.edu.cn |
| 唐剑武 Dr. Tang Jianwu | 湿地生态学; 碳循环、全球变化生态学 Wetland Ecology; Carbon Cycling, Global Change Ecology | jwtang@sklec.ecnu.edu.cn |
| 王群 Dr. Wang Qun | 水生生物学 Aquatic Biology | qwang@bio.ecnu.edu.cn |

| 姓名 Title | 研究专长 Research Interest | Email |
|--|---|---------------------------|
| 汪亚平 Dr. Wang Yaping | 海洋沉积动力过程与数值模拟; 河口海岸物质循环与运输 Ocean Sediments Dynamic Process and Numerical Simulation; Substances Transports and Circulation in Estuarine and Coastal Areas | ypwang@sklec.ecnu.edu.cn |
| 王张华 Dr. Wang Zhanghua | 河口-三角洲沉积地貌环境演变 Sedimentary and Morphological Evolution of Estuary and Delta | zhwang@geo.ecnu.edu.cn |
| 吴莹 Dr. Wu Ying | 海洋有机地球化学; 海洋生物地球化学 Marine Organic Geochemistry; Marine Biogeochemistry | wuying@sklec.ecnu.edu.cn |
| 夏建阳 Dr. Xia Jianyang | 全球变化生态学 Global Change Ecology | jyxia@des.ecnu.edu.cn |
| 杨嘉龙 Dr. Yang Jialong | 海洋生物学 Marine Biology | jlyang@bio.ecnu.edu.cn |
| 杨世伦 Dr. Yang Shilun | 海岸湿地沉积动力过程; 河口对流域变化的响应 Sediment Dynamic Processes in Coastal Wetlands; Estuarine Response to Impacts from River Basin | slyang@sklec.ecnu.edu.cn |
| 杨毅 Dr. Yang Yi | 新型有机污染物研究 Emerging Organic Pollutants | yyang@geo.ecnu.edu.cn |
| 赵云龙 Dr. Zhao Yunlong | 水生生物学 Aquatic Biology | ylzhao@bio.ecnu.edu.cn |
| 张经院士 Dr. Zhang Jing Academician of CAS | 生物地球化学与化学海洋学 Biogeochemistry and Chemical Oceanography | jzhang@sklec.ecnu.edu.cn |
| 张卫国 Dr. Zhang Weiguo | 环境磁学; 环境演变; 环境污染 Environmental Magnetism; Environmental Change; Environmental Pollution | wgzhang@sklec.ecnu.edu.cn |
| 周俊良 Dr. Zhou Junliang | 污染物河口地球化学; 新型污染物分析; 污染物毒理学 Estuarine Pollutant Geochemistry; Emerging Contaminant Analysis; Environmental Toxicity | jlzhou@sklec.ecnu.edu.cn |
| 周旭辉 Dr. Zhou Xuhui | 生态系统生态学 Ecosystem Ecology | xhzhou@des.ecnu.edu.cn |
| 周云轩 Dr. Zhou Yunxuan | 海岸带资源与环境遥感; 土地利用与覆盖变化; 地理信息系统应用 Coastal Zone Remote Sensing; LUCC; Application of GIS | zhouyx@sklec.ecnu.edu.cn |
| 朱建荣 Dr. Zhu Jiangrong | 河口海岸海洋动力学; 河口海岸海洋数值模式 Estuarine, Coastal and Ocean Dynamics; Estuarine, Coastal and Ocean Model; | jrzhu@sklec.ecnu.edu.cn |
| Dr. Bernd Wünnemann | 气候与环境变化的湖泊地层记录 Lake Sedimentary Records for the Environmental and Climate Change | wuene@zedat.fu-berlin.de |

副教授 Associate Professors

| 姓名 Name | 研究专长 Research Interest | Email |
|-------------------------|--|------------------------------|
| 曹芳 Dr. Cao Fang | 海洋水色遥感 Ocean Color Remote Sensing | fcao@sklec.ecnu.edu.cn |
| 陈启晴 Dr. Chen Qiqing | 微塑料的复合污染与生态效应研究; 颗粒污染物对水生生物的生物富集和致毒机理研究 Compound Pollution and Ecological Effect of Microplastics; Biological Enrichment and Toxic Mechanism of Particulate Pollutants on Aquatic Organisms | chenqiqing@sklec.ecnu.edu.cn |
| 陈雪初 Dr. Chen Xuechu | 湿地生态学 Wetland Ecology | xcchen@des.ecnu.edu.cn |
| 邓兵 Dr. Deng Bing | 沉积地球化学; 沉积学; 古环境 Sedimentary Geochemistry; Sedimentology; Paleoenvironment | dengbing@sklec.ecnu.edu.cn |
| 高磊 Dr. Gao Lei | 河口海岸地区营养盐的生物地球化学过程 Nutrient Biogeochemistry in Estuarine and Coastal Areas | lgao@sklec.ecnu.edu.cn |
| 葛建忠 Dr. Ge Jianzhong | 水动力及泥沙运动数值模拟; 可视化系统及高性能计算 Numerical Modeling of Hydrodynamics and Sediment Transport; Visualization System and High-Performance Computing | jzge@sklec.ecnu.edu.cn |
| 郭磊城 Dr. Guo Leicheng | 河口海岸动力地貌及模拟 Morphodynamic Modelling in Estuarine and Coastal Areas | lcguo@sklec.ecnu.edu.cn |
| 何利军 Dr. He Lijun | 谱系生物地理学; 种群遗传学 Phylogeography; Population Genetics | ljhe@sklec.ecnu.edu.cn |
| 李占海 Dr. Li Zhanhai | 河口海岸沉积动力学 Coastal and Estuarine Sediment Dynamics | zhli@sklec.ecnu.edu.cn |
| 刘演 Dr. Liu Yan | 全新世气候与环境演变; 环境考古 Holocene Climatic and Environmental Changes; Geoarchaeology | liuyan@sklec.ecnu.edu.cn |
| 梅雪菲 Dr. Mei Xuefei | 流域-河口水文地貌过程; 河口海岸动力、沉积、地貌 River-Estuary Hydrological and Geomorphological Process; Estuarine and Coastal Dynamics, Sedimentation, Landform | xfmei@geo.ecnu.edu.cn |
| 史本伟 Dr. Shi Benwei | 短周期潮滩沉积动力过程与机制; 生物作用影响下潮滩生物地貌学 Short Period Tidal Flat Sedimentary Dynamic Process and Mechanism; Tidal Beach Biogeomorphology under the Influence of Biological Processes | bwshi@sklec.ecnu.edu.cn |
| 田波 Dr. Tianbo | 海岸带遥感; 地理信息系统开发与应用 Coastal Zone Assessment and Remote Sensing; GIS Development and Application | btian@sklec.ecnu.edu.cn |
| 童春富 Dr. Tong Chunfu | 湿地生态学与系统生态学 Wetland Ecology and Systems Ecology | cftong@sklec.ecnu.edu.cn |
| 王宪业 Dr. Wang Xianye | 泥沙运动; 河流动力学 Sediment Transport; River Dynamics | xywang@sklec.ecnu.edu.cn |
| 吴辉 Dr. Wu Hui | 河口海岸动力过程及其三维数值模拟; 盐水入侵 Estuarine Dynamics and 3D Numerical Simulation; Saltwater Intrusion | hwu@sklec.ecnu.edu.cn |

| 姓名 Name | 研究专长 Research Interest | Email |
|---------------------------|---|---------------------------|
| 闫中正 Dr. Yan Zhongzheng | 植物生理生态; 海洋水色遥感 Plant Ecophysiology; Ocean Color Remote Sensing | zzyan@sklec.ecnu.edu.cn |
| 袁琳 Dr. Yuan Lin | 湿地生态; 资源环境遥感 Wetland Ecology; Remote Sensing Monitoring of Nature Resource | lyuan@sklec.ecnu.edu.cn |
| 张芬芬 Dr. Zhang Fenfen | 新技术(核磁共振、Raman光谱等)应用于海洋学的研究 Application of New Techniques (NMR and Raman spectroscopy) in Marine Science | ffzhang@sklec.ecnu.edu.cn |
| 朱卓毅 Dr. Zhu Zhuoyi | 有机地球化学; 生物地球化学 Organic Geochemistry; Biogeochemistry | zyzhu@sklec.ecnu.edu.cn |

讲师 Lecturers

| 姓名 Name | 研究专长 Research Interests | Email |
|-------------------------|---|--------------------------|
| 鲍俊林 Dr. Bao Junlin | 第四纪地质年代学 Quaternary Geochronology | jlbao@sklec.ecnu.edu.cn |
| 年小美 Dr. Nian Xiaomei | 泥沙运动; 河流动力学 Sediment Transport; River Dynamics | xmniao@sklec.ecnu.edu.cn |
| 徐江 Dr. Xu Jiang | 水污染控制与修复 Water Pollution Control and Remediation | jxu@sklec.ecnu.edu.cn |
| 许媛 Dr. Xu Yuan | 河口湿地底栖原生动物生态学; 原生动物分类学及分子系统学 Wetland Protozoan Ecology; Protozoan Taxonomy and Phylogeny | yxu@sklec.ecnu.edu.cn |

管理人员 Administrative Staff

| | | |
|--|---|--|
| 俞世恩 实验室党委书记 Dr. Yu Shien, Communist Party secretary | 江红 实验室副主任 Dr. Jiang Hong, Deputy Director | 李俊红 主任助理 Ms. Li Junhong, Director Assistant |
| 吴辉 实验室副主任 (兼) Dr. Wu Hui, Deputy Director (part time) | 张卫国 实验室副主任 (兼) Dr. Zhang Weiguo, Deputy Director (part time) | 高磊 主任助理 (兼) Dr. Gao Lei, Director Assistant (part time) |

技术人员 Technical Staff

| 姓名 Title | 技术领域 Position | 姓名 Title | 技术领域 Position |
|--|--|---------------------------------------|--|
| 瞿建国 副教授 Mr. Qu Jianguo, Associate Professor | 无机分析 Inorganic Elements Analysis | 崔莹 工程师 Dr. Cui Ying, Engineer | 有机及无机分析 Organic and Inorganic Elements Analysis |
| 顾靖华 工程师 Mr. Gu Jinghua, Engineer | 野外仪器设备管理 Field Surveying Instrument | 张国森 工程师 Mr. Zhang Guosen, Engineer | 有机及无机分析 Organic and Inorganic Elements Analysis |
| 张文祥 高级工程师 Dr. Zhang Wenxiang, Senior Engineer | 野外仪器设备管理 Field Surveying Instrument | 张婧 工程师 Ms. Zhang Jing, Engineer | 有机分析 Organic Elements Analysis |

李为华 高级工程师
Dr. Li Weihua, Senior
Engineer 野外仪器设备管理
Field Surveying Instrument

博士后 Postdoctoral Fellows

| 姓名 Name | 研究专长 Research Interest | Email |
|-------------------------|---|--------------------------------|
| 黄颖 Dr. Huang Ying | 滨海陆面过程与植被定量遥感 Land Surface Processes and Quantitative Remote Sensing in Coastal Wetlands | yhuang@sklec.ecnu.edu.cn |
| 张文霞 Dr. Zhang Wenxia | 近海生态动力学 Coastal Dynamics and Ecosystem Simulation | wenxia.zhang@sklec.ecnu.edu.cn |
| 林磊 Dr. Lin Lei | 海洋环境动力学和数值模拟 Marine Environmental Dynamics and Modelling | llin@sklec.ecnu.edu.cn |
| 江山 Dr. Jiang Shan | 海洋生物地球化学 Marine Biogeochemistry | sjiang@sklec.ecnu.edu.cn |
| 王锦龙 Dr. Wang Jinlong | 同位素海洋学 Isotope Oceanography | jllwang@sklec.ecnu.edu.cn |
| 杨阳 Dr. Yang Yang | 海洋沉积动力学 Marine Sediment Dynamics | yyang@sklec.ecnu.edu.cn |
| 周亮 Dr. Zhou Liang | 古风暴学和沉积动力学 Paleotempestology and Sediment Dynamics | lzhou@sklec.ecnu.edu.cn |
| 赵世焯 Dr. Zhao Shiye | 近岸河口生态与环境 Estuarine and Coastal Ecology and Environment | syzhao@sklec.ecnu.edu.cn |
| 谭凯 Dr. Tan Kai | 激光雷达与海岸遥感 LiDAR and coastal remote sensing | ktan@sklec.ecnu.edu.cn |
| 常燕 Dr. Chang Yan | 化学海洋学和同位素地球化学 Marine Chemistry and Isotopic Geochemistry | ychang@sklec.ecnu.edu.cn |
| 晏达达 Dr. Yan Dada | 介形虫、沉积动力、气候环境重建 Ostracod, Sediment Dynamics and Process, Climate and Environmental Reconstruction | ddyann@sklec.ecnu.edu.cn |
| 刘阳 Dr. Liu Yang | 河口海岸学 Estuarine Coastal Science | yliu@sklec.ecnu.edu.cn |
| 梅衍俊 Dr. Mei Yanjun | 海洋地质学 Marine Geology | yjmei@sklec.ecnu.edu.cn |
| 屈卡乐 Dr. Qu Kale | 历史地理学 Historical Geography | 13110760008@fudan.edu.cn |
| 尚媛 Dr. Shang Yuan | 自然地理学 Physical Geography | yshang@sklec.ecnu.edu.cn |
| 魏稳 Dr. Wei Wen | 河口动力沉积与动力地貌 Dynamic Sedimentation and Geomorphology of Estuary | wwei@sklec.ecnu.edu.cn |

| | | |
|---------------------|-----------------------------|-------------------------|
| 徐凡 Dr. Xu Fan | 自然地理学 Physical Geography | fxu@sklec.ecnu.edu.cn |
| 徐佳奕 Dr. Xu Jiayi | 海洋生物 Marine Biology | jyxu@sklec.ecnu.edu.cn |
| 周鹏 Dr. Zhou Peng | 自然地理学 Physical Geography | pzhou@sklec.ecnu.edu.cn |

客座人员 Guest Scientists

| | | |
|--|---|--|
| Dr. Svante Bojorck, Professor svante.bojorckgeol.lu.se | Dr. Edward A Boyle, Professor eaboyle@mit.edu | Dr. Venugopalan Ittekkot, Professor ittekkot@uni-bremen.de |
| Dr. Willard S Moore, Professor moore@geol.sc.edu | Dr. Eiji Matsumoto, Professor e2.matsumoto@nifty.com | Dr. Boris Koch, Professor Boris.Koch@awi.de |
| Dr. Jian Shen, Professor shen@viDr.edu | Dr. Bob (Z) Su, Professor b_su@itc.nl | Dr. Norbert Hertkorn, Professor hertkorn@gsf.de |
| Dr. William Mitsch, Professor mitsch.1@osu.edu | Dr. Wouter Verhoef, Professor verhoef@nlr.nl | Dr. Brian Finlayson, Professor brianlf@unimelb.edu.au |
| Dr. Changsheng Chen, Professor c1chen@umassd.edu | Dr. Huib J. de Vriend, Professor H.J.deVriend@sDr.utwente.nl | Dr. Michael Webber, Professor mjwebber@unimelb.edu.au |
| Dr. Christopher Craft, Professor ccraft@indiana.edu | Dr. Z.B. Wang, Professor zheng.wang@deltares.nl | Dr. Wayne Stephenson, Professor waynejs@unimelb.edu.au |
| Dr. Timothy I. Eglinton, Professor timothy.eglinton@erdw.ethz.ch | Dr. J.C. Winterwerp, Professor J.C.Winterwerp@tudelft.nl | Dr. Eric Wolanski, Professor Eric.Wolanski@jcu.edu.au |
| Dr. Bernhard Peucker-Ehrenbrink, Professor bpeucker@whoi.edu | Dr. M.J.F. Stive, Professor stive51@xs4all.nl | Dr. Ulo Mander, Professor ulo.mander@ut.ee |
| Dr. Frank Oldfield, Professor oldfield.f@gmail.com | Dr. T. Ysebaert, Professor Tom.Ysebaert@nioz.nl | Dr. Zhaoqing Yang, Professor zhaoqing.yang@pnnl.gov |
| Dr. Andrew J. Plater, Professor Gg07@liverpool.ac.uk | Dr. Peter M.J. Herman, Professor Peter.Herman@nioz.nl | Dr. Ian Townend, Professor I.Townend@soton.ac.uk |
| Dr. John A. Dearing, Professor J.Dearing@soton.ac.uk | Dr. Dano Roelvink, Professor d.roelvink@unesco-ihe.org | Dr. Victor N de Jonge, Professor v.n.de.jonge@planet.nl |
| Dr. Yoshiki Saito, Professor yoshiki.saito@aist.go.jp | Dr. Gerhard Kattner, Professor Gerhard.Kattner@awi.de | Dr. Jeanette M Rotchell, Associate Prof. J.Rotchell@hull.ac.uk |
| Dr. Keqi Zhang, Professor keqizhang8@gmail.com | Dr. Eiji Matsumoto, Professor e2.matsumoto@nifty.com | Dr. Boris Koch, Professor Boris.Koch@awi.de |
| Dr. Isaac Santos, Professor isaac.santos@scu.edu.au | Dr. Henner Hollert, Professor henner.hollert@bio5.rwth-aachen.de | Dr. Alfonse Dubi, Professor alfonsedubi@gmail.com |
| Dr. Christiaan van der Tol, Associate Prof. c.vandertol@utwente.nl | Dr. Mark Baskaran, Professor Baskaran@wayne.edu | Dr. Wang Xiaohua, Professor. X.Wang@adfa.edu.au |

| | | |
|---|---|--|
| Dr. Shunqi Pan, Professor PanS2@cardiff.ac.uk | Dr. Huan Feng, Professor fengh@mail.montclair.edu | Dr. Penjai Sompongchaiyakul penjai@hotmail.com |
| Dr. Moritz Mülle Associate Prof. mmueller@swinburne.edu.my | Dr. Zhi Huang, Senior Research Scientist Zhi.Huang@ga.gov.au | Dr. Alfred N. N. Muzuka, Professor alfred.muzuka@nm-aist.ac.tz |
| 吴加学 教授 Dr. Wu Jiaxue, Professor wujiaxue@mail.sysu.edu.cn | Dr. Samina Kidwai, Senior Re- searcher skidwaipk@gmail.com | Dr. Neven Cukrov ncukrov@irb.hr |
| 王爱华 教授级高工 Dr. Wang Aihua njywa@qq.com | 范代读 教授 Dr. Fan Daidu, Professor ddfand@tongji.edu.cn | 洪义国 研究员 Dr. Hong Yiguo, Professor yghong@scsio.ac.cn |
| 王有基 副教授 Dr. Wang Youji, Associate Prof. yj_wang@shou.edu.cn | 郑建 Principal Researcher Dr. Zheng Jian zheng.jian@qst.go.jp | 高建华 教授 Dr. Gao Jianhua, Professor jhgao@nju.edu.cn |
| 高 峥 副教授 Dr. Gao Zheng, Associate Prof. gaozheng@sdau.edu.cn | 吴捷 副研究员 Dr. Wu Jie, Associate Prof. jjewu@sippe.ac.cn | 沙龙滨 副教授 Dr. Sha Longbin, Associate Prof. shalongbin@nbu.edu.cn |
| 张亚娟 副教授 Dr. Zhang Yajuan, Associate Prof. zyj0212@126.com | 宏波 副教授 Dr. Hong Bo, Associate Prof. bohong@scut.edu.cn | 肖德荣 副教授 Dr. Xiao Derong, Associate Prof. xiaoderong1@163.com |
| 韩秋影 副研究员 Dr. Han Qiuying, Associate Prof. hanqiuying0312@sina.com | 左书华 副研究员 Dr. Zuo Shuhua, Associate Prof. zsh0301@163.com | 边昌伟 副教授 Dr. Bian Changwei, Associate Prof. bianchangwei@ouc.edu.cn |
| 于谦 副教授 Dr. Yu Qian, Associate Prof. qianyu.nju@gmail.com | 马小川 副研究员 Dr. Ma Xiaochuan, Associate Prof. mxch@qdio.ac.cn | 张衡 副研究员 Dr. Zhang Heng, Associate Prof. zhangziqian0601@163.com |
| 蔡华阳 副教授 Dr. Cai Huayang, Associate Prof. caihy7@mail.sysu.edu.cn | 孟翊 副教授 Dr. Meng Yi, Associate Prof. ymeng@sklec.ecnu.edu.cn | 张国安 副教授 Dr. Zhang Guoan, Associate Prof. gazhang@sklec.ecnu.edu.cn |
| 李茂田 副教授 Dr. Li Maotian, Associate Prof. mtli@sklec.ecnu.edu.cn | 张二风 副教授 Dr. Zhang Erfeng, Associate Prof. efzhang@sklec.ecnu.edu.cn | 孙千里 副教授 Dr. Sun Qianli, Associate Prof. qlsun@sklec.ecnu.edu.cn |
| 吕建树 讲师 Dr. Lv Jianshu, Lecture lvjianshu@126.com | 范中亚 讲师 Dr. Fan Zhongya, Lecture zyfan@scies.gov | 李恒翔 讲师 Dr. Li Hengxiang, Lecture hxli@scsio.ac.cn |
| 杜金秋 工程师 Dr. Du Jinqiu, Engineer jinqiu609@163.com | 郑崇伟 工程师 Dr. Zheng Chongwei, Engineer chinaoceanzcw@sina.cn | 布乃顺 工程师 Dr. Bu Naishun, Engineer bunaishun@163.com |
| 沈晓腾 博士 Dr. Sheng Xiaoteng xiaoteng.shen@kuleuven.be | 王涛 博士 Dr. Wang Tao haidawangtao@163.com | 许春阳 博士 Dr. Xu Chunyang cyxu@hhu.edu.cn |

| | | |
|--|--|--|
| 王艳娜 讲师 Dr. Wang Yanna, Lecture nywang@sklec.ecnu.edu.cn | 袁 瑞 讲师 Dr. Yuan Rui, Lecture ryuan@shmtu.edu.cn | 叶 祁 讲师 Dr. Ye Qi, Lecture qye@sklec.ecnu.edu.cn |
| 王龙升 讲师 Dr. Wang Longsheng, Lecture 52wls@163.com | 许 一 讲师 Dr. Xu Yi, Lecture xuyi@sklec.ecnu.edu.cn | 徐 皓 讲师 Dr. Xu Hao, Lecture xuhao@nbu.edu.cn |
| 毕倩倩 工程师 Ms. Bi Qianqian, Engineer qqbi@sklec.ecnu.edu.cn | 张 丹 工程师 Dr. Zhang Dan, Engineer dzhang@sklec.ecnu.edu.cn | 袁庆 工程师 Mr. Yuan Qing, Engineer qyuan@sklec.ecnu.edu.cn |
| 胡进 工程师 Mr. Hu Jin, Engineer jinhu@sklec.ecnu.edu.cn | 钱伟伟 助理工程师 Mr. Qian Weiwei, Assistant Engineer qianww89@163.com | 李 月 工程师 Dr. Li Yue, Engineer yli@sklec.ecnu.edu.cn |
| 郑媛予 助理工程师 Ms. Zheng Yuanyu, Assistant Engineer zhengyuanyu2018@163.com | | |

固定人员在国际期刊和国际组织任职情况

Serving in International Academic Organizations and Journals

| Name | International Organizations/Journals | Position | During |
|--------------------------|---|--------------------------|-----------------|
| 陈中原 Chen Zhongyuan | Environmental Management of Enclosed Coastal Seas | SPC Member | 2004- |
| | IAG-Large Rivers Working Group | Member | 2001- |
| | IGBP-LOICZ Scientific Steering Committee | Member | |
| | IGCP-582:Tropical Rivers | Chair | |
| | Geomorphology | Editors-in-Chief | 2017.7-2019.12 |
| | Earth Surface Processes and Landforms | Editorial advisory board | 2008- |
| 程和琴 Cheng Heqin | Estuarine Coastal and Shelf Science | Associate Editor | 2013.1- |
| | Journal of Geology, Geophysics and Geosystems | Editorial board member | 2009- |
| 丁平兴 Ding Pingxing | Acta Oceanologica Sinica | Editorial board member | 2003- |
| | China Ocean Engineering | Editorial board member | 1999- |
| 戴志军 Dai Zhijun | Scientific Reports | Editorial board member | 2016.12-2018.12 |
| | Frontiers of Earth Science | Associate Editors | 2017- |

| Name | International Organizations/Journals | Position | During |
|---------------------|---|----------------------------|----------------|
| 高抒 Gao Shu | Anthropocene Coasts | Founding Co-Editor | 2017.1- |
| | Marine Geology | Editors-in-Chief | 2018.1- |
| | Continental Shelf Research | Associate Editors | |
| | Acta Oceanologica Sinica | Associate Editors-in-Chief | |
| | Chinese Journal of Oceanology and Limnology | Editorial board member | |
| | China Ocean Engineering | Editorial board member | |
| | Ocean Science Journal | Editorial board member | |
| 何青 He Qin | INTERCOH | SSC Member | 2003- |
| 侯立军 Hou Lijun | Estuaries and Coasts | Associate Editors | 2017.1-2020.12 |
| | Scientific Reports | Editorial board member | 2015.12- |
| 李道季 Li Daoji | UNESCO IOC/WESTPAC, Marine Microplastic Project | PI | 2017- |
| | UNEP-Global Environment Outlook-6 Review panel | Expert | |
| | UNESCO-intergovernmental Oceanographic Commission | Expert | |
| | PICES- Marine microplastics research group | Member | |
| | UNEP- North-West Pacific Action Plan | Expert | |
| 刘东艳 Liu Dongyan | Frontier in Marine Science: Marine Ecosystems | Editor | 2018-2023 |
| 李秀珍 Li Xiuzhen | International Association for Landscape Ecology | Council Chair | 2011.1-2019.12 |
| | Ocean and Coastal Management | Associate Editor | 2014.10- |
| | Journal of Conservation Planning | Editorial board member | 2001-2017.12 |
| | Ecological Engineering | Editorial board member | 2008.8- |
| | Chinese Geographical Science | Editorial board member | 2009.6- |
| Richard Bellerby | SCAR Action Group on Ocean Acidification | Leader | 2010- |
| | AMAP Working Group on Ocean Acidification | Leader | 2010- |
| | SCOR/SCAR Expert Group in Oceanography | Member | 2006- |
| | SCAR SOOS Implementation Group | Member | 2007- |
| | SCAR Integrated Climate and Ecosystem Dynamics (ICED) | SSC Member | 2009- |
| | IMBeR - Future Earth Coasts Continental Margins working group | Chai | 2017- |

| Name | International Organizations/Journals | Position | During |
|-------------------------|---|------------------------|-----------------|
| 唐剑武 Tang Jianwu | Ecosystem Health and Sustainability | Editor | |
| | Ecological Processes | Editor | |
| | The Coastal Carbon Research Coordination Network (CCRCN) | Steering Committee | |
| 汪亚平 Wang Yaping | Anthropocene Coasts | Associate Editor | 2017.1- |
| 吴辉 Wu hui | Geoscience Letters | Editorial board member | 2018- |
| 吴莹 Wu Ying | IGBP/IMBER Scientific Steering Committee | Member | 2018- |
| Wünneman | Nature Group | Editorial board member | |
| 杨世伦 Yang Shilun | Scientific Reports | Editorial board member | |
| 张经 Zhang Jing | IOC/WESTPAC-CorReCAP | Project Leader | 2008- |
| | IGBP/IMBER -Capacity Building Working Group | Chair | 2009- |
| | SCOR-Committee on Capacity Building | Member | 2009- |
| | Water, Air and Soil Pollution | Editorial board member | 1994- |
| | Water, Air and Soil Pollution: Focus | Editorial board member | 1999- |
| | Journal of Marine Systems | Editorial board member | 2008- |
| | Acta Oceanologica Sinica | Editorial board member | 2003- |
| 张卫国 Zhang Weiguo | Future Earth Coasts | SSC Member | 2016.1-2018.12 |
| | Current Pollution Reports | Editorial board member | 2014- |
| | Estuarine Coastal and Shelf Science | Associate Editor | 2013- |
| | Geomagnetism and Paleomagnetism, Frontiers in Earth Science | Review Editor | 2015.11-2018.11 |
| 周俊良 Zhou Junliang | Scientific World Journal | Editorial board member | 2009- |

新聘人员 New Appointees



唐剑武 教授

主要经历:

美国加州大学伯克利分校 博士 (2003)
美国芝加哥大学海洋生物研究所 研究员 (2008-2019)
华东师范大学 教授 (2018-)

研究专长:

湿地生态学;
碳循环、全球变化生态学

Dr. TANG Jianwu, Professor

Education and Major Experience:

Ph.D., the University of California, Berkeley (2003)
Professor, Institute of Marine Biology, University of Chicago (2008-2019)
Professor, ECNU (2018-)

Research Interests:

Wetland Ecology;
Carbon Cycling, Global Change Ecology



董宏坡 教授

主要经历:

厦门大学/美国马里兰大学 联合培养博士 (2007-2011)
美国马里兰大学海洋生物研究所 博士后 (2011-2012)
暨南大学赤潮与海洋生物研究中心 副研究员 (2012-2016)
广东海洋大学海洋学院 副研究员 (2016-2018)
华东师范大学 教授 (2018-)

研究专长:

海洋微生物分子生态;
海洋微生物适应环境的分子基础;
海洋微生物参与生物地球化学循环的过程和机理

Dr. DONG Hongpo, Professor

Education and Major Experience:

Joint-trained Ph.D., Xiamen University/ University of Maryland (2007-2011)
Post doctor, University of Maryland Center for Marine Biology (2011-2012)
Associate Professor, Research Center of Marine Biology, Jinan Univeristy (2012-2016)
Associate Professor, School of Oceanography, Guangdong Ocean University (2016-2018)
Professor, ECNU (2018-)

Research Interests:

Molecular ecology of marine microorganisms;
Molecular foundation of marine microorganisms for environmental adaptation;
Processes and mechanisms of marine microorganisms involved in biogeochemical cycles



周旭辉 教授

主要经历:

美国俄克拉荷马大学 博士 (2003-2007)
美国俄克拉荷马大学 博士后 (2007-2019)
美国俄克拉荷马大学 研究助理教授 (2009-2011)
复旦大学 研究员 (2011-2014)
华东师范大学 教授 (2014-)

研究专长:

全球变化生态学;
生态系统生态学;
土壤生态学

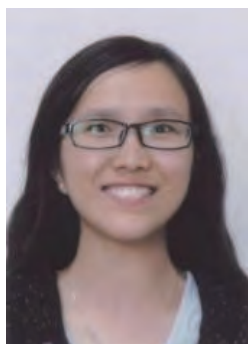
Dr. ZHOU Xuhui, Professor

Education and Major Experience:

Ph.D, University of Oklahoma, USA (2003-2007)
Post-Doctor, University of Oklahoma, USA (2007-2009)
Research Assistant Professor, University of Oklahoma, USA (2009-2011)
Professor, Fudan University (2011-2014)
Professor, ECNU (2014-)

Research Interests:

Global Change Biology;
Ecosystem Ecology;
Soil Ecology



杨毅 教授

主要经历:

奥地利维也纳大学 博士, 博士后
(2003-2008)
华东师范大学 副教授 (2008-2012)
美国弗吉尼亚理工大学 研究员 (2013)
华东师范大学 教授 (2012-)

研究专长:

新型有机污染物研究

Dr. YANG Yi, Professor

Education and Major Experience:

Ph.D, Post-Doctor, The University of Vienna Austria
(2003-2008)
Associate Professor, ECNU (2008-2012)
Research Scientist, Virginia Tech, CEINT (2013)
Professor, ECNU (2012-)

Research Interests:

Emerging Organic Pollutants



夏建阳 教授

主要经历:

中国科学院大学 博士 (2005-2011)
美国俄克拉荷马大学 博士后 (2011-
2015)
华东师范大学 教授 (2015-)

研究专长:

全球变化生态学;
陆地生态系统模型的不确定性溯源;
湿地碳循环对气候变化的响应机理

Dr. XIA Jianyang, Professor

Education and Major Experience:

Ph.D, Chinese Academy of Sciences (2005.9-
2011.1)
Post-Doctor, University of Oklahoma, USA (2011.3-
2015.5)
Professor, ECNU (2015-)

Research Interests:

Global Change Ecology;
Traceability Analysis on Global Land Model
Uncertainty;
Response of Wetland Carbon Cycle to Climate Change



王群 教授

主要经历:

华东师范大学 博士 (1998-2002)
华东师范大学 副教授 (2000-2005)
美国奥本大学 访问学者 (2004-2005)
华东师范大学 教授 (2005-)

研究专长:

水生生物学

Dr. WANG Qun, Professor

Education and Major Experience:

Ph.D, ECNU (1998-2002)
Associate Professor, ECNU (2000-2005)
Visiting Scholar, Auburn University, USA (2004-2005)
Professor, ECNU (2005-)

Research Interests:

Aquatic Biology



姜晓东 教授

主要经历:

纽约州立大学石溪分校 博士 (2006-
2010)
华东师范大学 教授 (2017-)

研究专长:

浮游动物生态学

Dr. JIANG Xiaodong, Professor

Education and Major Experience:

Ph.D, Stony Brook University, USA (2006-2010)
Professor, ECNU (2017-)

Research Interests:

Zooplankton Ecology



赵云龙 教授

主要经历:

华东师范大学 博士 (1989-1992)
华东师范大学 教授 (2000-)
上海市第七届“曙光”学者称号
(2001)

研究专长:

水生动物生物学及生态学

Dr. ZHAO Yunlong, Professor

Education and Major Experience:

Ph.D, ECNU (1989-1992)
Professor, ECNU (2000-)

Research Interests:

The Biology and Ecology of Aquatic Animal



杨嘉龙 教授

主要经历:

中国科学院海洋研究所 博士 (2008-2011)
中国科学院烟台海岸带研究所 助理研究员 (2011-2012)
美国杜克大学医学中心 博士后 (2012-2016)
华东师范大学 紫江青年学者 研究员 (2017-)
2018年上海市“浦江人才计划”

研究专长:

水生动物免疫学

Dr. YANG Jialong, Professor

Education and Major Experience:

Ph.D, Institute of Oceanology, Chinese Academy of Sciences (2008-2011)
Assistant Professor, Yantai Institute of Coastal Zone Research, Chinese Academy of Sciences (2011-2012)
Post-Doctor, Duke University Medical Center, USA (2012-2016)
Professor, ECNU (2017-)
Be supported by Shanghai Pujiang Talent Plan in 2018

Research Interests:

Immunology of Aquatic Animals



李超 教授

主要经历:

中国科学院遗传与发育生物学研究所/
北京生命科学研究所
联合培养博士 (2008)
美国马萨诸塞大学 博士后 (2008-2016)
华东师范大学 教授 (2016-)

研究专长:

发育生物学

Dr. LI Chao, Professor

Education and Major Experience:

Joint-trained Ph.D., Institute of Genetics and Developmental Biology, Chinese Academy of Sciences/National Institute of Biological Sciences (2008)
Post-Doctor, University of Massachusetts, USA (2008-2016)
Professor, ECNU (2016-)

Research Interests:

Developmental Biology



陈雪初 副教授

主要经历:

上海交通大学 博士 (2006 -2009)
上海交通大学 讲师 (2009-2015)
美国 (伍茨霍尔) 海洋生物实验室 访问科学家 (2014-2015)
华东师范大学 副教授 (2015-)

研究专长:

水域及滨海湿地碳氮循环;
生态工程

Dr. CHEN Xuechu, Associate Professor

Education and Major Experience:

Ph.D, Shanghai Jiao Tong University (2006-2009)
Lecturer, Shanghai Jiao Tong University (2009-2015)
Visiting scientist, Marine Biological Laboratory, USA (2014-2015)
Associate professor, ECNU (2015-)

Research Interests:

Carbon and Nitrogen Cycle in Aquatic Waters and Coastal Wetlands;
Ecological Engineering



陈启晴 紫江青年学者

主要经历:

同济大学 博士 (2012-2015)
德国亚琛工业大学 博士后 (2015-2017)
华东师范大学 学科博士后 (2017-2018)
华东师范大学 紫江青年学者 (2018-)
2018年获得上海市浦江人才计划资助
2019年获得国家自然科学基金青年基金资助

研究专长:

微塑料的复合污染与生态效应研究;
颗粒污染物对水生生物的生物富集和致毒机理研究

Dr. CHEN Qiqing, Zijiang Young Scholar of ECNU.

Education and Major Experience:

Ph.D, Tongji University (2012-2015)
Post-Doctor, RWTH Aachen University, Germany (2015-2017)
Post-Doctor, ECNU (2017-2018)
Zijiang Young Scholar of ECNU, ECNU (2018-)
Be supported by Shanghai Pujiang Talent Plan in 2018

Be supported by the fund of NSFC in 2019

Research Interests:

Compound Pollution and Ecological Effect of Microplastics;
Biological Enrichment and Toxic Mechanism of Particulate Pollutants on Aquatic Organisms



曹芳 副教授

主要经历:

美国佐治亚大学 博士 (2009-2015)
美国纽约城市大学 博士后 (2015-2018)
华东师范大学 副教授 (2018-)

研究专长:

海洋水色遥感

Dr. CAO Fang, Associate Professor

Education and Major Experience:

Ph.D, The University of Georgia, USA (2009-2015)
Post-Doctor, City University of New York, USA (2015-2018)
Associate Professor, ECNU (2018-)

Research Interests:

cean Color Remote Sensing



史本伟 副教授

主要经历:

华东师范大学 博士 (2007-2012)
南京大学 博士后 (2012-2018)
路易斯安那州立大学 访问学者 (2016-2017)
华东师范大学 副教授 (2018-)
2015年获得国家自然科学基金面上项目

研究专长:

短周期潮滩沉积动力过程与机制;
生物作用影响下潮滩生物地貌学

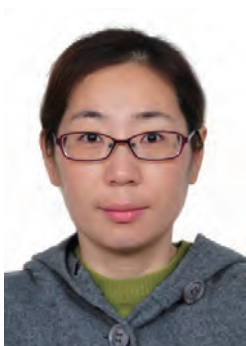
Dr. SHI Benwei, Associate Professor

Education and Major Experience:

Ph.D, ECNU (2007-2012)
Post-Doctor, Nanjing University (2012-2018)
Visiting Scholar, Louisiana State University (2016-2017)
Associate Professor, ECNU (2018-)
Be supported by the General Program of NSFC in 2015

Research Interests:

Short Period Tidal Flat Sedimentary Dynamic Process and Mechanism;
Tidal Beach Biogeomorphology under the Influence of Biological Processes



梅雪菲 副教授

主要经历:

荷兰代尔夫特理工大学 博士 (2008-2013)
华东师范大学 博士后 (2014-2018)
华东师范大学 副教授 (2018-)

研究专长:

流域-河口水文地貌过程;
河口海岸动力、沉积、地貌

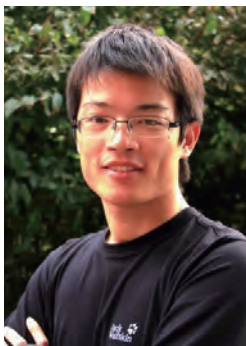
Dr. MEI Xuefei, Associate Professor

Education and Major Experience:

Ph.D, Delft University of Technology, Netherlands (2008-2013)
Post-Doctor, ECNU (2014-2018)
Associate Professor, ECNU (2018-)

Research Interests:

River-Estuary Hydrological and Geomorphological Process;
Estuarine and Coastal Dynamics, Sedimentation, Landform



刘演 副教授

主要经历:

华东师范大学 博士 (2008-2014)
同济大学 博士后 (2014-2016)
华东师范大学 博士后 (2016-2018)
华东师范大学 副教授 (2018-)

研究专长:

全新世气候与环境演变;
环境考古

Dr. LIU Yan, Associate Professor

Education and Major Experience:

Ph.D, ECNU (2008-2014)
Post-Doctor, Tongji University (2014-2016)
Post-Doctor, ECNU (2016-2018)
Associate Professor, ECNU (2018-)

Research Interests:

Holocene Climatic and Environmental Changes;
Geo-archaeology